ÇUKUROVA UNIVERSITY
INSTITUTE OF NATURAL AND APPLIED SCIENCES

Ph.D. THESIS

Akhtar ALI

EVALUATING THE EFFECT OF MICRO-CATCHMENT WATER HARVESTING ON WATER AND SOIL LOSSES IN THE DRYLAND CATCHMENT

DEPARTMENT OF AGRICULTURAL STRUCTURES AND IRRIGATION

ADANA, 2007

ÇUKUROVA UNIVERSITY
INSTITUTE OF NATURAL AND APPLIED SCIENCES

EVALUATING THE EFFECT OF MICRO-CATCHMENT WATER HARVESTING ON WATER AND SOIL LOSSES IN THE DRYLAND CATCHMENT

Akhtar ALI

Ph.D. THESIS

DEPARTMENT OF AGRICULTURAL STRUCTURES AND IRRIGATION

This Thesis was Approved on 28/9/2007 Date by the Following Juri with Unanimous/Majority Consensus.

Signature:........................ Prof. Dr. Attila YAZAR Chairman

Signature:........................ Prof. Dr. Selim KAPUR Member

Signature:........................ Prof. Dr. Cafer GENÇOĞLAN Member

Signature:........................ Asst. Prof. Dr. Fatih TOPALOĞLU Member

Signature:........................ Asst. Prof. Dr. Erhan AKÇA Member

This Thesis has been prepared in the Agricultural Structures and Irrigation Department.

Code No:

Prof. Dr. Aziz ERTUNÇ
Director of Institute

ÇUKUROVA ÜNİVERSİTESİ
FEN BİLİMLERİ ENSTİTÜSÜ

KURAK ALANLARDA MİKRO-HAVZA SU HASADININ SU VE TOPRAK KAYIPLARINA ETKİSİNİN DEĞERLENDİRİLMESİ

Akhtar ALI

DOKTORA TEZİ

TARIMSAL YAPILAR ve SULAMA ANABİLİM DALI

Bu tez 28/9/2007 Tarihinde Aşağıdaki Jüri Üyeleri Tarafından Oybirliği/Oyçokluğu İle Kabul Edilmiştir.

İmza:.................................
Prof. Dr. Attila YAZAR
DANIŞMAN

İmza:.................................
Prof. Dr. Selim KAPUR
ÜYE

İmza:.................................
Prof. Dr. Cafer GENÇOĞLAN
ÜYE

İmza:.................................
Yrd. Doc. Dr. Fatih TOPALOĞLU
ÜYE

İmza:.................................
Yrd. Doc. Dr. Erhan AKÇA
ÜYE

Bu tez Enstitümüz Tarımsal Yapılar ve Sulama Anabilim Dalında hazırlanmıştır.

Kod No:

Prof. Dr. Aziz ERTUNÇ
Enstitü Müdürü

ABSTRACT

Ph.D. THESIS

EVALUATING THE EFFECT OF MICRO-CATCHMENT WATER HARVESTING ON WATER AND SOIL LOSSES IN THE DRYLAND CATCHMENT

Akhtar ALI

ÇUKUROVA UNIVERSITY
INSTITUTE OF NATURAL AND APPLIED SCIENCES
DEPARTMENT OF AGRICULTURAL STRUCTURES AND IRRIGATION

Supervisor	**:**	**Prof. Dr. Attila YAZAR**
Year	**:**	**2007, Pages: 255**
Jury	**:**	**Prof. Dr. Selim KAPUR** **Prof. Dr. Cafer GENÇOĞLAN** **Asst. Prof. Dr. Fatih TOPALOĞLU** **Asst. Prof. Dr. Erhan AKÇA**

Micro-catchment water harvesting (MCWH), by inducing and conserving surface runoff, can alleviate the water stresses in arid environments. It brings the changes in land surface, concentrates local runoff at plant location and reduces the downstream flows. It has serious implications on the water and soil losses as well as survival and growth of vegetative cover. This study evaluated the effects of the MCWH on the water, soil and vegetation in an area with an annual rainfall about 110 mm. A small catchment of 2.5 km^2 was equipped with weather station, runoff stage sensors, runoff plots, bridge frames and Gerlach troughs to measure runoff and sediment loss at micro-catchment, site/rill and catchment scales. RUSLE2 model was used to compute the sediment delivery across the ridges.

The results revealed that the rainfall is too low to support rainfed agriculture, but with 4 mm threshold value for runoff generation, the MCWH can capture a runoff between 5 and 80% of incidental rainfall that can help in rehabilitation of the range. At micro-catchment scale, the annual runoff yield was between 200 and 400 m^3 ha^{-1}, which reduced to about half at the site scale and increased to 425 m^3 ha^{-1} at the catchment scale. High contribution of the upper catchment raised the runoff yield at catchment scale. The annual sediment yield was about 1.6 times higher with MCWH (1.2 Mg ha^{-1} yr^{-1}) than the control (0.77 Mg ha^{-1} yr^{-1}). However, the sediment delivery across the ridges was less than 1/5th of the sediment loss. At the catchment scale, the annual sediment yield was about 1.5 Mg ha^{-1}, which was due to the contribution of gully erosion. On an average, the sediment yield in the study area was below the soil loss tolerance limits set by the different studies elsewhere. The study estimated the effective life of the MCWH structures between 20 and 30 years. It concluded that the MCWH increased the shrub survival rate from less than 5% for control to about 70% with MCWH. It has been found that *Atriplex halimus* recorded high survival and growth rates and found best suited for this area. The study showed that the MCWH induced local runoff, but it did not affect the runoff yield at the catchment scale adversely.

Keywords: Micro-catchment water harvesting, runoff, soil loss, soil-water, shrub survival and growth.

ÖZ

DOKTORA TEZİ

KURAK ALANLARDA MİKRO-HAVZA SU HASADININ SU VE TOPRAK KAYIPLARINA ETKİSİNİN DEĞERLENDİRİLMESİ

Akhtar ALI

ÇUKUROVA ÜNİVERSİTESİ
FEN BİLİMLERİ ENSTİTÜSÜ
TARIMSAL YAPILAR ve SULAMA ANABİLİM DALI

Supervisor	**:**	**Prof. Dr. Attila YAZAR**
Year	**:**	**2007, Pages: 255**
Jury	**:**	**Prof. Dr. Selim KAPUR**
		Prof. Dr. Cafer GENÇOĞLAN
		Yrd. Doc. Dr. Fatih TOPALOĞLU
		Yrd. Doc. Dr. Erhan AKÇA

Mikro-havza su hasadı (MCWH) teknikleri, yüzey akış sularını biriktirerek, kurak alanlarda su stresinin etkilerini azaltabilir. Bu teknik arazi üzerinde bir değişikliği gerektirir ve yersel yüzey akış sularını bitki yetiştirilen noktalarda biriktirerek aşağı doğru olan yüzey akış miktarını azaltır. Ayrıca, bu teknik toprak ve su kayıpları üzerinde önemli etkilere sahip olup aynı zamanda vejetasyonun canlı kalmasına yardımcı olur. Bu çalışmada yıllık ortalama yağışı 110 mm olan bir alanda mikro-havza su hasadı (MCWH) tekniklerinin su, toprak ve vejetasyon üzerine etkileri değerlendirilmiştir. Alanı 2.5 km^2 olan küçük bir havzada yürütülen bu araştırmada otomatik iklim istasyonu, yüzey akış sensörleri, yüzey akış parselleri, mikro-havzada, oyuntuda ve havza düzeyinde yüzey akışı, sediment kayıplarını ölçmek için Gerlach aparatı gibi aygıtlar kullanılmıştır. Ayrıca, RUSLE2 Modeli sırtlar arasında sediment taşınımını hesaplamak amacıyla kullanılmıştır.

Araştırma sonuçları çalışmanın yapıldığı alanda düşen yağışların kuru tarımı sürdürebilmek için yeterli olmadığını göstermiştir. Ancak, yüzey akışın oluşabilmesi için en az 4 mm'lik bir yağışa gereksinim olduğu belirlenmiştir. Mikro-havza su hasadı tekniği ile yüzey akışın %5-80'nin mera alanlarının iyileştirilmesinde yararlı olabileceği kestirilmiştir. Mikro-havza ölçeğinde yıllık yüzey akış miktarı 200-400 m^3 ha^{-1} arasında belirlenmiştir. Araştırmanın yapıldığı küçük havza bazında bu değer yarı yarıya azalmış, ancak tüm havza bazında ise 425 m^3 ha^{-1} olmuştur. Yıllık sediment miktarı mikro-havza su hasadı tekniğiyle kontrol konusuna göre 1.6 kat daha fazla bulunmuştur. Ancak, sırtlara ulaşan sediment miktarı toplam sediment kayıplarının 1/5'inden daha az olmuştur. Havza bazında yıllık sediment verimi oyuntu erozyonunu katkılarıyla 1.5 Mg ha^{-1} belirlenmiştir. Çalışma alanında. Belirlenen ortalama sediment verimi başka alanlarda yapılan çalışmalardaki izin verilebilir toprak kayıplarından daha düşük bulunmuştur. Çalışmada mikro-havza su hasadı yapılarının ömürlerinin 20-30 yıl arasında olabileceği tahmin edilmiştir. Ayrıca, mikro-havza su hasadı tekniğinin canlı çalı oranını kontrol parsellerindeki %5'e karşılık %70'e çıkardığı gözlenmiştir. *Atriplex helimus* çalısının çalışmada denemeye alınan diğer çalılara kıyasla daha fazla canlı kalma özelliğine sahip olduğu da ayrıca belirlenmiştir. Çalışma sonuçları, mikro-havza su hasadı uygulamasının yüzey akışı artırdığı ancak havza bazında yüzey akışa etkisinin fazla olmadığını göstermiştir.

Anahtar kelimeler: Mikro-havza su hasadı, toprak kaybı, toprak suyu, çalı canlı kalma oranı

ACKNOWLEGEMENT

I gratefully acknowledge and sincerely thank my advisor Prof. Dr. Attila Yazar, Professor, Department of Agricultural Structures and Irrigation of Çukurova, University for his efficient guidance, encouragement and support from the start to the completion of this dissertation. He has always been keen to see that the results of the research are relevant and replicable. My special thanks go to Prof. Selim Kapur, Dr. Fatih Topaloğlu, Prof. Riza Kanber and other teachers and students from the department for their constructive views and encouragement during the seminars.

I am especially grateful to Dr. Mahmoud Solh, Director General, Dr. William Erskine, Assistant Director General and Dr. Theib Oweis, Director, Integrated Water and Land Management Program and other colleagues from ICARDA for their generous support. The valuable suggestions by Drs. Zuhair Masri and Adriana Bruggeman; review by Dr. Fadel Rida; and editing by Mr. Venkataramani Govidan are gratefully acknowledged.

The cooperation rendered by the project staff from Syria, namely Mr. Atef Abdal Aal, National Project Coordinator; General Commission for Scientific Agricultural Research (GCSAR), Mr. Kasem Salameh, Director, Mehesseh Research Center, Ms. Amira Khazal, Project Engineer, and Messer Ahmad Abdalla and Aymin Bakhit in project implementation and data collection is highly appreciated.

The author wishes to acknowledge the help of the ICARDA staff namely Messer Pierre Hayek, Ali Haj-Dibo, Jihad Abdalla and Issam Halimeh in the data collection. Particular thanks are due to Ms. Rima El-Khatib for formatting the publication. Administrative support by the ICARDA and the University staff is deeply acknowledged.

I acknowledge the SWISS Development Cooperation (SDC) for its generous funding the Vallerani Water Harvesting Project, which made this study possible.

Most importantly, the completion of this study is not my achievement alone. Credits are due to my father, late mother, my wife, daughter and son, who have endured great difficulties with me, and always encouraged me to pursue the study.

CONTENTS

LIST OF FIGURES

PAGE

LIST OF PHOTOS

PAGE

LIST OF TABLES

PAGE

ABBREVIATIONS AND SYMBOLS

CA	: Catchment area
CDI	: Cumulative departure index
EI_{30}	: Storm energy intensity
ET_o	: Potential evapotranspiration
FAO	: Food and Agriculture Organization of the United Nations
HEC	: Hydrological Engineering Center
ICARDA	: International Center for Agricultural Research in the Dry Area
KE	: Kinetic Energy
MCWH	: Micro-catchment water harvesting
Min-N	: Mineral nitrogen
MSL	: Mean sea level
MUSLE	: Modified Universal Soil Loss Equation
NRCS	: Natural Resources Conservation Service
OM	: Organic matter
P	: Pakistani
PA	: Planted area
Ppm	: Parts per millions
P/E_o	: Precipitation to evaporation ratio
RAI	: Rainfall anomaly index
RH	: Relative humidity
RUSLE	: Revised Universal Soil Loss Equation
SCS	: Soil Conservation Services
Sc	: Semi-circular manual bunds
T_{min}	: Minimum temperature
T_{max}	: Maximum temperature
T_{avg}	: Average temperature
t_c	: Time of concentration
t_p	: Time to peak
Vc	: Vallerani continuous
Vi	: Vallerani intermittent
UNDP	: United Nation Development Program
UNEP	: United Nation Environmental Protection
USDA	: United State Department of Agriculture
USLE	: Universal Soil Loss Equation
USR	: Unit Sediment Rate
m^3	: Cubic meter
ha	: Hectare
h	: Hour
yr	: Year
$Mg\ ha^{-1}\ yr^{-1}$	: Mega grams per hectare per year (= ton per hectare per yearr)
$m^3\ ha^{-1}$	: Cubic meter per hectare
$m^3\ ha^{-1}\ yr^{-1}$	: Cubic meter per hectare per year
$^{\circ}C$	: Degree Celsius

1. INTRODUCTION

1.1 The Drier Environment

Drylands are known for their water scarcity, land degradation and declined livelihood. They represent about 40% of the global area—of which 60% is located in developing countries, spread over 110 nations, sheltering more than 700 million population and their contribution in food security is well-acknowledged (FAO, 1978). Falkenmark *et al.* (1990) described drylands as areas with highly variable and dry hydro-climate, where water is identified as a limiting factor in biomass production. When combined with fragile and inherently low fertile soils, it is exposed to higher degree of vulnerability. FAO (1981) defined the arid and semi-arid environments as areas where rainfall under normal conditions does not support rainfed farming. Per capita freshwater availability in dry areas is low (1250 m^3) when compared to the world average of 7500 m^3. In most of the dry areas, agriculture used to share more than 75% of the water resources, and water availability is declining due to continuous diversions to domestic and industrial sectors. The drylands face contradicting situation of demand for more food for ever-increasing population and land degradation intimidating their production capacities. Rainfed farming and livestock husbandry are the main sources of livelihood of majority of the rural population. Poverty and land degradation are generally linked to the poor management of the water resources and over-exploitation of the vegetation cover. In the past, the drylands were commonly viewed as wastelands; not worthy of economic concern or political importance. But now they are getting attention because of the need to produce more food and environmental sustainability.

Range is a major land use in dry areas that constitutes about one-quarter of land surface (FAO, 1980). In Eastern Mediterranean countries, range is a predominant land use (Table 1.1) and is a main source of livelihood for millions of people. The rangelands are highly degraded and their carrying capacity has drastically reduced. Grazing pressure and very low potential of natural re-generation and sustaining the vegetation under harsh climatic conditions contributed to the degradation. Rangeland rehabilitation is a great challenge for ensuring livelihood security and environmental protection, and it can be addressed by adopting innovative techniques (FAO, 1980). Syria alone has about 8.3 million hectares of rangeland (Syrian Ministry of Environment and UNDP, 1997). Moderate land slopes with hilly to semi-hilly terrains, shallow soils (30–80 cm) and sparse vegetation characterize the Syrian rangeland. Its average annual rainfall varies between 50 and 200 mm and its unproductive losses are high. Rain on degraded land develops surface crust, reduces infiltration and encourages a large part of rainfall to runaway with little benefits to local environment. It leads to a vicious cycle of declining vegetation and land degradation. The rangeland's carrying capacity has reduced to about one-fourth of the referenced conditions existed 3 to 4 decades ago. Similar situation exists in rangelands in other East Mediterranean countries. The very low shrub survival rate under natural conditions in Syria (2–5%) emphasized the need of water harvesting in range rehabilitation (Somme *et al.* 2004).

Table 1.1. Rangelands in East Mediterranean Countries (Source: WRI, 2003)

Country	Total Land Area (10^3 ha)	*Total Dry Area (10^3 ha)	Shrub Lands, Savanna and Grasslands (% of Total Land Area)	Sparse Vegetation or Barren (% of Total Land Area)	Shrub + Sparse Vegetation (% of Total Land Area)
Algeria	238174	48530	9	89	98
Egypt	100145	7709	1	95	96
Palestine/ Israel	2106	1427	33	26	59
Jordan	8921	6467	52	43	95
Lebanon	1040	607	36	0.0	36
Libya	175954	36817	2	98	100
Morocco	44655	37232	42	49	91
Syria	18518	18436	54	22	76
Tunisia	16361	14565	31	59	90
Turkey	77482	60138	33	0.0	33

*Based on 1950–1981 information. All other data is based on status as of 2000.

1.2 Water Harvesting: An Unrealized Potential of Dryland Catchments

In contrast to humid regions, overland flow in dryland catchments, due to the absence of developed soils and vegetative cover, and presence of frequent impervious surfaces, generates and dissipates quickly. It is largely associated with on-site water and soil losses. Two specific features of dryland catchments describe its unrealized water harvesting potential.

- Raindrop impact on bare soil degrades the soil structure, seals the surface and prohibits infiltration, and can generate local runoff from a small amount of rainfall. This low threshold value of rainfall for runoff generation helps to produce more runoff events from same rainfall as compared to humid areas where vegetation cover induces high initial abstractions. Martinez-Mena *et al.* (1998), based on four small catchments (0.3–0.75 ha) in semi-arid Spain, found that Hortonian overland flow dominated on more degraded and poorly permeable soils leading to more accentuated runoff response (3.6 mm rainfall as threshold value for runoff initiation; runoff coefficient 9%) as compared with humid areas (threshold value 8 mm and runoff coefficient < 3%). Bull *et al.* (2000) found runoff producing rainfall threshold value 5–10 mm for areas of marl and 20 mm for areas of mica-schist in southeast Spain. In rocky northern Negev Desert with 100 mm of annual rainfall, Shanan and Schick (1980) quantified initial losses (the amount of storm rainfall lost until runoff initiation), about 5 mm of rain was lost during each storm in a 1–7 ha catchment due to crust wetting (2.5 mm) and overland flow losses (2.5–3 mm).

- A small catchment can produce high runoff per unit area, when runoff efficiency can significantly decrease with the increase in catchment area. Stern (1979) inferred that under same hydrological conditions, a runoff equal to 50% of incident rainfall may be expected from a small area as compared with river basin where it hardly reaches to 5% of the rainfall. Beven (2002) also described that runoff may generate locally when the catchment is dry or as a result of short duration storm. Nevertheless, in most of the runoff events in drylands, water is lost during transmission in ephemeral gullies or in shallow depressions and it does not reach to stream network or water bodies. Bergkamp (1998), on the basis of study on cultivated terraced slope, found that in extreme natural events overland flow was generated on several parts of the slope, but did not reach to the channel.

Low rainfall-runoff threshold value, together with high runoff efficiency of small catchments in drylands, provides opportunity to harvest this runoff at or near the source. Micro-catchment water harvesting (MCWH) can capture this local runoff and concentrate it into the plant basins before it is lost in the water conveyance network. Benefits of water harvesting are mentioned as speeding up of tree establishment and deep root development (Boers, 1994), increase in crop productivity and diversity and decrease in soil erosion (Gatot *et al.*, 1999), and stabilizing crop yield in poorly distributed rainfall areas (Oweis *et al.*, 2001).

1.3 Evaluation Rationale

Water harvesting depends on seasonal rainfall amount and pattern (Reij *et al.*, 1988) and water storage capacities of the host soils (Huibers, 1985). Catchment characteristics are also a major factor in runoff production. High spatial and temporal rainfall variability, long dry spells between rainfall events, and high water transmission losses and low annual water yield can be the main constraints to harvest water in dryland catchments, which need to be adequately incorporated in water harvesting planning. Tikue (2002) also emphasized the need of integrating the geophysical, agro-hydrological and socio-economic factors with water harvesting planning including field and high value crops and fodder shrubs and grasses. This adds complexity to sustainable water harvesting planning. Charles *et al*. (2002) and Shiferaw and Holden (1998), criticized that inappropriate water harvesting in dryland environments can lead to inequity, and initial negative return can undermine the households' incentive to invest in this technology. They emphasized that development of ecologically sound land management practices and to avoidance of negative consequences requires a clear understanding of how the potential interventions will affect the hydrology of the ecosystem. FAO (1990a) also indicated that improved management of soil and water resources is a pre-requisite for achieving sustainable agricultural and rural development. Prinz and Singh (2000) recommended that developing strategies for water harvesting for arid regions should be accorded a top priority. This leads to the evaluation of the MCWH for vegetative cover improvement and water and soil conservation. The key research questions can be,

- What are the runoff and sediment production and harvesting potentials of a micro-catchment?
- What is the effect of MCWH on runoff and sediment at different spatial scales?
- What is the effect of MCWH on shrub/vegetation establishment?

A better understanding to find the answer to all or any of these questions can be the rationale of evaluation of MCWH.

1.4 Preposition

MCWH ridges catch the overland flow before it reaches the rills and gullies and lost during transmission or by evaporation. These small check structures modify the land surface and interrupt the hydro-sediment pattern. They affect the overland flow hydrology by reducing the slope length, flow velocity and kinetic energy. The consequences could be increased infiltration in the structures' basins and reduced runoff and sediment at downstream of the structures. Up-scaling these structures could also affect water and soil at landscape or catchment scale. Evaluation of these effects can provide better insight into the suitability of MCWH. Nevertheless, these effects have rarely been quantified in the dryland catchments. The proposed study is designed to evaluate such effects. *The preposition of this study is that the micro-catchment water harvesting conserves water and reduces soil loss in the dryland catchments.*

1.5 Objectives

The overall objective of this study is to evaluate the effects of micro-catchment water harvesting on runoff and sediment in a small catchment in marginal dryland. The specific objectives of the study are:

1. To develop/evaluate a methodology to measure water and soil losses from a dryland catchment at micro- and macro-catchment scales;

2. To evaluate the effect of MCWH on soil-water storage and shrub establishment; and
3. To simulate the effect of contour ridges on soil erosion induced by overland flow.

1.6 Scope of Work

The MCWH in this research was limited to land slope between 2 and 6%. This is site-specific situation and is related to technical and economic factors. The steeper land slopes may require higher bunds—difficult to construct using the available implements, and high maintenance cost. On the contrary, flat areas may require modifications to create slope conducive to adequate runoff production. The study, through improved understanding, would contribute to the knowledge of water and soil loss in general and water and soil loss assessment in particular, in the dryland catchments experience with MCWH.

2. LITERATURE REVIEW

2.1 Context

Micro-catchment Water Harvesting (MCWH) requires the development of small structures across mild land slopes, which capture overland and semi-concentrated flows and store it in soil profile for subsequent use by plants. These structures also harvest the sediment generated in upstream areas. By doing so, MCWH cuts the flow kinetic energy and downstream sediment flow to zero and modifies the entire hydro-sediment process governed by overland flow. Nevertheless, in exceptional cases, overflowing or damages to these structures can cause high sediment loss. Water harvesting capacity of a MCWH system depends on its runoff production potential and soil-water storage that involves hydrology of a micro-catchment and hydraulics of corresponding small storage basin and soil profile. The hydrology may consist of runoff (= rainfall less abstractions; mainly infiltration in dryland catchments) and its impact on erosion and sedimentation at inter-rill and rill scales. Although, less likely, but it is possible that an extensive MCWH system may affect runoff and sediment dynamics in gullies at catchment-scale. Nature can also induce high rainfall that may generate a runoff more than absorbing capacity of corresponding basins and cause outflows either along or over the structures. This chapter reviews the literature to describe these processes and related implications.

2.2 Dryland Catchments and Hydro-Sediment Process

Drylands, including the arid, semi-arid and dry sub-humid environments, occupy 50% of land area, support 20% of the World's population and form highly significant global environment (UNEP, 1992; Middleton and Thomas, 1997). It is ecologically diverse and economically important area of the most resilient people (Behailu, 2001). Rainfed farming and livestock husbandry are the main sources of livelihood of majority of the rural population. Erratic rainfall and frequent dry spells on one hand, and sparse vegetation and fragile soils on the other hand characterize the dryland environment. In agricultural context, arid environment is referred to as areas where rainfall alone is not sufficient for regular rainfed farming (FAO, 1981). UNESCO (1977) defined the arid zones by rainfall and potential evapotranspiration ratio (P/PET) between 0.03 and 0.2; P/PET< 0.03 as hyper arid, and 0.2<P/PET< 0.5 as semi-arid zone. Simmers (2003) defined arid environment with annual rainfall 80–150 mm in winter and 200–350 mm in summer rainfall areas; inter-annual rainfall variability 50–100%, scattered nomadic livestock rearing and agriculture based on local rainfall possible through rainwater harvesting techniques. The rainfall is highly spatially and temporally variable, with variability possibly increasing with aridity (Bell, 1979). Ratios of evapotranspiration to precipitation are generally large in drylands, exceeding 95% in some areas (Branson, 1976). As a result, soil-moisture remains low during dominant period of the year and poses constraint to vegetative growth. The main implications of dryland environments can be prolonged drought and water shortages (Bull and Kirkby, 2002), soil erosion and land degradation (Sala *et al*. 1991) and desertification (UNEP, 1991).

Arid and semi-arid climates produce a characteristic balance of hillslope and channel process, which give dryland flows their special features (Bull and Kirkby, 2002). In dryland catchments, overland flow is i) a major form of flow, ii) a main determinant of sediment and nutrient transport by water (Kiepe, 1995) and iii) it shapes the size and shape of flood peak (Troch *et al*., 1994). Due to low total transmission losses, the proportionate yield per unit catchment area of overland flow is much higher than the channel flows. Often, rainfall in dry areas generates overland flow, but channel flow rarely occurs. Sparse vegetation, absence of developed soils and relatively steep topography create favorable conditions for high rate of overland flow in dryland catchments. The hydrological processes of rainfall and runoff drive erosion and sediment process. The process is initiated by free falling raindrops on bare soil that breakdown and detach the particles from soil mass and create surface crusting and sealing. Surface sealing reduces infiltration and causes rapid and high runoff rate downslope. The rapid runoff is largely generated as infiltration access in the form of sheet-flow, dominated by Hortonian overland flow. Sheet-flow transports detached soil particles at downstream, until kinetic energy of flow reduces and deposition starts.

Although, the overland flow is usually analyzed as a broad sheet flow, it often concentrates in many small definable channels called the rills (Foster, 1971). Erosion caused by flow in rills is called rill erosion and erosion on areas in between rills is called inter-rill erosion (Meyer *et al*.1975b). Both rill and inter-rill are overland flow rated processes, denoted by upland erosion. Rills discharge the runoff into gullies or streams. The flow in dryland streams is ephemeral, occurring only for a short period during and after rainstorms, hence fluvial process especially, the magnitude and frequency of their operation differs considerably from humid regions (Graf, 1988; Thornes, 1994). Another important feature of the dryland catchments is low runoff threshold, which reflects low on-site infiltration. Due to low and erratic precipitation in drylands, ephemeral or intermittent streams are common. Floods are also not uncommon in drylands and can occur during the rare period of prolonged and excessive rainfall.

A hydro-sediment process involves several factors (Fig. 2.1). Spatial and temporal variations in behavioral interactions among these factors (rainfall, infiltration, overland flow, ponding and erosion and sedimentation) add complexity, which are reflected in this natural system process in real world.

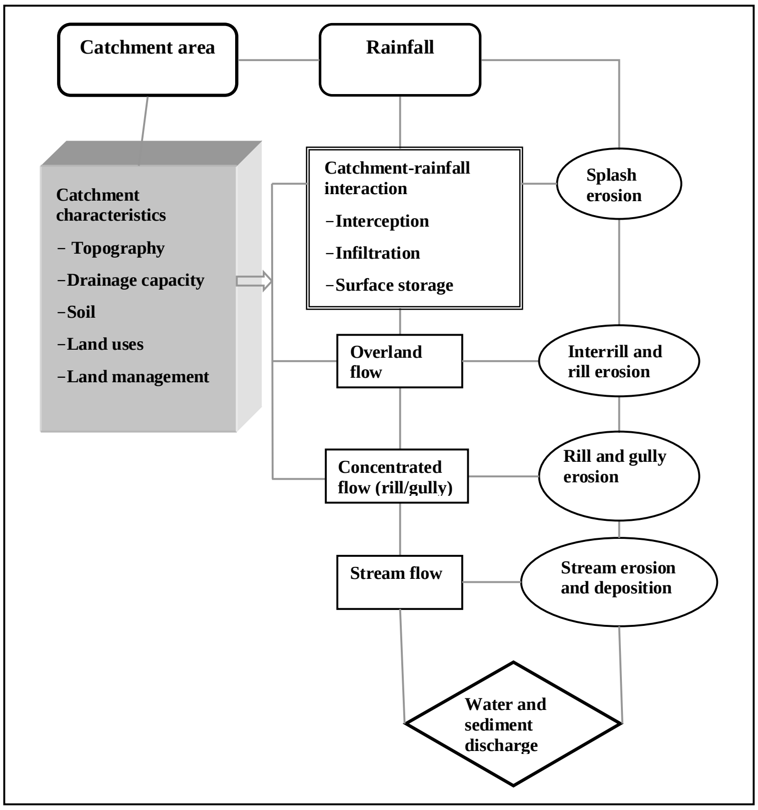

Figure 2.1. A Flowchart Showing Hydro-sediment Processes

2.3 Runoff Generation Mechanisms and Assessment Methods

Two different mechanisms generate runoff. The first, defined by Horton (1933), says that runoff develops when rainfall intensity exceeds the infiltration rate of the soil. Hence, surface runoff occurs before the soil has become fully saturated. The second mechanism proposed by Dunne and Black (1970a) describes that runoff develops when the volume of water exceeds the storage capacity of the soil. This mechanism dominates in areas of shallow groundwater. Horton method is more appropriate for upper slopes and Dunne and Black is more suitable for areas near drainage channels (Freeze 1982). In dryland catchments, where groundwater is deep, runoff development follows the Hortonian flow. Runoff occurs as a result of rainfall in excess to initial abstractions (retentions, infiltration) at a point and routing of rainfall excess by catchment actions. Rainfall and soil characteristics at a particular location greatly influence the rainfall excess or local runoff and catchment characteristics shape the direct runoff hydrograph at the outlet point. The subsequent sections present the mechanisms and methods that describe the rainfall excess and direct runoff.

2.3.1 Rainfall

Rainfall is a basic input parameter in runoff production. In arid environments, the rainfall variability and seasonality play a key role in the exploitation of water resources. As compared to temperate regions—standard deviation of annual rainfall is about 10–20% and annual amounts are between 75% and 125% of the mean, the annual rainfall variability in arid climates ranges between 40% and 200% of the average annual rainfall in 19 out of 20 years with mean annual rainfalls of 200–300 mm. For 100 mm mean annual rainfall, it can vary between 30% and 350% (FAO, 1981). Seasonal variability and frequent dry spells of variable lengths are often observed between rainstorms.

Spatial variability of the annual rainfall is also high. Often, point rainfall at one gauge is not observed at neighboring rain gauge. Areal extent of rainfall in mountainous regions is much smaller and the localized nature of storms is very significant. For example at Yangping station in northern Shanxi province in China, the measured 12-h rainfall was 408.7 mm on 25 July 1971, while 24-h, 31.7 mm rain was observed at about 20 km away at the Taihezai station (Lin, 1999). The observations in Mediterranean climate in Qaryatein hilly area in Syria during this study period showed that rainfall greatly varied within 10–15 km distance. Rainfall localization was very prominent in some extreme cases, when one rain gauge at about 15 km distance missed the entire storm. Sharon (1972) showed that spatial distribution of rainfall produced from convective storms cluster in core area of 1 to 5 km in diameter and reduced to zero over a distance less than 10 km. About 96% of rainfall events at a station were representative of an area of 2.5 km^2 surrounding a rain gauge in the semi-arid Southwestern USA (Murphy *et al.* 1977 quoted Dorroh, 1960).

Event rainfall depth, which is partly consumed in initial abstraction before runoff begins, is also important for runoff production. Initial abstractions for semi-arid climates in Southwestern USA: 6.6 mm (Kincaid et al., 1963), 12.7–17.8 mm (Murphy *et al.* 1977 quoted Dorroh, 1960), 8.1 mm (Fogel and Duckstein, 1973). For Israel: 3–4 mm for dry soil surface, approximately half that for wet surface; for sandstone 0.37 mm (Bryan et al., 1978), 1–2 mm for solid rock and 3–5 mm for stony soil surface (Yair *et al.* 1978). The highest threshold value of rain was determined as 5 mm for stream beds in Israel (Yair and Klein, 1973). Tenbergen (1991) showed that 3–5 mm of rainfall can generate runoff in Negev desert.

Rainfall intensity is another parameter that influences the runoff. Five-minute intensity is considered as maximum followed by 10, 15, 20, 30 minutes or entire rainfall duration, which makes the comparisons difficult. Determining the threshold rainfall intensity may be more difficult than the rainfall depth (Taur and Humborg, 1992). Rainfall duration is equally important in runoff generation. For West Africa, where rainfall intensity rarely lasts longer than 30 minutes (Chevallier *et al.* 1985), even in small catchment area, the entire catchment is unlikely to contribute to the runoff in channels. This shows the complexity of rainfall effect on runoff. The intensity of rare storms is always high, especially in the case of short duration storms. Fogel (1969) reported the effects of storm rainfall variability on runoff from small watersheds in the Southwest USA. Obsorn and Lane (1969) studied the relative sensitivity of rainfall variables and watershed characteristics on runoff from intense, short duration thunderstorm rainfall. They found that for four small watersheds (of less than 5 ha) runoff volume was strongly correlated to total rainfall, peak runoff rate was best correlated to maximum 15-minutes rainfall, flow duration was best correlated to watershed length and that lag time was best correlated to watershed area. Wei and Larson (1971) showed the effect of areal and time distribution of rainfall on runoff hydrographs from a small watershed in Southern Minnesota.

Rainfall coverage of catchment area plays key role in runoff generation. Partial area concept of runoff generation (Betson, 1964) offers opportunity to incorporate heterogeneity of catchment area in space and time, was originally developed for humid climate, but can also be applied to semi-arid and arid environments (Arteaga and Rantz, 1973; Yair and Lavee, 1974; Yair *et al.* 1978). The effective rainfall from certain partial area of catchment undergoes translation and retention effects of catchment and channels, reaches the outlet with certain time delay depending on the characteristics of catchment and the channel. Interflow is important for humid areas (Hewlett and Hibbert, 1967), but is missing or play subordinate role in semi-arid or arid regions.

Wind velocity affects the runoff—if wind direction coincides with direction of main valley slope, rainfall more or less moves parallel to the runoff and thus produces higher peak discharge, while the rain moving in opposite direction produces low runoff. Wind direction also influences the angle of rainfall. A lower rainfall amount reaches the ground if the angle of the rainfall follows the slope of incline (Yair *et al.* 1978).

2.3.2 Catchment Area

Size and shape of catchment area are important governing factors for runoff generation including peak discharge, time to peak, runoff volume and water harvesting potential (Taylor and Schwarz, 1952; Benson, 1962; Gregory and Walling, 1968; Alexander, 1972). Dominant effect of size of catchment area on runoff resulting from heavy rainfall in semi-arid regions was also emphasized by Puech and Chabi-Gonni (1984b) for West Africa and by Murphy *et al.* (1977) for

Southwestern USA. However, most of the times, the catchment area-runoff relationship is non-linear. Both runoff rate and peak runoff decreases with increase in catchment size (Renard and Keppel, 1968; Foggel and Duckstein, 1973; Wallace and Lane 1976). Increase in retention losses with catchment size and translation losses are the main causes for this reduction. It is generally accepted that runoff efficiency decreases with the increase in catchment area. Stern (1979) inferred that under the same hydrological conditions, a runoff equal to 50% of incident rainfall may be expected from a small area as compared with the river basin where it hardly reaches to 5% of the rainfall. Catchment slope has positive effect on runoff. Rodier and Ribstein (1988) showed that an increase in slope from 0.5% to 5% can increase runoff coefficient by 25–30%. The effect of catchment shape on runoff is generally known qualitatively that elongated catchment area produces elongated hydrograph, whereas circular catchments produce more compact runoff hydrographs. Table 2.1 shows some shape indexes that have been used in rainfall-runoff modeling.

Table 2.1. Some Catchment Shape Factor Indexes that Effect Runoff (Compiled from Taur and Humborg, 1992).

Description	Functions	Reference
Compactness index	$K_c = \frac{C}{2(\pi A)^{0.5}} = \frac{0.28C}{A^{0.5}}$; where, K_c is compactness index (dimensionless), C is circumference of catchment area (km) and A is size of catchment area (km^2). K_c is 1 for circular catchment area.	Horton (1932)
Circularity index	$RC = \frac{A}{A_c}$; where, RC is circularity index (dimensionless), A is catchment area (km^2) and A_c is circular area with same circumference as catchment area km^2).	Gray (1961)
Length of the Equal area rectangle	$L = \frac{C}{4} + \left(\frac{C^2}{16} - A\right)^{0.5}$; where, L is length of equal-area rectangle (km), C is circumference of catchment area and A size of catchment area (km^2)	Roche (1963)
Length-width ratio	$F = \frac{A}{L_c^{\,2}}$; where F is length-width ratio, A is size of catchment area (km^2) and L_c is maximum channel length (km)	Horton (1932)
Elongation index	$RL = \frac{D}{L'}$; where, RL is elongation index, D is diameter of circle having the same area as the catchment area (km), L' is maximum length of the catchment area parallel to the main channel (km)	Gray (1961)

2.3.3 Main Abstraction and Rainfall Excess

Rain after falling on land surface is transformed into runoff through a process of interception, infiltration, retention and evapotranspiration that altogether are referred as abstractions. These abstractions depend on catchment characteristics, climate, land use and management practices. Vegetation type, density and growth, rainfall intensity and wind speed affect the amount of interception. A dense forest may intercept 25% of annual rainfall and 10 mm from event rainfall, but it can be considerably low for mixed type cover (Hann *et al.* 1994). In dryland catchments, where vegetation is sparse, interception may form an insignificant proportion of total abstraction.

Surface storage and detention result from build-up depth of sheet flow to begin surface runoff. Terstriep and Stall (1974) recommended 5 mm for detention storage for bluegrass turf. Wright-McLaughlin Engineers (1969) in a study of urban hydrology in Colorado recommended the values of surface storage for impervious area as 1.3 mm for sloping roofs and 2.5 mm for flat roofs and large paved areas and for pervious area as 7.6 mm for lawn grass and 10.1 mm for open fields. Linsley *et al.* (1949) recognized that runoff begins after filling of small storages, when relatively larger storages still continue to fill. An exponential relationship between volume of water in surface storage and available surface storage, is given in the form of

$$V_d = S_d[1 - e^{-k_d(P-F)}] \tag{2.1}$$

Where, V_d is volume of water in surface storage, S_d is available surface storage, P-F is the accumulated mass of surface storage supply (accumulated rainfall minus infiltration and other losses except surface storage) and K_d is a constant (see more detail in Hann *et al.* 1994, pp 53).

Evapotranspiration is a combination of evaporation from soil surface and transpiration from vegetation. It forms a large fraction of annual rainfall. In arid climate, most of the rainfall, 90% or more may be lost through evapotranspiration. In more humid climates, it may account 40–70% of annual precipitation (Hann *et al.* 1994).

Infiltration forms an important component of abstractions from rainfall and depends on soil properties, rainfall characteristics, land slope, vegetation and antecedent moisture conditions. Characteristics of only the soil surfaces in semi-arid regions affect the variation of surface runoff more than do the rainfall characteristics (Bryan et al., 1978), although its verification is difficult (Betson and Maurius, 1969) due to variability of soil characteristics in space (horizontally and vertically) and time. Intensive rainstorm can produce quick runoff allowing low infiltration. Raindrops on bare soils by breaking down of soil aggregates seals surface and reduce infiltration. Steep topography through increased sheet flow velocity, discourages infiltration. Antecedent moisture conditions also affect the infiltration rate (Scoging and Thornes, 1979). However, in arid climate with longer dry period between rainfall events and wetting of top few centimeters—upper 2 cm (Blanchard et al., 1981), the effect of antecedent moisture on runoff can be very low. Osbern and Renard (1973) showed the effect of antecedent moisture conditions on runoff, which was not increased by 10% in semi-arid Southwestern USA. Vegetation density also increases the infiltration as well developed root system causes higher infiltration rates (Linsley *et al.* 1958; Kincaid *et al.* 1963). Land use practices also affect the infiltration rate. Albergel (1988) inferred that the cultivated areas in Sahel zone have higher infiltration rates than do the fallow, untilled areas. Combination of all these factors governs infiltration. The infiltration at some locations can be too high to produce surface runoff. However, low infiltration in some other areas can generate surface runoff even from light rainfall and are called runoff source areas (Betson, 1964). Many infiltration loss models for estimation of rainfall excess from a rainfall event have been presented in literature on hydrology (for example, Chow *et al.*, 1988; Hann *et al.*, 1994; USACE-HEC, 2000). These models can be classified on empirical and theoretical basis, whereas most common infiltration loss models are given in Annex A-1.

2.3.4 Transformation of Rainfall Excess into Direct Runoff

Two methods of transformation of rainfall excess into direct runoff are presented. A unit hydrograph is an empirical model that attempts to establish a casual link of runoff and rainfall excess without detailed consideration of the internal processes. The equations and parameters of the models have limited physical significance. Kinematic wave model of overland flow can describe the physical mechanism that governs the movement of the rainfall excess over the land surface and in small channels in a catchment (USACE-HEC, 2000).

2.3.4.1 Unit Hydrograph Approach

A hydrograph is graphical representation of stream flow with time at a location. It can comprise of the surface, sub-surface and base flow. In dryland catchments, surface flow generally constitutes hydrographs as sub-surface and base flow components are greatly missing. Catchment, land use and rainfall characteristics interact together to shape up a hydrograph. A hydrograph can be described by three main components; rising limb, crest segment or peak and recession limb. A unit hydrograph is a direct runoff hydrograph resulting from one unit (1 inch or 1 cm) of rainfall excess generated uniformly over the drainage area at a constant rate for an effective duration (Chow *et al.*, 1988). It can be used to derive a runoff hydrograph from any amount of rainfall excess by using simple linear model principle. Following basic assumptions are made in the derivation of a unit hydrograph.

i. A unit hydrograph is a lumped response of a catchment at its outlet. The excess rainfall and losses are treated as basin-average quantity.
ii. The direct runoff hydrograph resulting from a given increment of rainfall excess is independent of time of occurrence of the rainfall excess or whatever may the season of the year (assumption of time invariance).
iii. The ordinates of direct runoff hydrograph corresponding to rainfall excess of given duration are directly proportional to the volume of rainfall excess (assumption of linearity).
iv. The rainfall excess has a constant intensity within the effective duration.
v. The rainfall excess is uniformly distributed over the entire drainage area.

vi. The base time of the direct runoff hydrograph resulting from rainfall excess of given duration is constant.

vii. Since a unit hydrograph results from rainfall excess, the antecedent or subsequent storm conditions have no action in its derivation.

A unit hydrograph of a catchment can be developed from observed rainfall hyetograph and runoff hydrograph data at outlet of a gauged basin or it can be determined by using catchment parameters. The latter is known as synthetic unit hydrograph. The synthetic unit hydrograph can be divided into conceptual and empirical models of runoff (USACE, 1994). Single-linear Reservoir, Nash and Clark models are conceptual, where Snyder and SCS dimensionless are empirical models. These models, their basic concepts, development and uses are discussed in literature on hydrology (for example, Chow *et al*. 1988; Hann *et al*., 1994; USACE-HEC, 2000; Patra, 2002; Mays, 2004). Snyder's and SCS dimensionless unit hydrographs have been widely used and are given in Annex A-2.

2.3.4.2 Overland Flow and Kinematic Wave Model

Overland and channel flows are the two main types of surface runoff. It generates when inflow and /or rainfall at a place exceeds the infiltration and travels some distance before reaching a rill or channel (Emmett, 1970). Ponce (1989) defined overland flow as surface runoff that takes place in the form of sheet flow on the land surface without concentrating in clearly defined channel. Overland flow can be characterized by the flow depth varying between 10 and 100 mm as compared with the flow depth in rills, which may vary between 10 and 50 cm. Shallow depth and hydraulic boundary roughness combined with wind and rain actions cause frequent change in overland flow depth and make it heterogeneous. It adds complexity, which is normalized by assuming overland flow as a shallow sheet of average depth (Huggins and Burney, 1982). Figure 2.2 shows an overland flow element. Kinematic wave model can describe overland flow.

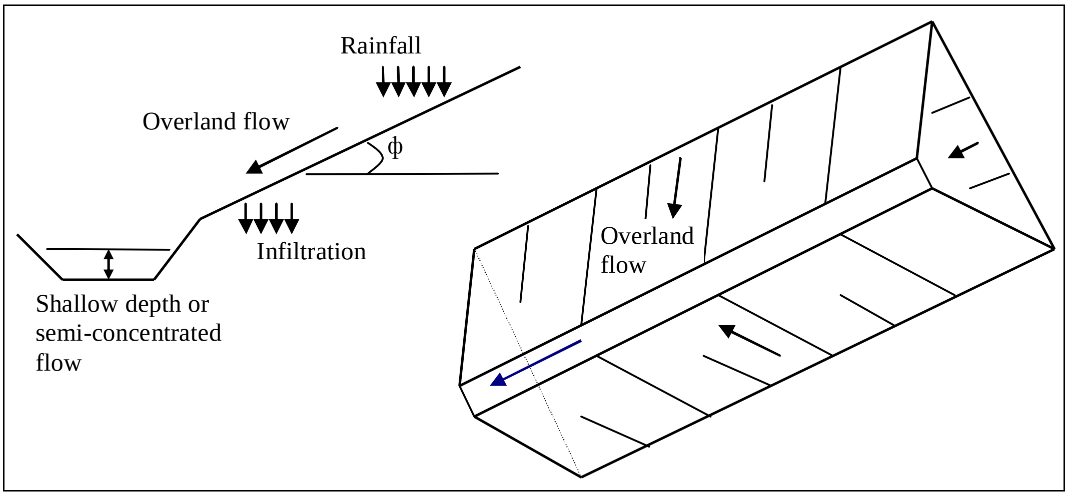

Figure 2.2. Definition Sketch of Overland Flow

A kinematic wave model is simplification of Saint-Venant equation. It has the advantages of offering analytical solutions of simple geometries and flow boundary conditions. The model can be derived from the continuity and momentum equations as described by Chow *et al.* (1988).

$$\frac{\partial Q}{\partial x}+\frac{\partial A}{\partial t}-q=0 \tag{2.2}$$

$$\frac{1}{A}\frac{\partial Q}{\partial t}+\frac{1}{A}\frac{\partial}{\partial x}\left(\frac{Q^2}{A}\right)+g\frac{\partial y}{\partial x}-g(S_0-S_f)=0 \tag{2.3}$$

Where, Q is flow rate, q is lateral inflows, A is cross-sectional area, g is gravitational acceleration, x is distance along the flow path, y is water depth and S_0 and S_f are the bed and frictional slopes, respectively. Equation (2.3) is conservation form of the momentum equation, where the first term is called local acceleration, the second convective acceleration, the third pressure force term, and the fourth and fifth is gravity and friction force terms, respectively. The non-conservation form of the momentum equation is:

$$\frac{\partial v}{\partial t} + v\frac{\partial v}{\partial x} + g\frac{\partial y}{\partial x} - g(S_0 - S_f) = 0 \tag{2.4}$$

Kinematic wave equation
Diffusion wave equation
Dynamic wave equation

Where, v is flow velocity. Equation (2.4) contains four terms. The fourth term alone of equation (2.4) is called kinematic wave equation, terms third and fourth together as diffusion wave equation and four terms altogether called dynamic wave equation. The momentum equation can also be expressed in the form of

$$A = aQ^b \tag{2.5}$$

Where, A and Q are previously defined and a, b are constants. Differentiation of equation (2.5) in time, results in

$$\frac{\partial A}{\partial t} = abQ^{b-1}\frac{\partial Q}{\partial t} \tag{2.6}$$

Combining continuity equation (2.2) with equation (2.6) yields in equation with one variable.

$$\frac{\partial Q}{\partial x} + abQ^{b-1}\frac{\partial Q}{\partial t} = q \tag{2.7}$$

Equation (2.7) being a one-variable can be solved for Q, given that values of α and β are known. The value of α and β can be computed from Manning equation of flow, which can be written as

$$Q = \frac{1}{n}\sqrt{S_0}\,\frac{A^{\frac{5}{3}}}{P^{\frac{2}{3}}} \tag{2.8}$$

Where, Q, S_0 and A are already defined, n is Manning roughness coefficient and P is wetted perimeter. Manning equation (2.8) can be rearranged as

$$A = \left[\frac{nP^{\frac{2}{3}}}{\sqrt{S_0}} \right]^{\frac{3}{5}} (Q)^{3/5} \tag{2.9}$$

Comparing equation (2.5) with equation (2.9) yields

$$a = \left[\frac{nP^{\frac{2}{3}}}{\sqrt{S_0}} \right]^{(0.6)} , b = 0.6 \tag{2.10}$$

Knowing the values of α and β, the equation (2.7) can be solved for Q and provides the solution of kinematic wave equation. It is physical based formulation, which can take distributed effects of overland flow and has strong theoretical base.

2.4 Soil Erosion by Water

2.4.1 Erosion Perspective

Soil erosion adversely affects land productivity at site and its transport and deposition can cause stream's malfunctioning and flooding, reduction in reservoir's capacity and water quality degradation at downstream. An annual global loss of agriculture land was three million ha due to soil erosion and two million ha due to desertification (Buringh, 1981). The off-site damages caused by sediment in the United States were estimated at 6 billions US$ annually (Clark, 1985). Since the beginning of the settled agriculture, soil erosion has destroyed about 430 million ha of productive land worldwide (Kovda, 1983). Vogel (1990) reported that in Haraz, Yemen, water-erosion reduces the soil depth by 1–3 cm yearly. Young (1969) quoted annual rate of soil loss under natural conditions from 0.0045 Mg per ha for areas of moderate relief to 0.45 Mg per ha in areas of steep relief as compared with agriculture land, which ranged 45 to 450 Mg per ha. However, the severity of soil loss is theoretically judged among others the rate of soil formation. Langbein and Schumm (1958) showed that erosion reaches a maximum in areas of effective mean annual rainfall of 300 mm. Over 300 mm annual rainfall, the development of vegetation cover provides protection, when below 300 mm, the soil erosion is reduced due to less numbers of erosion producing runoff events. Morgan (1995) compiled annual rates of soil erosion from many sources for some selected countries (Table 2.2).

Table 2.2. Annual Rates of Erosion in Some Countries (Source: Morgan, 1995)

Country	Rate of soil erosion (Mg ha^{-1} yr^{-1})		
	Natural	Cultivated	Bare soil
China	0.1–2	150–200	280–360
USA	0.03–3	5–170	4–9
Australia	0.0–64	0.1–150	44–87
Ivory Coast	0.03–0.2	0.1–90	10–750
Nigeria	0.5–1	0.1–35	3–150
India	0.5–5	0.3–40	10–185
Ethiopia	1–5	8–42	5–70
Belgium	0.1–0.5	3–30	7–82
UK	0.1–0.5	0.1–20	10–200

Dudal (1981) reported that current rate of agricultural land degradation by soil erosion and other factors is leading to annual irreversible loss of productivity on about six million ha of fertile land, worldwide. Soil erosion is among the most critical environmental hazards of modern times. There is a need for more basic research to generate data that are accurate, reliable and obtained by standardized methods (Lal, 1994). Also, there is a serious lack of information on the most basic issues, on the actual degree of soil erosion and full extent of its consequences (ISNAR 1992).

2.4.2 Water-erosion Mechanism and Process

Cohesion among individual particles in a soil-mass provides binding force to these particles. Soil-mass resists the external disturbances through the cohesion force. Whenever falling energy of raindrops increases the cohesion force of the particles, it detaches and displaces the hit particles from the mass. Weathering and rainfall actions further disintegrate the detached particles. Once a particle is separated and disintegrated, it can easily be transported by running water. Overland flow carries the detached particles and continues to concentrate along shallow-wide paths. As rainfall continues, the flow along these paths also continues to concentrate and gain more energy. The concentrated flow detaches and picks soil particles from its flow path to its carrying capacity. The scouring along this developed path continues till sediment load balances the sediment carrying capacity of the flow. The continuous scouring creates small channel on the soil surface (Moss *et al.* 1982). More flow converges, if process continues and results in a relatively clearer channel called rill. Any flow entrainment that occurs in these channels is called rill erosion (Foster *et al.* 1985). The non-rilled area, which largely contributes to rill can be divided into: i) upper-catchment area drains downslope to the rill, and ii) interrill area that drains towards the rill and may not necessarily follow downslope. The interrill area largely contributes sediment to rills (Foster, 1982). The detachment, transport and deposition of the sediment are three integral parts of soil erosion process (Rose, 1985).

The severity of erosion depends on the quantity of detached material, which works as supply and carrying capacity of the running water. Erosion progresses, if carrying capacity of flow is higher than the sediment supply by detachment. Deposition starts when the sediment supply exceeds the flow carrying capacity. Erosion-causing energy takes two forms: potential energy ($PE = mgh$) and kinetic energy ($KE = ½\, mv^2$). Most of this energy is dissipated in friction with the surface over which the particles moves so that only 3–4% of energy of running water and 0.2% of that of falling raindrops is expended in erosion (Pearce, 1976). Morgan *et al.* (1986) based on over a 900-day of soil loss measurement in England on an 18% slope on a sandy soil, showed that transport across a centimeter width slope amounted to 19,000 grams of sediment by rills, 400 grams by overland flow, and 20 grams by rain-splash. Soil erosion by concentrated flows in rills and gullies mostly depends on their carrying capacity, which is a combination of boundary resistance forces, residual kinetic energy and energy due to channel or friction slope. Depending on the type of actions, natural and human-induced factors can accelerate or reduce erosion.

The study site contains 24 gullies in 100 ha area. Twenty one gullies start as rills and develop into gullies within the study site. However, three gullies generate in upper catchment area and pass through the study site. MCWH, because of capturing sheet-flow can directly affect the inter-rill and rill erosion, which is the main focus of this study. Nevertheless, due to lack of clarity between end point of rill and start of gully, some of these gullies may receive indirect impact of MCWH. Therefore, literature on gully development and assessment has also been reviewed here.

2.4.3 Splash Effect and Particle Detachment

Falling raindrop hits the soil surface causing consolidation, breaking down the coarse aggregate and creating a small cavity. The interaction of raindrop and soil surface transforms vertical compressive stress of the drop into lateral shear stress that jets the soil particles away from the center of the cavity (Sharma, 1996). The disruptive effects on sloping land create locally flowing jets with almost double the velocities of raindrops (Huang *et al*., 1982). Detachment occurs when the shear stress of flow exceeds the tensile strength of the soil particles. Laboratory experiment showed that 3.5 to 6.2 mm drops falling from 0.7 to 6.2 m, the measured stress ranged from 2 to 6 MPa (Ghadiri and Payne, 1981). Kinetic energy ($KE = ½ mv^2$) and momentum (mv) are the most used erosivity parameter for single water drops. Sharma and Gupta (1989) showed that the threshold kinetic energy or momentum exists before the detachment process is initiated by raindrop impact. Many soil variables including soil texture, organic matter, bulk density, water potential, aggregate size and shear strength influence the splash. Al-Durrah and Bradford (1981) proposed a simple relationship between splash weight and a linear function of the ratio of water drop kinetic energy to soil shear strength.

The movement of the detached soil particles by raindrops follows a trajectory path to a distance variable along and against the slope. Splash produces random particles movement in all directions; however, net transportation of the sediment is influenced by the slope or wind. Although theoretically valid, but practically this component of particle detachment is almost insignificant due to the low shear stress of sheet-flow (in a range of 'Pascal') as compared with the tensile strength of the soil particles (usually in the range of kilo-Pascal) (Nearing 1991). For interrill erosion prediction purposes, the detachment of soil by shallow overland flow alone is assumed negligible (Foster, 1982).

2.4.4 Interrill Erosion

Erosion on areas between rills and at upper part of rill head is referred as interrill erosion. It also includes areas that directly drain at the head of a rill. Interrill erosion process consists of i) transport of detached particles, ii) detaching the soil particles during concentration of flow along poorly defined paths, and iii) deposition of the particles. Transport of the detached particles includes the transport by raindrops (splash erosion) and transport by flow (sheet erosion or wash erosion). The quantity of the splashing particles decreases with the increase of runoff depth on the surface. Moss (1988) showed that splash effect was almost negligible on a runoff covering surface by a depth of about 2 mm. As the runoff starts, the sheet-flow carries the loose or detached particles in the direction of downslope. Governed by the slope and roughness, the sheet-flow can only transport small-sized particles mainly in suspension. Coarse particles are not transported till the action of raindrops causes their breakdown or carried away by splash impact of the drop. The sediment starts deposition as the transport capacity of the sheet-flow reduces due to friction induced by surface roughness. Decreasing slope steepness, vegetation barrier or human-induced factors can be the main causes of increased surface roughness. Depending on the depth of flow and the extent of rain-induced flow transport, the process of deposition is highly selective and the rate of deposition is indirectly proportional to the velocity of flow and directly related to the concentration and density of given sediment size (Hairsine and Rose, 1991).

2.4.5 Rill Erosion

Rill is small and intermittent water courses that can be removed by conventional tillage methods. Rill erosion is referred as detachment and transport of soil particles by concentrated flow. Studies on the hydraulic characteristics of the flow show that change from overland flow to rill flow passes through four stages:1) un-concentrated channel flow, 2) overland flow with concentrated flow paths, 3) micro-channels without headcuts, and 4) micro-channels with headcuts (Morgan, 1995). The first and second stage show clear difference. The flow regime changes from sub-critical to super-critical at point of rill initiation (Savat, 1979). The overall change in flow conditions through the four stages seemingly takes place smoothly as the Froude Number increases from about 0.8 to 1.2 (Torri et al, 1987; Slattery and Bryan, 1992). Success has been achieved in relating rill initiation to the exceedance of critical shear velocity of runoff. Govers (1985) found that sediment concentration in the flow increased with shear velocity more rapidly once a critical value of about 3.0–3.5 cm s^{-1} is achieved. This critical shear velocity of 3.5 cm s^{-1} applies to non-cohesive soils. For other soils excluding soil with high clay contents, Rauws and Govers (1988), proposed that critical shear velocity (u_{*cr}) for rill initiation is linearly related to the shear strength (τ_s) of the soil.

$$u_{*cr} = 0.89 + 0.56t_s \quad (2.11)$$

Brunori *et al*. (1989) presented a similar relationship

$$u_{*cr} = 0.9 + 0.3t_s \quad (2.12)$$

Govers (1992) found experimentally that the flow velocity in rills could be related to discharge by

$$v = 3.52Q^{0.294} \quad (2.13)$$

Theoretical basis of water erosion at rill and interrill scales are given in Annex A-3.

2.4.6 Surface Crusting and Sealing

Crusting of soil surface and sealing reduce infiltration and induce runoff and soil erosion. Rainfall (amount, intensity, raindrop kinetic energy) and soil properties (texture, structure, clay contents, mineralogy and cationic composition of the exchange phase), sediment deposition and vegetative cover are main governing factors in surface crusting and sealing. Wischmeier and Smith (1951) found that larger the drop size, higher is the final velocity and higher the rainfall intensity, higher the percentage of large drops. The rate of seal formation was found to depend on median drop diameter and rain intensity (Ellison, 1947). Some studies have also related rain drop kinetic energy (KE) to the seal formation. Agassi *et al.* (1985) showed that when soil was exposed to drops with KE below 0.01 J $mm^{-1}m^{-2}$ (fog-type rain), no seal was formed. But a seal with a very low permeability was formed when the KE of rain was 23.0 J $mm^{-1}m^{-2}$ (KE of high-intensity rainstorm). Increasing clay content in soil tends to increase their structural stability. Clay particles act as cementing material binding the particles together in the aggregates (Kemper and Koch, 1966), thus aggregate stability against the impact action of the raindrops should also increase with an increase in clay content and increasing clay content should result in less erodibility.

Change in infiltration rate from high at initial stage to a constant rate afterwards, causes drop in water energy, deteriorate soil structure and leads to partial sealing of the soil profile. It is well-known that seal formation at the soil surface predominates in the decrease of infiltration during rain (Duley, 1939; Epstein and Grant, 1973; Morin and Benyamini, 1977). Agassi *et al.* (1981) suggested i) physical disintegration of soil aggregates and their compaction due to raindrop impact and ii) chemical dispersion and movement of clay particles into a region at 0.1–0.5 mm depth, where they lodge and clog the conducting pores, as the complementary mechanism of seal formation. On non-arable lands, which are not subjected to frequent disturbances as of agricultural lands, crust sealing continue to strengthen with time under the action of rainfall. Owing to this phenomenon, non-arable lands allow less infiltration and generate higher runoff and soil losses.

Surface crusting is classified as structural crust (characterized by in-situ rearrangement of soil particles without a distinct evidence of lateral movement), erosion crust (results from soil erosion) and depositional crust (characterized by sediment sorting as a result of deposition process). The effect of water-erosion on crust formation process varies with topography, soil texture and erosion intensity itself. On the other hand, the surface crusting has pronounced effect on soil erosion. Bristow *et al.* (1994) noted that surface sealing or crusting altered the way water was partitioned at soil surface, resulting into decreased infiltration and increased overland flow. Overland flow concentration instigates the soil erosion at a faster rate. Generally, the process beginning with the formation of soil crusts precede to runoff and an increase in soil loss through erosion (Visser and Leenders, 2004). However, in the case of wind erosion, Chepil (1953) estimated that erosion rate at the crusted soil was approximately 6–60% lesser than the erosion rate at freshly cultivated field. Largely, both surface crusting and water-erosion complement each other interactively, whereas surface crusting reduces the wind erosion.

2.4.7 Other Main Factors Affecting Interrill and Rill Erosion

Erosivity (a measure of impacting force of raindrop), detachability (tendency of soil-matrix yields to raindrop impact) and transportability (capability of flow to overcome the shear stress or surface roughness) influence the erosion and deposition in area contributing a rill. The erosivity of raindrop and flow depends on many factors such as size of raindrop, kinetic energy, intensity of rainfall, overland flow depth and velocity, ground slope and surface cover and roughness. Kinetic energy, because of representative of raindrop size and impact velocity, is commonly used as a measure of raindrop erosivity. The total energy of a rainfall event is simply a summation of kinetic energies of individual raindrops combined with drop-size information.

Depth of sheet-flow on surface provide cushion to the impact of raindrop and reduces its impact. The greater the flow depth, the smaller will be the detachment rate. Palmer (1965) observed that detachment and transport by raindrops increased to a flow critical depth (y_c), approximately equal to the drop diameter (d), but decrease sharply as the flow depth (y) increases beyond critical depth (y_c). Mutchler and Young (1975) suggested that $y \geq 3d$ essentially eliminated detachment by raindrop impact.

Velocity is an indicator of carrying capacity of flow and influences the sediment transport. Moss (1988) showed that transport rates tend to vary linearly with flow velocities. Surface roughness also helps in reducing the flow velocity thus decreasing the potential of sheetflow erosion.

Local slope, either natural or manmade, has direct effect on the erosivity of overland flow. The slope influences the stream power (product of hydraulic shear stress $\tau = gRS$ and average flow velocity v) (Nearing *et al.* 1991).

Surface cover directly intercepts the raindrops and dissipates their kinetic energy before they impact the soil surface. The type and height of the cover affects the energy dissipation potential. Shorter and bushy canopy may dissipate the energy of falling raindrops completely. On the other hand, taller canopies by reshaping and producing large-size drops may result in higher detachment efficiency than similar size raindrops falling at terminal velocity (Moss and Green, 1986; Sharma and Gupta, 1989).

Mulch reduces the soil erosion by protecting the land surface from direct raindrop impact and by reducing the overland flow velocity (Foster, 1982). By reducing surface sealing, the mulch also helps in infiltration. Increasing the surface roughness, increases the surface area and redistribute the raindrop impact resulting in a decrease in energy per unit area (Sharma, 1996).

Detachability of soil particles depends on the soil strength and aggregate stability, which are the function of aggregate size and density, amount and type of clay, organic carbon content and inorganic constituents such as iron, sodium, calcium and magnesium (Foster *et al.* 1985). Antecedent wet condition increases the soil strength (Kemper *et al.* 1987) and aggregate stability (Truman *et al.* 1990) resulting in less erosion.

The transportability depends on the flow energy, particle size and surface roughness. Fine (clay and silt) and course aggregates are the main constituents of the detached sediment. Course particles move on the surface as bed load given that flow energy is adequate for their movement. Aggregates settled down if the total energy is less than the energy required for their movement. Nevertheless, finer particles remain in suspension and move with flowing water to a farther distance till their fall velocity is higher than the flow velocity.

2.4.8 Universal Soil Loss Equation for Sheet and Rill Erosion

Universal Soil Loss Equation (USLE) (Wischmer and Smith, 1978) is the most widely used regression model for predicting soil erosion. It is an empirical equation that can estimate soil loss due to sheet and rill erosion (Simons *et al.*, 1982). The equation was developed from over 10,000 plot-years of runoff and soil-loss data, collected from experimental plots in 23 states by the US Department of Agriculture. A 22.13 m (72.6 ft) long plot on a 9% uniform slope in bare fallow soil and tilled to break surface crusts was arbitrarily selected to serve as a reference of evaluation. The equation predicts average annual soil loss. Mathematically, USLE is described by a number of factors given below.

$$E = R\,K\,LS\,C\,P \tag{2.14}$$

Where E is spatial and temporal average annual soil loss per unit area ($Mg\ ha^{-1}yr^{-1}$), R is rainfall erosivity factor, K is soil erodibility factor, L is the slope length factor, S is slope steepness factor, C is cropping and management factor and P is supplemental erosion control practices factor. *L, S, C* and *P* are dimensionless and E has a time period of R and soil loss dimension of K. Since K represents mean annual soil loss per unit of R, E has the same units as K. Thus, if K is in $t\ ha^{-1}$ for one unit of metric R, multiplication by metric R value will give the value of E in $t\ ha^{-1}$.

Rainfall-runoff erosivity factor, i.e. R-factor, quantifies the effect of raindrop impact and also reflects the amount and of runoff likely to be associated with precipitation events. The R-factor is calculated as total storm energy (E) times the 30-minute intensity (I_{30}), or EI_{30} and referred as Rainfall erosivity index. If E in foot-Mgs/acre and I_{30} is in in hr^{-1}, R in Imperial units is given by,

$$R=EI_{30}/100 \tag{2.15}$$

If E is in J/m^2 and I_{30} is in mm/h, R in metric units is given by,

$$R=EI_{30}/1,000 \tag{2.16}$$

Procedure for calculation of EI_{30} is given in literature (e.g. Chow *et al.* 1988; Wischmeier and Smith, 1978).

K, soil erodibility factor, is the rate of soil loss per rainfall erosion index unit or it is defined as mean annual soil loss per unit of *R* for referenced conditions (22.13-m long plot on a 9% uniform slope in bare fallow soil and tilled to break surface crusts). Wischmeier *et al.* (1971) found *K* as a function of percent of silt, percent of coarse sand, soil structure, permeability of soil, and percent of organic matter and developed monograph, which can be used with caution if measured data are not available.

Topography factor (*LS*) was defined as the ratio of soil loss from any slope and length to soil loss by referenced plot (22.13-m long plot on a 9% uniform slope in bare fallow soil and tilled to break surface crusts). Slope length was defined as the distance from the point of overland flow origin to the point where either the slope decreases to the extent that deposition begins or runoff water enters a well-defined channel. *LS* can be estimated from monograph (Wischmeier and Smith, 1978). Based on data for slopes between 3% and 20% and with length up 122 meters, Wischmeier and Smith (1965) proposed the estimation of the topographic factor *LS* by using the following empirical equation.

$$LS = \left(\frac{l}{72.6}\right)^{n}\left(\frac{430(\sin q)^{2} + 305.6q + 0.43}{6.613}\right) \tag{2.17}$$

Where, l is horizontal projection of slope length (not distance parallel to soil surface), 72.6 is RUSLE unit plot length in ft, q is slope angle and n is exponent depending on slope.

n = 0.3, for slope ≤ 3%

n = 0.4, for slope = 4%

n = 0.5, for slope ≥ 5%

The above values of *n* are indicative. Renard *et al.* (1997) suggested an improved method for estimation of value of *n*. Morgan (1995) proposed following equation to estimate the topographic factor *LS*.

$$LS = \left(\frac{x}{22.13}\right)^n \left(0.065 + 0.045S + 0.0065S^2\right) \tag{2.18}$$

Where *x* is slope length in meters, 22.13 is standard USLE plot length in meters and *S* is slope gradient in percent. The value of *n* can be estimated from Renard *et al.* (1997). Arnold et al., (1995) used the following equation to compute the topography factor *LS* in SWAT model.

$$LS = \left(\frac{l}{22.13}\right)^n \left(0.065 + 4.565S + 65.41S^2\right) \tag{2.19}$$

Where *l* is slope length in meters (22.13 m is standard USLE plot length) and *S* is slope gradient as percentage. They suggested calculating the value of *n* from the following function.

$$n = 0.6\left[1 - \exp(-35.835S)\right] \tag{2.20}$$

Cropping management factor *C* was defined as the ratio of soil loss from land cropped under specific conditions to corresponding loss from tilled, continuously fallowed ground. The factor ranges from approximately zero to 1.0 depending on the vegetation cover, crop season and other management practices. The value of *C* can be set 1.0 for bare soil and 0.001 for forest or dense shrub. The cropping factor *C* for various conditions is tabulated and referred to USDA, Agriculture Handbook No. 537 (Wischmeier and Smith, 1978).

The erosion-control practices factor *P* account for the effect of conservation practices such as contouring, strip cropping and terracing on erosion. It is defined as the ratio of soil loss using one of these practices to the loss due to using straight row farming up and down the slope. For straight farming or wild land, it is set to be 1.0 (no-erosion control practice). It decreases with interventions; for contouring 0.5, terracing 0.14 and tied ridging value of *P* varies between 0.1 and 0.2. Values for other conditions are given in USDA, Agriculture Handbook No. 537 (Wischmeier and Smith, 1978). Some limitations of USLE have been documented in literature (Simons et al., 1982; Morgan, 1995) that include,

- Rainfall factor *R* in the equation may vary significantly in different arid areas (intensity, duration, and thunderstorm). Further, the weathering process between two rainstorms can significantly influence the erodibility factor “K” by supplying easily erodible material. It estimates for individual storm and their summing over a year can be significantly different from the estimates on average annual basis and therefore should not be used for individual storm.
- One limitation of regression-type equations like USLE is that these do not take in to account the distributed effect of space and time, which means that the data for their development are restricted to certain collection period at specific locations and do not necessarily represent long term variations in the system.
- The USLE is designed to predict average annual soil losses by sheet and rill erosion on upslope areas such as farm land and construction sites. Its estimates do not include the contributions from gully erosion and land slides. It also does not consider the sediment loss and gain between the fields and streams or reservoirs. These items must be evaluated separately.
- The equation was developed from the data collected at small plots. Its use on larger areas should be made with caution.
- It was developed for a sediment load of 1 mm and finer. Soil erosion by larger sediment size should be considered separately.

2.4.9 Revised Universal Soil Loss Equation (RUSLE)

During a workshop on soil erosion in 1985, it was decided to update USLE by incorporating the considerable amount of erosion information that had accumulated since the publication of the USDA Agriculture Handbook 537 (Wischmeier and Smith, 1978) and to specifically address the application of USLE to land uses other than agriculture. This has resulted in fully computerized technology of RUSLE as fully described in USDA Agriculture Handbook 703 (Renard et al., 1997).

RUSLE accounts a wide range of land uses by incorporating many variables. Some researchers (Weltz et al., 1987; Renard and Simanton, 1990; Benkobi et al. 1993) mentioned that RUSLE underestimated the soil loss as compared with some other methods, but Renard (1999) stated that their method of evaluation, single storm simulations may or may not reflect an annual average as RUSLE is designed to estimate.

Renard *et al.* (1996), by comparing RUSLE with USLE see that RUSLE technology is superior to USLE, as it does allow application to the situation, which USLE technology cannot. Nevertheless, empirical basis of the model may not avoid uncertainties. Inadequate data to make the results verifiable may also reduce its reliability. Despite this weakness, the technology because of its enhanced capabilities of estimating *R*, *K* and topographic factors and support practices greatly improved its reliability in using it in the USA and in developing countries. RUSLE model has flexibility to use readily inbuilt available values of factors in database or modification addition in these values is also possible. The RUSLE predicts interrill and rill erosion from rainfall and associated runoff. It is a useful tool for conservation planning, inventory and assessment. However, soil loss values estimated by RUSLE should better be used for comparison purposes rather than being considered as absolutely accurate erosion rate. RUSLE computes the average annual interrill and rill erosion for landscape profiles. Its projection over an area depends on the representativeness of the landscape profile to that area. RUSLE does not compute sediment yield.

While comparing RUSLE with WEPP, it is seen that both RUSLE and WEPP have limitations of slope length. However, WEPP model is more complex in variables to be estimated. The users need to gather a great deal more on-the-ground information to use the model effectively, which may need a big deal of resources. The WEPP model has proven so complex in its application that RUSLE will remain the primary tool for estimating soil loss for the foreseeable future (Renard, 1999). RUSLE technology was developed over decades of research and field-testing by US

Federal Agriculture Agencies and the Universities, despite of its limitations, RUSLE is easy to use and the resources to apply it are generally readily available. It can provide useful information to examine how management practices influence range use and soil conservation (Jones, 2001). While it is likely that application of more complex models than RUSLE can provide more accurate estimates of soil erosion for specific sites, the data requirements of these models make them difficult to use on a regional scale. By comparison, the data for utilization of RUSLE can be relatively easy to obtain.

2.4.10 Modified Universal Soil Loss Equation (MUSLE)

It can be recognized from the above discussions that application of USLE is limited to soil loss. Williams and Berndt (1977) developed a procedure to compute sediment yield from a watershed. The procedure estimates sediment yield for single storm event. The modification suggests replacement of rainfall in USLE with runoff factor. The resultant equation is called as Modified Universal Soil Loss Equation (MUSLE). By virtue of its structure, the MUSLE is more applicable to arid regions. The equation is given below.

$$Y_S = a\left(Q_v q_p\right)^b KLSCP \qquad (2.21)$$

Where, Y_s is the sediment yield in Mg for a storm event. Q_v is runoff volume in acre-ft, q_p is peak runoff rate in cubic feet per second and a and b are coefficients. All other terms are previously defined. In MKS units, sediment yield Y_s, runoff volume Q_v and peak runoff rate q_p are represented in Mg, m^3 and m^3sec^{-1}, respectively. Soil and Water Assessment Tool (SWAT) (Arnold *et al.*, 1995) uses values of a and b as 11.8 and 0.56, respectively, for MKS system. Simons *et al.* (1982) suggested a procedure to estimate also annual sediment yield by using MUSLE. The procedure is as follows:

- Determine sediment yield for events of various return periods. Recommended return periods are 2, 10, 25, 50 and 100 years.

- The sediment yields are weighted according to their incremental probability, resulting in weighted storm average.
- Multiply weighted storm yield by the ratio of annual water yield to an incremental probability-weighted water yield.

For certain recommended return periods the computation can be followed by using following relationship.

$$A_S = \left[\frac{Q_A \left(0.01Y_{S100} + 0.01Y_{S50} + 0.02Y_{S25} 0.06Y_{S10} + 0.4Y_{S2} \right)}{\left(0.01Q_{V100} + 0.01Q_{V50} + 0.02Q_{V25} + 0.06Q_{V10} + 0.4Q_{V2} \right)} \right] \quad (2.22)$$

Where A_S is the annual sediment yield, Q_A is the average annual water yield, Y_S and Q_V are referred to single storm sediment and water yields respectively for respective return periods. The general form of the above equation is

$$A_S = \frac{Q_A \sum Y_S}{\sum Q_V} \quad (2.23)$$

One of the limitations of USLE and MUSLE methods is that these are generally applicable to wash load (sediment size less than one millimeter). Sediment transport theory is used for the situations where sediment size increases from one mm in order to estimate the total load, particularly in the channel. It requires knowledge of the hydraulic characteristics and sediment transport capacity of the streams and sediment size of bed load. It is assumed that the transporting capacity of material larger than one mm is controlled by the transport rate, while supply controls transport of smaller sizes. The transport capacity of the channel can be determined by combination of Meyer-Peter, Muller bed-load equation and Einstein integration for suspended load. The supply of smaller sediment is determined using MUSLE.

2.4.11 Gully Erosion

2.4.11.1 What is Gully?

Gullies are known by their key role to linking upland areas to regular streams, transferring runoff and sediment at downstream and causing mass erosion of adjacent lands. Gully erosion is defined as the erosion process whereby runoff water accumulates and often recurs in narrow channels and, over short periods, removes the soil from this narrow area to considerable depth (Poesen *et al.*, 2002). Gullies for agriculture land are often defined as channels too deep to easily ameliorate with ordinary farm tillage equipment, typically ranging from 0.5 m to as much as 25 to 30 meters (Soil Science Society of America, 1996). The term ‘ephemeral gully erosion’ was introduced in 1980s to emphasize the concentrated flow erosion larger than rill erosion, but smaller than classical gully erosion (Foster, 1986; Grissenger, 1996a, 1996b). Soil Science Society of America (1996) describes ephemeral gully as small channel eroded by concentrated overland flow that can easily be filled by normal tillage, only to reform again at the same location by additional runoff event. Hauge (1977) and Poesen (1993) used critical limit of the squared ft criterion of cross-sectional area (channel cross-sectional area of 1 ft^2 or 929 cm^2) to distinguish rill from gully. The other criteria include a minimum width of 0.3 m and a minimum depth of 0.6 m (Brice, 1966), or minimum depth of 0.5 m (Imeson and Kwaad, 1980). Despite of many efforts to classify hydraulically-related erosion (micro-rills, rills, mega-rills, ephemeral gullies, gullies) transition from rill erosion to ephemeral gully erosion to some extent remains subjective (Grissenger, 1996a, 1996b).

2.4.11.2 Gully Development

Gullies have been classified as ephemeral and permanent gullies, valley-head, valley-floor and valley-sides (Brice, 1966), V- and U-shaped gullies (Imeson and Kwaad, 1980) and axial gullying with single headcut, digitate gullying involving several headcuts and frontal gullying (with pedimentation) (De Poly, 1974). Poesen (1993) further subdivided ephemeral gullies according to width/depth ratio (w/d). According to him a wide ephemeral gully would be with $w/d > 1$ and cause significant crop damages. This gully type can cause a high percentage of soil loss by removing fertile top soil with high organic matter. Contrary to high damages wide and shallow gullies can be removed by conventional tillage. Narrow and deep ephemeral gullies with $w/d \leq 1$, cause little crop damages and less percentage of total soil loss, but require heavy equipment to rehabilitate the area of their occurrence.

A gully can result either by the expansion of a rill or by the concentrated flow over a localized weak spot on hillslope, depression or knick formation. Flow concentration on these weak sections of hillslope continues to develop larger and larger and gully forms as a result of connections of such depressions in a series. Two main processes cause the expansion of a gully i.e. headcutting and sides scouring. The runoff over the headcut contributes to gully growth by i) exerting force on the channel boundary, ii) removing deposited soil from channel and iii) eroding channel bank by undercutting them and gravity (moisture) loading to a level greater than critical shear strength (Piest *et al.*, 1975). To initiate and develop a gully, the mean shear stress of concentrated flow τ should be large enough to overcome the resistance to detachment and transport of the topsoil and to scour channel with a cross-section equal to or exceeding the square foot criterion. Whereas rill in loamy cultivated topsoil develops once $\tau > 1$ Pa (Govers, 1985), ephemeral gullies develop with higher flow intensity i.e. $\tau > 4$ Pa (Poesen *et al.*, 2002). Once a gully develops, several processes and combination of processes such as headcutting, bank scouring and sloughing, piping, tension cracking, mass failure and channel bifurcation, lead to its expansion. The total sediment outflow from eroding gullies, though large, is usually less than that produced by sheet erosion (Glymph, 1951; Leopold *et al.* 1966), although the economic losses from dissection of upland fields, damage to roads and drainage structures, and deposition of relatively infertile overwash on floodplains are disproportionately large.

2.4.11.3 Assessment of Gully Erosion

Many empirical relations were developed to estimate the gully expansion (Annex A-4). Most of these relations deal with the progression of gully head. These empirical models were based on site-specific data, which reduce the reliability of prediction using these equations for other areas. With all their limitations, these models can be used for a preliminary assessment for conservation planning, but they are not a substitute to on-site observations.

2.5 Water Harvesting

2.5.1 Need of Water Harvesting for Dryland Agriculture

Rainfed production system in drylands is important to meet the food and fodder demand and to maintain the ecological balance. It is the only source of livelihood for the rural-poor in many dry areas. The low cost inputs needed and the vast potential areas make it a better choice for future harvest. Parr and Stewart (1990) consider that due to high investment cost and declined water storages for irrigated-agriculture; rainfed agriculture will be an alternate source of food production in the foreseeable future. FAO (1988a) emphasized an ever-increasing food demand in drylands. FAO (1993) suggested two principal options to increase water productivity in the dryland; (i) through maximizing water infiltration and water retention in soil and (ii) by supplying water during periods of crop-water deficit. Water productivity is closely linked to soil moisture and nutrients (especially, phosphorous and nitrogen). Diminishing vegetative cover and low organic matter can easily result in the collapse of soil structure (Valentin *et al.*, 1991). Root-zone water deficit combined with the inherent low-fertility of soils is a main limiting factor for biomass production in arid and semi-arid regions (Falkenmark *et al.* (1990). Water harvesting induces, collects and stores the runoff for crop production or other uses. Management/ conservation of stored water for optimum benefits can greatly enhance the effectiveness of water harvesting systems. It can improve root-zone soil-moisture and stabilize crop yield. Nevertheless, human endeavor in the development of water harvesting must match the replenishing capacity of nature and it must be sustainable.

2.5.2 Development in Water Harvesting

Review of literature on water harvesting showed that water harvesting was practiced in many dry regions across the globe, since ancient times (Table 2.3). The old water harvesting system had necessary elements of water capturing, spreading and storing. It served dryland agriculture and domestic water supplies in arid and semi-arid environments, in the past. Nevertheless, the role water harvesting seems to be diminished with time and little work is reported on it from the fifteenth century onwards. This opens an important dimension of research in water harvesting with key research questions;

- Why did the role of water harvesting diminish with time?
- What contributed to the failure of large water harvesting structures?

Water harvesting again has received attention since middle of twentieth century (Reij *et al.* 1988; Critchley & Siegert 1991; FAO, 1994; Prinz and Singh, 2000). Research on water harvesting focused on floodwater diversions for crops and fruit trees (MRMP, 2000), MCWH for crops, fruit trees and range rehabilitation (Somme *et al.*, 2004; Ali *et al.*,2007) and rooftop/ courtyard water harvesting for domestic uses (UNEP, 2000). A considerable attention was paid to the design of MCWH in relation to geophysical and agro-climatic conditions (Boers, 1994), but high soil and rainfall variability and their implications to runoff assessment and water availability to the plants pose the real challenges for the successful use of this technique. Floodwater harvesting in northwest Egypt during 1996–2001, stimulated discussion among communities and decision-makers on the sustainability of interventions in the context of watershed and upstream downstream linkages (Ali *et al.*, 2007). Rooftop and ground catchment water harvesting in cisterns for drinking uses face the challenges of water quality and reliable source of water.

Table 2.3. Main Regions of Water Harvesting Practices in History.

Area / Region	WH System	Main Uses	Historical Time	Reference
Southern Spain	Not mentioned	Agriculture	Prehistoric time	Chapman, 1978
Jordan	Water collection structures	Drinking and domestic	7000 B.C. (9000 yrs.)	Prinz, 1994
Southern Mesopotamia	WH structures	Agriculture	4,500 B.C. (6500 yrs.)	Bruins *et al.* 1986
Palestine	Cistern	Drinking and domestic	2200–1200 B.C. (3200–4200 yrs.)	Wahlin 1997
Negev desert	Tanks for hillside runoff	Drinking and domestic	2000 B.C. (4000 yrs.	UNEP, 2000
Northern Yemen	floodwater for 20,000 ha	Agriculture	1000 BC (3000 yrs.)	Eger 1988
Northwestern Egypt	Roman Cistern	Drinking and domestic	300 B.C. (2300 yrs.)	MRMP, 1992
Morocco, Algeria, Tunisia	Lacs collinaires Meskat and Jessour	Agriculture	300 B.C. (2300 yrs.; Roman time)	Prinz, 1994
Thailand	Rooftop	Drinking and domestic	1 B.C. (2000 yrs.)	UNEP, 2000
North-western Saudi Arabia	Flood irrigation (Nabatean)	Agriculture	After 3rd century (1700 yrs.)	Bowersock 1994
Istanbul, Turkey	World's largest rainwater tank	Drinking and domestic	5th Century (A.D. 527–565; 1000 yrs.)	UNEP, 2000
Negev desert	Runoff irrigation systems	Agriculture	10th Century (1000 year)	Evanari *et al.* 1971
Desert of Arizona and northern Mexico	Floodwater farming	Agriculture	10th Century (1000 yrs.)	Zaunder and Hutchinson 1988
Northern-western Egypt	Wadi terracing and run-on	Agriculture	15 Century (500 yrs.) Roman time	El-Naggar *et al.* 1988
Libya (hundreds kilometers inland; 50 mm rainfall)	WH structures served 400 yrs.	Crops, fruit trees and animal	15th Century (500 yrs.)	Prinz 1994
Northern Jordan	Cistern	Drinking and domestic	1100 to 1516 A.D (400–500 yrs.)	Lenzen, *et.al*, 1985
Balochistan, Pakistan	Sailaba and Khushkaba	Agriculture	15th century (500 yrs.)	Oosterbaan, 1983
Rajasthan, India	Tank and Khdin systems	Agriculturre, Drinking	15th Century (500 yrs.)	Kolarkar *et al.* 1983
Bihar, India	Ahar system	Agriculture	15th Century (500 yrs.)	UNEP, 1983; Pacy & Cullis, 1999
Sudan	Haffir	Dom., animal	Not known	UNEP, 1983
Burkina Faso	Zay, rock bunds	Agriculture	Not known	Reij *et al.* 1988
Niger	Rock bunds	Agriculture	Not known	Prinz, 1994
Mali	Basin systems	Agriculture	Not known	Prinz, 1994
Quaddai, Chad	WH techniques	Agriculture	Not known	Somerhalter, 1987
Chaco Canyon, New & central Mexico	Rock bunds, terracing	Agriculture	Not known	UNEP 1983
Hiraan region of central Somalia.	Caag system	Agriculture	Not known	Critchley *et al.* 1992

2.5.3 Water Harvesting Definitions and Systems

Although history witnessed the water harvesting practices, the systematic scientific research on it was initiated in 1950s, when Gedes gave the first definition of the water harvesting (Boers, 1994). Some of the most common definitions of water harvesting include;

- Collection and storage of any farm waters, either runoff or creek flow, for irrigation use (Gedes quoted in Myers, 1975 and Boers, 1994),
- A method for inducing, collecting, storing and conserving local surface runoff for agriculture in arid and semi-arid regions (Boers and Ben-Asher 1982),
- An hydro-agronomic term covering a whole range of methods of collecting and concentrating various forms of runoff (Reij *et al.* 1988),
- Collection of runoff for its productive use (Critchley and Siegert 1991),
- The process of concentrating rainfall as runoff from a large catchment area to be used in a smaller target area (Oweis *et al.* 1999).

Traditional water harvesting largely consists of rooftop, micro- and macro-catchment water harvesting techniques mainly for domestic uses, range rehabilitation and raising the fruit trees. With many improvements during last three decades, these techniques have successfully been practiced in the US and Australia for the domestic and livestock water supplies and in East Mediterranean countries for growing olive, almonds and pistachio nuts (Critchley and Siegert 1991). In Sub-Saharan Africa, water harvesting has been used to stabilize yield from annual crops (Critchley and Reij, 1988). More recently, rooftop and hillside water harvesting for storage and subsequent uses have been practiced in China and Ethiopia. Water harvesting for irrigation (spate irrigation), soil conservation and groundwater recharge have been used in Afghanistan, Pakistan and India. Fig. 2.3 shows some common water harvesting practices.

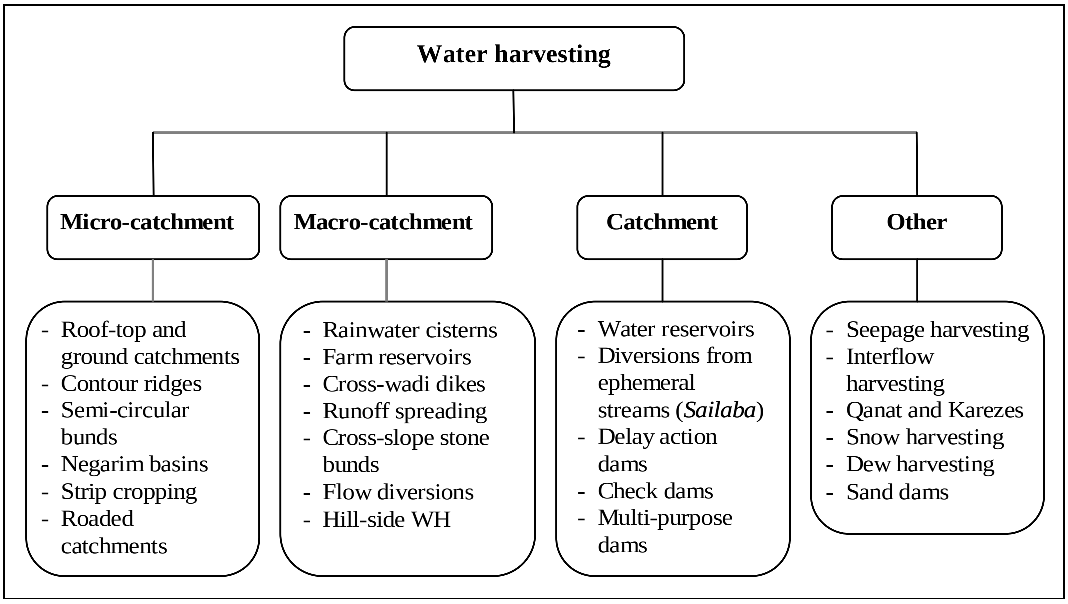

Figure 2.3. Main Water Harvesting Systems

2.5.4 Emerging Trends in Water Harvesting

Limited freshwater resources and burgeoning demand for food production have increased the demand of water harvesting in arid and semi-arid regions. To be sustainable, the water harvesting faces two-fold challenges.

- Developing possible ways and means that ensure sustainable water harvesting vis-à-vis maximize its productive use. The development should have either no or low/mitigable negative impacts.

- The developed water harvesting system must be in tune with the existing agro-ecological and socio-economic conditions.

A sustainable water harvesting system should not negatively affect the hydrological cycle capacity of a system. Reduction in groundwater recharge and drying out of Qanat and Karezes (sub-surface flow channels) in many dry areas could be result of disproportionate water harvesting at upstream (Author's experience in Syria and Pakistan). To meet these challenges one needs to adopt a systems approach based on water, sediment and nutrients balance and dealing with the initial negative returns that many water harvesting systems, particularly, raising fruit trees and range rehabilitation, face. Further, many water harvesting systems (catchment and other in

Fig. 2.3) that did not get due attention in the past, should be incorporated in developmental research in future. These systems have great improvement potential as well as challenges. Water harvesting, now-a-days, is seen expanding from domestic to regional and national levels and from micro-catchment to basin scales. In the future, water harvesting for flood mitigation, environmental management (reduced land degradation, dilution and eco-system management), streams restoration, groundwater recharge and for other developmental purposes will be on board. These emerging trends in water harvesting call for a comprehensive definition that encompasses all these elements. A new definition, "*Water harvesting is a process of concentrating, capturing, storing and regulating the run-on, runoff, inter- or stream flows for in-situ, on-site or off-site uses for conservative and/or sustainable developmental purposes*[1]*",* is proposed. This is a broad-based definition, which also reflects "water use" as a rationale for water harvesting. The concepts of sustainable contemporary water harvesting can thus be built on this definition by considering demand- and supply- sides as an integral part of the system.

2.5.5 Micro-catchment Water Harvesting (MCWH)

MCWH is a method of collecting surface runoff from a small catchment area and storing it in the root zone of an adjacent infiltration basin with plant (Boers and Ben-Asher, 1982). Frasier *et al.* (1979) describe that water yields of operational water-harvesting catchments usually related to the water yields measured at small-instrumented plots. Size of catchment has bearing on the yield of runoff. Under the same hydrological conditions, small area may generate runoff up to 50% of rainfall as compared with river basin where runoff may remain only 5% of the rainfall (Stern 1979). The higher runoff generation per unit area from a small catchment forms the basis of micro-catchment water harvesting as an alternative option.

Some common types of MCWH structures include continuous and intermittent contour ridges, semi-circular bunds, contour strips and Negarim basins. Small earthen or stone-made structures are constructed across the land slope along the

[1] This definition was first presented in PhD seminar in 2005, at Çukurova University Adana, Turkey.

contour. Construction along the contour ensures smooth water spreading. Land slopes between 2% and 8% are considered suitable for MCWH. Nevertheless, these structures have been constructed on flat lands and slopes up to 20%. Excavation in slope to the pit or location of plant—generally in centre of the micro-catchment, can develop a micro-catchment on flat land. Rectangular or hexagonal shapes are suitable for this purpose. Frequent damages and high maintenance cost are main implications of development of MCWH on steep slopes.

The performance of a micro-catchment depends on many factors including rainfall, soil and crop genotype. The design of micro-catchment area is important as it is responsible for adequate water supply on one side and it affects plant density (number of plants per unit area) on the other side. A micro-catchment area is designed by;

$$\frac{Catchment\ area}{Plant\ area} = \left[\frac{Crop\ water\ requirement - Design\ rain}{Design\ rain * Runoff\ coefficient * Runoff\ coefficient}\right] \quad (2.24)$$

Water requirement of crops depends on the crop genotype, climate and crop growing stage. FAO (1992) presented water requirements of common crops and the methodology for the estimation of crop water requirements. The simplest method of micro-catchment design is based on annual rainfall and annual runoff coefficient. However, crop water requirement in relation to crop growing season and rainfall events during these seasons by using event runoff coefficient can improve the design quality significantly. Although, this method is simple and practicable, the rainfall and soil variabilities and operation of MCWH between low and high extremes add uncertainties to the design parameters.

Runoff coefficient is important while determining the water availability to the plant. Critchley and Siegert (1991) presented runoff coefficient in relation rainfall depth and rainfall intensity, duration and antecedent soil moisture for agricultural land. Pacey and Cullis (1999) presented runoff coefficient for different treated and untreated catchments in rural areas, particularly in the context of water harvesting for storage and domestic uses. Sharma (1986) found that micro-catchments can harvest runoff from about 13 to 45% of the rainfall for slopes ranging between 0.5 and 10%

by proper selection of micro-catchment areas. Based on seven years of study, he concluded that the threshold rainfall to generate runoff decreased from 4.7–6.0 mm to 2–3 mm and runoff efficiency increased from 22–36% to 52.56% with an improvement of rainfall-runoff correlation coefficient from 0.643–0.751 to 0.988–0.993 due to crusting of the catchment area. Thus intensifying crust caused an increase in runoff 1.3 to 2.7 times that of original level. The runoff efficiency is related to the fraction of collected water used by plants excluding evaporation from water surface and deep percolation. Anschutz *et al.* (1997) showed that 75% of collected runoff is used by plants when 25% is lost in evaporation and deep percolation.

Infiltration plays a key role in runoff generation and affects runoff coefficient. It also determines the rainfall threshold to generate runoff that is equally important in the design of micro-catchment. Infiltration depends on many factors including rainfall, soil type, vegetation and soil-moisture. In plant basin area, the available water holding capacity and plant rooting effective depth also affect the water available to plant and thus to the design of micro-catchment. Table 2.4 shows the typical infiltration rate and water holding capacity of various soils.

Table 2.4. Infiltration Rates and Water Holding Capacities of some Common Soils (Source: Anschutz, 1997)

Soil type	Infiltration rate (mm h^{-1})	Available water (mm m^{-1} of soil depth)
Sand	< 30	55
Sandy loam	20–30	120
Loam	10–20	-
Clay loam	5–10	150
Clay	1–5	135

The size of micro-catchments varied between 0.5 m^2 (Aldon and Springfield 1975) to 1000 m^2 (Evenari *et al.* 1968) and average annual rainfall ranged from 100 mm (Boers *et al.* 1986b) to 650 mm (Anaya and Tovar 1975). Boers (1994) developed a methodology for design of MCWH by using infiltration model, SWATRE, and kinematic sheet-flow model in drier environment in Niger. The model's predictions of micro-catchment design were reasonable, and of academic interest. Nevertheless, using this approach is cumbersome and requires high technical skill and a lot of data, which makes its practical use very difficult.

2.5.6 Hydraulics of MCWH

MCWH is a combination of rainfall, infiltration and runoff from micro-catchment area and storage in drainage basin and soil profile at plant location. The excess rainfall on micro-catchment area is routed along slope length of the micro-catchment and transforms into direct runoff at the location of drainage basin. Direct runoff is stored in drainage basin until it exceeds the storage capacity and runs off. Surplus flows take two ways; overflowing across the ridge or flow along the ridge to find its way to downstream. Zero flow in catchment and in drainage basin is assumed as initial conditions. The boundary conditions assume zero flow at upstream boundary and no flow, overflowing sections and channel flow along ridge can be assumed as downstream boundary conditions. Inflows to and outflows from the drainage basin can be treated as a very small reservoir. Therefore, the reservoir routing principles can be applied, which allows to model the MCWH as it appears in the study area (Fig. 2.4),

Water balance can be estimated by analyzing the rainfall, interception, deep percolation, evapotranspiration and retentions in micro-catchment and planted areas. The runoff from the micro-catchment area would be the rainfall less all the above-mentioned abstractions. This runoff from the micro-catchment would be an inflow component to the planted area. Therefore change in storage in planted area would be the runoff and rainfall on the planted area (inflows) less the outflows (deep percolation, evapotranspiration and spillage). The concept of flow routing through reservoirs can be use to rout the flow through the planted basins or ditches by using continuity equation.

$$I_t - O_h = \frac{dS}{dt} \tag{2.25}$$

Where, inflow I_t is function of time and outflow O_h is function of overflow head h over the basin. Change in storage dS is function of time and can be represented by $A_h dh$.

$$I_t - O_h = A_h \frac{dh}{dt} \quad \text{or} \tag{2.26}$$

$$\frac{dh}{dt} = \frac{(I_t - O_h)}{A_h} \tag{2.27}$$

These routing equations can be used to compute the water balance.

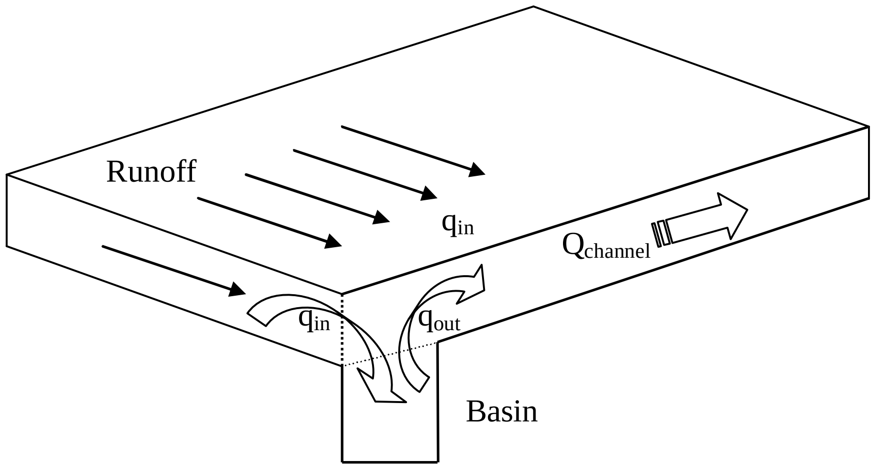

Figure 2.4. Runoff Pattern as Modified by the MCWH in the Study Site

3. MATERIALS AND METHODS

3.1 The Research Environment

The research site is located in the foothills of Tool el-Raous mountains at latitude $34^{\circ}08'$ (N), longitude $37^{\circ}09'$ (E) and altitude 894 m in Syrian steppe area. It is at about 120 km northeast of Damascus, 13 km southwest of Qaryatin village and 12 km from Mehesseh Research Center (Fig. 3.1). It consists of a small catchment (~ 2.5 km^2) and about half of that is upper catchment. The upper catchment is semi-hilly to hilly with land slope between 5 to 10% in upper plateau and greater than 10% along hillsides. The soils are shallow and gravel covers about 30–35% of the upper area. Rocky outcrops are common along the drainage courses. Four main gullies exist in the upper catchment. A village road crosses three gullies, where culverts with sizes greater than the gully cross-section have been provided. The average bed slopes of these gullies vary between 2.7 and 4% in the lower and upper reaches, respectively. The cross-section of the gullies measured between 2 and 4 m^2. The lower catchment forms about 50% of the total catchment area. It is located along the foothills with land slopes ranging between 2 and 6%. Twenty one small gullies and rills exist in the lower catchment. About hundred hectares of the lower catchment is defined as the research site. It is mostly a rangeland. The vegetation is sparse and exists along water courses or in depressions. Its soil depth varies from 30 to 80 cm, excepting the depressions and alluvial fan areas, where depths of more than 100 cm can be found. The drainage density is high.

The winter is cool and the temperature drops below zero on an average for 22 days during December, January and February. The summer is hot and remains dry. The average annual rainfall is 117 mm with coefficient of variation of 0.35 (Table 3.1). Rainfall occurs from October to April. Mostly, May to September is the rainless period, and April to November is the soil-water stress period. The average annual evapotranspiration (ET_o) is 1671 mm. The annual rainfall was just 8% of the reference evapotranspiration. UNESCO (1977) climatic zoning, on the basis of rainfall-evaporation ratio, places the research environment closer to the margin of arid to hyper-arid zone. This environment poses limitation to plant survival and growth. On an average, 3 to 4 runoff events occur in an average rainfall year. The drainage density is high and runoff generates and dissipates quickly into the gullies. Local runoff may occur more frequently, but it is often lost as transmission losses in rills and small gullies before joining the stream network.

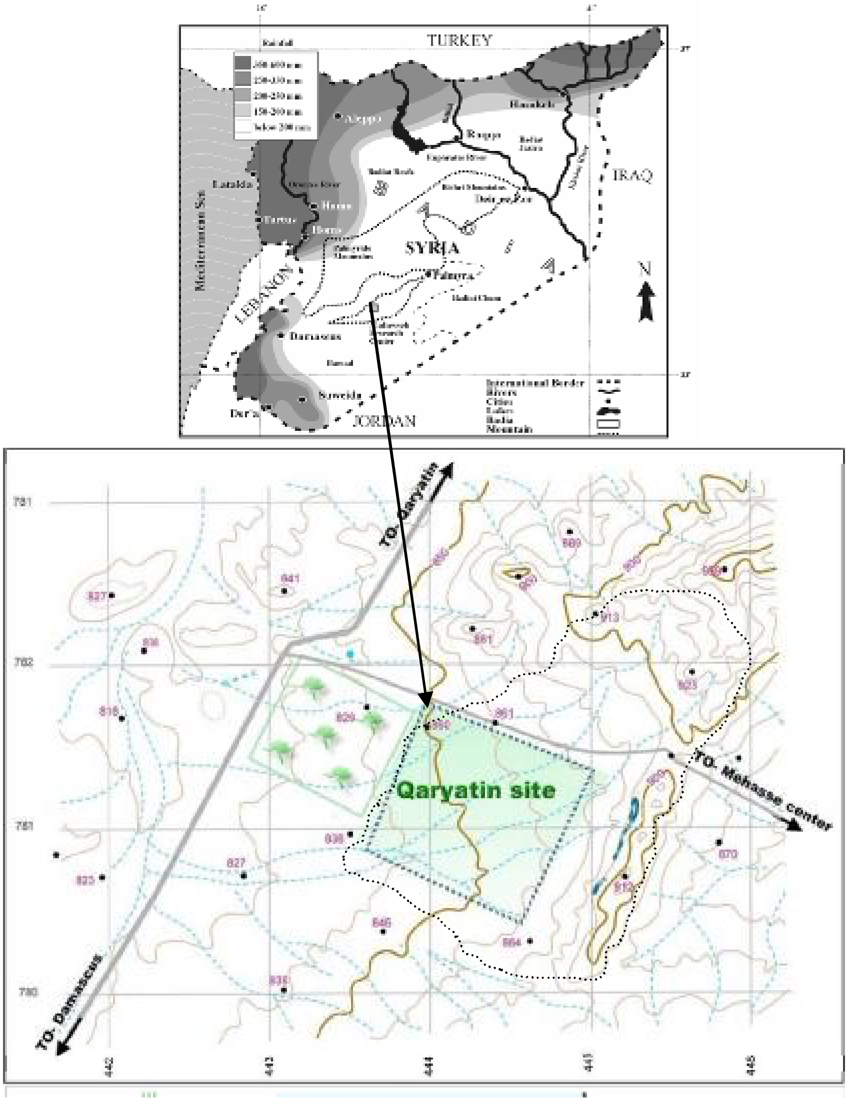

Figure 3.1. Location Map of the Research Site and the Catchment

Table 3.1. Mean-monthly Climatic Parameters at Qaryatin near Research Site

Climatic Parameters	Jan	Feb	Mar	Apr	May	Jun	July	Aug	Sep	Oct	Nov	Dec	Annual
[1]Mean rainfall (mm)	13.6	14.6	23.7	13.7	17.4	0.1	0.0	0.0	0.2	8.7	12.6	12.6	117.2
Mean temp. °C	6.4	6.5	8.84	13.8	21.3	23.7	26.6	25.7	22.8	17.7	11.8	7.0	16.0
Mean max. temp °C	10.5	12.3	14.5	22.0	29.1	32.8	34.3	34.0	30.5	25.2	18.6	12.8	23.0
Mean mini. temp. °C	0.7	-0.2	2.0	6.2	11.7	14.8	17.5	16.3	13.1	8.2	5.9	1.6	8.1
Mean RH (%)	73.9	64	58.2	51.7	34.7	43.9	45.2	48.7	48.2	50.6	61.7	73.1	54.5
[2]Mean wind speed (m/s)	3.4	3.73	3.74	4.05	4.15	4.6	5.9	4.3	3.8	3.2	3.6	4.1	4.0
ETo (mm)	40	60	87	136	222	222	218	223	194	147	79	43	1671

[1]Based on data from 1956 to 1993; [2]Based on data from 1967 to 1983;
ETo is based on data from 1958 to 1988; Underlines figures represents annual total.

3.2 Research Approach

The research objectives, within stipulated scope, were pursued by integrating field investigations, monitoring water, soil and shrubs parameters and simulations wherever needed for elaboration. Characterizing the research environment, diagnostic analysis and development of the research site laid the foundation for the research work. The description of the main elements of water, soil and vegetation relevant to the proposed research, identified the need for data collection and defined the simulation domain. Data analysis yielded results with respect to each component. The results were interpreted to understand the combined effects (Fig. 3.2). The experiment generated data on runoff, soil-water, soil loss and shrubs survival and growth. The necessary data for simulation was processed and used to run a mathematical model for various scenarios.

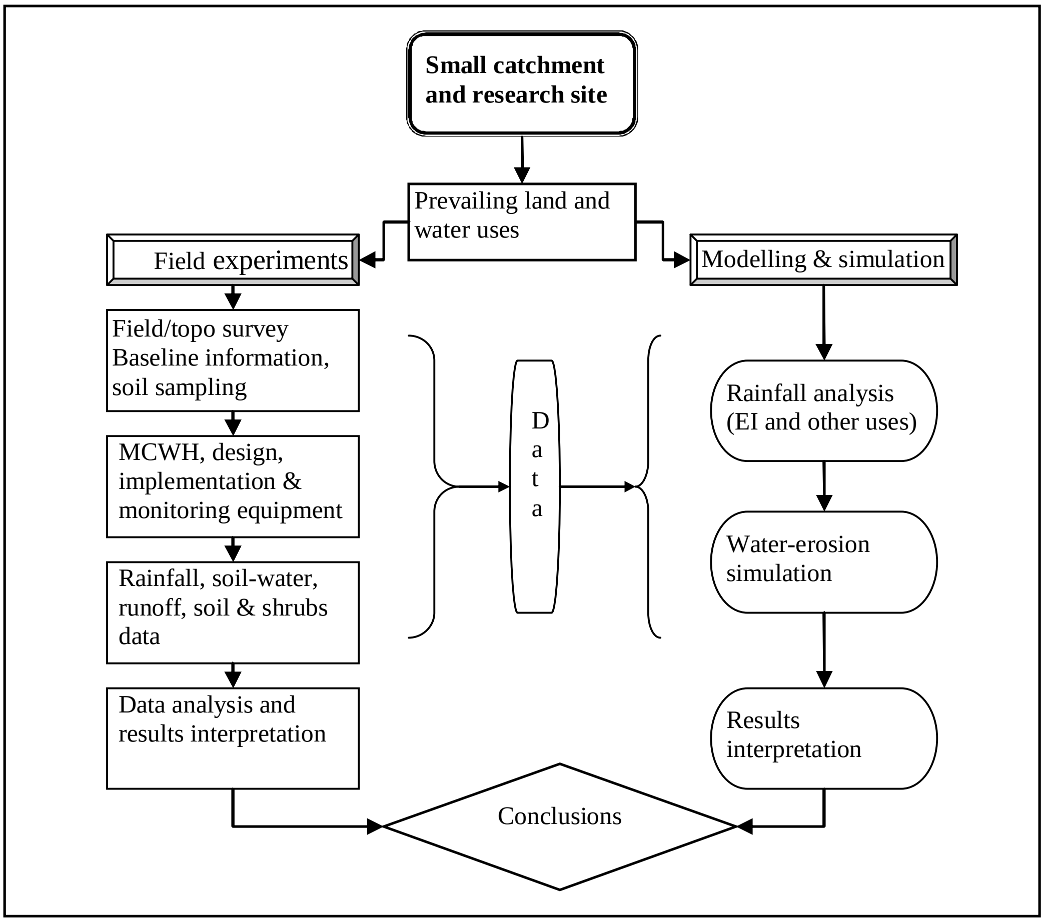

Figure 3.2. A Framework for MCWH Evaluation for Water and Soil Losses

3.3 Setting up Research

3.3.1 Diagnostic Analysis

Diagnostic analysis was used for subjective evaluation and to identify the main bio-physical drives responsible for land degradation and their probable impacts in the context of study environment. It consists of problem visualizing, objective analysis and investigating the cause and effect scenarios. The secondary data, field investigations and meetings with the communities and staff of research and development organizations formed the basis of the diagnostic analysis. Topographic survey, soil depth and a survey of drainage system showed that ground relief varied between 3–8% in Block A, 2–3% in Block B and 1–2% in Block C (Fig. 3.3).

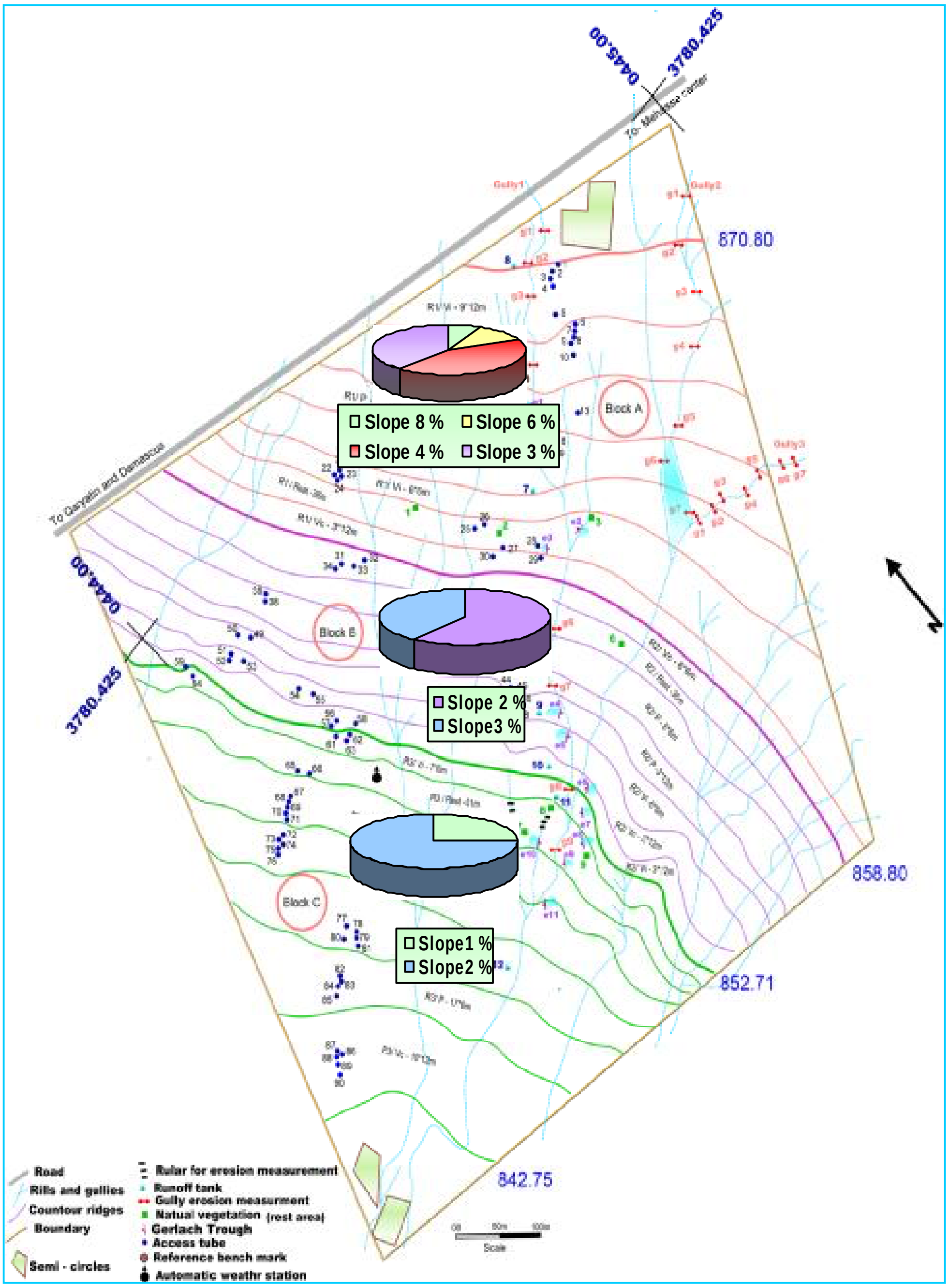

Figure 3.3. Topography and Drainage System in the Study Site

Slope steepness due to flow residence time can affect infiltration and soil losses, however; a decreasing trend in slope from up to downstream is a common phenomenon. Twenty four gullies and rills in 100 ha area is quite a high drainage density. The drainage density is high in upper areas and low at downstream. High drainage density may results in low time of concentration and sharp peak discharges.

The soil depth at randomly selected 90 locations varied between 25 and 90 cm. It is 60–90 cm in downstream areas of mild slopes (1–3%), 45–70 cm in middle reaches of moderate slope (3–5%) and 20–45 cm in upstream areas of 5–8% slopes (Fig. 3.4). Largely, sandy loam, the soils in mild slope areas, contained about 25% stones and its average salinity (represented by electrical conductivity) varied between 2 and 16 dS m^{-1}.

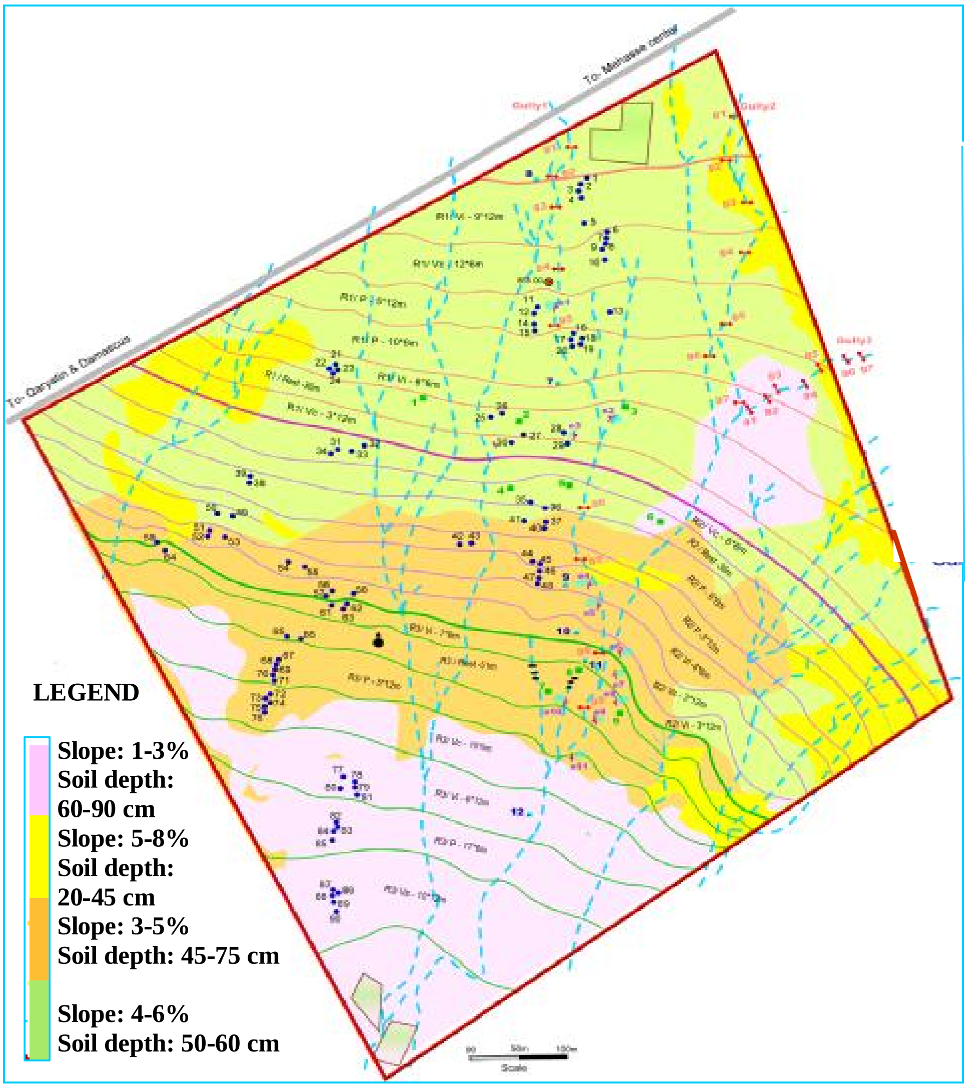

Figure 3.4. Variation of Soil Depth and Slope in the Study Area

Soils in areas of medium slopes contain 15% granular material and salinity range 8 to16 dS m-1. The gullied area contained about 45% granular material. Runoff transported most of this material from the upper catchment. In general, sparse vegetation cover and fine aggregates dominate that can be the main causes of surface crusting, low on-site infiltration and quick runoff generation. Fig. 3.5 shows probable causes and effects of the prevailing conditions in the study area.

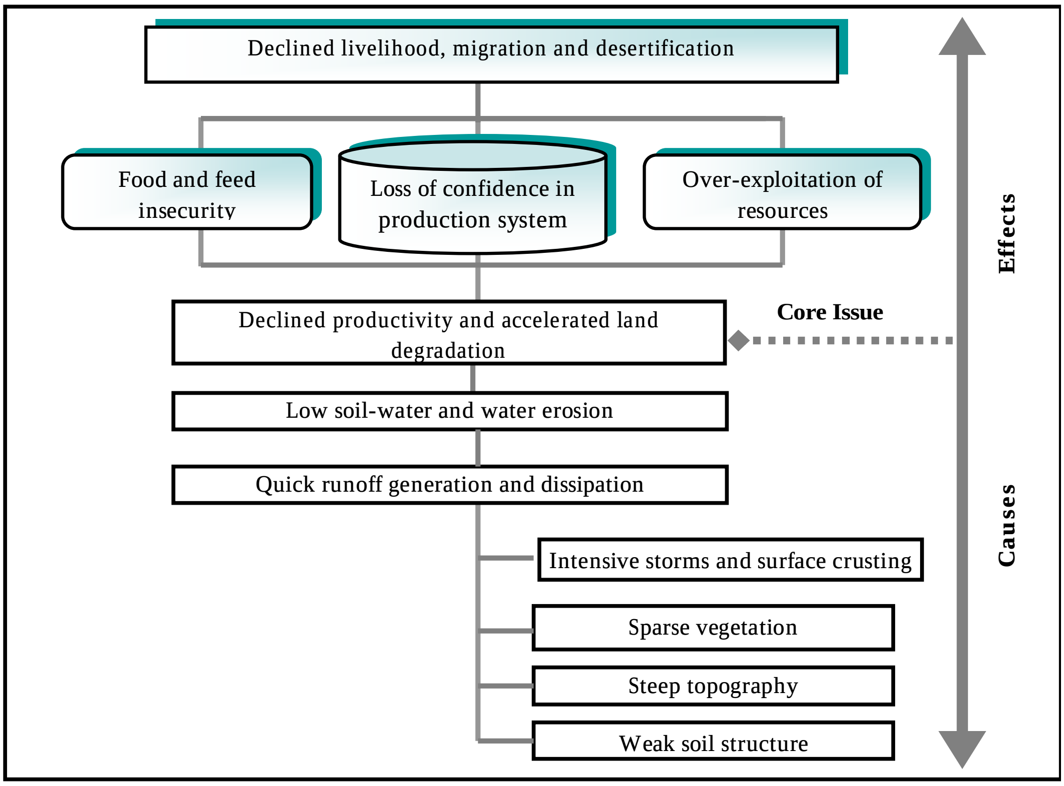

Figure 3.5. Problem Analysis by Using Cause and Effect Approach

3.3.2 Research Site Development

The main features of the site were captured by topographic survey and site plan. The main drainage network was marked on the map, land slopes were computed and the intervention area was estimated. The site was divided into three blocks for the convenience of research. The experimental layout followed the randomized complete block design (RCB) that created about 85 km long contour ridges on 2 to 5% slope. The design included two management options (MCWH, and control area); three implementing techniques (Vallerani intermittent, *Vi*; Vallerani continuous, *Vc*; and Pakistani, *P*); and two spacings (6 and 12 m). The agronomic options included three shrubs (***Atriplex halimus***, AH; ***Salsoal vermiculata***, SV; and ***Atriplex leucucolada***, AL) and two methods of plantation - seedling transplantation (T) and direct seeding (S). The control area was left without any treatment. The cross-combinations resulted in 37 pairs (Table 3.2). Each treatment was replicated three times in blocks A, B and C. Each block has many rows of variable length. The shrub to shrub distance was 4 m along the ridges. The micro-catchment area per shrub for 6 and 12 m spacing was estimated as 24 and 48 m^2 respectively. About 10,000 shrubs were planted over an area of 100 ha. Experimental design and a typical field layout are given in Annex B-1 and B-2, respectively. A longitudinal section of micro-catchment with shrub basin and ridge is shown in Fig. 3.6.

Table 3.2. Combination Pairs of Techniques and Treatments.

No.	Techniques	Shrub Species and plantation methods					
		1	2	3	4	5	6
		Seedling transplantation			Direct seeding		
		AH-T	SV-T	AL-T	AH-S	SV-S	AL-S
1	Vi-6	****	****	****	****	****	****
2	Vi-12	****	****	****	****	****	****
3	Vc-6	****	****	****	****	****	****
4	Vc-12	****	****	****	****	****	****
5	P-6	****	****	****	****	****	****
6	P-12	****	****	****	****	****	****
7	Rest (R)	One treatment including three replica					
	Total combinations pairs including one for rest area						37

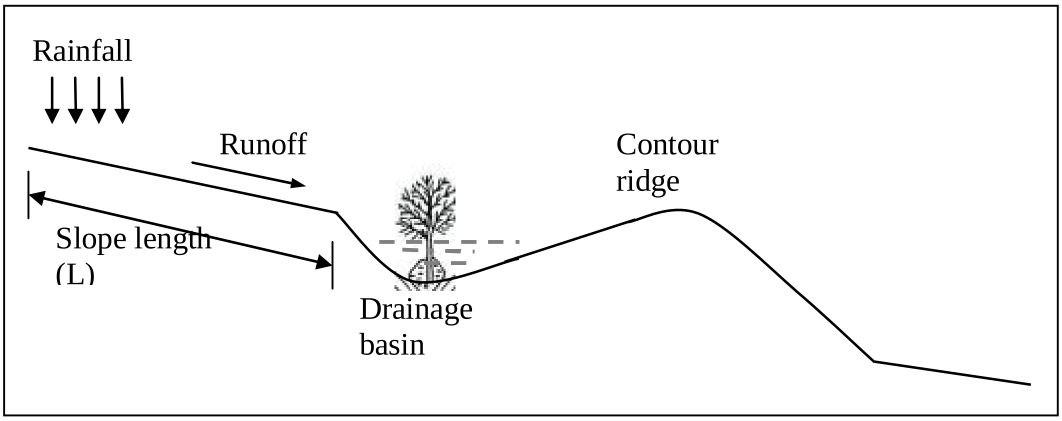

Figure 3.6. A Typical Layout of the Micro-catchment

3.3.3 Instrumentation

A spatially designed monitoring experiment was developed and maintained during the study period. The research site was equipped in order to measure the climatic parameters, soil-water, runoff and soil losses. Grow-Weather; an automatic weather station, was installed within the research site to measure the rainfall and other climatic parameters (Fig. 3.7). This integrated weather station and data logger measures, calculates, displays and stores wind speed and direction, solar radiation, solar energy, air temperature, temperature/humidity index, growing degree-days, soil temperature, humidity, dew point, leaf wetness, barometric pressure, evapotranspiration, rainfall and the rate of rainfall. Another recording rain gauge was installed near the foothill within the research site in order to incorporate spatial rainfall variability and hill-side effects.

One hundred and eight access tubes were installed at randomly selected locations in micro-catchments and in shrub basins. Water and soil loss from the micro-catchments were measured by runoff plot method. Twenty six runoff collecting tanks were installed to take into account, the effect of the different MCWH techniques and treatments. Nine rills were selected to measure the soil losses. Three to five cross-sections on each rill were equipped with graduated cross-section measuring frame. A grid of pin (mesh = 2m×2m) was installed in interrill area of each rill to measure inter-rill erosion. A rill trap was provided at the outlet of each rill. Three sharp-crested weirs were constructed on three major gullies and each was equipped with stage recording sensor. The sensors recorded the stage hydrograph. The sediment delivery at the weirs was measured by using the grid-pin method. Six Gerlach troughs were installed to measure the sediment loss from micro-catchments. Twenty four frames were installed to measure the erosion of different ridges and the data were used to develop ridge-decay function. The shrubs were randomly selected for measurement and flagged. A temporary hut was also built for the guard to ensure the security of instruments and other interventions at site. Fig. 3.8 shows field layout of monitoring system.

Figure 3.7. An Automatic Weather Station at Research Site (Davis Instrument Corporation, 1996)

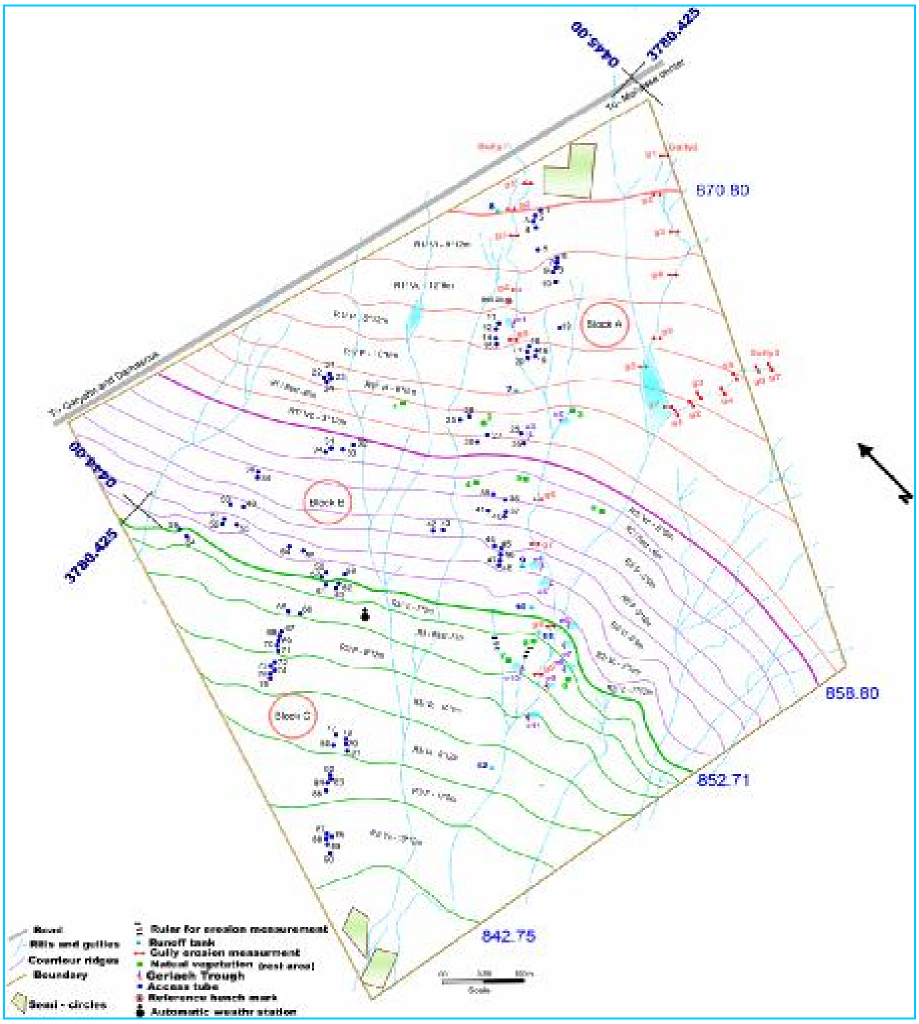

Figure 3.8. Field Layout of Water and Soil Loss Monitoring Network

3.4 Soil Characterization

3.4.1 Soil Sampling and Analysis

Twenty one sampling sites were randomly selected across the blocks A, B and C from upstream to downstream. This resulted in three samples from each treatment (Vc-6, Vc-12, Vi-6, Vi-12, P-6, P-12 and Rest area) and seven samples from each block. Three depth-integrated soil samples at 20 cm incremental depth (0–20, 20–40 and 40–60 cm) were taken from each site by using manually operated auger (steel, ϕ = 10 cm). This depth represents the zone of most biological activities and has particular significance in soils of marginal dry areas such as the research site. It resulted in 63 spatial- and depth-integrated samples. Each soil sample was preserved in a polyethylene bag and properly tagged with location, profile number, sampling layer and date. The samples were transported in boxes and stored in a refrigerator box so that they do not loose soil moisture. The samples were oven-dried (air-forced) at 30°C for 36 hours. Seven samples from each block for each layer (0–20, 20–40 and 40–60 cm) were mixed together to get one representative sample for each layer. This resulted in nine depth-integrated representative samples from blocks A, B and C. The samples were prepared and passed through 2 mm sieve. Each depth-integrated sample was then divided into two – one each for physical and chemical analysis. Table 3.3 shows the samples summary.

Table 3.3. Location and Numbers of Sub-samples and Samples (June, 2005).

Location	Block A			Block B			Block C			Total
Depth (cm)	0-20	20-40	40-60	0-20	20-40	40-60	0-20	20-40	40-60	
No of sub-samples	7	7	7	7	7	7	7	7	7	63
No. of rep. samples	1	1	1	1	1	1	1	1	1	9

3.4.2 Some Physical and Chemical Properties of Soil

The representative soil samples were analyzed in ICARDA Soil Laboratory for physical and chemical properties. Mechanical analysis of the soil was carried out by using hydrometer with Bouyoucos scale (Bouyoucos, 1962). The soil organic matter, total nitrogen and electrical conductivity were estimated by using Walkley (1947), (Bremner and Mulvaney (1982), and (Richard (1954), respectively. Table 3.4 shows the methods of analysis.

Table 3.4. Methods of Soil Analysis for Main Parameters.

Soil parameters	Method of analysis
Mechanical analysis (Texture)	Extraction method/ Hydrometer method (Bouyoucos, 1962). Pipette gravimetric method
Particle size	Richard, 1954
pH	Deionized water and Potentiometer
Electrical conductivity (EC)	Deionized water and Potentiometer
Organic matter (%)	Extracting solution 1N Potassium Dichromate ($K_2Cr_2O_7$), wet oxidation (Walkley, 1947; FAO, 1974)
Total N (ppm)	Extraction/ Kjeldahl (Bremneran Mulvaney, 1982)
Mineral Nitrogen (ppm)	Extraction/ Kjeldahl (Bremneran Mulvaney, 1982)
Total/Olsen-P (ppm)	Extraction Method, cholorimetery (Olsen and Sommers, 1982)
Gypsum	Precipitation with acetone
Extractable Ca, Mg, Na and K	Extraction by 1 Normality, Ammonium Acetate, pH 7.0
Soluble Ca, Mg, Na and K	By distilled water (Richard 1954). Ca and Mg by titration with Ethylene di-amino tetra acetic acid (EDTA)
Chlorides (Cl)	By deionized water and titration with $AgNO_3$ (Richard, 1954)
Sulphate (SO_4) (meq/L)	By deionized water and precipitation (Richard, 1954)
Carbonate (CO_3) and Bi-carbonate (HCO_3)	Deionized water treatment with H_2SO_4; use pH 8.3 for carbonate and 4.5 for bicarbonate.
Field capacity and wilting point (%)	Pressure Plate Extractor
Moisture (%)	Gravimetric method and oven dry

3.4.3 Aggregate Stability Analysis

Nine soil samples were collected from surface (maximum of 5 cm depth from surface) for aggregate stability analysis. These included three samples each from gully, continuous and intermittent ridge areas. The samples were preserved, tagged and analyzed for soil texture and wet sieving including micro- and macro-aggregate. The dry sieving analysis is related to wind erosion and was not included in this study. The procedures followed for soil sampling, air drying, separation, weighing, and preparation for assessing dry aggregate fraction and water stable aggregate by wet sieving in the laboratory, were run with negligible mechanical disruption to avoid any significant changes in the size of the aggregates and to preserve their sizes as they existed in the field.

3.4.3.1 Macro-aggregate Analysis: Wet Sieving

The soil batch was dried in the shade to allow loss of excess moisture. The soil was passed through sieves having mesh sizes 10, 5, 4, 2, 1, 0.5, and 0.1 mm with minimum vibration for adequate fragment separation with limited disruption. Following dry sieving, three replicates of 50 g dry aggregates were proportionally sampled to the total weight distributed/retained on different sieves. Samples were moistened slowly by micro-cracking on filter paper and were placed on small dishes. After 30 minutes, wet-sieving was carried out for 2 minutes. Sieves were oscillated (amplitude 10 cm) 100 times, removed from the tank, and dry weights of the water-stable aggregates retained on a 0.5 mm sieve were determined to provide macro-aggregation measurements. Sieves of 2.0, 1.0, 0.5 and 0.20-mm mesh were used. The test was replicated three times for each soil sample.

3.4.3.2 Micro-aggregate Analysis: Wet Sieving

Micro-aggregate analysis was carried out by passing the dry aggregate-size fraction through 2 mm sieve to wet sieving (USDA-NRCS, 1996). After 30 minutes of immersing in the deionized water the aggregates, wet-sieving was carried out for 2 minutes. Sieves were oscillated (amplitude 10 cm) 100 times, after which the water-stable aggregates on a 0.5 mm sieve were removed from the tank, dried and weighed. This determined the water-stable sand contents of greater than 0.5 mm size.

3.4.4 Bulk Density

Bulk density is defined as the ratio of mass of dry soil to its volume. Climate, cultivation and compaction affect the bulk density. Bulk density was computed from $Bulk\,density = dry\,weight\,of\,\,soil \div Sample\,volume$. Table 3.5 shows a range of bulk densities for various soil descriptions. Eight samples (profiles) from each treatment at randomly selected locations were taken in February 2005, to a maximum soil depth of 60 cm at an incremental depth of 15 cm. It resulted in a total of 32 samples. The desired sampling depth for most of the cases for irrigated and non-irrigated areas is 60 and 100 cm, respectively. Each soil sample was preserved in a plastic bag and was tagged. A steel auger of 4.8 cm diameters was used to collect the samples. A soft rock layer was encountered at a depth of about 60–80 cm at various locations. The soil was processed, dried in oven at 105°C for 48 hours and analyzed in ICARDA soil testing laboratory for moisture content and bulk density. The bulk density of study falls within the standard range for non-compacted soils (Table 3.5). It increased with depth, which also indicated increasing clay contents with depth. The soil compaction was not problem in the study site.

Table 3.5. Standard Bulk Densities for Different Soil Conditions (After Stocking and Murnaghan, 2000).

Soil Description	Range of Bulk Densities (g cm^{-3})	[1]Average Bulk Density (g cm^{-3})
Recently cultivated	0.9–1.2	1.1
Surface mineral soils*	1.1–1.4	1.3
Compacted		
Sand and loam	1.6–1.8	1.7
Silt	1.4–1.6	1.5
Clay	Variable	1.3

[1]An average value of 1.3 g/cm^3 is generally acceptable.
*not recently cultivated and not compacted

3.5 Rainfall Measurement and Analysis

3.5.1 Data Source

An inventory list of long-term rainfall and climatic data in the vicinity of the study site was prepared. The inventory of the data source (Table 3.6) showed that the monthly and annual rainfall data was available for about 35 years (1958–93) at Qaryatin gauging station, which is located at about 13 km in the northeast of the study site. The Qaryatin station is situated at an altitude of 760 m above mean sea level (MSL). The rainfall data from 1994 to 2004 was available at Mehesseh Research Center, which is located at about 12 km in southwest of the study site at an altitude of about 900 m MSL. The weather station and an additional rain gauge were located at altitudes of about 850 m above sea level in the study site.

Table 3.6. Inventory of Climate Data Sources

Location	Latitude & Longitude	Altitude (m)	Distance from the Study Site	Data Type	Years of Record
Study site	34° 08′ N 37° 09′ E	850	At the site	P, T_{min} and T_{max}, RH, Wind, Et_o	2004-2007
Mehesseh Research Center	34° 13′ N 37° 03′ E	900	12 km in south	P, T_{min} and T_{max}, RH, Wind speed, Et_o	1993-2004
Qaryatin Town (Met st)	34° 14′ 45″ N 37° 14′ 30″ E	760	13 km in east	P, T_{min} and T_{max}, RH, Et_o, Wind speed	P, Temp, RH (1958-93) Wind (1967-83) Et_o (1958-88)

3.5.2 Long-term Rainfall Data

The long-term rainfall data at these stations was collected from their respective organizations and processed (Table 3.7). The data was analyzed for mean, standard deviation and coefficient of variance. It was also analyzed for minimum and maximum rainfall and percentage of time for annual rainfall below and above average annual rainfall.

Rainfall anomaly index (RAI) for annual rainfall variability (van Rooy, 1965) and modified to account for non-normality (Tilahun, 2006) were computed from:

$$RAI = +3\left[\frac{RF - M_{RF}}{M_{H10} - M_{RF}}\right] \text{; for positive anomaly} \quad (3.1)$$

$$RAI = -3\left[\frac{RF - M_{RF}}{M_{L10} - M_{RF}}\right] \text{; for negative anomaly} \quad (3.2)$$

Where RAI is rainfall anomaly index, RF is rainfall for year under consideration, M_{RF} is mean for total record period, M_{H10} is the mean of 10 highest values and M_{L10} is mean of 10 lowest values of rainfall on the record.

The cumulative departure index (CDI), is a measure of annual variability and shows long-term trends. It can be computed from a rainfall record by using following expression:

Table 3.7. Long Term Monthly Rainfall Data[1]

No	Year	Sept	Oct	Nov	Dec	Jan	Feb	Mar	Apr	May	Jun	Jul	Aug	Annual
1	58–59	0	6.1	9.2	7.5	9.5	8.1	15.5	10.1	5.3	0	0	0	71.3
2	59–60	0	5.1	8.1	10.6	7.8	5.7	13.7	9.1	2.4	0	0	0	62.5
3	60–61	0	7.9	5.4	11.8	12.1	13.9	20.1	14.2	8.6	0	0	0	94.0
4	61–62	0	13.0	17.8	18.3	20.1	19.5	28.2	18.9	10.1	0	0	0	145.9
5	62–63	0	17.1	15.2	20.1	13.6	24.2	22.7	28.3	24.6	0	0	0	165.8
6	63–64	0	8.2	12.3	17.1	19.8	15.6	25	3.2	10.2	0	0	0	111.4
7	64–65	0	10.4	13	0.2	9.5	16.3	19.29	10.3	8.7	0	0	0	87.69
8	65–66	2.3	12.4	14.1	16.2	15.2	17.1	14.5	11.7	13	0	0	0	116.5
9	66–67	0.2	11.3	19.8	14.8	28.3	22.7	30.1	18.9	22.1	0	0	0	168.2
10	67–68	0	9.3	19.2	27.5	14	15.1	13.2	13.3	17.3	0	0	0	128.9
11	68–69	0	8.1	15.2	13.3	13.5	14.2	21	13.9	17.2	0	0	0	116.4
12	69–70	0	4.9	5.1	15.8	15.3	17.3	9.1	19.8	33.2	0	0	0	120.5
13	70–71	0.1	5.6	14.3	6.8	9.5	5.7	8.1	10.2	8.9	0	0	0	69.2
14	71–72	0	9.1	23.5	23.1	13.4	27.5	34.6	42.5	17.2	0	0	0	190.9
15	72–73	0	2.7	3.4	6.1	8.2	6.5	9.9	12.1	11.2	0	0	0	60.1
16	73–74	0.3	13.2	22.8	13.6	23	18.3	24.1	9.2	41.3	0	0	0	165.8
17	74–75	0	9.1	12.5	10.2	9	14.6	19.1	8.9	18.7	0	0	0	102.1
18	75–76	3.1	6.7	0	18.5	15.1	15.3	22.3	17.2	18.9	0	0	0	117.1
19	76–77	0	9.1	13.1	16.4	14.2	22.3	42.2	19.2	13.8	0	0	0	150.3
20	77–78	0.5	7.2	9.6	3.2	11.9	5.5	18.2	6.6	13.1	0	0	0	75.8
21	78–79	0	2.6	1.1	6.6	13.7	10.3	16.2	13.1	16.2	0	0	0	79.8
22	79–80	0	12.3	22.1	23.4	20.2	21.7	22.6	7.4	39.2	0	0	0	168.9
23	80–81	2.1	18.2	12.6	16.9	30.4	14.6	17.1	13.9	17.2	0.8	0	0	143.8
24	81–82	0	9.3	7.2	9.7	9.1	7.5	23.1	11	15.2	0	0	0	92.1
25	82–83	0	10.5	20.3	14.7	7.5	14.6	27.1	21.7	27.8	0	0	0	144.2
26	83–84	0	3.0	2.7	19.5	6.7	3	16.3	8.3	2.1	0	0	0	61.6
27	84–85	0	19.5	24.3	8.8	15.7	21.1	36.2	23.2	25.7	0	0	0	174.5
28	85–86	0	7.8	12.7	10.6	4.6	8.6	13.8	2.6	24.6	0	0	0	85.3
29	86–87	0	3.0	23.4	5.4	10.7	0	27.1	4.8	3.5	0	0	0	77.9
30	87–88	0	9.9	13.8	20.6	12.5	32.6	15.1	10.6	27.9	0	0	0	143.0
31	88–89	0	8.9	6.5	21.2	13	5.5	20.2	3.9	0	1	0	0	80.2
32	89–90	0	12.0	5.9	3.1	2	18.8	114.2	15.3	0	0	0	0	171.3
33	90–91	0	2.0	2	9.4	20.9	14.5	57.9	25	2.4	0	0	0	134.1
34	91–92	0	7.5	4	0	9.7	14.2	2.5	0	81.6	2.5	0	0	122.0
35	92–93	0	0	30	0	16.6	17.2	10.4	21	11.5	0	0	0	106.7
36	93–94	1.5	5.6	22	18	19	22	6	9.9	0	0	0	0	104
37	94–95	1.2	2.0	13	16	34	38	7.8	8	7	0	0	0	127
38	95–96	0	0.8	0.8	1	19.7	24.9	28.9	2.1	2.5	0	0	0	80.7
39	96–97	0	0.3	65	78.5	17.7	2.6	17.6	5.1	6.5	0	0	0	193.3
40	97–98	0	32.0	65.7	6	0	27.4	25.5	10.7	0.4	0	0	0	167.7
41	98–99	5.4	0	0	9	12.8	6	6.8	2.8	0	0	0	0	42.8
42	99–2000	0	3.9	0	1.6	12.3	2	6.7	4.6	0	0	0	0	31.1
43	2000– 01	0	8.8	1.1	6.2	4.1	17.1	1.3	11.9	16.2	0	0	0	66.7
44	2001– 02	0	0	3.6	4	26.2	9.8	7.5	1.3	10	0	0	0	62.4
45	2002–03	0.8	4.2	22	12.2	0.1	20.4	14.5	0.2	0.1	3.1	0	0	77.6
46	2003–04	0	0	24.8	4.4	24.2	1.6	4.2	0.4	0.8	0	0	0	60.4
47	2004–05	0	2.6	40.4	14.1	21.7	25.6	1	8.2	13.8	0.1	0	0	127.5
48	2005–06	0	2.4	7.5	2.2	14.4	7.6	0.2	9.2	0.6	0	0	0	44.1
49	2006–07	0	32.8	0.3	2.3	3.3	10	19.2	9.2	48.8	0	0	0	125.9
Mean monthly		0.3	8.0	14.4	12.8	13.5	14.5	20.9	11.9	14.7	0.2	0	0	110.55

[1]Data from 1958/59–1992/93 at Qaryatin town, 1993/94–2003/2004 at MRC and 2004/2005–2006/2007 at study site

$$CDI = \sum_{i=1}^{n} \frac{(x_i - x_o)}{x_o} \tag{3.3}$$

Where, CDI is cumulative departure index, x_i is annual rainfall, x_o is average annual rainfall and n is numbers of years of record.

3.5.3 Rainstorm Erosivity

The erosivity of the rainfall, expressed by the R-factor in the Universal Soil Loss Equation (USLE), is a function of the total energy and the maximum 30-minutes intensity of a storm event. The kinetic energy of a storm depends on the size and terminal velocities of the raindrops, which are related to rainfall intensity. Renard *et al.* (1977) observed that the soil loss from the cultivated fields is directly proportional to EI30 parameter, which is the product of total storm energy (E) and maximum 30-minutes intensity (I_{30}). To compute the energy of a storm, the storm is divided into increments with relatively uniform intensity. Individual storm energy intensity is computed by the relationship (Foster *et al.*, 1981).

$$EI_{30} = \sum_{n=1}^{n=d} [(0.119 + 0.0873 \log_{10} i_n)] I_{30} \quad for \quad i_n \leq 76 \; mm\, h^{-1} \tag{3.4}$$

$$EI_{30} = 0.283 I_{30} \qquad for \quad i_n > 76\, mm\, h^{-1} \tag{3.5}$$

Where, EI_{30} is storm energy intensity (MJ mm ha^{-1} h^{-1}), i_n is rainfall intensity (mm h^{-1}) of the *n*th time increment, ***d*** is storm incremental duration (h) and I_{30} is maximum 30-minute intensity (mm h^{-1}).

The annual RUSLE factor (R) is the sum of the energy intensity values computed from equations 3.4 and 3.5, of all storms in a given year. The average annual value of R-factor (Equation 3.6) is derived from rainfall intensity data over extended periods (Renard *et al.*, 1997):

$$R = \frac{\sum_{i=1}^{j} (EI_{30})_i}{N} \tag{3.6}$$

Where, R is rainfall-runoff erosivity factor (MJ mm ha^{-1} h^{-1} yr^{-1}), EI_{30} is storm energy intensity for storm *i* and *j* is number of storms in *N* year period

3.6 Soil Moisture Measurement and Analysis

One hundred and eight access tubes to a depth of 100 cm were installed at randomly selected locations in the micro-catchment, plant basins and control/rest areas (Table 3.8). Ninety access tubes were installed in mechanically constructed micro-catchments, while 18 were in manually developed micro-catchment. The Neutron Probes (Type: I.H.II; Radioactive source: N5; Material: 4570NE) were used to measure soil-water. The Neutron Probes were calibrated to actual site conditions at the start of every season. The data of water volume fraction (WVF) was plotted versus count ratio (counts in actual field condition/ counts in fresh water).

A typical calibration curve for one Neutron probe for year 2005 is given in Fig. 3.9. A linear regression equation (3.7) fit better.

$$Pv = 0.7328\,CR + 0.0011 \;\; (R^2 = 0.91) \qquad (3.7)$$

Where, *Pv* is the volumetric water content, *CR* is the count ratio.

The resultant regression equation is comparable with the equations developed by the ICARDA for ICARDA research station at Tel Hadya, Syria (3.8) and for Hobs, Khanasir project area, Syria (3.9).

$$Pv = 0.76\,CR - 0.052 \;\; (R^2 = 0.93) \qquad (3.8)$$

$$Pv = 0.64\,CR + 0.03 \;\; (R^2 = 0.78) \qquad (3.9)$$

The soil-water was measured at an interval of 14 days and after 24–36 hours of each rainfall event to incremental depths of 15–30, 30–45, 45–60, 60–75, and 75–90 cm. soil water from top 0–15 cm depth was estimated by using gravimetric method. A lag time of 24 hour was estimated from the field observations on the calcareous soils/ Aridisol that revealed the rainwater flow through soil profile could reach to stability in 24 hours.

Table 3.8: Layout of Access Tubes for Soil-water Measurement at Site

Block/ line no	Treatment	Numbers of access tubes in		
		Micro-catchment area	Seedling plant basins*	Direct seeding basins
A1	V_i – 12	1	2	2
A2	V_c – 6	1	2	2
A3	P – 12	1	2	2
A4	P – 6	1	2	2
A5	V_i – 6		2	2
A6	Rest		1	1
A7	V_c – 12		2	2
B1	V_c – 6		2	2
B2	Rest		1	1
B3	P – 6	1	2	2
B4	P – 12		2	2
B5	V_i – 6	1	2	2
B6	V_c – 12	1	2	2
B7	V_i – 12		2	2
C1	V_i – 6	1	2	2
C2	Rest		1	1
C3	P – 12	1	2	2
C4	V_c – 6	1	2	2
C5	V_i – 12	1	2	2
C6	P – 6		2	2
C7	V_c – 12	1	2	2
Total		12	39	39
Manually developed semi-circular area				18
G. total				108

* One access tube for Atriplex and one for Salsola

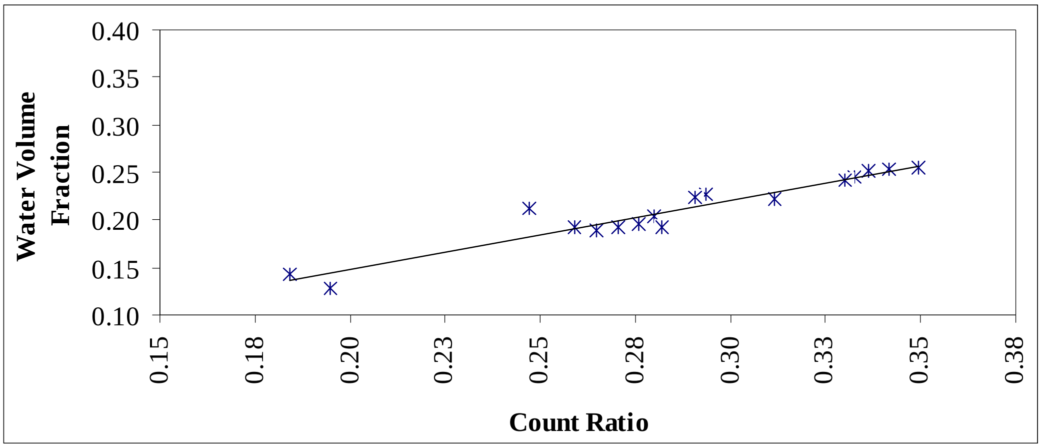

Figure 3.9. Calibration Curve for One of the Neutron Probe at Study Site (February, 2005)

Soil-water by gravimetric method for top soil layer was computed from;

$$Soil\ moisture\ contents = (Weight\ of\ moisture \div Dry\ weight\ of\ soil) \times (100)$$

Soil moisture measurement at study site prior to its development (September 2004) developed soil-water contours (Fig. 3.10) that shows soil-water variations between 3 and 7% for upper and lower areas. The contour map is based on the sample of a horizon of 45 cm. It also estimated field capacity and wilting point 25.8 and 11.4% respectively.

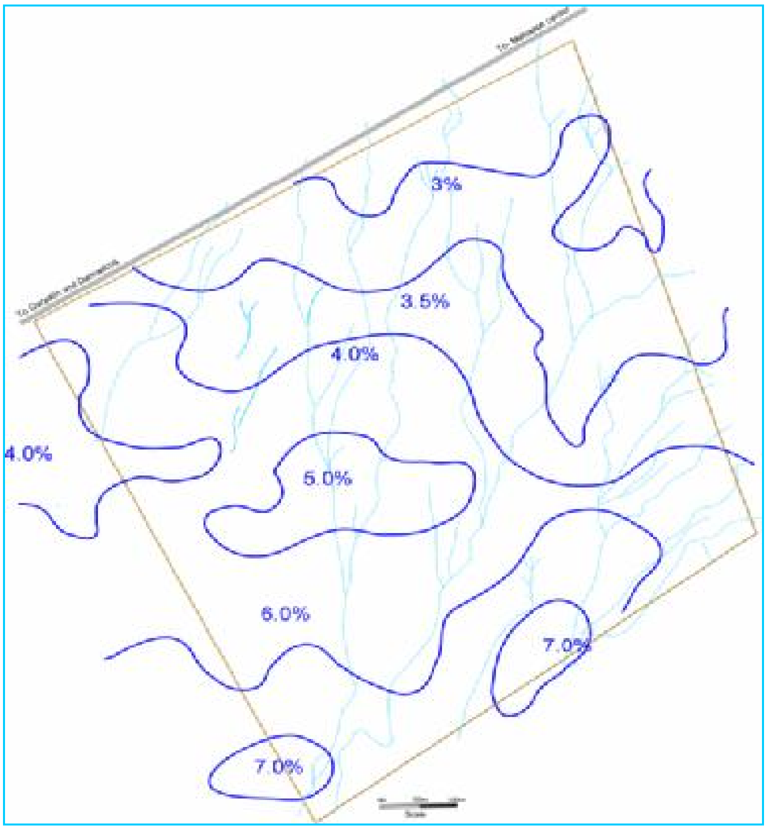

Figure 3.10. Soil-water Isohyets (45 cm Soil Horizon) in the Study Site on September 2004

3.7 Runoff Measurement and Analysis

3.7.1 Runoff Measurement at Micro-catchment Scale by Runoff Plot Method

This method involves the collection of runoff from a small plot into a runoff tank installed at the outlet of each plot. Twenty six runoff tanks were installed at the study site covering different treatments and catchment areas. The tanks were spatially distributed to incorporate the variations in micro-topography and soil. In continuous contour ridge area, (6×4 m) and (12×4 m) plots created catchment areas 24 and 48 m^2 (Fig. 3.11). In intermittent ridge areas, shape and layout difference created slope lengths of 12 and 24 m for the same catchment area (Fig. 3.12). Because of the techniques and treatments, this difference is considered to be a positive factor. Tanks of adequate size were used to accommodate runoff from moderate to high runoff events. The runoff plots were also used to measure the sediment loss from the plots. Runoff and sediment in the tanks were measured after every runoff event. This method lumps the runoff at plot scale.

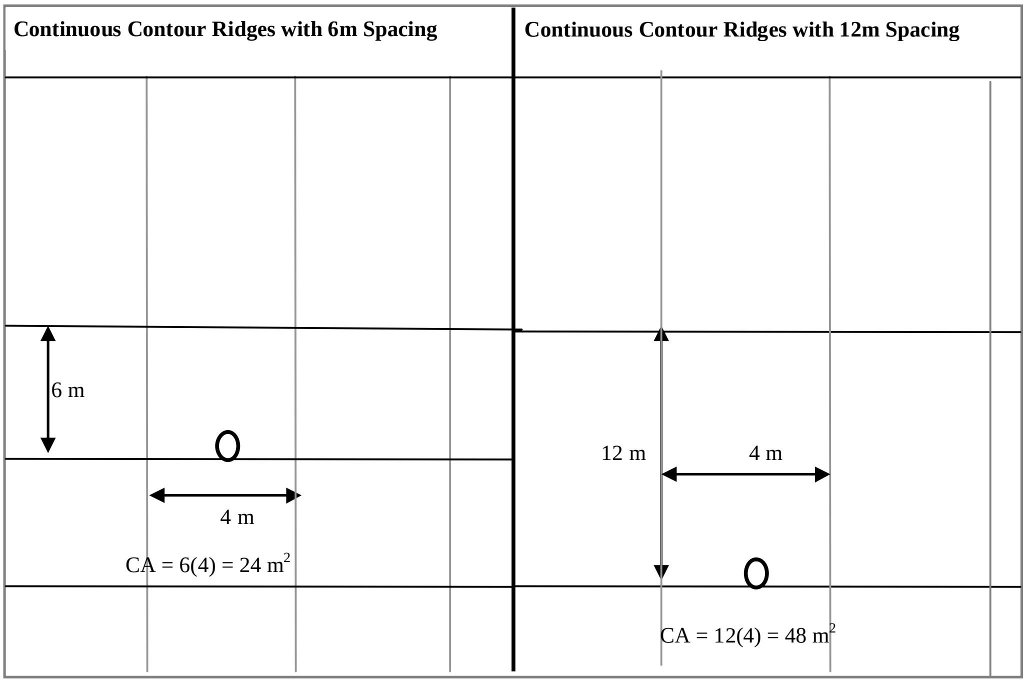

Figure 3.11. Typical Layout of Runoff Plots in Continuous Contour Ridge Area

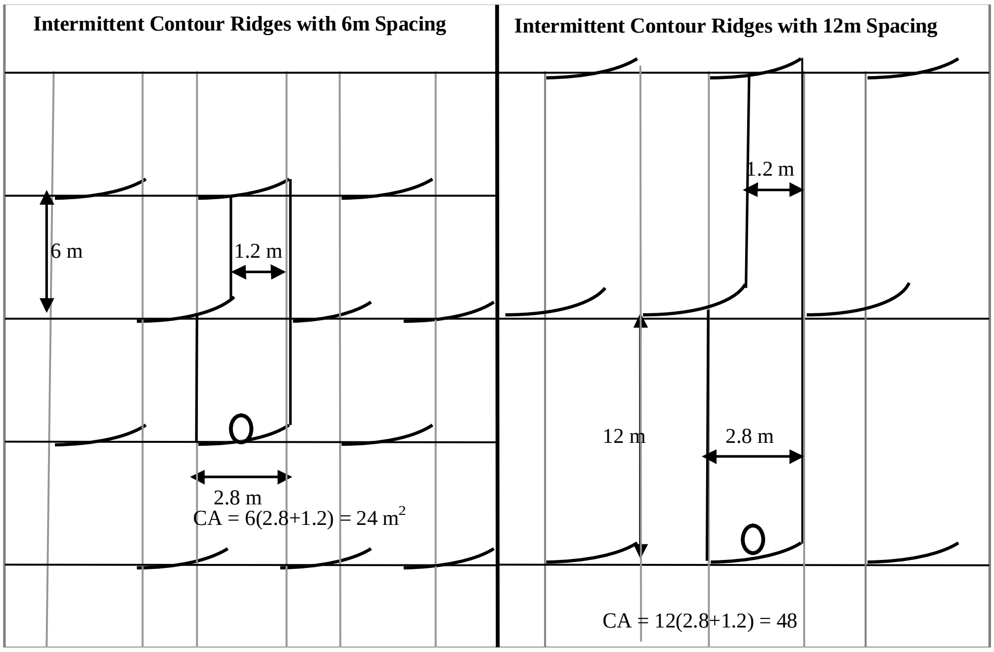

Figure 3.12. Typical Layout of Runoff Plots in Intermittent Contour Ridge Area

3.7.2 Runoff Assessment at the Site Scale by Soil-Water Accounting and Water Balance

Direct runoff measurements at site-scale (100 ha) were difficult due to i) entire site does not drain at one outlet point, ii) variations in micro-relief, soils and drainability add heterogeneity and complexity and iii) it requires bigger structure for water storage. Therefore, indirect runoff measurement approach based on soil-water accounting and water balance was used to estimate runoff at this scale. MCWH by concentrating runoff from a catchment to a target area downslope creates a micro hydro-environment. The water balance approach accounts for a change in soil-water storage in this micro-environment and relates this change to incident rainfall, evapotranspiration and deep percolation. The net difference in the soil-water storage in the target and the catchment areas was considered as the runoff from the micro-catchment. Integrating the soil-water changes in the micro-catchment and the planted areas resulted in the runoff from that area at the site scale. The water balance approach in this study is explained by considering a micro-catchment area of sloping length (L_s) bounded by upper and lower ridges, runoff area (R_a) and runoff collection basin or catch-basin (R_b) at the lower end with shrub plantation (Fig. 3.13).

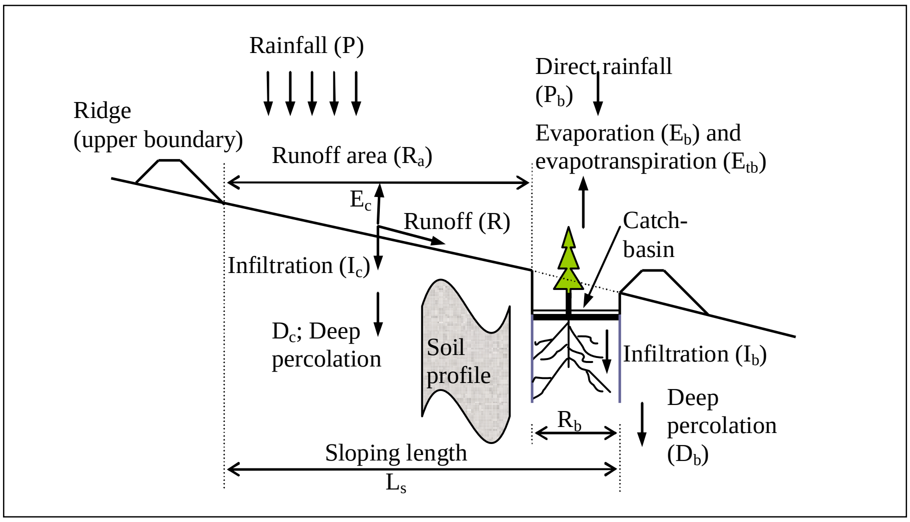

Figure 3.13. Rainfall, Runoff and Infiltration Processes in a Micro-catchment

The rainfall on micro-catchment (*P*) transformed into runoff (*R*) after infiltration in the catchment (I_c), retention into micro-relief (S_c), evapotranspiration (*Eto*) and deep percolation (D_c). The runoff (*R*) was collected into a catch-basin and was subjected to evapotranspiration (*Eto*), infiltration (I_b) and deep percolation (D_b). Rainfall on catch-basin (P_b) directly contributed to basin storage. The water balance equation for the micro-catchment can be written as:

$$P = I_c + D_c + Eto + S_c + R \tag{3.10}$$

The soil-water for this study was measured for soil layers from 1–15 cm by gravimetric means, 15–30, 30–45 and 45–60 cm by using pre-calibrated neutron probe.

$$I_c = I_{c(layer1)} + I_{c(layer2)} + \ldots\ldots + I_{c(layer,n)} = \sum_{i=1}^{i=n} I_{c(i)} \tag{3.11}$$

Soil- water storage was estimated for each incremental layer by using,

$$SWS = (q_{n2} - q_{n1})\frac{D}{100} \tag{3.12}$$

Where *SWS* is soil-water storage (mm), θ_{v1} and θ_{v2} are volumetric water contents (%) and *D* is the thickness of soil layer. The seasonal soil-water storage was determined by summing the increase in soil storage during the rainy season. The water balance equation for catch-basin was derived from reservoir water balance equation,

$$Inflow = Outflow + Change\ in\ storage \qquad (3.13)$$

Considering inflows equal to direct rainfall on catch-basin (P_b) and runoff from micro-catchment (R), outflows equal to evapotranspiration, deep percolation and spills and change in soil-moisture storage in various soil-layer as infiltration transforms into water balance equation for the catch-basin;

$$\underbrace{P_b + R}_{Inflow} = \underbrace{D_b + Eto_b + Spills}_{outflow} + \underbrace{\Delta S_b}_{change\ in\ storage} \qquad (3.14)$$

Where, ΔS_b is change in storage i.e. soil-water before and after rainfall in different soil layers and the spills are the outflows from the catch-basin either occur as overflow or through breaches. All other parameters have been already defined.

Assuming deep percolation and retention in micro-catchment insignificant and infiltration as soil-water storage, the equation 3.10 can be written as

$$R = P - SWS - Eto \qquad (3.15)$$

Where *R* is runoff depth, *P* is rainfall and *SWS* is soil-water storage and Et_o is evapotranspiration, all in mm. RHS of the equation 3.15 is known through measurements. The weather station uses Penman-Monteith, Blaney-Criddle and Evanove methods to calculate evapotranspiration from climatic data (air temperature, relative humidity, wind run and solar radiation). This study used Penman-Monteith method. Runoff was computed from equation 3.15. Knowing the *R* (runoff from catchment) and P_b (rainfall on catch-basin), the LHS of the equation 3.15 (inflows to catch-basin) can be estimated. Change in soil-water storage (ΔS_b) is known by soil-water measurement. Regarding outflows in equation 3.14; deep percolation is rare phenomena and can be ignored at the study site considering rainfall pattern and the type of structures. Evapotranspiration is already known. Therefore spillage can be estimated by using equation 3.14. The spillage from the catch-basin may occur as a result of heavy rain in two ways;

- In the case of continuous contour ridges, the flow in access to the catch-basin will run along the contour ridge as channel flow and is directly beneficial for other shrubs. However, it can cause breaching of the ridge and other consequences.
- In the case of intermittent ridges, the flow in access to the catch-basin is likely to spread downstream acting ground surface as control (weir flow case). This may result little-bit more infiltration in catchment until the flow reaches to downstream catch-basin.

In both the cases, the spillage is useful for other shrubs at the site scale, but flow mechanism will be different. Therefore, averaging soil-water storage can be a better measure of runoff or water conserved by the techniques. The reasons for neglecting water retention and deep percolation in the micro-catchment include:

- Small flow path (5–15m) and smooth topography in the case of MCWH can assume water retention by the micro-relief as zero.
- Surface crusting and low rainfall reduces the infiltration rate. Sheet flow without impoundment also discourages infiltration and thus deep percolation. This is also in-line with the concept of MCWH, where the abstractions in the micro-catchment are minimized in order to induce the runoff in the catch-basin. The soil-water data also supported this assumption.

3.7.3 Catchment-Scale Runoff Estimation by Measuring Stage Hydrograph

The runoff from small catchments at the study site was measured at the outlets of the three catchments. Three small catchments drained by gullies 1, 2 and 3 were selected. It was not possible to find catchments that are totally located in the intervention areas. Therefore, two catchments that were partly covered with MCWH were selected in order to measure the effect of interventions on water and soil loss. The third catchment was located in the control area. Three sharp-crested weirs were constructed and water level loggers were installed to measure runoff depth over the weir (Fig. 3.14). The weirs were designed to operate within one meter of depth of flow over the crest; limit for water level logger. The height of crest from the stream bed (P) was fixed 0.4 m minimum in order to achieve full contraction of nappe for accuracy in measurement. Using Francis formula, estimated the runoff of coefficient 2.08 $m^{1/2} s^{-1}$. Main design parameters of the weirs are given in Table 3.9.

Catchment parameters and shape of observed hydrographs at Weir-1 were used to compute the discharge hydrographs at Weir-2 and 3 that due to instrument fault could not record the first runoff event. The methodology follows a combination of dimensionless hydrograph at Weir-1, peak runoff rates and catchment parameters at weirs 2 and 3. The time parameters for weirs 2 and 3 were estimated from the catchment characteristics including time of concentration, travel time and time to peak. Time of concentration was estimated by using Kirpich equation (1940).

$$t_c = 0.01947 L^{0.77} S^{-0.385} \qquad (3.16)$$

Where, t_c is time of concentration in minutes, L is maximum length of water path in meters, and S is catchment slope.

Figure 3.14. Sharp-crested Weir and Automatic Data Sensor to Record Real-time Stage Hydrograph.

Table 3.9. Main Catchment Characteristics and Weirs Design Parameters.

Catchment/Weir ID	Drainage Area (ha)	Stream Length (m)	Average Slope	Altitudes (m)	Crest Length (m)	P (m)
1 (W-1)	36.3	1993	0.039	852–930	1.35	0.36
2 (W-2)	21.0	1650	0.042	854–923	1.36	0.40
3 (W-3)	5.1	780	0.038	850–880	0.33	0.40

The time of concentration was also estimated by using travel time approach. Summation of travel time (t_t) for overland flow and for stream results in total travel time or time of concentration.

$$t_c = \sum_{i=1}^{i=n} \frac{L_i}{v_i} \quad (3.17)$$

Where L_i and v_i are lengths and velocities in different segments along the drainage path.

Travel time for overland flow was estimated by dividing the length of overland flow by the overland flow velocity. Length of overland flow was estimated from the catchment characteristics and using the following equation estimated the overland flow velocity.

$$v = aS^{1/2} \quad (3.18)$$

Where v is velocity in ft-s^{-1}, and S is slope, a is constant and was used as 10.1 for bare and untilled land. The results were multiplied by 0.305 to convert velocity in m s^{-1}.

The travel time within the stream was estimated from stream hydraulics. The stream velocity was estimated by using Manning formula and stream hydraulic radius. The cross-sections of each stream were measured at five locations and channel representative cross-sections were developed. The areas and perimeters for each stream were computed from the representative cross-sections and dividing area by the perimeters yielded the hydraulic radius. Bed slope of each stream was computed from the measured cross-sections. The travel time of flow within the streams was estimated from the following equation.

$$t_t = \frac{n\,L}{R^{2/3} S^{1/2}} \tag{3.19}$$

Where n is Manning roughness coefficient and was estimated from condition survey of the channels, R is hydraulic radius (m), S is channel slope and L is channel length (m).

The travel time of overland and channel flows were added to get total travel time or time of concentration in seconds. It was converted into minutes for comparison with the travel time computations by using Kirpich equation.

The lag time (l) and time to peak (t_p) were estimated from the following equations.

$$l = 0.6 t_c \text{ (for medium and large catchments)} \tag{3.20}$$

$$l = t_c \text{ (for small catchment: Subramanya, 1994)} \tag{3.21}$$

$$t_p = \frac{\Delta D}{2} + l \tag{3.22}$$

$$t_p = \frac{\Delta D}{2} + t_c \text{ (for the catchments in consideration)} \tag{3.23}$$

Where ΔD is time base of rainfall in minutes.

3.8 Measurement of Erosion by Rainfall-runoff

3.8.1 Erosion Measurement at Plot Scale

3.8.1.1 Runoff Plot Method

The twenty-six runoff plots, as described earlier, for runoff measurement were also used for measurement of sediment loss from those plots for various rainfall conditions. Steel tanks at the outlet of each plot collected the eroded soil. The sediment sample from each tank was collected after each runoff event. The sediment laden water was stirred and well mixed at the time of sampling. The samples were weighed and oven-dried at 105°C. The dry weight of sediment from sample was used to estimate total sediment in the tank in proportionate to water. Three slope lengths (6, 12 and 24 m) resulted from the MCWH ridges.

3.8.1.2 Gerlach Trough Method

A Gerlach trough is a two meters long metallic channel or sediment collecting gutter (Fig. 3.15). The 2-m long inlet opening converges into five splitters of 2.5 cm each at the outlet point. Five splitters (12.5 cm) and 4 recesses (10 cm) totals 22 cm outlet plate width. The height of each splitter is equal to the height of the trough. One splitter is provided with a steel cylinder (6.9 cm diameter) that is connected to sediment collecting jute bag. The bag allows water flow and retains sediment. The other four splitter discharge water freely at downstream. A cut channel at downstream end guide the surplus flows to the outlet channel. The collected sediment from one splitter is multiplied by 5, in order to get total sediment. The Gerlach trough was installed at lowest point of plot. The plot size is kept within the sediment harvesting and runoff disposal capacities of the trough (12.5 cm opening for outflow). A bigger size plot may generate runoff more than the trough capacity that may overflow and results in inaccurate measurements. A cover at the top of the trough protects it from sediment entry from the top and allows cleaning it. Eleven Gerlach troughs were installed on micro-catchments of slopes between 2 and 6% and catchment areas between 11 and 90 m^2.

Figure 3.15. Gerlach Trough for Soil Loss Measurement at Micro-catchment Scale.

3.8.2 Erosion Measurement in Rill and Inter-Rill Scale

3.8.2.1 General

Interrill and rill represent an important component of hillside landscape in marginal dryland. It is a catchment within a catchment, where sediment can generate, transport and deposit. Eroded soil from interrill area (catchment of a rill including upper area that drains down-slope and area between two adjacent rills that drains towards rill) is carried down to rill by the runoff and is routed during its transport at downstream. The erosion and deposition process within the rills depend on its carrying capacity and kinetic energy of inflow. Figure 3.16 shows a typical layout of a rill. Nine rills; five with and four without effect of MCWH were selected. The land slope and catchment areas of the rills vary between 2.5 and 4.5%, and 263 and 1372 m^2, respectively. Interrill erosion was measured by grid-pin method. Erosion and deposition within the rills were measured by graduated ruler frames installed at appropriate cross-sections. Each rill was surveyed and suitable areas for measurement and instrumentation were identified. Three to five cross sections were selected on each rill (Table 3.10).

Table 3.10. Locations, Slope and Drainage Areas of Selected Rills.

Rill no	Block	Technique	Slope (%)	Drainage area (m^2)	No of cross-sections
1	C	Rest	3.0	289	1–1, 1–2, 1–3
2	C	Rest	4.0	935	2–1, 2–2, 2–3
3	C	Rest	3.0	350	3–1, 3–2, 3–3, 3–4, 3–5
4	C	Vi-6	2.5	266	4–1, 4–2, 4–3, 4–4, 4–5, 4–6, 4–7
5	B	Rest	3.0	1372	5–1, 5–2, 5–3, 5–4, 5–5, 5–6, 5–7, 5–8
6	B	Vc-6	3.6	426	6–1, 6–2, 6–3
7	B	Vc-12	4.0	263	7–1, 7–2, 7–3
8	A-B	Vc-12	4.5	293	8–1, 8–2, 8–3
9	C	Vi-12	2.5	431	9–1, 9–2, 9–3

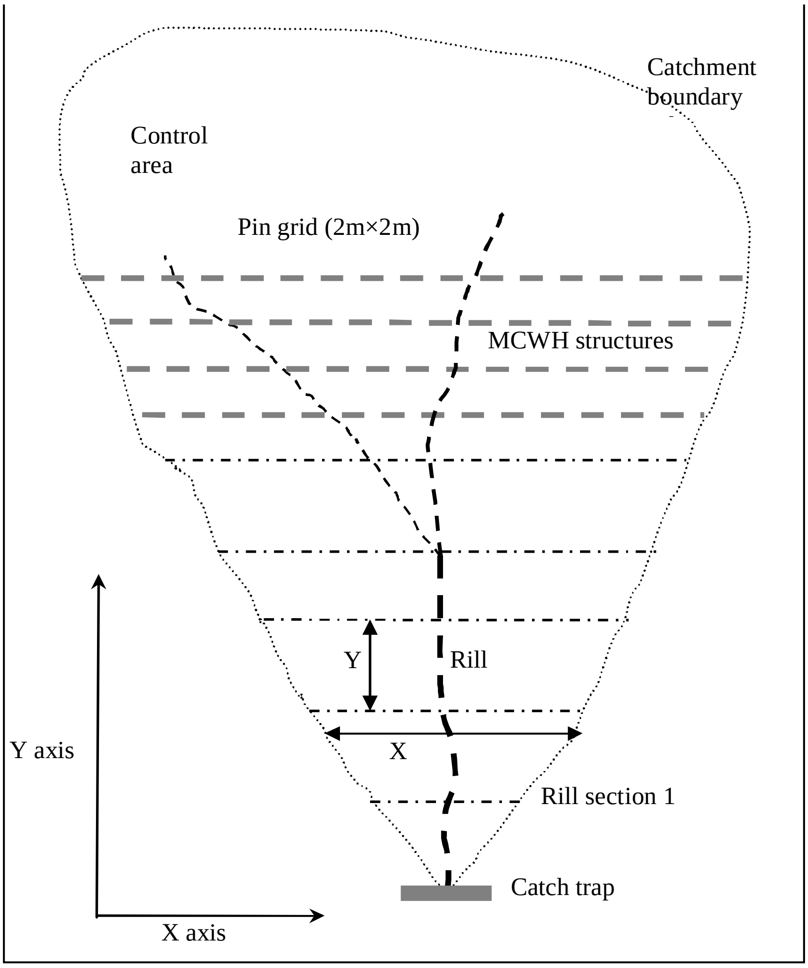

Figure 3.16. A Typical Layout of Rill and Interrill Area with MCWH Structures

3.8.2.2 Measurement of Sheet Erosion by Pin-grid Method in Inter-Rill Area

This method is also known as point measurement method, and it consists of driving a pin into the soil in such a way that the top of the pin gives a datum from which changes in the soil surface level can be measured (FAO, 1993). It requires pins of adequate length. A typical pin length of 30 cm is generally recommended. However, it can vary depending on the soil depth; less for shallower and more for deeper soils. A smaller diameter (5 mm) is preferable in order to avoid the interference of surface runoff and consequently add scour depth. Rectangular or square grid layout on randomly selected locations can be used. Takei *et al.* (1981) measured soil erosion by installing pegs at 2 meters square grid on three 100 m^2 square plots at 30° slope at one month interval. Pin method installed at 1.5 m interval at six profiles lines in 5 ha basin in Colorado, measured the effect of single heavy rainfall event on soil erosion (Hadley and Lusby, 1967). Using metal washer with pins could be advantageous to accurately measure and also to check any deposition, if occurred on the metal washer. However, it may prohibit or reduce the erosion underneath the collar.

The erosion in interrill area was measured by 2×2 m grids of pins. A total of 1335 pins of about 3 mm diameter were installed. The numbers of pins vary between 76 and 333 per rill depending on the catchment size. The cap of each pin was kept 10 cm above the ground surface as a reference for subsequent measurements. The pin area was secured by a boundary rope. The measurement at pin P_i at location X_iY_i and comparing it with the baseline values resulted in erosion (shown by –ve sign) or deposition (+ve values) for each rainfall-runoff event. The average value of erosion/deposition was computed from,

$$e/d = \mu \frac{\sum_{i=1}^{i=n} \{P_i(X_iY_i)\}_{t_0} - \{P_i(X_iY_i)\}_{t_1}}{n} \tag{3.24}$$

Where ***e/d*** shows the average value of erosion ***(-ve value***) or deposition ***(+ve value)*** in the dimension of ***P***, ***P*** is the depth of ground surface from pin-top and t_0 and t_1 show the time of measurement of baseline value and measurements after the runoff event under consideration. For subsequent event the values of the earlier event serve as baseline.

3.8.2.3 Measurement of Erosion/Deposition in Rills Cross-sections

Ruler frames were installed at each section on rills that were used to measure changes in the cross-sections after each runoff event. Thirty-eight ruler frames (3–8 per rill) were installed in order to measure erosion/deposition in the 38 cross-sections on nine rills. The frames were fixed across the sections so that they do not interrupt flow within the rills and provide benchmark for time-variant measurement. The measurement of the cross-sections at the time of installation of frame provided the baseline values. The erosion/deposition (***e/d***) from the measured cross-sections were computed by calculating ***e/d*** at point 1 at time t_0 previous ruler measurement minus the measurement at time t_1 after runoff event from

$$(e/d)_i = \left(r_{t_0} - r_{t_1}\right)_i \tag{3.25}$$

Where $(e/d)_i$ is erosion (-ve sign) or deposition (+ve value) at i^{th} point and r_{t0} and r_{t1} are time-variant measurements of change in section at that point or ruler measurements. The (***e/d***) at the section under consideration was then computed from

$$(e/d)_{\sec_1} = \sum_{i=1}^{n} \frac{(e_i + e_{i+1})}{2} * \left(D_{i+1} - D_i\right) \tag{3.26}$$

Where $(e/d)_{sec1}$ is erosion (-ve sign) or deposition (+ve value) at section under consideration, e_i and e_{i+1} are erosions at two neighboring points in the section and D_{i+1} and D_i are the distances of the points under consideration from reference point at that section. Summation of e/d at all sections gives the erosion or deposition within the rill.

3.8.2.4 Measurement of Sediment Yield from a Rill Catchment

One sediment trap was built at the outlet of each rill to measure the sediment yield from the rill catchments. The masonry catch traps with cemented-base facilitated the measurement of deposited material. Fig. 3.17 shows the construction of rill trap, where the Bridge Frame can also be seen in the background. The sediment was collected after each runoff event, dried and weighed.

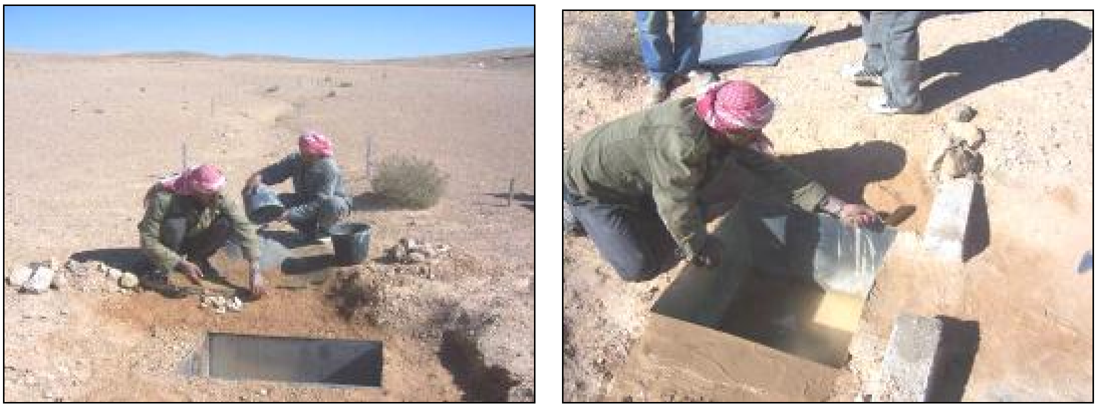

Figure 3.17**.** Catch-trap for Measurement of Sediment Yield at Rills Scale

3.8.3 Erosion Measurement at Catchment Scale

Catchment-scale sediment delivery was measured in three streams upstream of purposely constructed weirs for runoff and sediment measurement (see section on runoff measurement). Two weirs represented the area under the effect of MCWH, while the third under control conditions. However, ground-truth, unsuitability of upper catchments for MCWH and human-induced modifications to land use did not allow to selecting a catchment under the strict effect of MCWH. A pin-grid network was installed. Benchmark information before sediment deposition at weirs locations were collected. The sediment deposition was measured after every runoff event (Fig. 3.18). The sediment data was analyzed.

Figure 3.18. Sedimentation at Immediate Upstream of a Weir

3.8.4 Measurement of Decay of Runoff Ridges

The decay of runoff ridges is important for determining their effective life and maintenance requirements. The impact of raindrops on sloping and relatively loose shoulders of the ridges causes their decay. Runoff ridges at 24 locations were randomly selected for various treatments. A rill bridge frame (RBF) was designed, manufactured in ICARDA workshop and they were fixed on the selected locations (Fig. 3.19). The RBF was also modified in order to enhance the accuracy in the measurements. The ridge height was measured on a monthly basis.

Figure 3.19**.** Bridge Frame for Ridge-decay Measurement

3.8.5 Mathematical Modeling of Soil Loss Assessment with RUSLE2

3.8.5.1 Model Concepts

Universal Soil Loss Equation (USLE) was upgraded by incorporating new erosion information that had accumulated since the publication of Agriculture Handbook 537 (Wischmeier and Smith, 1978) and to specifically address the application of USLE to land uses other than agriculture. This has resulted in fully computerized technology of Revised Universal Soil Loss Equation (RUSLE) as described in Agriculture Handbook 703 (Renard *et al.*, 1997). RUSLE2 estimates the soil loss from hill slopes. Best results were obtained by using this model on 3 to 20% slopes. It computes soil loss from eroded area and sediment delivery by incorporating effects of different land uses and management practices. It takes into account the uniform and complex slope along overland flow path. It computes interrill and rill erosion, sediment yield from overland flow slope length and sediment yield from terrace channels and simple sediment control basins.

3.8.5.2 Model Structure

RUSLE2 is an advance version of RUSLE and RUSLE1.06 models that computes average annual soil loss on the i^{th} day as:

$$a_i = r_i\, k_i\, l_i\, S\, c_i\, p_i \tag{3.27}$$

Where a_i = average annual soil loss for ith day per unit area (Mg $ha^{-1}yr^{-1}$), "r_i" is rainfall erosivity factor for the i^{th} day, "k_i" is soil erodibility factor, "l_i" is the slope length factor, "S" is slope steepness factor, "c_i" is cover-management factor and "p_i" is supporting erosion control practices, all on i^{th} day. Slope steepness factor is same for every day. Values of these factors are average annual for a particular day—not for the year. Factors *l, S, c* and *p* are dimensionless and "*a*" has a time period of "*r*" and soil loss dimension of "*k*". Since *k* represents mean annual soil loss per unit of *r*, *a* has the same units as *K*. Thus, if *k* is in Mg ha^{-1} for one unit of metric r, multiplication by metric *r* value will give the value of *a* in Mg ha^{-1}.

RUSLE2 is based on the assumption that net detachment caused by single storm is directly proportional to the product of storm's energy E and its maximum 30-minute intensity I_{30}, which allow summation to get monthly and annual loss. This also assumes a linear function. Average annual erosivity is the sum of the storm erosivities over n number of years.

$$R_j = \frac{\sum_{n=1}^{N} \sum_{j=1}^{J(m)} (EI_{30})_j}{N} \tag{3.28}$$

Where *R* is average annual erosivity, EI_{30} is the erosoivity of individual storms, *j* is an index for each storm, *J(m)* is number of storms in the m^{th} year, and is an index for the year. Total energy for a storm is computed from

$$E = \sum_{k=1}^{m} e_k \Delta V_k \qquad (3.29)$$

Where e is unit energy (energy per unit of rainfall), ΔV is rainfall amount for the k^{th} period, k is an index of periods during a rain storm where intensity can be considered as constant, and m is number of periods. Unit energy is computed by

$$e = 0.29[1 - 0.72\ \exp(-0.082i)] \qquad (3.30)$$

Where e is unit energy (energy per unit of rainfall), ΔV is rainfall amount for the k^{th} period, k is an index of periods during a rain storm where intensity can be considered as constant, and m is number of periods. Unit energy is computed by

The coefficient in the above equation (-0.082) was modified for RUSLE2 model. Brown and Foster (1987), used -0.05 in the original equation. Average annual *R* value was also estimated from rainfall data 1997–2006 (Observed by rain gauges at MRC and the study site). The main model structure consists of database for climate, topography, soil and land use.

3.8.5.3 Model Suitability

RUSLE can be used for estimating a wide range of land uses. The RUSLE predicts interrill and rill erosion from rainfall and associated runoff. It is a useful tool for conservation planning, inventory and assessment. However, soil loss values estimated by RUSLE should better be used for comparisons rather than being considered as absolutely accurate erosion rate. RUSLE computes the average annual interrill and rill erosions for landscape profiles. Its projection over an area depends on the representativeness of the landscape profile to that area.

Weltz *et al.*, (1987), Renard and Simanton, (1990) and Benkobi *et al.* (1993) noted that the RUSLE computed low soil losses for rangelands. Nevertheless, Renard (1999) found that their method of evaluation, single storm simulations may or may not reflect an annual average as RUSLE is designed to estimate. Renard *et al.* (1996), by comparing RUSLE with USLE saw that the RUSLE technology was superior to USLE, as it modeled the situations, where USLE technology could not be applied.

Nevertheless, the empirical basis of the model may not avoid uncertainties. Inadequate data to make the results verifiable may also reduce its reliability. Despite the weakness, the technology because of its enhanced capabilities of estimating R, K and topographic factors and support practices, greatly improved its reliability to using it in USA and in developing countries. RUSLE model has the flexibility to use readily inbuilt available values of factors in database and modifications/additions in these values are also possible.

The RUSLE2 model can be applied to estimate the soil loss in cropland, pasture and rangelands, disturbed forest land, construction sites and landfills areas. It takes in to account the effects of cover management, surface roughness, ridges, contouring, diversions and terraces. It also covers the effect of impoundment and considers hydraulic elements sequence.

3.9 Shrub Survival and Growth

It is observed that no shrub was germinated from the seeds in the study area. Therefore, the option of raising shrubs by seed broadcasting was not successful. The survival rate of shrubs planted with seedling and their growth rates were measured. A count of all the live shrubs in the trial in May 2005 and then in May 2006, estimated the shrub survival rate. The shrubs' growth was measured three times a year in April, August and December. This covered the main rainfall season (January-April), the dry period (May-August) and the low rainfall period (September-December). Measurement of shrub biomass by standard procedure—cutting and weighing, was not feasible during first three years until the shrubs grew to grazing level. Alternatively, an approach to measure shrub growth/volume at the site was adopted. The shrub canopy was measured through shortest diameter (d_1) and longest diameter (d_2). The canopy height (h) was directly measured from its bottom to top by using flat ruler and tape. The shrub volume was calculated using average diameter to estimate the area multiplied with the canopy height. This assumes that the canopy area remains the same along the height that may differ in reality. On an average 927 shrubs were measured from all the treatments, which was around 20% of the total shrubs.

4. RESULTS AND DISCUSSION

4.1 Rainfall

4.1.1 Annual Rainfall

The main characteristics of the annual rainfall - an indicator of runoff, soil loss and vegetation processes - were estimated from long term annual rainfall data. The rainfall series included the data from Qaryatin village (1958–93), Mahesseh Research Center (1994–2003) and the study area (2004–2007). Plotting the accumulative annual rainfall in relation to time checked the consistency of partial rainfall series (Fig. 4.1). The results show a strong linear correlation (R^2=0.9987). Probability distribution of annual rainfall for the complete (Qaryatin for 35 years) and partial series (Qaryatin + MRC + Study area; 48 years) (Table 4.1) does not show significant deviation. The results favor the use of partial rainfall series for long term trend analysis.

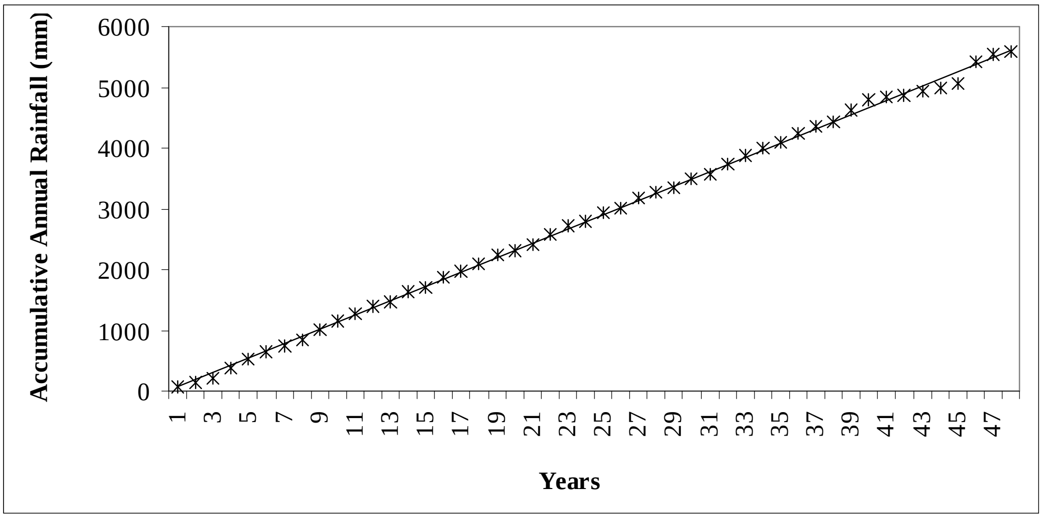

Figure 4.1. Accumulative Annual Rainfall in Relation to Years of Record

Table 4.1. Probability Distribution of the Annual Rainfall.

Rainfall Class (mm)	Mean of Class (mm)	Probability of Occurrence (Qaryatin) (%)	Probability of Occurrence (Qaryatin+MRC+Study area) (%)
0–50	25.0	0	6
50–75	62.5	14	17
75–100	87.5	23	21
100–125	112.5	23	19
125–150	137.5	17	17
150–175	162.5	20	17
175–200	187.5	3	4

The annual rainfall data was also analyzed for main statistical parameters such as mean, standard deviation and coefficients of variance and skewness. The results (Table 4.2) show that the average annual rainfall is 110±42.7 mm and the coefficient of variation is 39%. The standard deviation is high as compared to temperate climates where it varied between 10–20% (Thames, 1989). The annual minimum precipitation during the period of record was 31.1 mm (MRC, 1999–2000) and the maximum was 193.3 mm (MRC, 1996–1997). The annual minimum rainfall was 16% of the annual maximum and about 28% of the average annual rainfall. Annual rainfall varied between 28 and 175% of the average annual rainfall. Based on FAO (1981) criteria[2] the dry, average and wet conditions occurred in the study area for about 30, 59 and 11% of time respectively. The annual rainfall was just 8% of the reference evapotranspiration (Table 3.1). Similarity between mean (110 mm), median (111 mm) and mode (108 mm) shows that rainfall data is normally distributed. A value of coefficient of skewness (C_s) around zero shows that the data is symmetrically distributed across mean.

The Rainfall Anomaly Index (RAI) and the Cumulative Departure Index (CDI) estimated the annual rainfall variability for wet and dry spells and long term trends, respectively. The analysis (Fig. 4.2) shows that RAI varies between -4.6 and +4.4.

[2] FAO (1981) criteria narrate that dry conditions (annual rainfall below 75% of average annual rainfall), average conditions (annual rainfall between 75 and 125% of average annual rainfall) and wet conditions (annual rainfall above 125% of average annual rainfall) prevail.

The rainfall above and below average conditions recurred periodically, with consistent overall deviation. The analysis indicates that drought persisted during 1998/1999 and 2003/2004. The upward and downward movement of CDI (Fig. 4.3a-4.3c) shows the variations above and below the average rainfall. The CDI for partial series (48 yrs) showed an increasing trend (Fig. 4.3a). Similar trend was observed in complete series (35 yrs) (Fig. 4.3b). However, for shorter series (1993–2007), it showed a downward trend (Fig. 4.3c). This appeared due to persistent low rainfall during late nineties and early twenties, when 7 out of 9 years received low rainfall. The CDI analysis indicates a changing trend in annual rainfall.

Table 4.2. Results of Analysis of Long-term Rainfall Data.

Description	Qaryatin + MRC + Study area (48 yrs data)
Mean annual rainfall (mm)	110.2
Standard deviation (s) (mm)	42.7
Coefficient of variance (CV)	0.39
Coefficient of skewness (C_s)	3.1E-05
Annual maximum rainfall (mm)	193.3
Annual minimum rainfall (mm)	31.1
Ratio of maximum to minimum rainfall	6.2
Ratio of mean to minimum annual rainfall	3.2

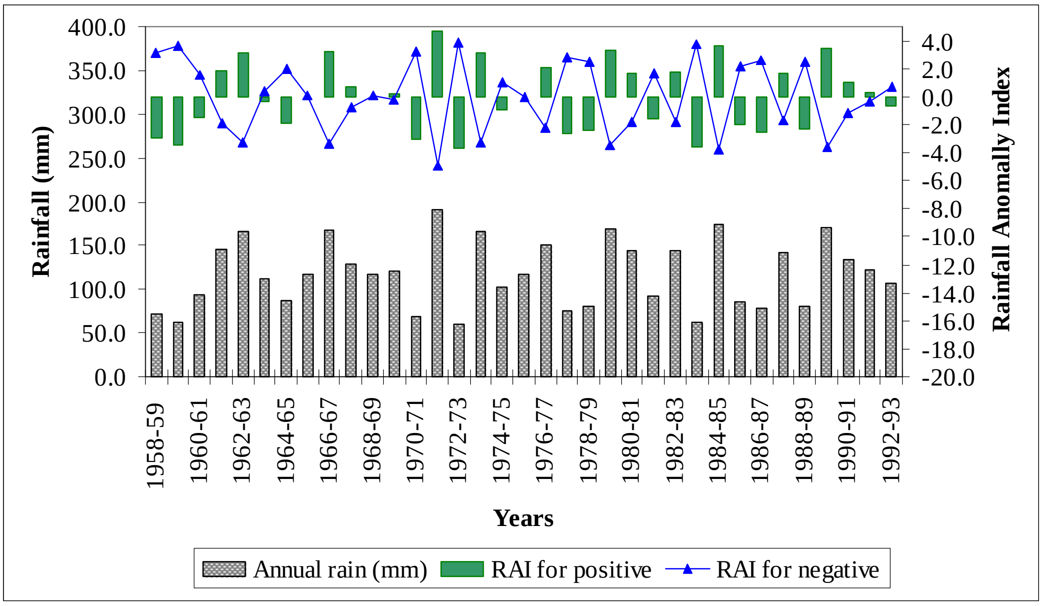

Figure 4.2. Rainfall Anomaly Index (+ve and –ve) for Partial Rainfall Series

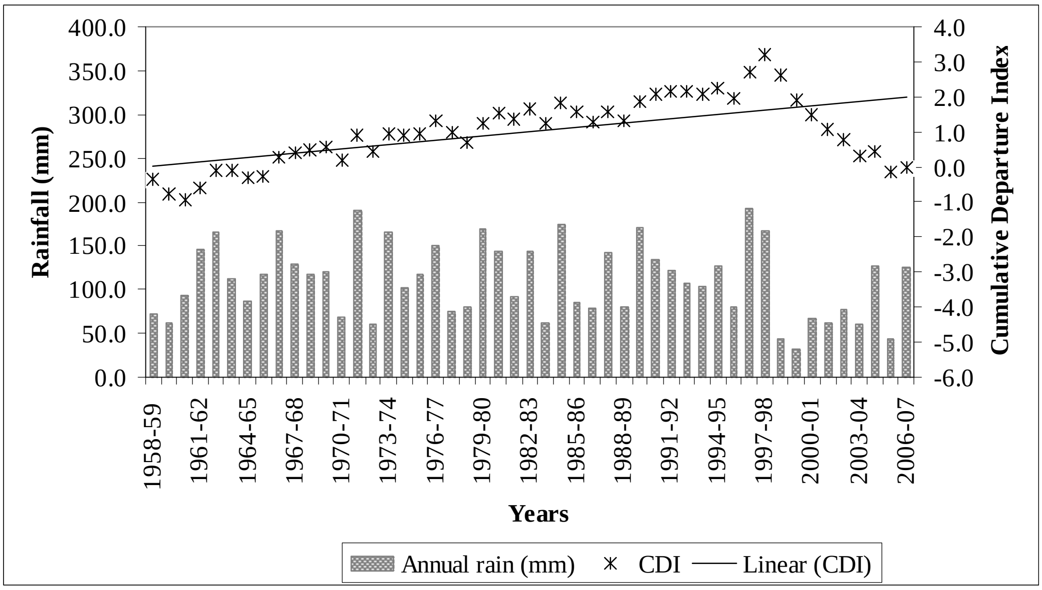

Figure 4.3 (a). Cumulative Departure Index of Annual Rainfall (Partial Series)

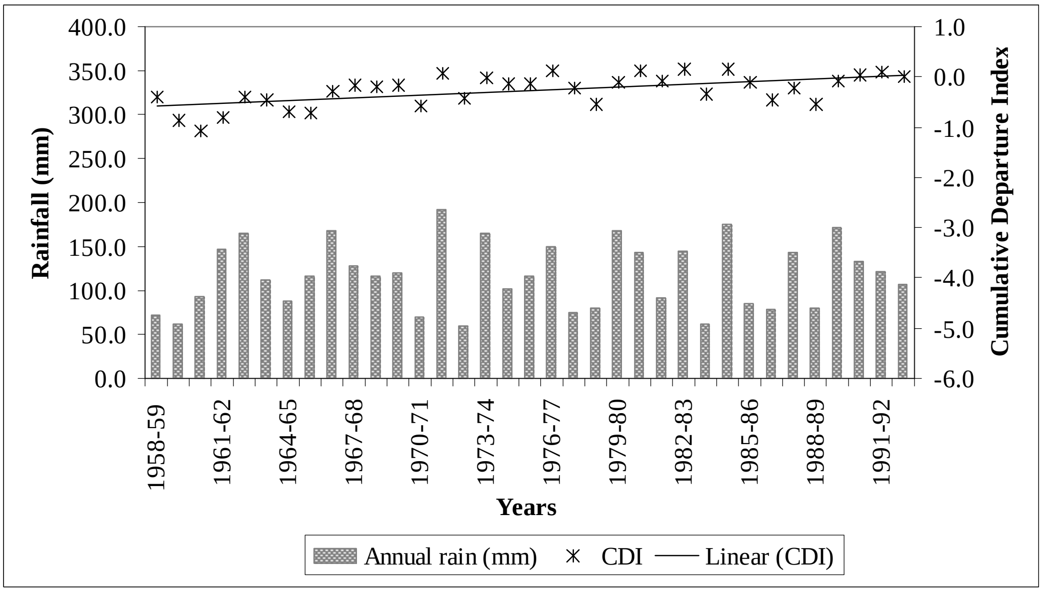

Figure 4.3 (b). Cumulative Departure Index of Annual Rainfall (Complete Series)

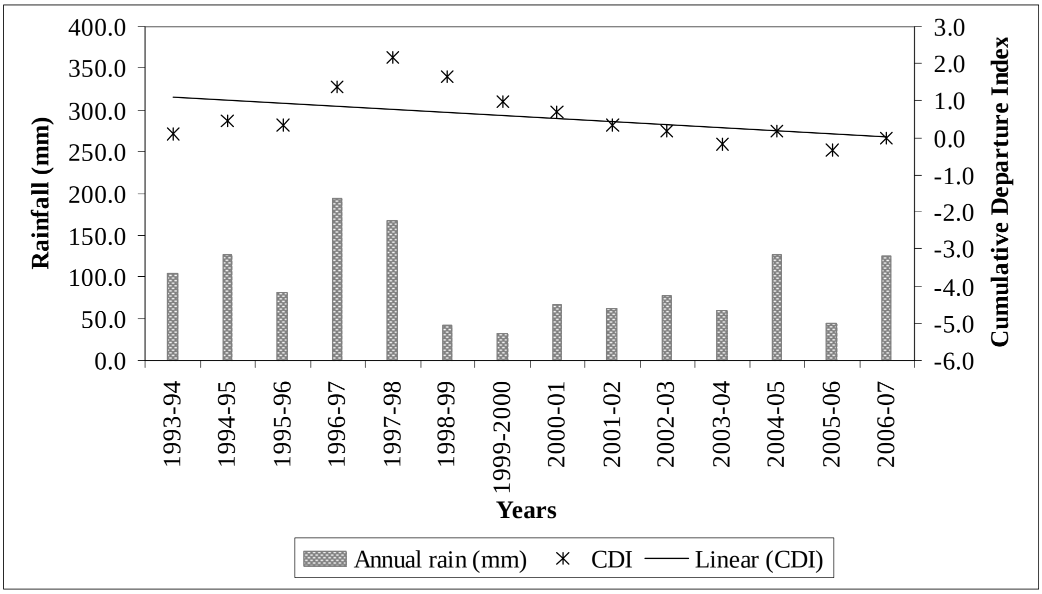

Figure 4.3 (c). Cumulative Departure Index of Annual Rainfall at Qaryatin

4.1.2 Monthly Rainfall

The mean-monthly rainfall in the study area (Table 4.3) shows September as dry period and December, March and April as low rainfall months as compared with long term average. The average annual rainfall during the study period was 89.5 mm (about 76% of long term average annual). However, reasonable rainfall in October, November, January, February and May shows fairly good seasonal distribution. Rainfall-evapotranspiration ratio (P/E_o) is an important indicator of the availability of soil-water to the plants. Monthly rainfall-evapotranspiration ratio (Fig. 4.4; Table 3.1) shows May to October as soil-moisture stress period. UNESCO (1977) climatic zoning, on the basis of rainfall-evaporation ratio, describes the study area at the margin of arid to hyper-arid environments. This environment poses limitation to plant survival and growth without additional water. It reveals that P/E_o varies between zero and 38% round the year. Reasonable P/E_o (25–38%) in a period from December to March, low in April and November (12–15%) and very low during May, September and October is an indicator of the temporal distribution of soil-moisture over a year. Monthly rainfall varies between 2.5% to about 40% of monthly evaporation and is more critical. Dry period from May to September also posses stress to crop growth.

Table 4.3. Monthly Rainfall (mm) in the Study Area

No	Year	Month												Annual
		Sept	Oct	Nov	Dec	Jan	Feb	Mar	Apr	May	Jun	Jul	Aug	
1	2003–04	0.0	0.0	24.8	4.4	24.2	1.6	4.2	0.4	0.8	0.0	0.0	0.0	60.4
2	2004–05	0.0	2.6	40.4	14.1	21.7	25.6	1.0	8.2	13.8	0.1	0.0	0.0	127.5
3	2005–06	0.0	2.4	7.5	2.2	14.4	7.6	0.2	9.2	0.6	0.0	0.0	0.0	44.1
4	2006–07	0.0	32.8	0.3	2.3	3.3	10.0	19.2	9.2	48.8	0.0	0.0	0.0	125.9
Mean monthly		0.0	9.5	18.3	5.8	15.9	11.2	6.2	6.8	16.0	0.0	0.0	0.0	0.0
Long term Mean-monthly		0.3	8.0	14.4	12.8	13.5	14.5	20.9	11.9	14.7	0.2	0.0	0.0	110.6

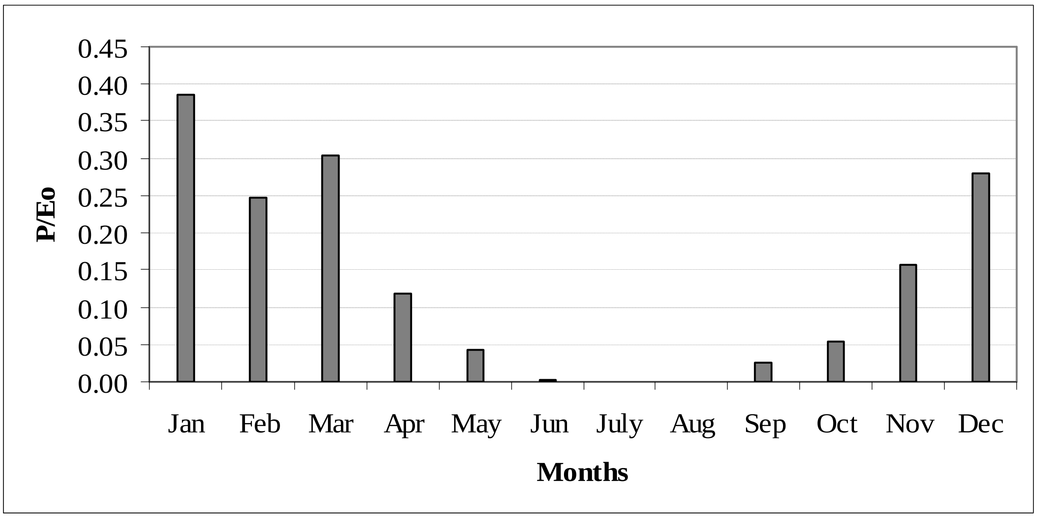

Figure 4.4. Precipitation to Evapotranspiration Ratio (P/E_o) at Qaryatin

4.1.3 Major Rainfall Events during the Study Period

Eight runoff producing rainfall events occurred during the study period. The events during 2006/07 contributed to about 66% of the annual rainfall. Remaining 34% of the rainfall occurred in the form of light showers, which was consumed as initial catchment abstractions. The rainfall data was analyzed for rainfall amount, duration, intensity and antecedent moisture conditions (Table 4.4). These parameters are important to know infiltration, runoff and soil loss processes. The rainfall events were separated by 6 hours rainless period between the two consecutive events (Foster, 2003) and dry antecedent conditions for 5 days rainless period (USDA-SCS, 1972). The rainfall amount varied from 2.9 to 21.8 mm and rainfall intensities varied from 0.12 to 3.3 mm h^{-1}. Four events occurred with wet antecedent moisture conditions.

Table 4.4. Summary of Major Rainfall Events during Study Period.

Rainfall Event	Rainfall Amount (mm)	Rainfall Duration (hours)	Rainfall Intensity (mm h^{-1})	Percentage of Event to Annual Rainfall (%)	Antecedent Conditions
4 May, 2005	13.1	4.66	2.8	10	Dry
4 Apr, 2006	6.1	12.0	0.5	14	Wet
2 Oct, 2006	5.1	3.5	1.5	4	Dry
24 Oct, 2006	21.1	12.9	1.6	17	Dry
15 Feb, 2007	2.9	24.6	0.12	2	Wet
1 Mar, 2007	15.4	7.25	2.1	12	Wet
12 May, 2007	17.1	12.0	1.4	14	Dry
17 May, 2007	21.8	6.6	3.3	17	Wet

The rainfall event on 15th February 2007 is not included in the analysis due to very low intensity and amount. However, it added soil-moisture and created favorable conditions for runoff generation. Event-wide analysis (Figs 4.5 to 4.11) showed that the event on 4th May 2005 occurred in dry antecedent conditions and poured 13.1 mm rainfall (Fig. 4.5). The storm duration was 4 hours and 40 minutes and average rainfall intensity of the storm was estimated 2.8 mm h^{-1}. The peak rainfall was 0.5 mm. The rainfall occurred in 5 major clusters of less than 6 hours gap that is used to separate rainfall events. The rainfall event on 4th April 2006 (Fig. 4.6) amounted to a rainfall depth of 6.1 mm. Prior events conditions were dry for 3 days and slight rain occurred on day 4 and 5 before the event. A rainfall of 2.0 mm occurred about 10 hours prior to the start of the major event on the same day. The duration of this small event was about 3.5 hours and average intensity was estimated about 0.5 mm h^{-1}. The main rainfall event started at 19:43 hours sharply rose to 0.8 mm in 2 minutes and poured 4.1 mm rainfall in 9 minutes. This resulted in rainfall intensity about 27 mm h^{-1}. The rainfall occurred in one cluster and the peak rainfall was 0.8 mm. The rainfall event on 2nd October 2006 amounted to a total rainfall of 5.1 mm in 3.5 hours (Fig. 4.7). The average intensity of this event was estimated about 1.5 mm h^{-1}. The antecedent conditions were dry. The peak rainfall was 1.5 mm and the rainfall occurred in two clusters. The rainfall event on 23rd and 24th October, 2006 amounted to 21.1 mm rain (Fig. 4.8). Its duration was about 12 hours and 50 minutes and its average intensity was estimated about 1.6 mm h^{-1}. Antecedent conditions prior to this event were dry. The peak rainfall was 1.5 mm. The rainfall occurred in six clusters. The rainfall event on 1st March, 2007 amounted to 15.4 mm rain (Fig. 4.9). Its duration was about 7 hours and 15 minutes and its average intensity was estimated about 2.1 mm h^{-1}. It occurred in the form of five clusters. The antecedent conditions prior to this event were wet.

The rainfall event on 12th May, 2007 amounted to 17.1 mm rain (Fig. 4.10). Its duration was about 12 hours and its average intensity was estimated as 1.4 mm h^{-1}. Antecedent conditions prior to this event were dry. The rainfall event on 17th May, 2007 poured 21.8 mm rain (Fig. 4.11). Its duration was about 6 hours and 35 minutes and its average intensity was estimated as 3.3 mm h^{-1}. Antecedent conditions prior to this event were wet.

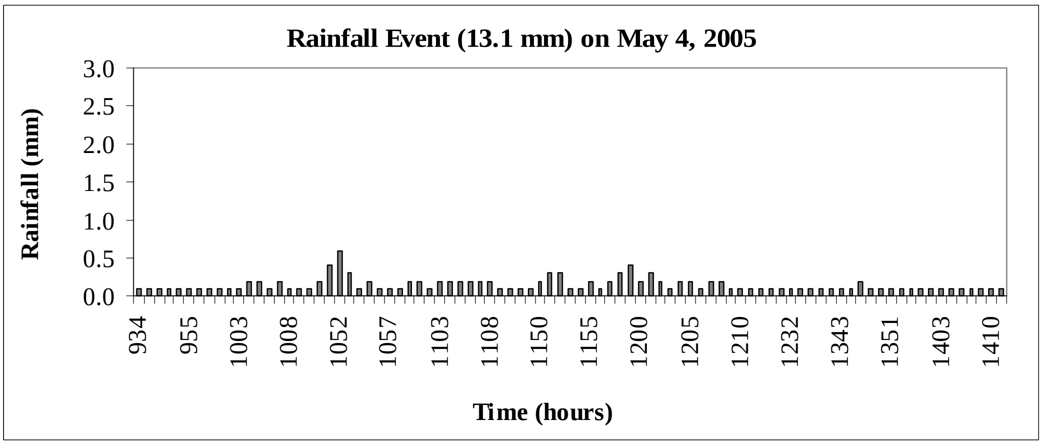

Figure 4.5. Rainfall Hyetograph on 4th May, 2005

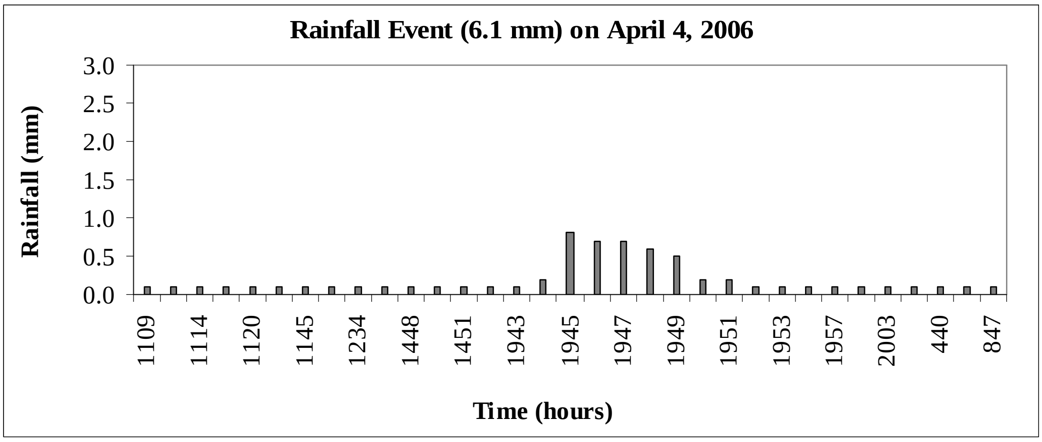

Figure 4.6. Rainfall Hyetograph on 4th April, 2006

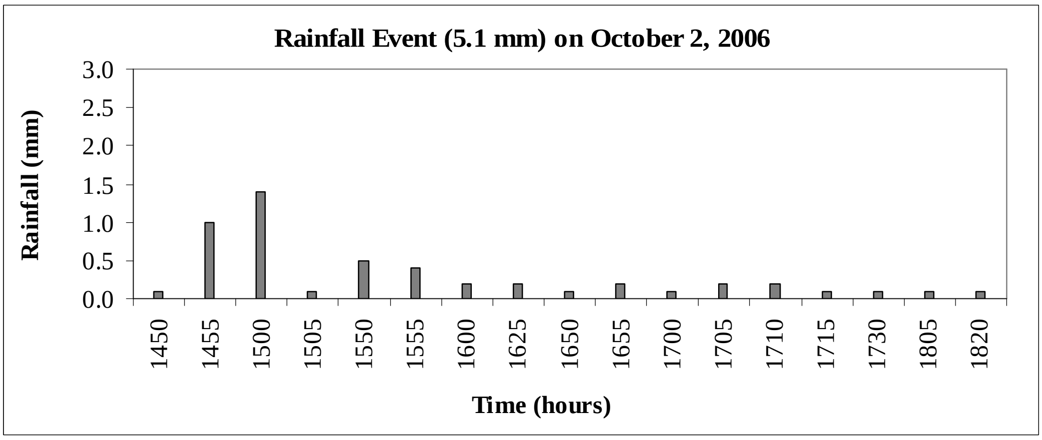

Figure 4.7. Rainfall Hyetograph on 2nd October, 2006

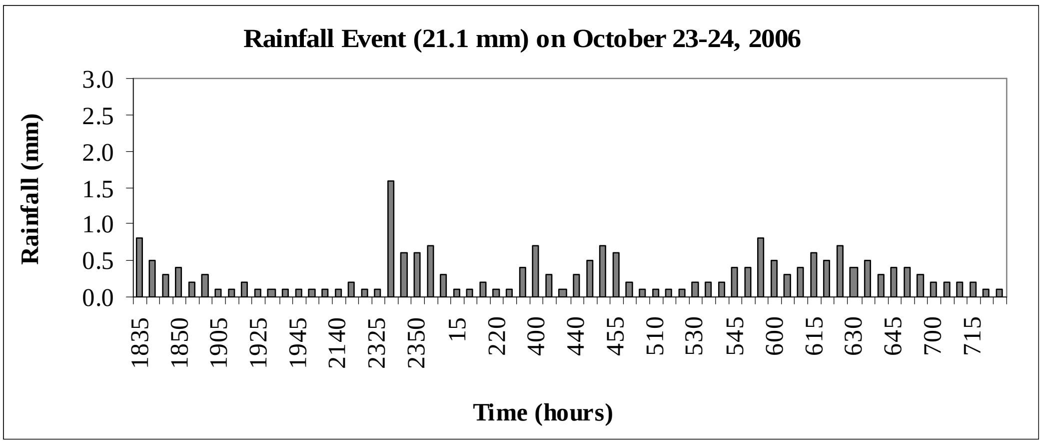

Figure 4.8. Rainfall Hyetograph on 23rd and 24th October, 2006

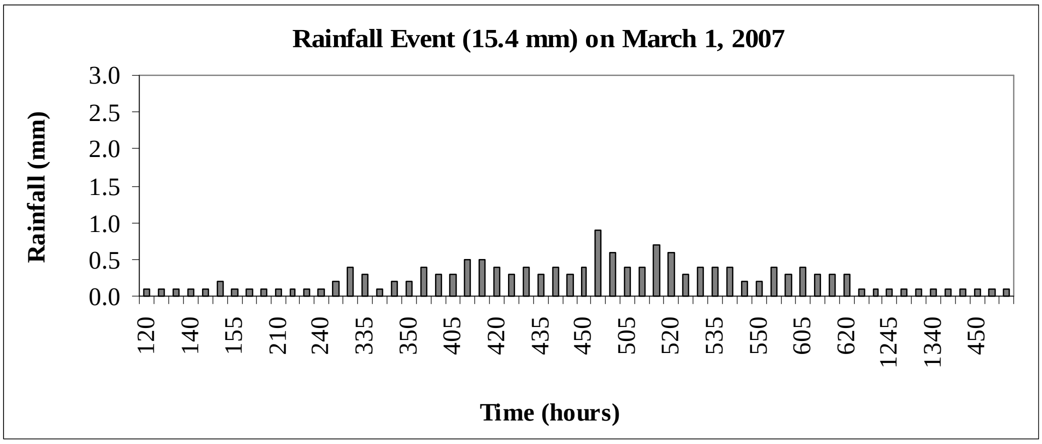

Figure 4.9. Rainfall Hyetograph on 1st March, 2007

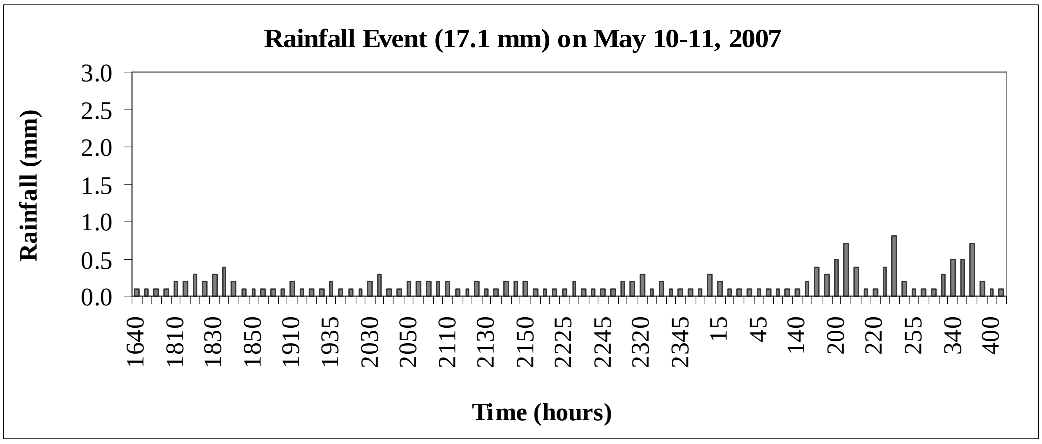

Figure 4.10. Rainfall Hyetograph on 10th and 11th May, 2007

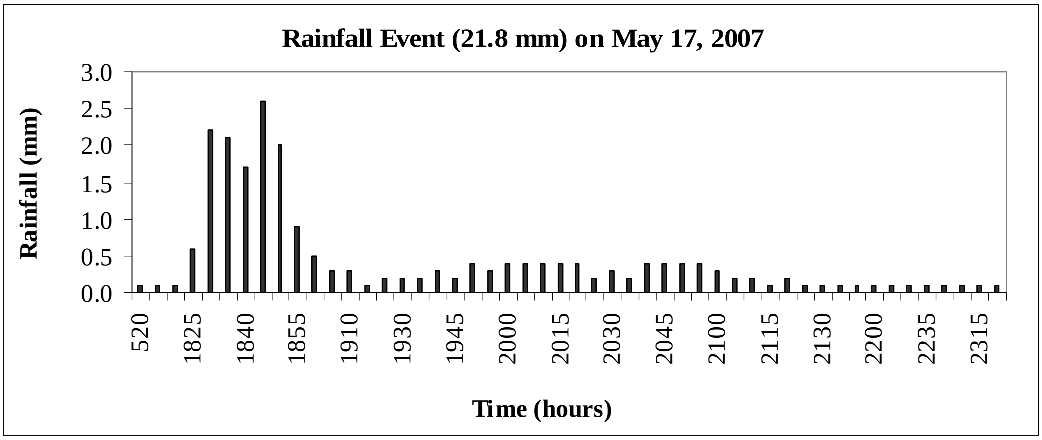

Figure 4.11. Rainfall Hyetograph on 17th May, 2007

4.2 Soil

4.2.1 Soil Properties

Results of depth-integrated soil samples (Table 4.5) showed sand and clay contents around 50 and 30%, respectively. USDA soil texture criteria describe the soil in the sandy-clay-loam domain. Clay contents slightly increase and sand decreases with depth. This soil has moderate water holding capacity. Comparing the soil properties at research site with critical values (Adepetu and Adebusyi, 1985; Sobulo and Adepetu, and Adepetu, 1990), show that total nitrogen is almost half the critical value (0.11% or 1100 ppm) and plant available P (Olsen-P) varied between 4 and 9 ppm and decreased with depth. A value of available P less than 6 ppm is considered as critical and between 6 ppm and 10 ppm, it requires fertilization for better crop. Landon (1984) reported that soil is saline if EC value exceeds 4 dS m^{-1} (0–2 salt free, 2–4 slightly saline, 8–15 moderately saline and >15 strongly saline). This type of soil is common in arid regions. Organic matter less than 2% are considered deficient. Exchangeable potassium (K) is higher than the critical value (0.2 meq/100g or 2 meq/L), which rank as medium to high fertility. The results also show that plant available nitrogen (NO_3^- and NH_4^+) vary with depth and location from one block to another block. The results show an overall nutrient deficiency, which increases with depth. Nevertheless, improving the fertility by artificial means for fodder shrubs in dryland farming is not a practice in the study area. The pH value ranges from 7.5 to 8.3. Field capacity and permanent wilting point (PWP) shows plant available water between 14 and 16% in top layer, 20 and 21% in mid layer and 18 and 21% in lower layer.

4.2.2 Bulk Density

The bulk density of the study area varies between 1.03 and 1.26 gcm^{-3} with an average of 1.13 g cm^{-3} (Table 4.6). The increase in soil density with depth corresponds to increase in clay contents with depth. The soil densities greater than 1.4 g cm^{-3} for clay and 1.6 gcm^{-3} for sand could have deleterious effects on plant growth (Ryan *et al.* 1997). Results show that the measured bulk density is within the range of the standard bulk density (Table 3.5) and compaction is not a major problem in the study area.

Table 4.5. Some Physical and Chemical Properties of the Soil at the Study Area (Sampling date: June 2005).

Block	A			B			C		
Sample no.	1	2	3	4	5	6	7	8	9
Sample depth (cm)	0–20	20–40	40–60	0–20	20–40	40–60	0–20	20–40	40-60
Total N (ppm)(Kjeldahl)	658	648	572	549	475	565	502	506	419
Olsen-P (ppm)	7.2	5.7	7.3	8.3	4.8	5	8.8	5.9	4.1
Gypsum	None	None	None	None	None	None	None	None	None
Mechanical Analysis									
Clay: <0.002 mm(%)	31.5	32.7	37.8	23.8	29.1	30.4	23.8	34.1	36.8
Silt: 0.002¯0.05 mm (%)	17.8	19	16.6	15.2	17.8	14	12.7	19.1	16.7
Sand: 0.05-2.0 mm (%)	50.7	48.3	45.6	61	53.1	55.6	63.5	46.8	46.5
Texture	SCL	SCL	CL	SC	SCL	SCL	SCL	SC	SC
Mineral Nitrogen									
NO_3-N (ppm)	2.28	5.3	2.67	11.38	12.2	2.81	3.24	5.09	9.11
NH_4-N (ppm)	12.77	20.6	16.79	9.46	22.09	19.14	8.18	16.47	17
Min-N (ppm)	15.05	25.9	19.46	20.84	34.29	21.95	11.42	21.56	26.11
pH (saturated paste)	7.5	7.5	7.7	8.3	7.7	7.7	8.2	7.7	7.7
EC (mS/cm)	7.7	18.3	14.9	0.78	12.01	13.8	1.4	12.66	16.6
Organic matter (%)	1.18	1.25	1.12	0.96	0.91	1.01	0.84	0.94	0.8
Potassium (K) (meq/L); 1 meq/L = 10 meq/100 g									
Extractable K	8.74	5.67	4.15	9.78	4.63	3.92	8.4	5.4	2.67
Soluble K	1.17	0.87	0.39	0.28	0.5	0.43	0.28	0.46	0.11
Exchangeable K	7.57	4.8	3.76	9.5	4.13	3.49	8.12	4.94	2.56
Calcium (Ca) (meq/L)									
Extractable Ca	176.8	189.4	181.8	166.7	166.7	156.6	166.7	166.7	176.8
Soluble Ca	20.2	52.1	38.3	2.7	23.4	23.4	4.3	29.8	35.1
Exchangeable Ca	156.6	137.3	143.5	164	143.3	133.2	162.4	136.9	141.7
Magnesium (Mg) (meq/L)									
Extractable Mg	54	51	56.2	54.5	52.1	50.2	54.5	49.7	73.3
Soluble Mg	16.1	39.1	39.2	3	34.4	28.6	6.5	28.1	34.5
Exchangeable Mg	37.9	11.9	17	51.5	17.7	21.6	48	21.6	38.8
Sodium (Na) (meq/L)									
Extractable Na	33.64	65.1	51.3	4.36	58	55.72	10.22	43	86.02
Soluble Na	8.19	22.74	19.11	0.62	15.79	20.52	1.61	17.08	22.74
Exchangeable Na	25.45	42.36	32.19	3.74	42.21	35.2	8.61	25.92	63.28
Chlorides (Cl) (meq/L)	71.49	178.72	139.57	2.77	112.34	125.96	13.62	117.45	156.6
Sulphate (SO_4) (meq/L)	6.01	11.76	9.18	2.23	7.21	17.17	3.86	9.18	5.84
CO_3 (meq/L)	0	0	0	0.1	0	0	0.05	0.05	0.05
HCO_3 (meq/L)	1	1	1.4	1.05	1	1.15	1.2	1	1.1
Field capacity (FC) %	26.6	32.8	30.7	28.6	31.5	29.7	26.7	32.4	34.8
Wilting point (PWP) %	12.0	12.0	11.9	10.9	11.9	11.1	11.4	11.2	13.3
Available moisture (%)	14.6	20.8	18.6	17.7	19.4	18.6	15.3	21.2	21.5

SCL = Sandy clay loam; CL = Clay loam; SC = Sandy clay

Table 4.6. Depth-Integrated Bulk Density at the Study Site.

Sampling Depth (cm)	Mean Bulk Density (g cm^{-3})
0–15	1.03
15–30	1.10
30–45	1.12
45–60	1.26
Average	1.13

4.2.3 Soil Properties in Relation to Water Erosion

Soil erosion is a function of soil physical and chemical properties. Two main systems were covered that include inter-gully area and gully banks, and gully cross-sections. Sheet flow is a main characteristic of inter-gully areas. Stream flow dominates in gullies. Results of soil samples analysis (0–5 cm from surface) for soil texture (Table 4.7), show that sand (particle size 0.05–2.0 mm) dominates (more than 60%) followed by silt (≈ 20%) and clay (≈ 15%) contents. According to USDA soil classification guidelines, the soil texture is sandy loam, which is most vulnerable to crust formation (Morgan, 1995). High sand (76.4%) and low silt (9.7) percentage in gully bed area and low sand (54%) and high silt percentage (29%) in near-gully area along banks is due to two different flow process - stream flow within the gullies and sheetflow in inter-gully areas prevail. High kinetic energy of concentrated flow transports coarser particles from catchment and deposits in gullies when flow carrying capacity drops down. Nevertheless, low carrying capacity of the sheetflow in inter-gully areas can only carry fine particles and deposit them in near-gully areas along banks, where sheetflow kinetic energy reduces due to change in slope. Poesen (1985) showed that particles between 0.063 mm and 0.25 mm because of minimal energy requirement for their transport are vulnerable to detachment. The results showed that more than 60% of the material falls in this range, which also infers erosive tendency of these soils.

Results of samples for chemical properties (Table 3.2) show that organic matter varies between 0.8 and 1.25%. Evans (1980) showed that soil with less that 3.5% organic contents (= 2% organic carbon) can be considered erodible. Wischmeier and Mannering (1996) also consider the organic matter as the second most influencing property affecting soil erodibility after soil texture. Results indicate the susceptibility of the soil to erosion.

Table 4.7. Soil Texture of Surface Samples (0–5 cm Depth; November, 2005).

No	Location	Clay (%) <0.002 mm	Silt (%) 0.002-0.05 mm	Sand (%) 0.05-2.0 mm	Texture	Very fine sand 0.05-0.1 mm (%)	Fine sand 0.1-0.2 mm (%)	Medium & coarse sand 0.2-2.0 mm (%)
1	Gully bed	13.88	9.68	76.44	SL	17.53	37.91	21.01
2	Gully sides	16.25	13.67	70.08	SL	18.54	30.62	20.92
3	Gully bank	16.72	29.19	54.09	SL	22.99	8.46	22.65
4	Intermittent ridge 1	14.47	14.91	70.63	SL	22.87	26.46	21.29
5	Intermittent ridge 2	14.78	18.55	66.67	SL	20.83	25.03	20.82
6	Intermittent ridge 3	13.47	17.26	69.27	SL	23.93	25.21	20.13
7	Continuous ridge 1	15.34	22.35	62.31	SL	22.63	19.42	20.25
8	Continuous ridge 2	15.84	21.97	62.19	SL	21.19	20.97	20.03
9	Continuous ridge 3	16.53	22.15	61.32	SL	21.08	19.34	20.91

SL = Sandy loam

4.2.4 Aggregate Stability and Soil Erosion

Assessment of the structural properties of discrete soil aggregates is fundamental to understanding soil erosion processes. The aim of aggregate stability tests is to give a reliable description and ranking of the behavior of soils under the effect of water and management. Response of soil aggregates to rainfall in wet condition (wet aggregate) is important for water erosion. This process conceptually refers to a system where dry aggregates at the soil surface are wetted, flooded and subjected to the disruptive action of both the flowing water and the eroding particles being suspended and carried in the water runoff. Wetting can weaken or disintegrate soil aggregate by disrupting cationic bridging, ionic hydration, and osmotic swelling force water in between clay platelets, separating them and causing aggregate swelling and wetting. Water soluble bonding materials can also destabilize aggregates. Macro-aggregate analyses used a proportion of soil sample retained on sieve sizes varying between 0.1-10 mm. The size distribution of the water-stable aggregates is essentially a measure of aggregate stability, in that the aggregate retained on the various sieves must have remained stable during the wetting and sieving process (Jastrow and Miller, 1991). In addition to analyzing the stability of macro-aggregates, the stability of the micro-aggregates was also analyzed to know the clay behavior (dispersible clay, but not appropriate to describe the flocculation-dispersion behavior of soil clays). The micro-aggregate analysis used the percentage of the soil finer than 2 mm. Both the analyses were carried out for soils within the gullies, along the gully banks and in the intervention areas between the gullies.

The results of wet-sieving analysis for micro- and macro-aggregates are given in Table 4.8. The results show that fine micro-aggregates (< 0.2mm) were about 54% in the gullies, 66% along the gully banks and 70% in intervention area. The coarser micro-aggregates (> 0.5 mm) were about 23% in the gullies, 18% along the gully banks and 16% in intervention area. A similar pattern can be seen in the case of aggregates between 0.2 and 0.5 mm. The results of micro-aggregate analysis depict 3–5 times higher percentage of finer material as compared with coarser material. It indicates moderate to high susceptibility of water erosion. Higher percentage of coarser material in gullies as compared with intervention area could be due to erosion in the channel, which washed away finer particles. Similarly, the erosion could also be responsible for lower percentage of finer material in gullies as compared with the intervention area.

The results of macro-aggregate analysis also showed lower percentage of coarser and higher percentage of finer aggregates. The finer aggregates (< 0.2mm) were about 62% in gully beds and 76–81% in intervention area. The coarser aggregates (>0.5 mm) were about 11 and around 7% in intervention area. Interestingly, no water stable aggregate was retained on sieve of 1 mm size. It is a special characteristic of the soils in the study area. Both the micro- and macro-aggregate analysis follows similar trends.

Soil aggregate size determines infiltration and runoff and depends on many factors including soil texture, clay mineralogy, organic matter, cations, ferrous and aluminum oxides, and calcium carbonate ($CaCO_3$). Aggregate stability increases with increased clay content (Gollany *et al.* 1991) and decreases with increased silt (0.002–0.05 mm) and sand (0.05–0.10 mm) fraction (Wischmeier and Mannering 1996. Ben-

Hur *et al.* (1985) found that the medium-textured soils (silt and loamy soils) are often more susceptible to crusting and erosion. Nevertheless, breakdown of course aggregate and surface sealing and crusting is an indicator of soil erosion rather than a clear relationship.

Table 4.8. Water Stable Aggregate (%) Retained on Different Sieve Sizes in the Micro- and Macro-aggregate Analysis (Sample depth 0–5 cm; Sampling date: November, 2005)

No	Locations	Micro-aggregate (%)			Macro-aggregate (%)		
	(mm)	>0.5[1]	0.5–0.2[1]	< 0.2[1]	>0.5[1]	0.5–0.2[1]	< 0.2[1]
1	Gully bed	23.3	22.8	53.9	11.3	26.4	62.3
2	Gully sides	23.4	22.0	54.6	14.8	26.7	58.5
3	Gully bank	18.1	15.8	66.1	7.1	16.6	76.3
4	Intermittent ridge1	14.3	14.0	71.7	6.5	15.3	78.3
5	Intermittent ridge2	16.5	15.3	68.3	6.8	16.6	76.6
6	Intermittent ridge3	14.2	12.5	73.4	5.5	13.4	81.1
7	Continuous ridge1	14.1	14.7	71.3	5.4	16.1	78.4
8	Continuous ridge2	16.6	14.6	68.8	6.8	16.1	77.2
9	Continuous ridge3	18.9	14.6	66.5	8.1	16.0	75.8

[1]of water stable aggregate; the values in the table represent average of three replicas

4.2.5 Soil-Water

4.2.5.1 Temporal Variability

Analysis of soil-water in 90 cm deep soil profile captured some of the observed seasonal variations (Fig. 4.12). The study area received 27 rainfall events in 2005–2006 and 2006–2007. Thirteen events produced local-scale runoff. Nevertheless, the results do not show visible increase in soil-water as a result of rainfall events in 2005. Low rainfall, dry antecedent conditions and weak runoff in micro-catchment were responsible for the insignificant change in the soil-water storage. Increasing trend in soil-water during January and February 2006 was due to frequent rainfall events during this period. The rainfall pattern resulted in wet antecedent moisture conditions that helped to generate runoff in micro-catchment and increase in soil-water storage in plant area. Following these relatively wet month, the sharp rise in soil-water in plant area in April, 2006 can be linked to wet antecedent conditions in previous month and intensive rainstorm on 4th April, 2006. The soil-water continued to drop in May to October 2006, when minimum soil-water was near to wilting point.

Soil-water started increasing with rainfall event on 4th and 5th October, 2006, continued to rise in October following rainfall event on 25th October, 2006. In November 2006, the soil-water was gradually decreased due to rainless period and it maintained a level in December 2006 to February 2007 as a result of low rainfall showers. Rainfall on 28th February, 2007 boosted up the soil-water, which touched to the peak of the season in May 2007.

The results indicate low soil-water in summer from May to September and reasonably good soil-water in winter during October to April with some exceptions of low spikes that reflect a longer dry period between subsequent rains. The second important phenomenon is low soil-water in micro-catchment area as compared with plant area for almost all techniques and treatments. This was due to runoff inducement by MCWH at plant locations.

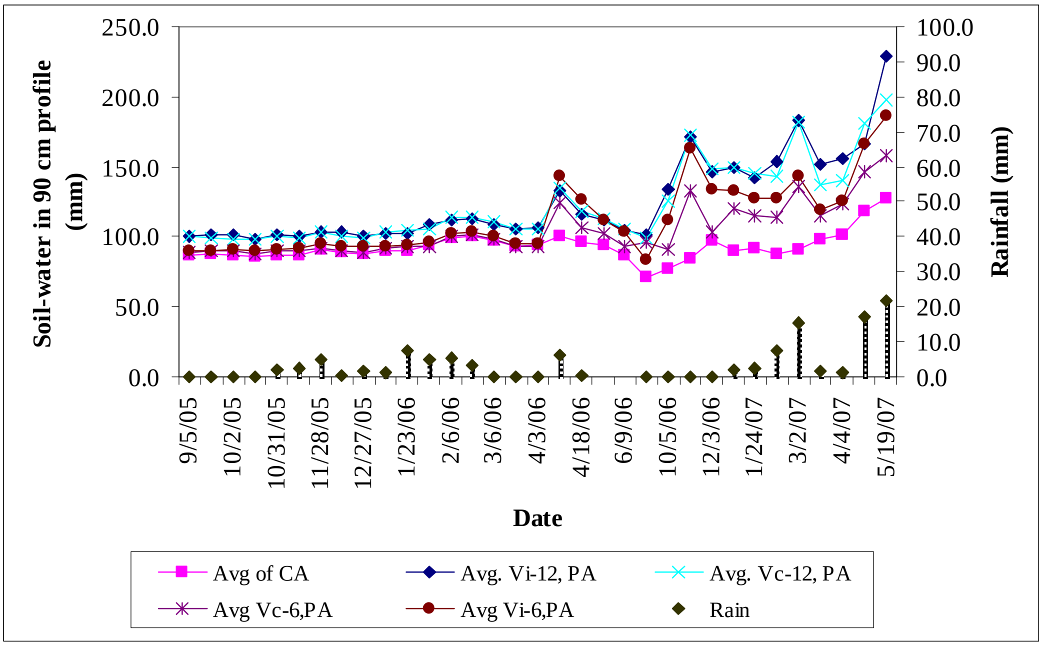

Figure 4.12. Temporal Variations of Soil-Water in Relation to Event Rainfall.

4.2.5.2 Spatial Variability

Spatial variability of soil-water from up to downstream (Blocks A, B and C) was captured by plotting soil-water to a depth of 60 cm in plant areas for two major rainstorms on 6th April and 26th October, 2006 (Fig. 4.13). The location of measurement covered entire site including shrubs and direct seeding areas. Block A, at most upstream has slightly a steeper slope than block C at downstream. The results on soil-water depicted two main features.

- High variations in soil-water in Block A followed by moderate in Block B and mild in Block C.
- Declining trend in soil-water from upstream to downstream (Block A to C).

The first phenomenon can be linked to the variations in micro-relief and relatively high crusting in upper areas. The second phenomenon is inter-related as conditions in upper areas seem to be favorable for local runoff generation and harvesting more water than downstream area. Local fluctuations can be linked to different catchment areas and micro-catchment techniques. Nevertheless, the series show a slight declining trend in soil-water from up to downstream with a poor fitting of regression equation ($r^2 < 0.2$).

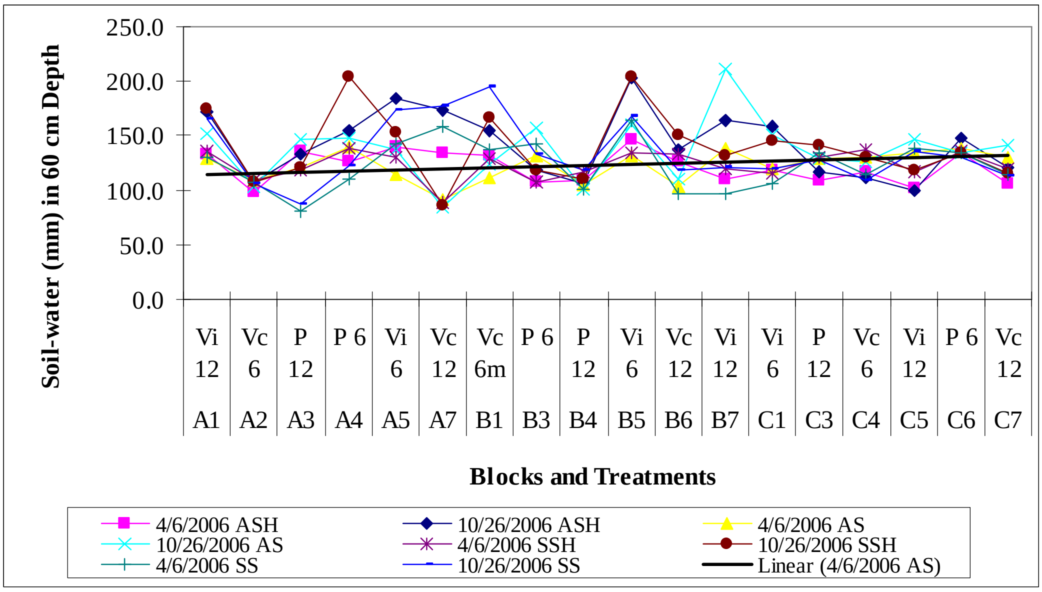

Figure 4.13. Spatial Variability of Soil-water in the Study Area

4.2.5.3 Effect of MCWH Techniques on Soil-Water

The effect of MCWH techniques on soil-water at the study area was gauged by measuring soil-water in catchment and target areas after major rainfall events (Table 4.9). In general, soil-water was low in micro-catchment area and high in planted areas. The effect of catchment area on soil-water showed that 12 m slope length (48 m^2 catchment area) performed better than ridges of 6 m slope length (24 m^2 catchment area) in water harvesting and soil-water storage. It did not show clear difference in soil-water due to techniques based on continuous and intermittent ridges except for two major rainfall events in April and October 2006 and March 2007, where Vi-6 areas performed relatively better than Vc-6 areas. It indicates that intermittent ridges can perform slightly better than continuous for high rainfall events due to their better water spreading capacity. Variation in soil-water for major rainfall events also showed that the soil-water increased from 17 to 70% in planted area with water harvesting as compared to 9 to 58% in catchment area for different rainfalls. For 26 mm rainfall, the increase in soil-water storage in planted area was 1.5–4 times higher than the catchment area for various treatments. It was 1.2–3 times higher for 13 mm and 1.2–1.5 times higher for 8 mm rainfall.

Table 4.9. Changes in Soil-Water in Micro-catchment and Planted Areas

Date	Event Rainfall (mm)	Soil-Water Contents (mm/90 cm) for Various Treatments											
		Vi-12		Vc-12		P-12		Vi-6		Vc-6		P-6	
		CA	PA	CA	PA	CA	PA	CA	PA	CA	PA	CA	PA
4/18/05		97.3	109.7	85.5	90.1	61.3	115.0	103.9	84.2	90.4	77.1	102.0	103.5
4/25/05	8.1	110.9	128.3	94.9	105.4	79.2	133.8	122.5	101.9	105.6	95.8	119.5	126.3
Change in water contents		13.6	18.6	9.4	15.4	17.9	18.8	18.6	17.8	15.2	18.7	17.4	22.8
Increase in water contents (%)		14.0	17.0	11.0	17.1	29.3	16.4	17.9	21.1	16.8	24.3	17.1	22.0
5/2/05		104.7	116.3	91.6	93.9	73.1	119.9	110.7	92.1	98.2	84.9	108.3	109.9
5/5/05	13.1	118.1	142.1	100.1	114.2	84.1	140.2	125.7	109.0	117.5	106.2	121.8	134.2
Change in water contents		13.4	25.8	8.5	20.3	11.1	20.3	15.0	17.0	19.3	21.4	13.5	24.3
Increase in water contents (%)		12.8	22.2	9.2	21.6	15.2	16.9	13.6	18.5	19.6	25.2	12.5	22.1
1/23/06		89.8	102.8	69.5	81.2	59.5	107.6	98.9	78.2	81.8	71.0	97.3	98.3
1/24/06	5.3	96.3	109.1	71.4	84.3	64.0	111.1	99.4	79.4	86.8	74.6	98.7	100.4
Change in water contents		6.6	6.3	1.9	3.1	4.5	3.5	0.5	1.1	5.0	3.7	1.4	2.1
Increase in water contents (%)		7.3	6.1	2.7	3.8	7.6	3.3	0.5	1.4	6.1	5.2	1.5	2.1
4/3/06		94.3	106.6	70.7	81.3	63.1	111.6	101.1	79.3	84.6	73.1	97.5	101.5
4/6/06	6.4	100.9	132.6	77.0	106.4	70.3	135.8	107.5	118.4	91.0	97.6	105.0	126.0
Change in water contents		6.6	26.0	6.2	25.1	7.2	24.2	6.4	39.1	6.5	24.5	7.5	24.5
Increase in water contents (%)		7.0	24.4	8.8	30.9	11.4	21.7	6.3	49.2	7.6	33.5	7.7	24.2
8/28/06		86.0	101.2	56.6	72.8	54.1	102.2	86.8	75.5	75.3	65.7	86.4	92.0
10/26/06	26.2	106.5	171.5	89.3	120.6	79.4	133.0	110.4	158.4	101.0	108.1	109.3	154.2
Change in water contents		20.5	70.4	32.7	47.8	25.3	30.8	23.7	82.9	25.8	42.4	22.9	62.1
Increase in water contents (%)		23.9	69.6	57.7	65.7	46.7	30.1	27.3	109.9	34.2	64.5	26.5	67.5

CA = Catchment area; PA = Planted area

4.2.5.4 Distribution of Water in Soil Layers

Distribution of soil-water in soil layers (15 cm incremental depth) responded differently to rainfall events (Fig. 4.14). There was a substantial increase in soil-water in top layer (0–15 cm) as a result of rainfall events such as in April and October 2006 and March 2007. The high spikes show the trend clearly. This response was less visible in layers 15–30 and 30–45 cm in April 2006. The soil-moisture in 45–60 cm layer responded only to very high rainfall event (October, 2006). Almost straight line behavior for soil layers 60–75 and 75–90 cm shows insignificant effect of rainfall in soil-water changes in these layers. It indicates that the highest soil-water zone was located in the first half of the soil profile. This infers to certain extent hydraulic conductivity, water holding capacity and root water extraction of different layers. It also depicts that the interventions under prevailing rainfall and land use conditions, can only help to store soil-water to a maximum depth of 45–60 cm, effectively and may be suitable for shallow rooted plants.

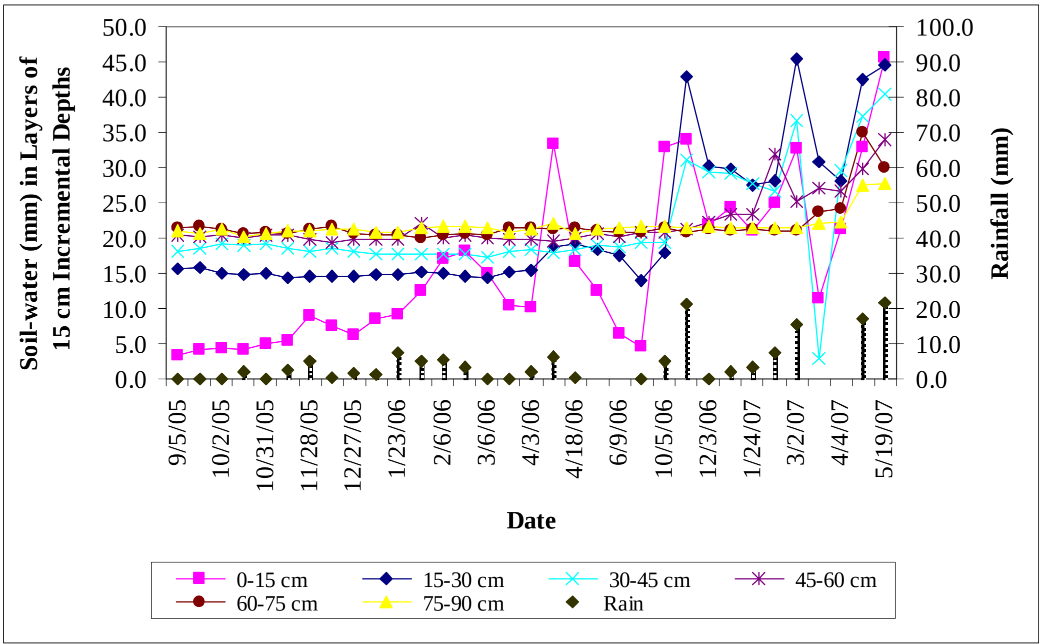

Figure 4.14. Distribution of Soil-Water in Different Soil Layers

The soil-water distribution in soil layers was also analyzed for the highest rainfall event during study period (October 2006) and after long dry period in summer (August 2006). The soil-water distribution after 36 hours of rainfall shows maximum soil-water storage in 15–30 cm layer followed by 30–45 cm layer (Fig. 4.15). The soil-water reduced to a minimum below 60 cm depth. In rainless period (June to August, 2006), the soil-water was between 10 and 20 mm in 15–30 and 30–45 cm soil layers (Fig. 4.16), which is a dominant rhizosphere. The soil-water during rainless period was below wilting point (13%) for most of the treatments. It shows water stress and plant dormant period. Nevertheless, it showed a critical situation in catchment area, when soil-water was less than or equal to wilting point even with rainfall. Soil-water below wilting point in micro-catchments minimizes the possibility of survival of shrubs under control conditions. On the other hand, the high soil-water contents in planted area for dominant period showed the strength of water harvesting by the micro-catchments.

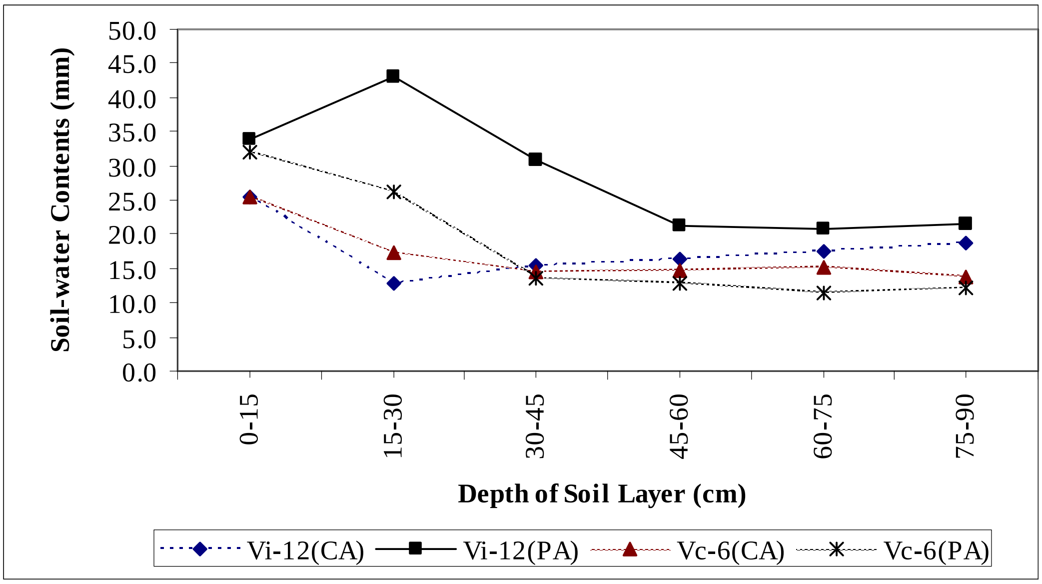

Figure 4.15. Soil-water Distribution after 36 hours of Rainfall on 24th Oct, 2006

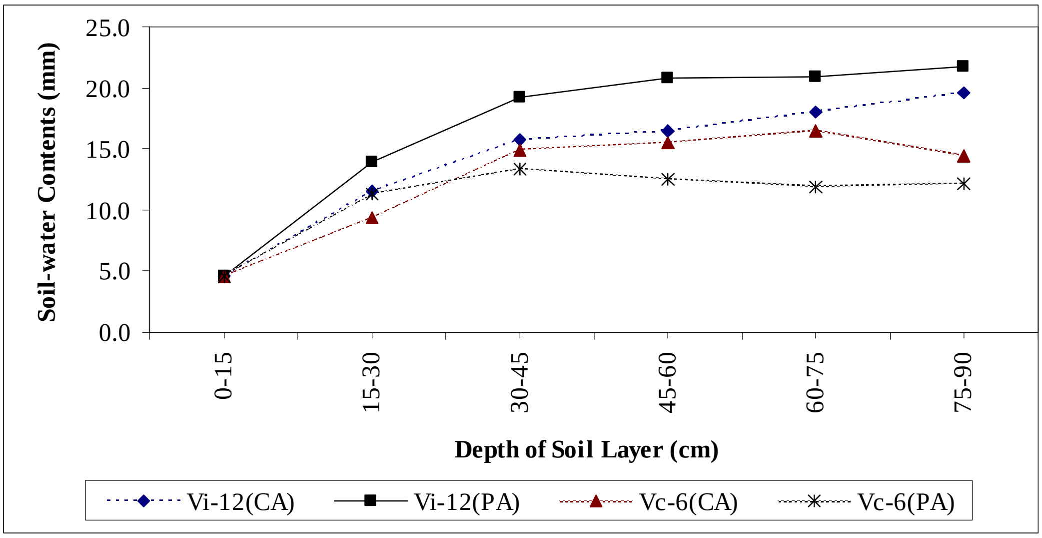

Figure 4.16. Soil-water Distribution during Rainless Period (28 August 2006)

The following points can be noted from the results

- Soil-water was many times higher in the planted area than micro-catchment
- The soil-water responded to the rainfall events. The response was obvious for the big storms, but unclear for weak rainstorms.
- Temporal variability of the soil-water was very clear for dry and wet periods, but spatial variability did not show clear trend.
- The soil-water variations were prominent in the first two top layers (0–15 and 15–30 cm), moderate into the third layer (30–45 cm), visible only for highest event in the fourth layer (45–60) and insignificant change in the 5th (60–75 cm) and 6th (75–90 cm) layers.
- The soil-water was high in the first 3 layers after rainfall, when it was very low during dry period and vice versa.

4.3 Runoff Assessment

The results of runoff measurement and analysis at three spatial scales are presented for various rainfall events occurred during the study period. The spatial scales included micro-catchment, site and catchment.

4.3.1 Runoff Assessment at Micro-catchment Scale

The analysis of five runoff producing rainfall events was carried out to estimate runoff yield and runoff coefficient. The runoff coefficient is an indicator of transformation of rainfall into runoff through catchment actions. The event-wide analysis is as follows.

4.3.1.1 Runoff Event on 4th May, 2005

A rainfall of 13.1 mm generated this runoff event. The event was measured in 12 plots of semi-circular and Vallerani intermittent shaped ridges having 6 and 12 m spacing. Two important water indicators—runoff yield and runoff coefficient, were plotted for micro-catchment area. The results show that runoff yield increases and runoff coefficient decreases with the increase in micro-catchment area (Fig. 4.17). Runoff yield represents the total runoff volume generated on the micro-catchment; therefore, it is logical that it increases with an increase in area. Reduction in runoff coefficient with increase in micro-catchment area is due to increased abstraction loss and reduced runoff per unit area. Power equations poorly fit to the data, which show relatively higher dependency of dependent variables (runoff yield and runoff coefficient) on other independent variables such as antecedent moisture conditions, soil characteristics and rainfall amount and intensity. High scatter in data was considered responsible for the poor fitting. Runoff yield per unit area is also a good indicator of rainfall-runoff relationship. Estimation of unit runoff yield in relation to MCWH techniques and treatments (Fig. 4.18) does not show any specific trend.

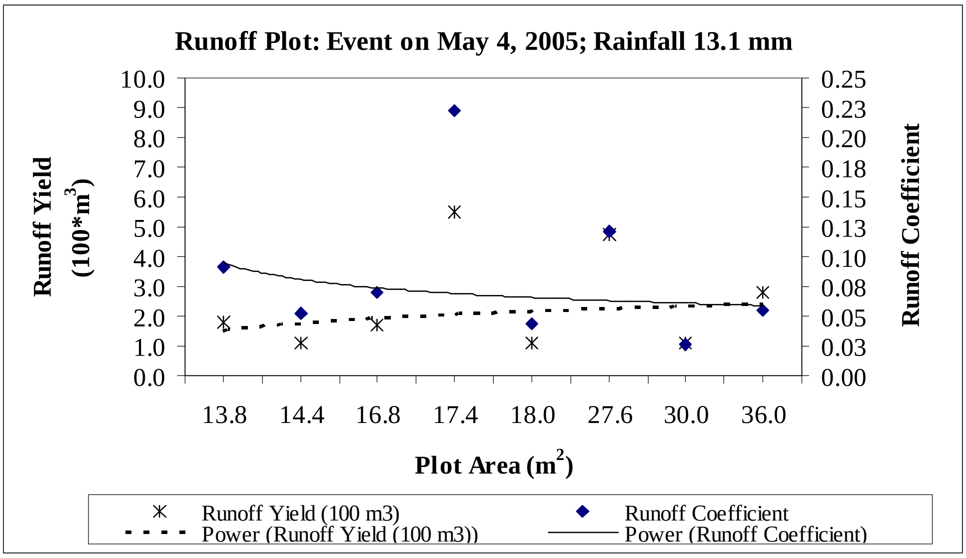

Figure 4.17. Runoff Yield and Coefficient for Different Micro-catchment Areas

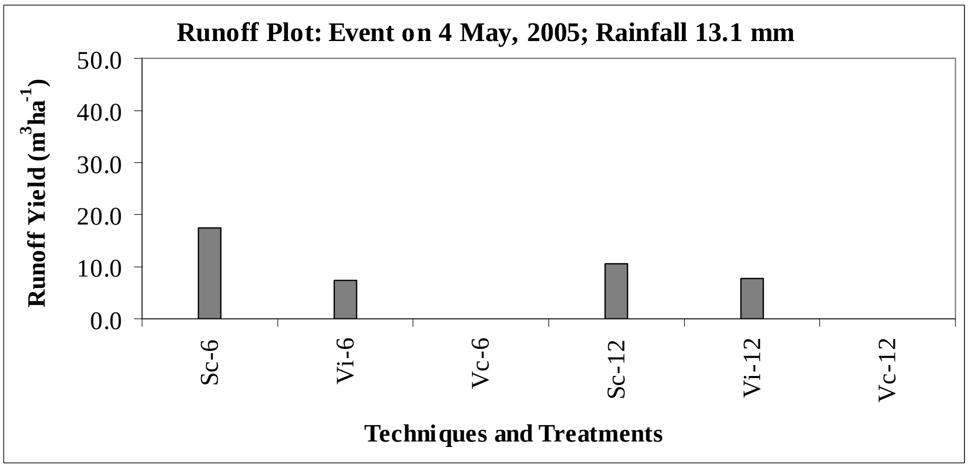

Figure 4.18. Runoff per Unit Area for MCWH Techniques and Treatments

4.3.1.2 Runoff Event on 4th April, 2006

Rainfall of 6.1 mm with wet antecedent conditions generated this runoff event. A micro-catchment of runoff yield and runoff coefficient shows that runoff yield increases and runoff coefficient decreases with the increase in micro-catchment area (Fig. 4.19) The runoff yield varied from about 0.05 m^3 to about 0.2 m^3 for micro-catchment area between 14 and 50 m^2. Power equation of the form $y = 3.4857x^{0.3784}$ ($r^2 = 0.1769$) poorly fits to the data. Where ‘x’ is catchment area in m^2 and ‘y’ is runoff yield in 100 m^3. The data of runoff coefficient in relation to micro-catchment area was highly scattered. A linear equation of the form y = -0.0105x + 0.6477 (r^2 = 0.046) poorly fit to the observed data. Where 'y' is runoff coefficient and 'x' is already defined. Average runoff yield for different MCWH techniques and treatments (Fig. 4.20) shows that runoff yield per unit area (m^3ha^{-1}) is higher for MCWH techniques with 6 m spacing as compared with 12 m spacing. This is in-line with the high yield per unit area from small catchment as compared with large catchment. Another interesting result depicts that runoff yield per unit area is low for semi-circular ridges and high for continuous contour ridges. The longer slope length in semi-circular ridges is responsible for relatively higher abstraction losses and low runoff yield. Contrastingly, continuous contour ridges hold shorter slope length thus low abstraction losses and high runoff yield per unit area.

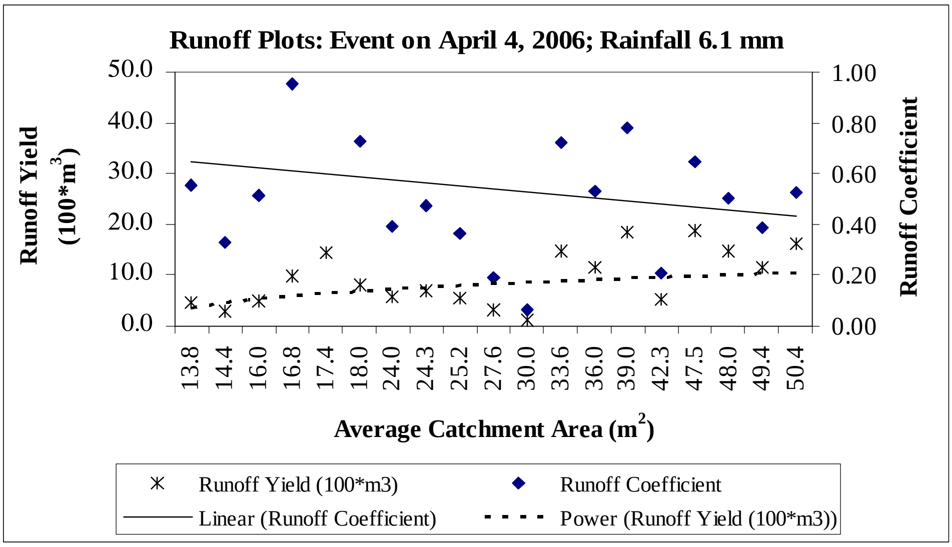

Figure 4.19. Runoff Yield and Coefficient for Micro-catchment Areas

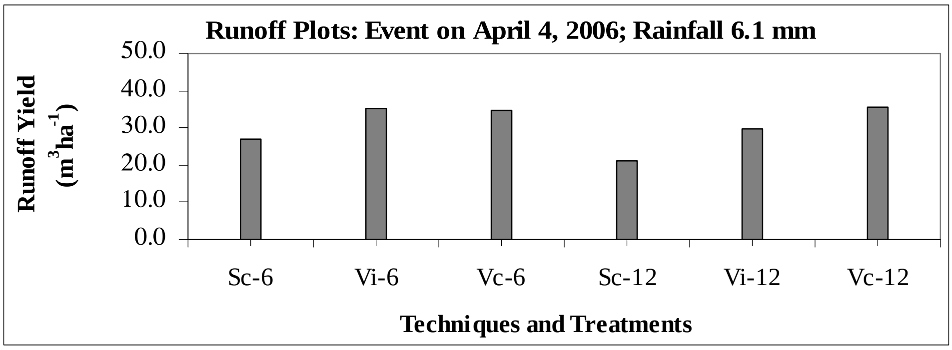

Figure 4.20. Runoff Yield in Relation to MCWH Techniques and Treatments

4.3.1.3 Runoff Event on 3rd October, 2006

A rainfall of 5.1 mm having rainfall intensity of 1.5 mm h^{-1} generated this runoff event. The results show that runoff yield increases and runoff coefficient decreases with the increase in micro-catchment area (Fig. 4.21). The runoff yield varied from about 0.005 m^3 to about 0.05 m^3 for micro-catchment area between 14 and 50 m^2. A polynomial equation of the form $y = -0.0027x^2 + 0.145x + 0.6146$ (r^2 = 0.019) poorly fit to the data. Where 'x' is catchment area in m^2 and 'y' is runoff yield in 100 m^3. The data of runoff coefficient in relation to micro-catchment area was highly scattered. A linear equation of the form $y = -0.0029x + 0.1472$ (r^2 = 0.0067) also poorly fit to the observed data. Where 'y' is runoff coefficient and 'x' is already defined. Average runoff yield for different MCWH techniques and treatments (Fig. 4.22) shows that runoff yield per unit area (m^3 ha^{-1}) in general is higher for MCWH techniques with 6 m spacing as compared with 12 m spacing. The runoff prediction for MCWH techniques for 12 m spacing also follows the general trend. However, lower runoff yield for continuous ridges (Vc-6, Vc-12) could not be explained.

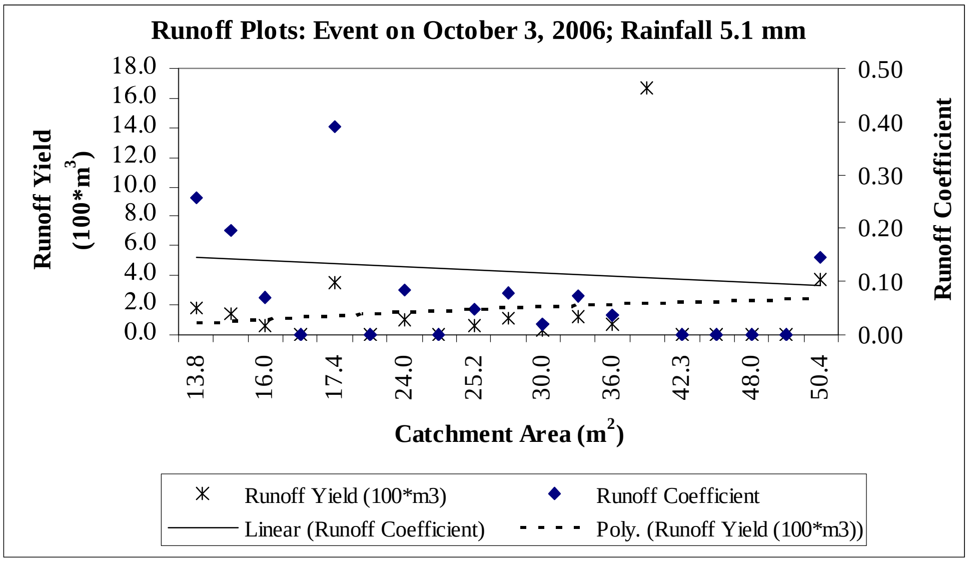

Figure 4.21. Runoff Yield and Runoff Coefficient in Relation to Micro-catchment Area

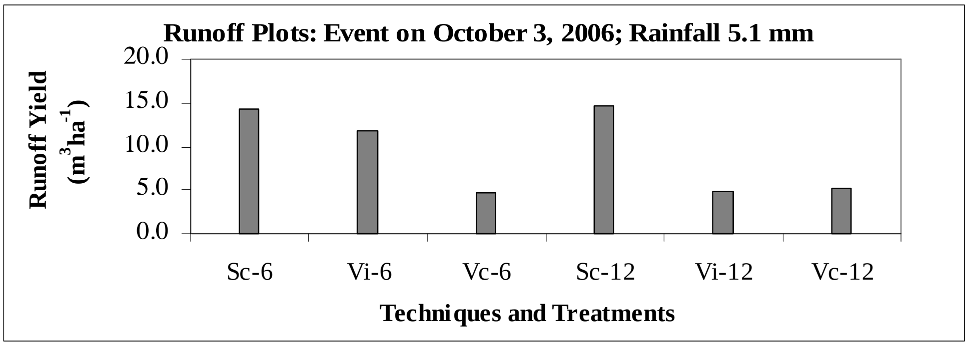

Figure 4.22. Runoff per Unit Area in Relation to MCWH Techniques and Treatments

4.3.1.4 Runoff Event on 25th October, 2006

A rainfall of 21.1 mm generated this runoff event. Results show that runoff yield increases and runoff coefficient decreases with the increase in micro-catchment area (Fig. 4.23). The runoff yield varied from about 0.02 m^3 to about 0.3 m^3 for micro-catchment area between 14 and 50 m^2. A power equation of the form $y = 6.3082x^{0.3877}$ ($r^2 = 0.231$) fits to the data. Where 'x' is micro-catchment area in m^2 and 'y' is runoff yield in 100 m^3. A linear equation of the form $y = -0.0072x + 0.2976$ ($r^2 = 0.1234$) fits to the observed runoff coefficient data. Where 'y' is runoff coefficient and 'x' is already defined. Average runoff yield for different MCWH techniques and treatments (Fig. 4.24) shows that runoff yield per unit area (m^3 ha^{-1}) is higher for MCWH techniques with 6 m spacing as compared with 12 m spacing. These results are in-line with the high yield per unit area from small catchment as compared with large catchment. Another interesting result depicts that runoff yield per unit area is low for semi-circular ridges and high for continuous contour ridges. The longer slope length in semi-circular ridges is responsible for relatively higher abstraction losses and low runoff yield. Contrastingly, continuous contour ridges hold shorter slope length thus low abstraction losses and high runoff yield per unit area.

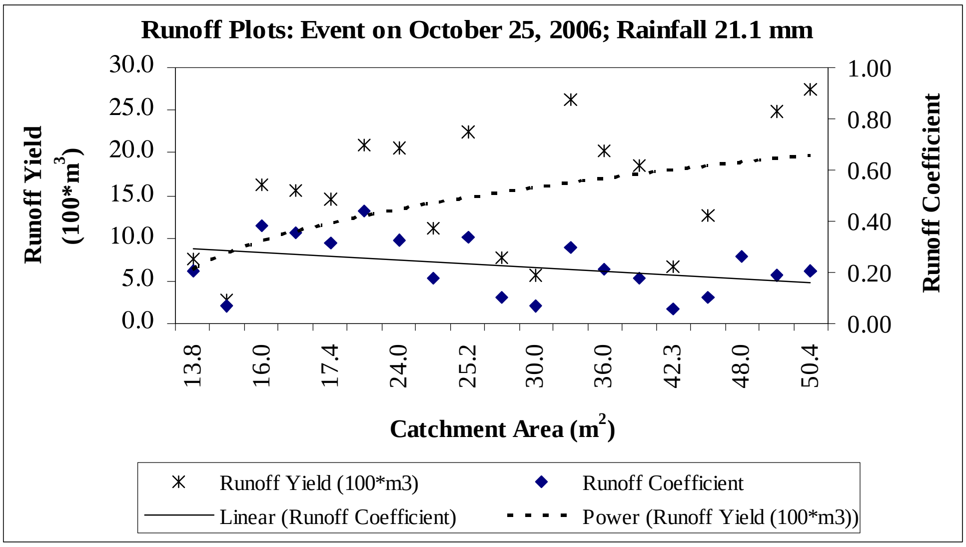

Figure 4.23. Runoff Yield and Coefficient for various Micro-catchment Areas

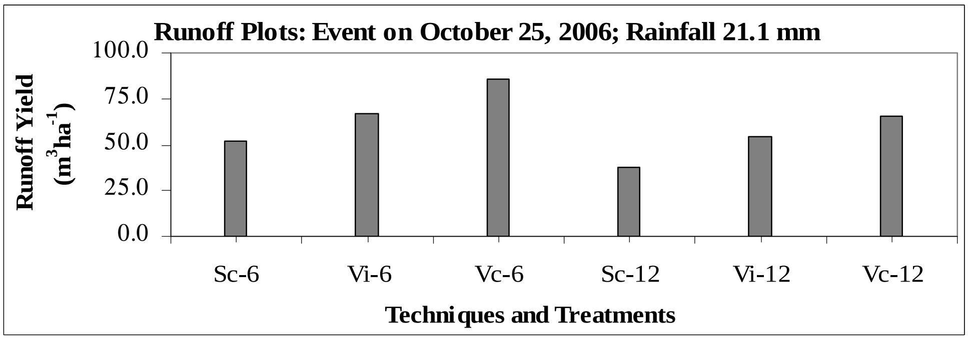

Figure 4.24. Runoff per Unit Area for MCWH Techniques and Treatments

4.3.1.5 Runoff Event on 1st March, 2007

Rainfall of 15.4 mm with wet antecedent conditions generated this runoff event. Results show that runoff yield increases and runoff coefficient decreases with the increase in micro-catchment area (Fig. 4.25). The runoff yield varied from about 0.02 m^3 to about 0.3 m^3 for micro-catchment area between 14 and 50 m^2. A power equation of the form $y = 4.259x^{0.4382}$ ($r^2 = 0.1938$) poorly fits to the data. Where 'x' is catchment area in m^2 and 'y' is runoff yield in 100 m^3. Runoff coefficient was computed from observed data by using rainfall and runoff depth. A linear equation of the form $y = -0.0089x + 0.3916$ ($r^2 = 0.0633$) poorly fits to the observed data. Where 'y' is runoff coefficient and 'x' is already defined. Average runoff yield for different

MCWH techniques and treatments (Fig. 4.26) shows that runoff yield per unit area (m^3 ha^{-1}) is higher for MCWH techniques with 6 m spacing as compared with 12 m spacing. These results are in-line with the high yield per unit area from small catchment as compared with large catchment. Another result depicts that runoff yield per unit area is low for semi-circular ridges and high for continuous contour ridges. The longer slope length in semi-circular ridges is responsible for relatively higher abstraction losses and low runoff yield. Contrastingly continuous contour ridges hold shorter slope length thus low abstraction losses and high runoff yield per unit area.

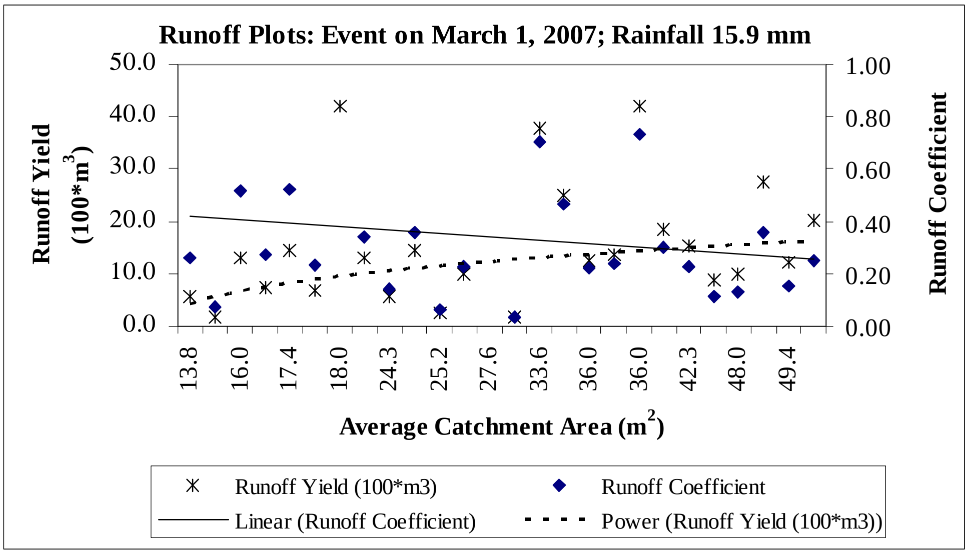

Figure 4.25. Runoff Yield and Runoff Coefficient in Relation to Micro-catchment Area

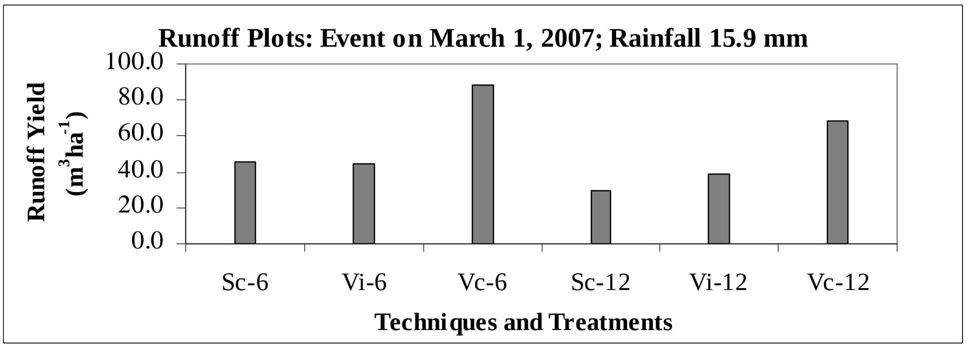

Figure 4.26. Runoff per Unit Area in Relation to MCWH Techniques and Treatments

4.3.1.6 Runoff Event on 13th May, 2007

Rainfall of 17.1 mm with dry antecedent conditions generated this runoff event. The results show that runoff yield increases and runoff coefficient decreases with the increase in micro-catchment area (Fig. 4.27). The runoff yield varied from about 0.025 m^3 to about 0.32 m^3 for micro-catchment area between 14 and 50 m^2. A power equation of the form $y = 5.3996x^{0.3951}$ ($r^2 = 0.25$) fits to the data. Where 'x' is catchment area in m^2 and 'y' is runoff yield in 100 m^3. Runoff coefficient was computed from observed data by using rainfall and runoff depth. A linear equation of the form $y = -0.0042x + 0.2711$ ($r^2 = 0.047$) poorly fits to the observed data. Where 'y' is runoff coefficient and 'x' is already defined. Average runoff yield for different MCWH techniques and treatments (Fig. 4.28) shows that runoff yield per unit area (m^3ha^{-1}) is higher for continuous contour ridges (Vc) and lower for semi-circular bunds (Sc) and intermittent ridges (Vi). Shorter slope length in continuous ridge was responsible to produce higher runoff per unit area. However; higher runoff yield by 12 m spacing techniques could not be explained.

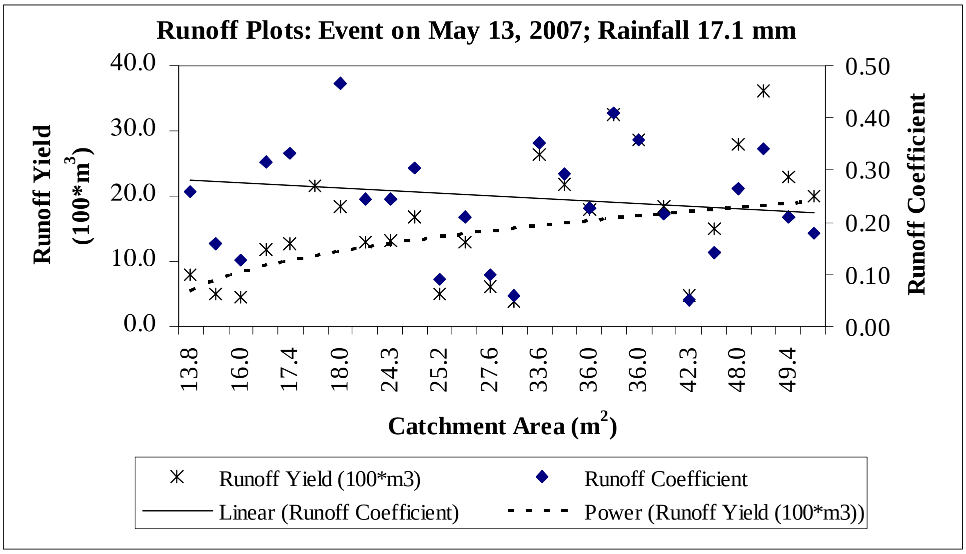

Figure 4.27. Runoff Yield and Runoff Coefficient in Relation to Micro-catchment Area

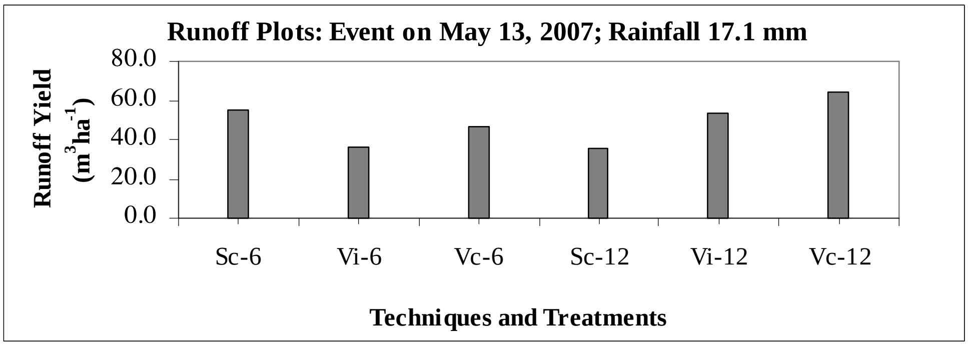

Figure 4.28. Runoff per Unit Area in Relation to MCWH Techniques and Treatments

4.3.1.7 Runoff Event on 18th May, 2007

A rainfall of 21.8 mm with wet antecedent conditions generated this runoff event. Results show that runoff yield increases and runoff coefficient decreases with the increase in micro-catchment area (Fig. 4.29). The runoff yield varied from about 0.1 m^3 to about 0.6 m^3 for micro-catchment area between 14 and 50 m^2. A power equation of the form $y = 16.51x^{0.2802}$ ($r^2 = 0.29$) fits to the data. Where 'x' is catchment area in m^2 and 'y' is runoff yield in 100 m^3. Runoff coefficient was computed from observed data by using rainfall and runoff depth. An exponential equation of the form $y = 0.6759e^{-0.0386x}$ ($r^2 = 0.26$) fits to the observed data. Where 'y' is runoff coefficient and 'x' is already defined. Average runoff yield of MCWH techniques and treatments (Fig. 4.30) shows that runoff yield per unit area ($m^3\ ha^{-1}$) is higher for small catchment (6m spacing) and lower for larger catchment (12 m spacing). Theory supports this phenomenon. Comparison between MCWH techniques shows that continuous ridges produced higher runoff from unit area as compared with semi-circles and intermittent contour ridges. The argument of the shorter slope length to produce higher runoff per unit area in case of continuous ridges is also valid here.

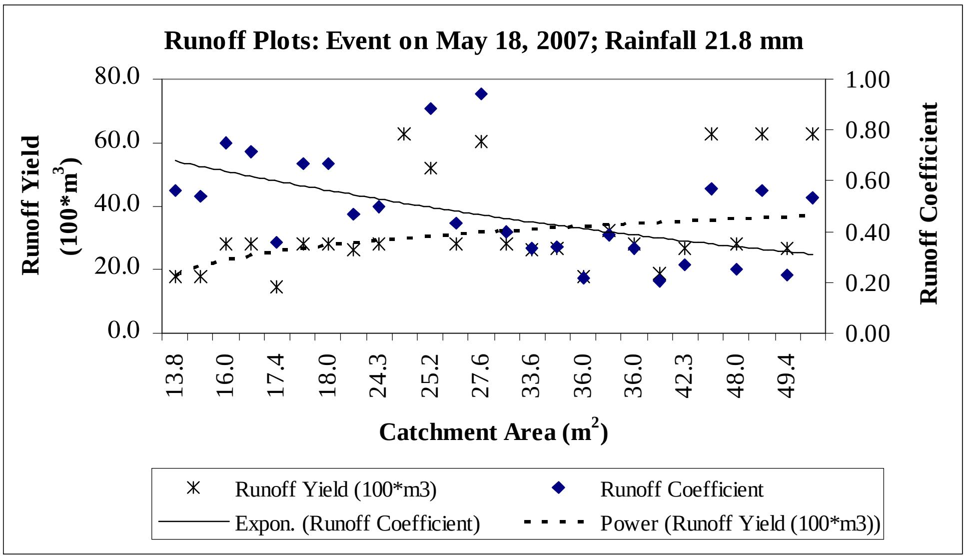

Figure 4.29. Runoff Yield and Coefficient for Micro-catchment Areas

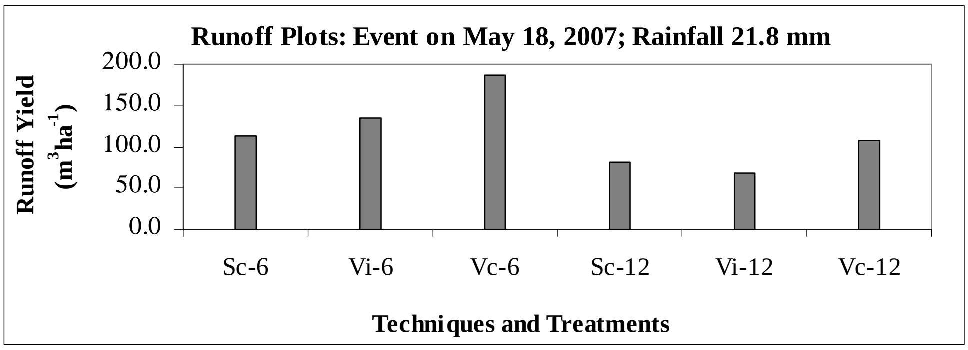

Figure 4.30. Runoff per Unit Area for MCWH Techniques and Treatments

4.3.1.8 Summary of Runoff Measurements and Analysis at Micro-catchment Scale

Event runoff yield of the micro-catchments varied between 0.03 to 0.6 m^3 for the micro-catchment areas between 14 and 50 m^2, event rainfall between 5 and 21 mm and three different MCWH techniques. The power equations fairly represent the event runoff yields. However, small R^2 values indicate that other variables such as rainfall intensity, antecedent moisture conditions and soil type play a significant role in runoff generation process. Runoff yield in relation to event rainfall (Fig. 4.31) shows increase in runoff with rainfall following an exponential trend (y = 4.6x-17.71; R^2 = 0.65). Where ‘x’ is event rainfall in mm and ‘y’ is runoff yield in m^3 ha^{-1}.

The relationship shows a rainfall threshold value of 3.85 mm to generate runoff, which represents the wet antecedent soil-moisture conditions.

Average runoff yield for different rainfall events (Table 4.10) varied between 33 and 64 m^3 ha^{-1}. It was between 46 and 64 m^3 ha^{-1} for 6 m spacing between the ridges (catchment area ~ 24 m^2) and between 33 and 50 m^3 ha^{-1} for 12 m spacing between the ridges (catchment area ~ 48 m^2). The annual runoff yield was between 220 and 413 m^3 ha^{-1}. Average annual runoff yield was 329 and 243 m^3 ha^{-1} for 24 and 48 m^2 catchment areas, respectively. The runoff yield per unit area was higher for smaller catchment and it decreased with the increase in micro-catchment area. It was also higher for continuous ridges and lower for intermittent ridges. Longer length of overland flow in the intermittent ridges and semi-circular bunds was responsible for more abstraction losses and lower runoff yield per unit area from them. The runoff coefficient varied between 5 and 80% with an average value of about 30% (Table 4.10). It shows that the micro-catchment could harvest rainwater up to 80% of the incidental rainfall.

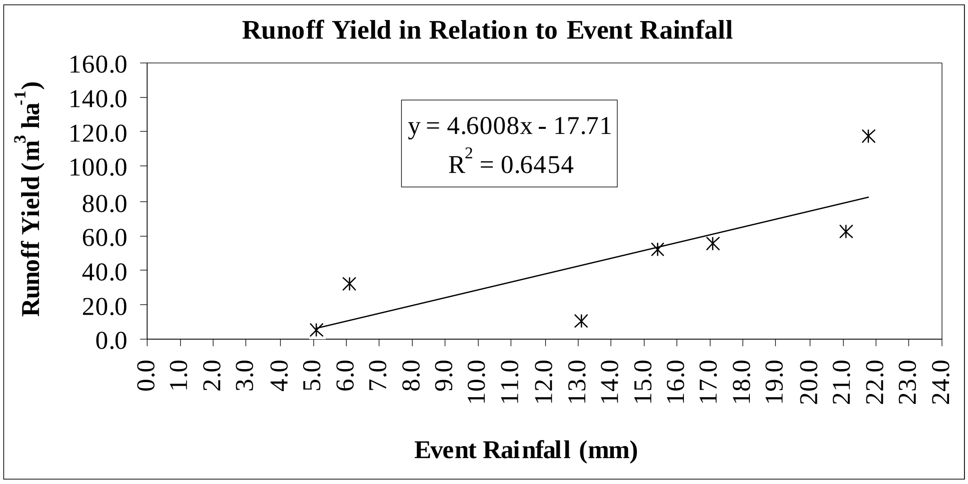

Figure 4.31. Runoff Yield in Relation to Event Rainfall for Runoff Plot Method

Table 4.10. Runoff Yield and Coefficient in Relation to Rainfall for Different MCWH Techniques and Treatments.

MCWH Techniques	Rainfall (mm)							Average
	5.1	6.1	13.1	15.4	17.1	21.1	21.8	
	Runoff Coefficient							
Sc-6	0.28	0.44	0.12	0.29	0.25	0.20	0.48	0.30
Vi-6	0.07	0.58	0.05	0.28	0.16	0.25	0.58	0.28
Vc-6	0.09	0.57	0.00	0.56	0.11	0.32	0.80	0.35
Sc-12	0.09	0.35	0.07	0.19	0.16	0.14	0.35	0.19
Vi-12	0.10	0.48	0.05	0.24	0.24	0.21	0.29	0.23
Vc-12	0.10	0.59	0.00	0.43	0.29	0.25	0.46	0.30
Average								0.28
	Runoff Yield (m^3 ha^{-1})							
Sc-6	14.35	26.96	17.40	45.61	55.24	52.29	112.92	46.40
Vi-6	11.75	35.26	7.48	44.42	36.43	66.57	135.03	48.13
Vc-6	4.65	34.86	0.00	88.62	46.99	85.70	187.39	64.03
Sc-12	14.54	21.11	10.49	29.85	35.72	37.59	80.74	32.86
Vi-12	4.96	29.52	7.78	38.54	53.77	54.17	68.19	36.70
Vc-12	5.28	35.73	0.00	68.90	64.45	65.02	108.18	49.65
Average								46.30

4.3.2 Runoff Assessment at Site Scale

The site (100 ha) included the rill and interrill area and areas between gullies. Natural drainage within the site follows several drainage paths. Further water harvesting ridges across the slope also modified the drainage pattern that added complexity and made the direct runoff measurement unfeasible at the site scale. Therefore, the runoff yield at this scale was estimated from the distribution of water in the soil layers as a result of runoff. The soil-water data was observed at 90 locations and it was analyzed for runoff yield and runoff coefficient for the Vallerani intermittent (Vi-6, and Vi-12) and Vallerani continuous ridges (Vc-6 and Vc-12). The parameters were estimated for each major rainfall event and averaged for various treatments. Results (Table 4.11) showed that runoff yield per unit area varied from 5.1 to 13.8 m^3 ha^{-1} for Vi-12 and 2.4 to 5.3 m^3 ha^{-1} for Vc-12 for different rainfall amounts. The runoff yields of Vi-6 and Vc-6 were between 10 and 30 m^3 ha^{-1} and 14 and 19 m^3 ha^{-1}, respectively. The average runoff yields were about 10 m^3 ha^{-1} for Vi-12, 3.9 m^3 ha^{-1} for Vc-12, 21.8 m^3 ha^{-1} for Vi-6 and 16.7 m^3 ha^{-1} for Vc-6 techniques. The average runoff coefficient was estimated 0.09 (Vi-12), 0.03 (Vc-12), 0.17 (Vi-6) and 0.16 (Vc-6). The unit runoff yield and runoff coefficient were higher for 6-m spacing (Vi-6 and Vc-6; catchment area 24 m^2) and lower for 12-m spacing (Vi-12 and Vc-12; catchment area 48 m^2). It shows that the runoff per unit area increases with the decrease in catchment area. The results also showed that intermittent ridges produced more runoff than continuous ridges. This is in contradiction to results obtained at micro-catchment scale where continuous ridges produced more runoff (Table 4.10). This can be explained through runoff measurement methodology.

At micro-catchment scale, the runoff was collected in a tank installed at the lowest end of each micro-catchment (Runoff Plot method). There was hardly any chance of the runoff to detour unless the tank overflowed. Therefore, the abstraction losses within the micro-catchments included the infiltration and evaporation. In reality, the runoff from the micro-catchments was spread in planted area along the ridges. A part of this runoff was retained in a ditch length between the two shrubs. The intermittent ridges by virtue of their design allowed overflowing and spreading of runoff over adjacent area or at downstream. This caused additional water losses, which remained unaccounted in the Runoff Plot method at micro-catchment scale. On the other hand at the Site scale, the soil-moisture measurement only accounted for the runoff concentrated to shrub location (access tube near the shrubs). It did not take into account the runoff spreading away from the shrub. This was the main cause of difference of runoff estimate at both the scales.

Table 4.11. Runoff Assessment at the Site Scale by Soil-Water Accounting Method.

Description	Soil-moisture (mm) in 90 cm deep soil profile					
Date	06/04/06	10/5/06	10/26/06	3/2/07	5/14/07	5/19/07
Rainfall (mm)	6.1	5.1	21.1	15.4	17.1	21.8
Catchment area (m^2)	Vi-12 & Vc-12	48	Vi-6 & Vc-6	24		
Vi-12 technique (average)						
Soil-moisture in catchment area (mm)	99.8	87.6	105.2	108.5	113.9	126.7
Soil-moisture in target area (mm)	151.1	112.2	152.1	163.1	165.7	192.9
Difference in soil-moisture (mm)	51.3	24.6	46.8	54.6	51.8	66.2
Runoff depth (mm)	1.1	0.5	1.0	1.1	1.08	1.4
Runoff volume (m^3)	0.1	0.02	0.045	0.06	0.05	0.07
Runoff yield ($m^3 ha^{-1}$)	10.7	5.1	9.76	11.4	10.8	13.8
Runoff coefficient	0.2	0.1	0.05	0.07	0.06	0.06
Vc-12 technique (average)						
Soil-moisture in catchment area (mm)	97.1	81.9	110.3	108.9	114.1	131.2
Soil-moisture in target area (mm)	115.4	93.59	125.1	134.2	133.0	153.5
Difference in soil-moisture (mm)	18.4	11.66	14.8	25.2	18.9	22.3
Runoff depth (mm)	0.38	0.24	0.31	0.5	0.4	0.5
Runoff volume (m^3)	0.02	0.01	0.01	0.03	0.02	0.02
Runoff yield ($m^3 ha^{-1}$)	3.8	2.4	3.1	5.3	3.9	4.6
Runoff coefficient	0.06	0.05	0.01	0.03	0.02	0.02
Vi-6 technique (average)						
Soil-moisture in catchment area (mm)	93.5	79.76	97.22	97.57	104.14	112.6
Soil-moisture in target area (mm)	130.3	105.64	162.94	152.55	162.94	184.8
Difference in soil-moisture (mm)	36.8	25.88	65.72	54.98	58.79	72.2
Runoff depth (mm)	1.5	1.08	2.7	2.3	2.5	3.0
Runoff volume (m^3)	0.04	0.03	0.07	0.05	0.06	0.07
Runoff yield ($m^3 ha^{-1}$)	15.3	10.8	27.4	22.9	24.5	30.1
Runoff coefficient	0.25	0.21	0.13	0.15	0.14	0.14
Vc-6 technique (average)						
Soil-moisture in catchment area (mm)	79.1	61.9	85.7	91.9	93.6	102.3
Soil-moisture in target area (mm)	120.2	98.28	129.34	131.52	128.27	148.0
Difference in soil-moisture (mm)	41.0	36.39	43.65	39.57	34.66	45.7
Runoff depth (mm)	1.7	1.5	1.8	1.7	1.4	1.9
Runoff volume (m^3)	0.04	0.04	0.04	0.04	0.03	0.05
Runoff yield ($m^3 ha^{-1}$)	17.1	15.2	18.2	16.5	14.4	19.0
Runoff coefficient	0.28	0.30	0.09	0.11	0.08	0.09

Runoff yield per unit area in relation to rainfall amount (Fig. 4.32) showed that runoff yield generally increased with rainfall amount for all techniques and spacing. The regression function differently fitted to the data for each technique. Largely, the performance of intermittent ridges was better than the continuous ridges and 6 m spacing better than 12 m spacing. The best fit regression function and R-squared values are given in Table 4.12 for Vi-6 and Vi-12. The Vc-6 and Vc-12 data poorly fitted, therefore not presented.

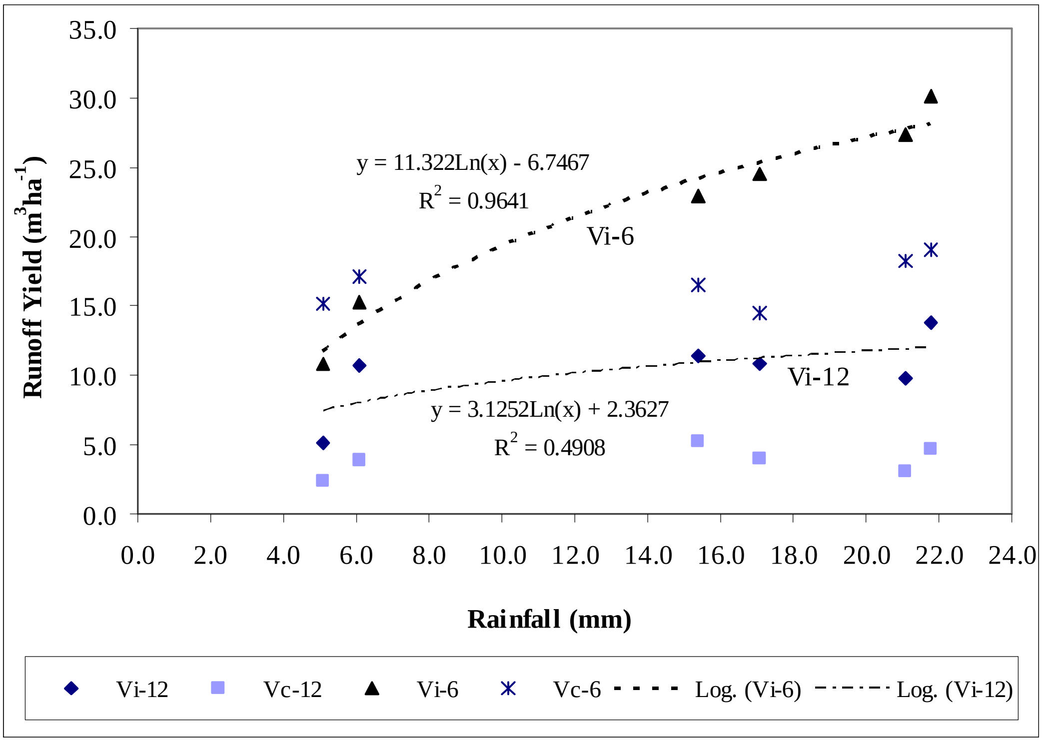

Figure 4.32**.** Runoff Yield in Relation to Rainfall Amount at Site Scale for Different MCWH Techniques and Treatments

Table 4.12. Regression Equations for Rainfall and Runoff Yield Relationship.

MCWH Technique	Regression Equation	Parametric Regression Equation	R^2
Vi-6	y = 11.32Ln(x) - 6.75	$q = a\,Ln(P) - c$, where q is unit runoff yield ($m^3\,ha^{-1}$), P is event rainfall in mm, a is coefficient (11.32) and c is intercept (-6.75).	0.96
Vi-12	y = 3.13Ln(x) + 2.36	$q = a\,Ln(P) + c$, where all variables and constants are already defined. a is 3.13 and b is 2.36.	0.49

4.3.3 Runoff Assessment at Catchment Scale by Measuring Stage Hydrograph

Runoff from small catchments was estimated by measuring stage hydrograph at outlets of three small catchments. Catchments 1 and 2 represented by Weir-1 and 2 are partially covered with MCWH interventions and experience land use changes. Catchment 3 represented by Weir-3 was kept as control. Stage-discharge ratings were used to convert observed stage hydrograph into discharge hydrograph. The data was analyzed for runoff volume and peak runoff rate and parameters such as runoff yield per unit area and runoff coefficient were estimated.

4.3.3.1 Runoff Event on 4th April, 2006

A 6.1 mm rainfall generated runoff and was recorded at Weir-1. The rainfall started at about 11:00 hours and continued until 15:00 hours. It was a very weak rainfall. It started again at 19:43 hours and sharply rose to 0.8 mm in 2 minutes. It subsided slowly by 19:52 hours and accumulated 4.1 mm rainfall in 9 minutes. The observed rainfall hyetograph at research site was analyzed for time base and rainfall intensity. It revealed a time base of rainfall events (ΔD) as 9 minutes and rainfall intensity of 27 mm h^{-1} for 9 minutes duration. The antecedent conditions were dry for 3 days and slight rain was observed on day 4 and 5 prior to this event. Stage hydrograph at the Weir-1 was translated into discharge hydrograph (Fig. 4.33) by using stage-discharge rating. The parameters of the discharge hydrograph were estimated as time base 1.5 hours, time to peak 30 minutes and peak runoff rate 0.42 $m^3 s^{-1}$. Total runoff under the hydrograph was estimated 33.72 m^3. This estimated a runoff yield of 0.93 $m^3 ha^{-1}$ from a catchment area of 36 ha.

Stage hydrograph at Weir-2 and 3 could not be recorded for this event due to low voltage problem of data loggers. However, manual gauges at these weirs recorded the elevation for the peak flood. The flood level was used to compute peak runoff rates by using weir formula. Peak runoff rates at Weir-2 and 3 were 0.72 and 0.092 $m^3 s^{-1}$, respectively. A combination of dimensionless hydrograph at Weir-1, peak runoff rates and catchment parameters at weirs 2 and 3 developed the discharge hydrograph for weirs 2 and 3. The time parameters for weirs 2 and 3 were estimated from the catchment characteristics including time of concentration, travel time and time to peak. Time of concentration and time to peak were estimated by using Kirpich equation (1940) and travel time approach (Table 4.13).

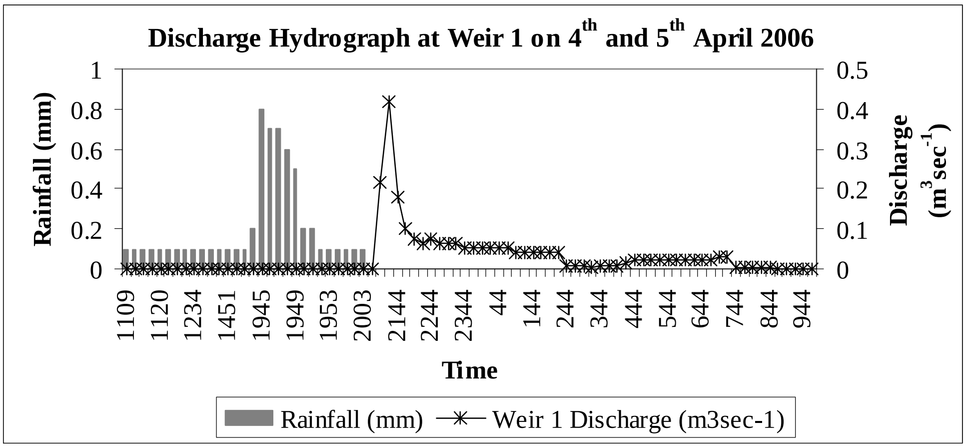

Figure 4.33. Discharge Hydrograph at Weir-1 on 4th and 5th April 2006.

Table 4.13. Computed and Observed Time Parameters of the Catchments.

Weir	Time of concentration (t_c) (min)		Time to peak (t_p) (min)		Time to peak (t_p) (min)
	Kirpich formula	Travel time approach	Kirpich formula	Travel time approach	Observed
1	23.54	12.19	28.04	19.19	30
2	19.84	9.32	24.34	17.93	–
3	11.51	4.46	16.01	10.80	–

Comparison of observed and computed values of time to peak for the Weir-1 by the two approaches showed that the estimate by Kirpich formula (28.04 minutes) was closer to the observed value of time to peak (30 minutes). The estimate of time to peak by the travel time approach (19.2) was far below the observed value. Therefore, Kirpich formula was used to develop hydrograph for Weir-2 and 3. A dimensionless discharge hydrograph at Weir-1 was computed and was used in combination with catchment and time parameters to estimate discharge hydrograph at Weir-2 and 3 (Figs. 4.34 & 4.35). The starting time of the discharge hydrograph (20:59 h) is same in all three cases. A summary of hydrograph parameters (Table 4.14) shows that runoff yield was high from catchment 3 (without MCWH) as compared with the catchment 1 and 2 partly covered by the MCWH ridges. It also shows that ridges have affected the runoff yield by retaining water and increasing catchment retention capacity. Catchment size is considered responsible for the difference in runoff yields from catchment 2 and 3.

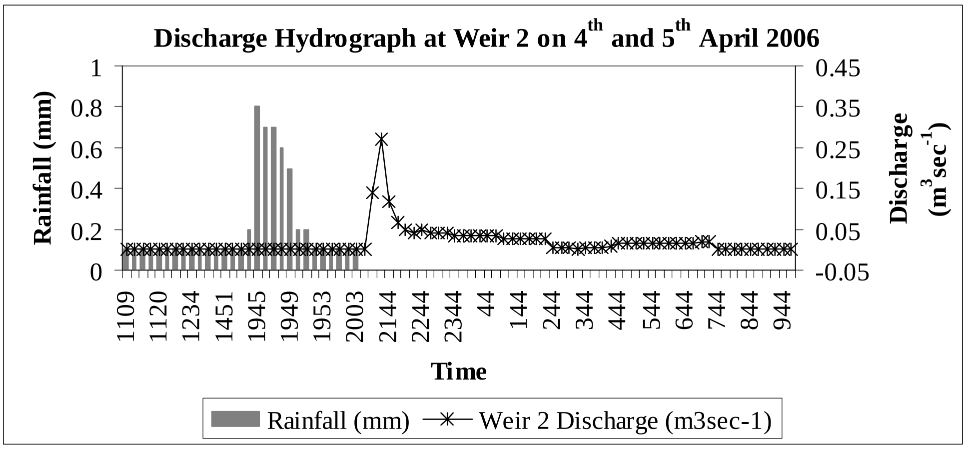

Figure 4.34. Computed Discharge Hydrograph at Weir-2 for Rainfall on 4th and 5th April

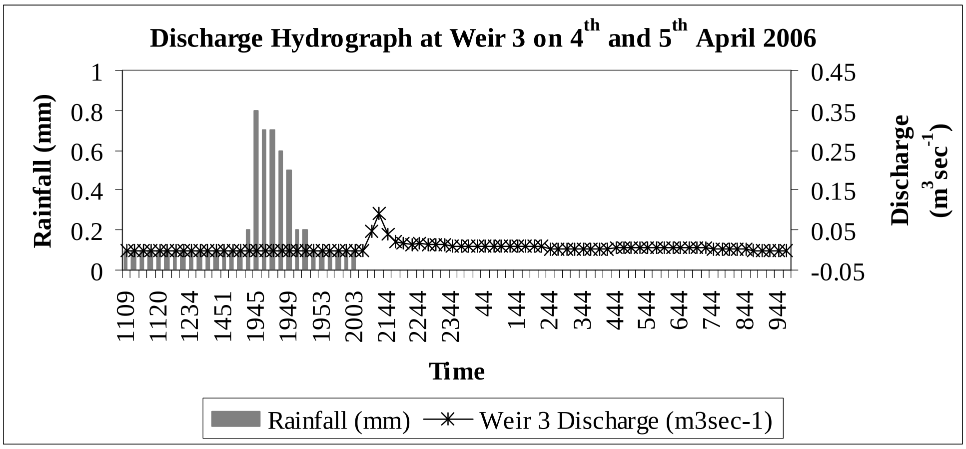

Figure 4.35. Computed Discharge Hydrograph at Weir-3 on 4th and 5th April

Table 4.14. Estimated Runoff Parameters on 4th April, 2006.

Description	Weir-1	Weir-2	Weir-3
Catchment area (ha)	36.3	21.0	5.1
Peak runoff rate ($m^3 s^{-1}$)	0.417	0.271	0.092
Runoff volume (m^3)	33.723	21.9	7.5
Runoff yield ($m^3 ha^{-1}$)	55.74	62.66	87.59

4.3.3.2 Runoff Event on 3rd October, 2006

A 5.1 mm rainfall occurred on 3rd October, 2006, which generated runoff and was observed at Weir-2. The runoff did not pass over the Weir-1 and 3, therefore could not be recorded. Rainfall started at 14:50 hours and accumulated to 2.5 mm by 15:00, 3.7 mm by 16:00, 4.3 mm by 17:00, 4.9 mm by 18:00 and 5.1 mm by 19:00 h. This was the first rainfall of the season that generated a weak runoff. Stage hydrograph at Weir-2 was analyzed to develop discharge hydrograph (Fig. 4.36), which shows a time lag of about 1 hour between rainfall and runoff. It generated a total runoff (passed over the weir) of about 0.5 m^3 with runoff yield equals to 0.24 m^3 ha^{-1}.

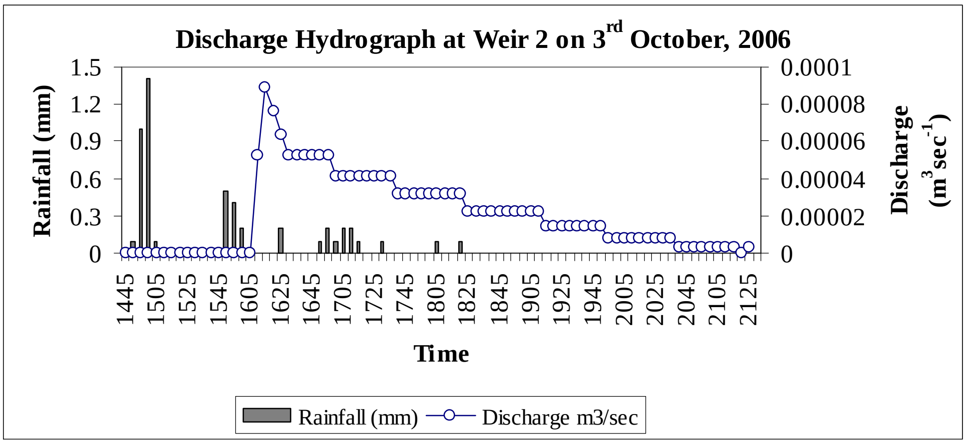

Figure 4.36. Discharge Hydrograph at Weir-2 on 3rd October, 2006

4.3.3.3 Runoff Event on 25th October, 2006

A 26.4 mm of rainfall was occurred on 24th and 25th October 2006. The rainfall started at 18:00 h on 24th October and continued until 15:00 h on 25th of October with four peaks on 18:35, 23:40, and 06:20 and 12:00 h. The rainfall pattern generated runoff with three peaks (Figs 4.37 to 4.39). The discharge hydrograph for each weir was computed from stage hydrograph. Maximum flood marks at manual gauges helped to verify peak runoff rate. The first peak of runoff hydrograph occurred at 0120 h at Weir-1, 0110 h at Weir-2 and 0115 h at Weir-3. The second and third peaks occurred after about 5.0 and 8.50 hours of the first peak. The second peak was the mildest when third peak was the highest at the three weirs. The analysis of rainfall hyetograph in relation to runoff hydrograph indicated that the earlier rainfall on 18:35 h was absorbed by the soil as initial abstractions to satisfy the micro-relief and soil-moisture requirements. The runoff peaks were sharp. The runoff parameters for each event are given in Table 4.15. The runoff yield and runoff coefficient for Weir-1 and Weir-2 followed the general trend. Nevertheless, the runoff at Weir-3 did not follow the general trends. No obvious reason was found except for relatively low rainfall in this catchment, which could not be proved, as no separate rain gauge was installed for this catchment.

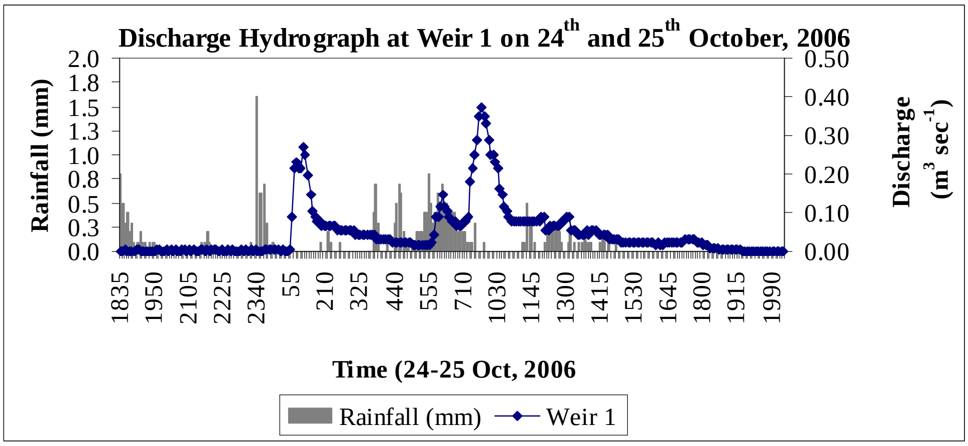

Figure 4.37. Discharge Hydrograph on 24th 25th October 2006 at Weir-1.

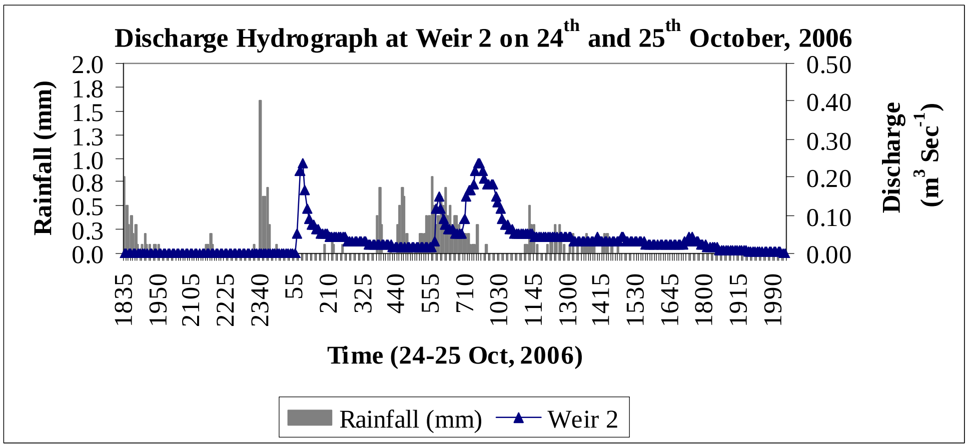

Figure 4.38. Discharge Hydrograph on 24th and 25th October 2006 at Weir-2.

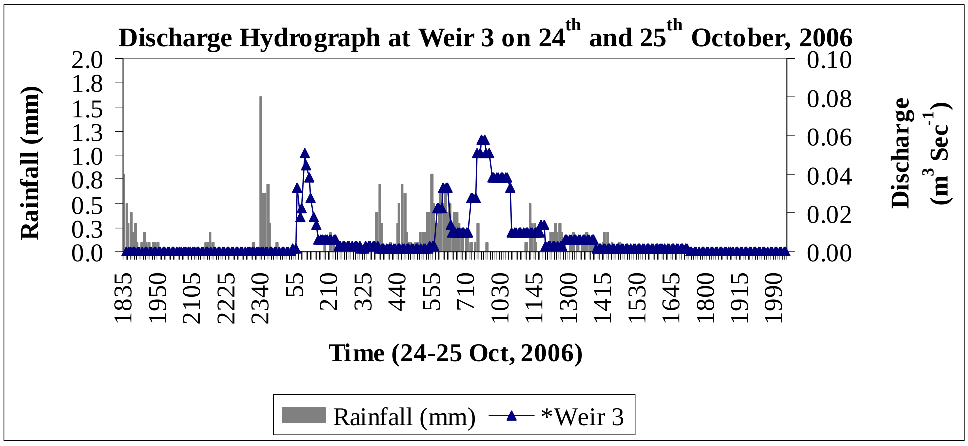

Figure 4.39. Discharge Hydrograph on 24th and 25th October 2006 at Weir-3.

Table 4.15. Estimated Runoff Parameters on 24th and 25th October, 2006.

Description	Weir-1	Weir-2	Weir-3
Total runoff (m^3)	4023.9	2985.2	297.5
Catchment area (ha)	36.30	21.00	5.1
Runoff yield ($m^3\ ha^{-1}$)	110.9	142.2	102.7
Runoff coefficient	0.42	0.54	0.39
Peak runoff rate ($m^3\ s^{-1}$)	0.37	0.23	0.057

4.3.3.4 Runoff Event on 11th and 12th of May, 2007

Runoff event on 11th May 2007 occurred due to 17.1 mm accumulative rainfall. The rain fell in several spells from 13:25 h to 15:50 h on 11th and 12th May, 2007. The rainfall events on 15:50 h generated sharp discharge hydrograph with single peak (Fig. 4.40). Nevertheless, the earlier rainfall created wet conditions and helped in runoff generation. A sharp subsidence of the hydrograph was due to rainfall pattern of the event immediate before the runoff. The runoff hydrograph followed the similar trend at Weir-2 (Fig. 4.41). Nevertheless, two earlier low peaks were observed at Weir-3 before main peak (Fig. 4.42). The earlier two low peaks can be linked to small catchment of the Weir-3, where earlier rains were able to produce runoff that concentrated at weir location. The third peak followed the similar trends as in case of hydrograph at Weir-1 and Weir-2.

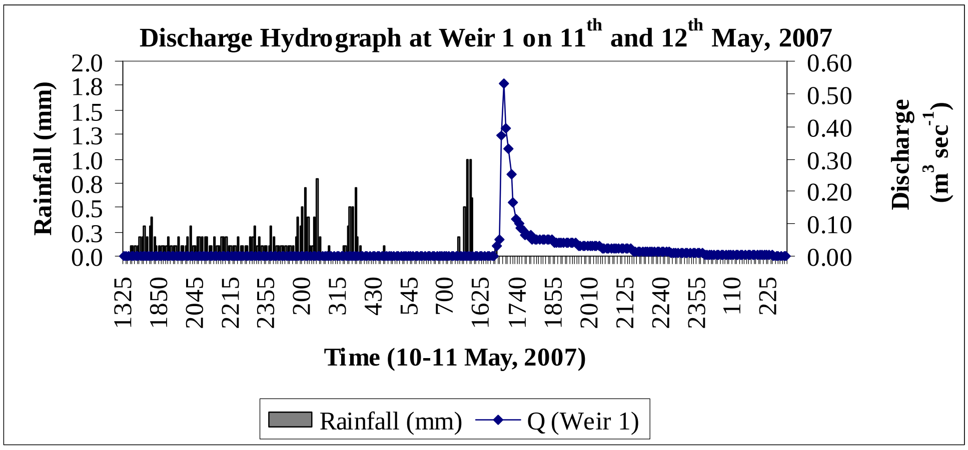

Figure 4.40. Discharge Hydrograph on 11–12 May, 2007 at Weir-1.

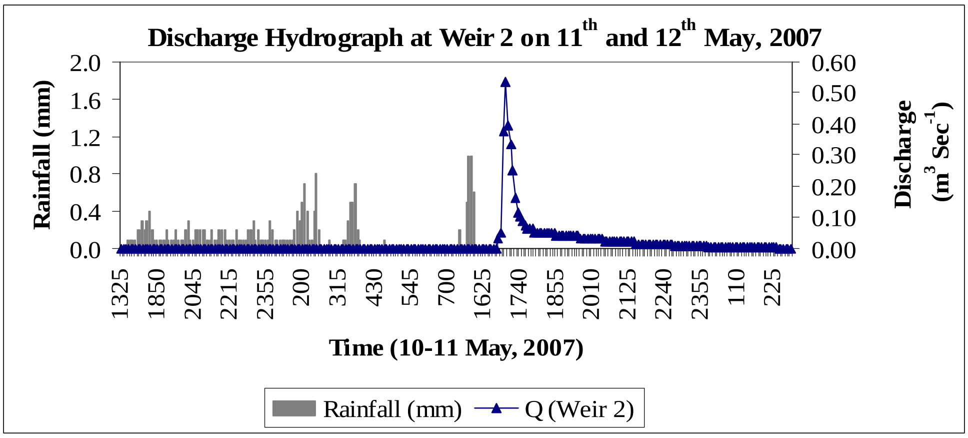

Figure 4.41. Discharge Hydrograph on 11th and 12th May, 2007 at Weir-2.

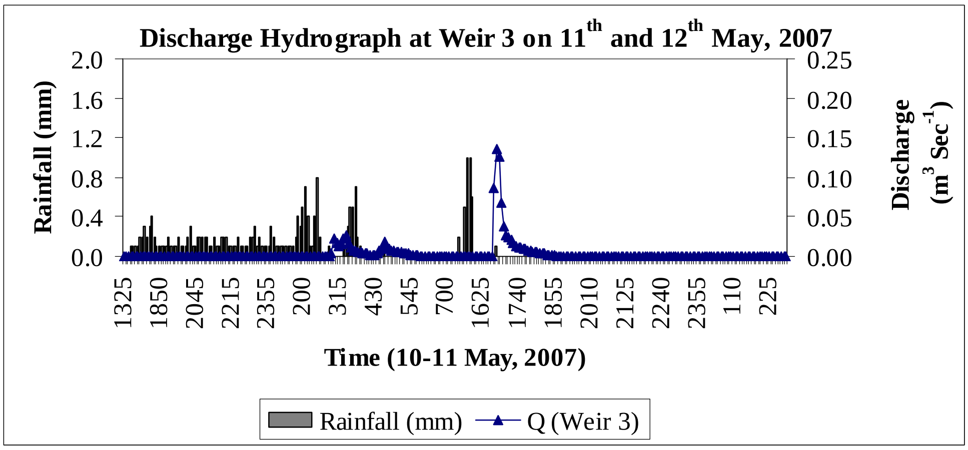

Figure 4.42. Discharge Hydrograph on 11th and 12th May, 2007 at Weir-3.

Comparing the runoff parameters (Table 4.16) shows that the runoff yield of catchment (Weir-3) was higher than the runoff yield of catchment drained by Weir-1, however, it was lower than the runoff yield of catchment drained by Weir-2. While former follows the general trends the later one does not.

Table 4.16. Estimated Runoff Parameters on 11th and 12th May, 2007

Description	Weir-1	Weir-2	Weir-3
Total runoff (m^3)	1384.07	1394.32	286.85
Catchment area (ha)	36.30	21.00	5.1
Runoff yield ($m^3 ha^{-1}$)	38.13	66.40	56.24
Peak runoff rate ($m^3 s^{-1}$)	0.53	0.54	0.14

4.3.3.5 Runoff Event on 17th and 18th May, 2007

A rainfall of 21.8 mm produced this runoff event. A major chunk of the rainfall occurred in continuous short duration spell and caused runoff. The hydrograph peak was sharp (Figs. 4.43, 4.44, and 4.45). A second rise in runoff hydrograph was a result of low intensity rainfall spell followed after the major rainfall spell. The discharge hydrograph followed similar trend at the three weirs except for very sharp peak at Weir-3. This shows a quick response of the catchment W-3.

Comparing the runoff parameters (Table 4.17) shows that the runoff yield of catchments draining at Weir-1 and 3 are comparable. The runoff yield of catchment draining at Weir-2 was relatively high. Catchment at Weir-2 showed consistency in responding to both the events in May 2007.

Table 4.17. Estimated Runoff Parameters on 17th and 18th May, 2007

Description	Weir-1	Weir-2	Weir-3
Total runoff (m^3)	4023.9	2985.2	297.5
Catchment area (ha)	36.30	21.00	5.1
Runoff yield ($m^3 ha^{-1}$)	238.0	280.5	211.2
Peak runoff rate ($m^3 s^{-1}$)	1.86	1.41	0.36

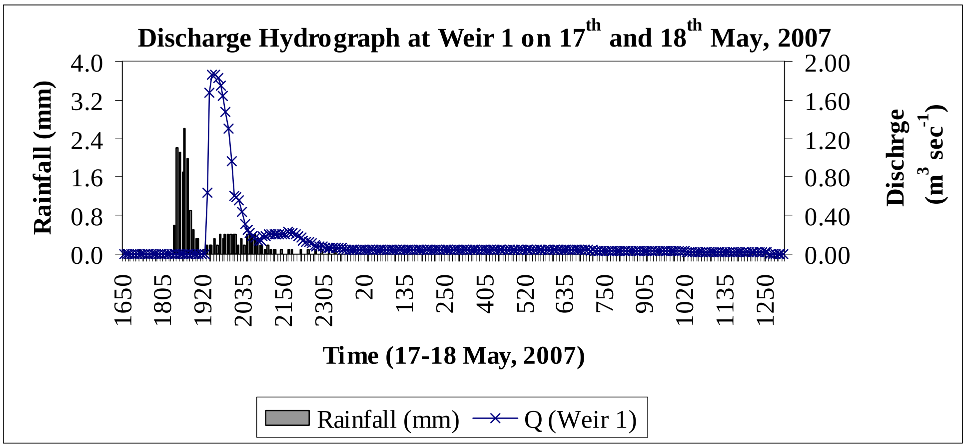

Figure 4.43. Rainfall and Runoff Hydrograph on 17th and 18th May, 2007 at Weir-1.

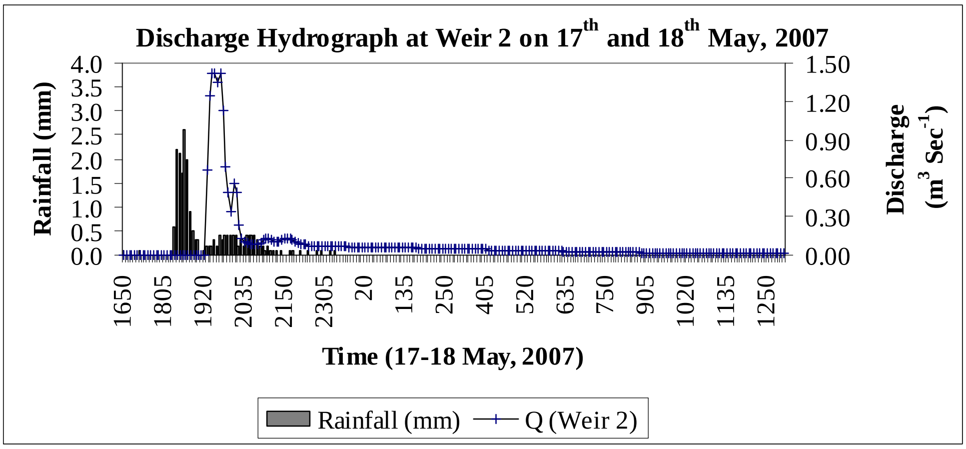

Figure 4.44. Rainfall and Runoff Hydrograph on 17th and 18th May, 2007 at Weir-2.

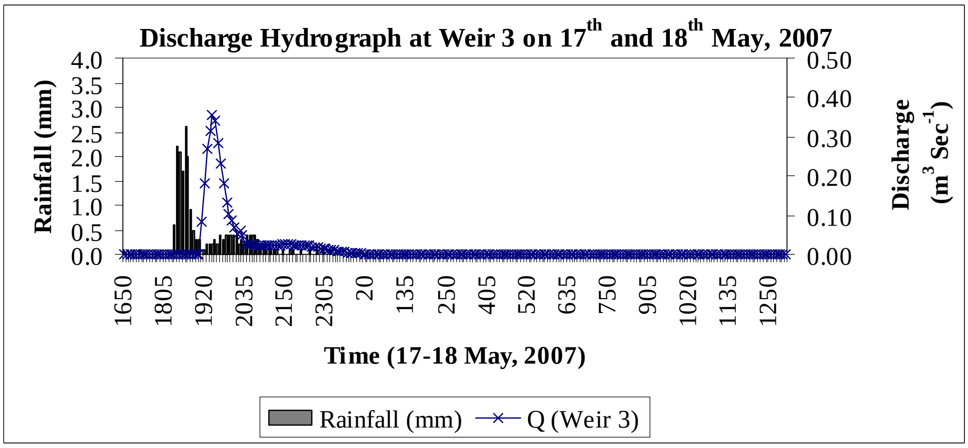

Figure 4.45. Rainfall and Runoff Hydrograph on 17th and 18th May, 2007 at Weir-3.

4.3.3.6 Summary of Runoff Measurement at three Different Scales

The runoff yield was higher at micro-catchment scale as compared with site scale, which included the effect of MCWH interventions (Table 4.18). The runoff yield at catchment scale was fairly high for catchment without influence of MCWH. Nevertheless, reasonably high runoff yield in other two catchments with MCWH revealed that upper catchment and its efficient drainage was more effective to raise runoff yield as compared with effect of MCWH to reduce it. This also indicates the influence of ground realities on assessment and limitations of assessment methods.

The results of micro-catchment-scale measurements showed the maximum potential of harvesting of runoff by the MCWH structures, when site-scale study depicted the runoff that was concentrated to plant location. There remained a wide gap between potential of runoff harvesting and flow concentrated to plant location. Variations in topography and effectiveness of MCWH structures to concentrate flow at plant location are responsible for this gap. This gap can reasonably be reduced by improving MCWH implementation methodology.

Runoff measurements at the three scales showed that runoff yield fairly responded to the rainfall amount. It indicated that rainfall amount had a fair share in contribution to runoff yield as an independent variable. The other independent variables such as rainfall intensity, antecedent soil-water conditions and catchment characteristics also played critical role in runoff generation. In reality, the combined effect of all these independent variables and interactions among them complicated the runoff process and its quantity estimate. Unraveling the effect of the each individual variable may require a great deal of time and resources inputs, which was beyond the scope of this study.

The different spatial scale measurement in this study revealed that MCWH did not significantly affect the runoff yield at catchment scale. High runoff production potential of the upper catchment and its unsuitability for MCWH for shrub raising (steep topography, shallow soils and high drainage density) overwhelmed the effect of MCWH on runoff reduction in the middle reaches. Therefore, dominance of runoff from the upper catchment diminished the effect of MCWH structures on lowering the runoff and resulted in relatively higher runoff yield at catchment scale.

This infers for insignificant consequences on water availability at downstream due to water harvesting at upstream.

Table 4.18. Summary of Runoff Yield Measurement

Event Date	Rainfall Amount (mm)	Runoff Yield (m^3 ha^{-1}) at Measurement Scales				
		Micro-catchment	Site	Catchment		
				W-1	W-2	W-3
4th April, 2006	6.1	27–36	4–15	55.7	62.7	87.6
3rd October, 2006	5.1	5–15	2.5–11	–	–	–
25th October, 2006	21.1	38–86	3–27	110.9	142.2	102.7
1st March, 2007	15.4	30–89	5–22	–	–	–
12th May, 2007	17.1	36–64	4–24	38.1	66.4	56.2
18th May, 2007	21.8	68–187	5–30	238.0	280.5	211.2
Annual		177–441	19.5–114	387.0	489.1	370.1

4.4 Soil Erosion by Water

4.4.1 Sediment Yield at Micro-catchment Scale

4.4.1.1 Runoff Plot Method

Sediment from the runoff tanks was collected after each runoff event and was analyzed for sediment yield per unit area or unit sediment rate (Mg ha^{-1}) and annual sediment rate (Mg ha^{-1} yr^{-1}) (Annex C-1). The unit sediment rate (USR) provided a consistent basis to know the response of the catchment to different rainfall, runoff and MCWH techniques. The annual sediment rate (ASR) helped to know the response of the catchment area to the sediment yield.

The ASR varied between 0.2 and 2.9 Mg ha^{-1} with an average value of 1.21 Mg ha^{-1} (Annex C: Table C-1.1). The relationship between annual sediment rate and micro-catchment area (Fig. 4.46) showed a decrease in ASR with the increase in the micro-catchment area. Power equation poorly fits to the data and takes the form of

$$q_s = aA^b \quad (R^2 = 0.19) \qquad (4.1)$$

Where 'A' is micro-catchment area in m^2, 'q_s' is annual sediment rate in Mg ha^{-1} yr^{-1} and 'a' and 'b' are coefficient and exponent, respectively. The values of 'a' and '*b*' in the equation 4.1 is *10.99* and *-0.7386*, respectively. This equation was developed in micro-catchment area domain between 13 and 50 m^2.

Relationship between Unit sediment rate and event rainfall lumped over the micro-catchment areas showed a linear trend (Fig. 4.47) and takes a form of

$$q_s = aP + c \quad (R^2 = 0.59) \tag{4.2}$$

Where '*P*' is event rainfall in mm, 'q_s' is sediment rate per unit area in Mg ha^{-1}, '*a*' is coefficient and '*c*' is constant. The values of '*a*' and '*c*' in the above equation is *0.02* and *-0.091*, respectively. The event rainfall varied between 5.1 and 21.8 mm for this estimate. The value of constant 'c' in this equation indicates that an event rainfall less than 5 mm is less likely to cause soil erosion. Sediment yield for individual rainfall events during the study period is given in Annex C: Figs C-1.1 to C-1.7.

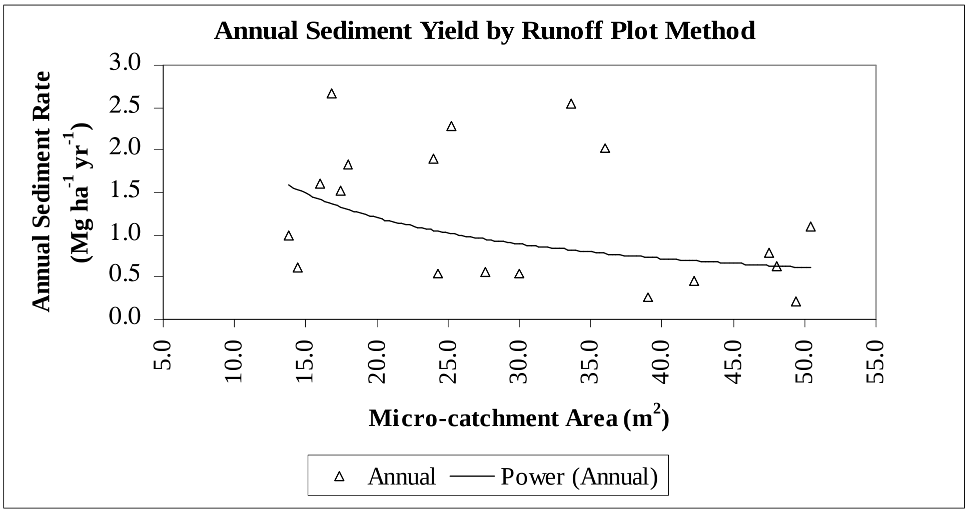

Figure 4.46. Annual Sediment Rate as a Function of Micro-catchment Area

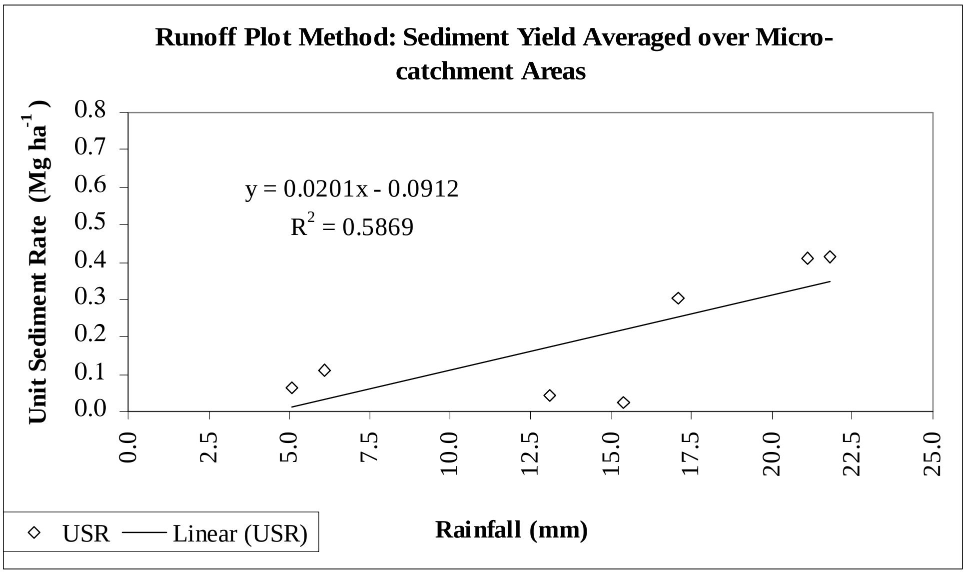

Figure 4.47. Unit Sediment Rate as a Function of Event Rainfall Lumped over Micro-catchment Areas

Variation of annual sediment rate in relation to MCWH techniques and treatments showed high ASR for 6 meter slope length (Sc-6 and Vi-6) and low for 12 meter slope length (Sc-12 and Vi-12) (Fig. 4.48). This behavior is unusual as kinetic energy of flow increases with uniform slope length and causes erosion under natural conditions. This effect is visible in case of Vc-12 and Vc-6 techniques. High erosion from disturbed land and ridges may have contributed more sediment to shorter slope lengths, when in case of longer length part of the eroded soil may have settled down along the flow paths. Among MCWH techniques, the annual sediment rate was low for semi-circular bunds and high for Vallerani intermittent and continuous ridges. It is due to the reason that the semi-circular bunds were constructed manually with minimum land disturbances. Nevertheless, the machine-made intermittent and contour ridges due to operation of heavy machinery and high land disturbances may have caused more erosion. Sediment data for each runoff event for different MCWH techniques and treatments is given in Annex C: Table C-1.2.

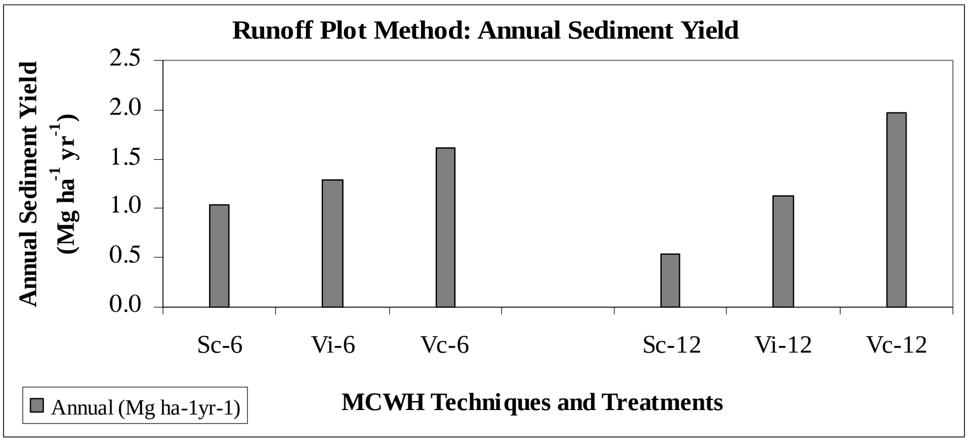

Figure 4.48. Annual Sediment Rate in Relation to MCWH Techniques and Treatment

The overall sediment yield per ha deceased with the increase in micro-catchment area for all events (Annex C: Figs C-1.1 to C-1.7). This is a usual trend and theory explains it clearly. Nevertheless, some data points greatly deviated from the general trend. For example, the micro-catchment area about 17 m^2 resulted in high sediment yield per unit area for majority rainfall events. On the other hand, the micro-catchment areas between 25 ad 30 m^2 resulted in low sediment yield per unit area in most of the cases. Although consistency largely prevails in these cases, but these can be the major contributors in determining degree of correlation between independent and dependent variables of the regression equations.

4.4.1.2 Gerlach Trough Method

Eleven Gerlach Troughs were installed on micro-catchments of slopes between 2 and 6% and micro-catchment areas between 11 and 90 m^2. The sediment was collected from one opening at downstream end in an attached bag. Remaining four openings allowed to passing the runoff at downstream. The sediment data from each trough was collected and weighed after each runoff event and it was analyzed for average annual soil losses (Annex C: Table C-1.3). The annual sediment rate varied between 0.09 and 1.47 Mg ha^{-1} with an average annual value of about 0.5 Mg ha^{-1}.

The relationship between micro-catchment area and annual sediment rate (Fig. 4.49) shows that the annual sediment yield (Mg ha^{-1} yr^{-1}) decreases with the increase in micro-catchment area. Power equation fairly fits to the annual sediment yield data.

$$q_s = aA^b \quad (R^2 = 0.32) \qquad (4.3)$$

Where '*A*' is micro-catchment area in m², 'q_s' is annual sediment yield in Mg ha^{-1} yr^{-1} and '*a*' and '*b*' are coefficient and exponent, respectively. The values of '*a*' and '*b*' in the equation 4.3 is *1.93* and *-0.4889*, respectively. This equation was developed in micro-catchment area domain between 11 and 90 m^2.

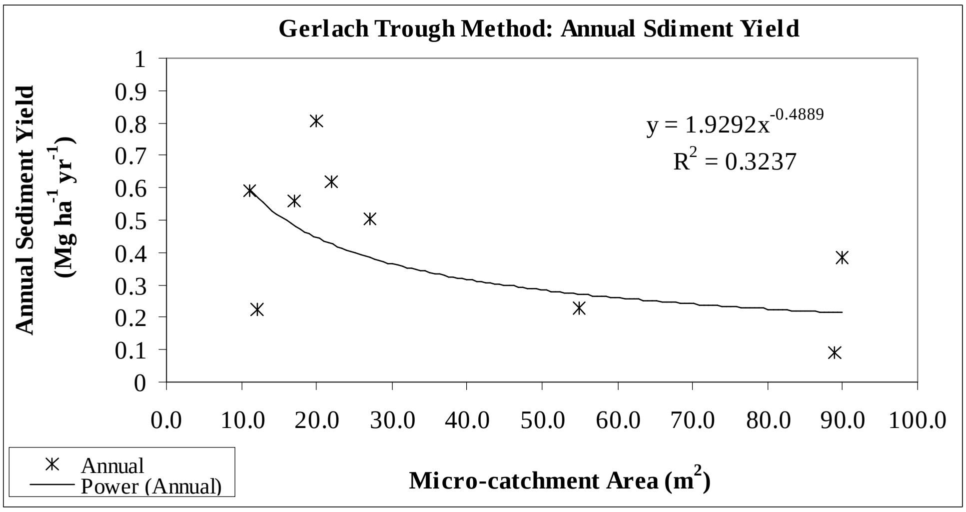

Figure 4.49. Annual Sediment Rate as a Function of Micro-Catchment Area (Gerlach Trough Method)

4.4.1.3 Discussion on Sediment Yield at Micro-Catchment Scale

Two methods were used to measure sediment loss from the micro-catchments. The runoff plot method was used in intervention area, where sediment laden runoff was collected at the outlet of the micro-catchments created by semi-circular bunds and Vallerani intermittent and continuous contour ridges. The Gerlach trough measured sediment loss from micro-catchment areas along the rills and gullies as it needs cut channel to guide surplus runoff at downstream. This area was without effect of the MCWH interventions.

A comparison of the unit sediment rate by the Runoff Plot and Gerlach Trough methods (Table 4.19) showed that the runoff plots estimated by about 2.4 times more annual sediment yield per unit area. Two missing events in case of Gerlach Trough may have introduced this major difference. The average sediment yield for rainfall events matched in both the cases. The annual sediment yield after adjusting for the two missing events by average sediment yield of available data yielded annual sediment yield of 0.77 Mg ha^{-1}, which is 64% of the sediment yield measured by Runoff Plot Method. Two main possibilities of this difference are discussed.

Firstly, the construction of MCWH interventions (bunds and ridges) loosened the soil and increased the angle of repose (bunds and ridges). Both loose soil and high angle of repose created favorable conditions for soil erosion and high sediment yield in runoff plots. Considering Gerlach Trough being non-intervention area as control and runoff plots in intervention area, the intervention area produced about 1.5 times more sediment yield than the control.

Secondly, the possibility of error in measurements was also explored. The errors in runoff micro-catchment method may occur due to non-horizontal installation of tanks and resulting in higher water depth on one side and lower on the other side, leakage from the tanks due to damages by rusting, overflowing and poor mixing of sediment with water at the time of sampling and processing and computational error. The first type of error was eliminated by installing tanks by horizontal control method using total station and manual levels. This method was used for all instruments installation at the site. The new tanks of galvanized iron were used in the study, which also eliminated the error of leakage. Further, to check the leakage problem the water in the tanks was monitored for several hours before emptying them. A 40–50 cm earthen ridge downstream of the collection tank prevented the overflowing of runoff. Proper mixing of sediment with water was ensured by stirring the water and taking 3–5 representative samples. Nevertheless, inadequate mixing of water and sediment should not over-estimate the sediment yield. Same team worked for entire study period, therefore human error if any should appear consistently in all measurements. The possibility of under estimation by the Gerlach Trough may include non-uniform flow though the slots, removal of sediment collection bag or capacity constraint of bag during high rainfall event. The runoff collection tray ensured the flow uniformity though the openings. Removal of bag means zero sediment, so under estimation in this case was not possible.

Table 4.19. Comparison of Sediment Rate Measurement by Runoff Plot and Gerlach Trough Methods.

Date	Rainfall (mm)	Sediment Rate by Runoff Plots (Mg ha^{-1})	Sediment Rate by Gerlach Trough* (Mg ha^{-1})
5/5/2005	13.1	0.04	0.02
4/4/2006	6.1	0.11	0.2
10/3/2006	5.1	0.06	–
10/25/2006	21.1	0.06	0.07
3/1/2007	15.4	0.41	0.17
5/12/2007	17.1	0.02	–
5/18/2007	21.8	0.31	0.24
Average		0.144	0.14
Annual	125.9	1.21	0.49

*Annual sediment rate after adjustment for two missing event 0.77

Relationship between runoff and sediment yields at micro-catchment scale for Runoff Plot and Gerlach Trough methods (Fig. 4.50) shows that the unit sediment yield increases with unit runoff yield following linear equation with zero intercept and takes form,

$$q_s = a\,Ln(q) + c \qquad (4.4)$$

Where 'q' is event runoff yield in $m^3\,ha^{-1}$, 'q_s' is sediment yield in Mg ha^{-1}, 'a' is coefficients and is equal to 0.066 and 0.071 for Runoff Plot and Gerlach Trough, respectively. The value of c is -0.085 for Runoff Plot and -0.124 for Gerlach Trough. The R^2 value for the regression equation was 0.23 for the Runoff Plot and 0.49 for Gerlach Trough. The trend lines for both the methods are comparable, but Gerlach Trough slightly under estimates the sediment yield for same runoff yield.

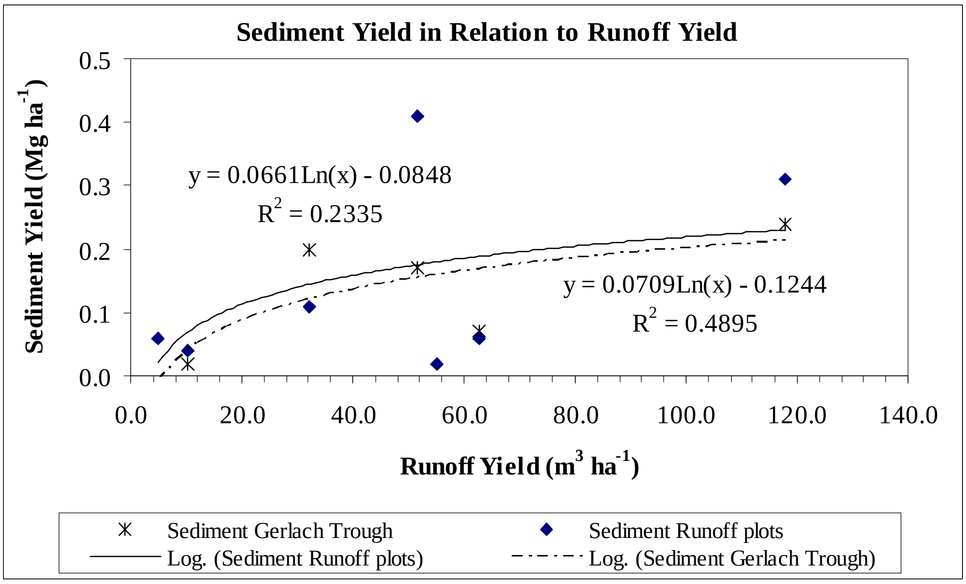

Figure 4.50. Sediment Yield in Relation to Runoff Yield at Micro-catchment Scale

4.4.2 Water Erosion at Rill Scale

4.4.2.1 Erosion/Deposition in Inter-Rill Area

Erosion pins measured the erosion and deposition in inter-rill area by measuring land surface from top of the pins for major rainfall events. The data was analyzed for soil loss and deposition in the inter-rill area. Bulk density of 1150 kg m^{-1} was used to compute the sediment load for the study area. The data (Table 4.20) showed the net erosion in interrill area of 1, 2, 6, 7 and 8 and net deposition in 3, 4, 5 and 9. The net erosion rate varied between -4.59 and -20.5 Mg ha^{-1}. Negative sign shows erosion. The net deposition ranged between 0.57 and 10.86 Mg ha^{-1}. This erosion rate is high and can be linked to measurement error associated with this method. The erosion and deposition in interrill area (Annex C-2.1) did not follow some specific pattern. Complexity due to interaction among rainfall amount and intensity, splashed material and sheetflow kinetic energy was responsible for unclear trend of the erosion/deposition with the pin no.

Table 4.20. Average Erosion and Deposition in Inter-rill Area

Rill No	Catchment Area (m^2)	Slope (%)	No of Pins	Average Erosion/Deposition (Mg ha^{-1}) for Rainfall Events on			
				4/4/2006	10/25/2006	3/1/2007	Net
1	289	3.15	141	-5.52	5.38	-6.20	-6.34
2	935	3.98	333	-9.61	13.04	-9.08	-5.65
3	350	3.03	83	-19.26	23.55	1.39	5.68
4	266	2.31	153	9.09	-1.20	-1.20	6.69
5	1372	2.9	261	-7.53	6.17	1.94	0.57
6	426	3.59	100	-5.75	-16.15	1.39	-20.50
7	263	4.15	76	-11.80	-5.06	12.28	-4.59
8	293	4.43	86	-3.88	0.81	-3.65	-6.72
9	431	2.5	102	3.16	7.48	0.23	10.86

Rill 1–3 and 5 are without and 4, 6–9 are with MCWH. Negative sign shows erosion and +ve deposition

4.4.2.2 Erosion/Deposition within the Rills

Erosion and sedimentation within the rills were measured by using Erosion Bridge Frame (EBF). The EBF measured the rill cross-sections at several locations along the rills. Aggradations and degradations at the cross-sections estimated the erosion and deposition for each runoff event. The results (Table 4.21) showed a net deposition in rills 1, 6, 7 and 9, and erosion in rills 2, 3, 4, 5 and 8 during the study period. The deposition in rills 1, 6 and 7 followed the erosion in their respective interrill areas, which meant that erosion in interrill areas caused sediment transport and deposition in these rills. Similarly, net deposition in interrill areas 3, 4 and 5 led to low sediment in their respective rills and caused erosion in these rills. Nevertheless, deposition in rill 9 and erosion in rill 8 followed the deposition in interrill area 9 and erosion in interrill area 8, respectively. This different phenomenon can be linked to the sediment carrying capacity of these rills for different runoff events. Probably, the rill 8 had more sediment carrying capacity than sediment inflow from the interrill area. Similarly, rill 9 may had less carrying capacity than sediment inflow and caused deposition. It should be noted that the sediment carrying capacity of rills depends on the kinetic energy of flow in the rills and vary from storm to storm.

Soil erosion and deposition within the rills was also analyzed at different sections. The section 1 was at the most downstream and section number increased in upstream direction. Erosion and deposition pattern at different cross-sections in the rills (Annex C-2.2) shows that in rill 1, erosion occurred in all the three sections during runoff event on 25th October, 2006 followed by deposition in March 2007. The rill remained stable during event in May 2007. Section 1 of the rill 2 remained also stable, when eroded material at section 3 was deposited immediately downstream at section 2. In rill 3, the section 1 experienced deposition till 16th May 2007 and erosion during runoff event on 18th May 2007. Deposition in early season at section 1 was due to erosion at section 4 upstream. In rill 4, erosion and deposition balanced each other in upper sections, when the section 1 showed stability. It was due to reason that the sections 3 and 6 reciprocated the erosion and deposition to each other. Rill 5 remained fairly stable, when deposition in 2006 followed the erosion in 2007. In rill 6, erosion at section followed deposition in May 2007. Similarly, deposition in section 2 in March 2007 followed erosion in May 2007. Section 3 almost remained stable with a fair balance of erosion and deposition in upper sections. In rill 7, erosion in section 3 followed by the deposition in section 2, when section 1 remained fairly stable. In rill 8, sections 2 and 3 experienced deposition in March 2007 and erosion in May 2007. Section 1 remained almost stable during the study period. Rill 9 largely experienced deposition with minor erosion at section 2. Erosion-deposition analysis within the rills showed that erosion in the upper sections followed by the deposition in the lower sections and vice versa. In most of the cases the most downstream section remained fairly stable.

Table 4.21. Erosion and Deposition Pattern in Rills

Rill No.	Description	Erosion/Deposition in Relation to Time (kg)					
		4-Apr-06	25-Oct-06	01-Mar-06	12-May-07	18-May-07	Total
1	Erosion	-9.2	-838.2	0.0	-24.0	-97.9	-969.4
	Deposition	97.4	0.0	927.0	131.0	77.2	1232.5
	Net	88.2	-838.2	927.0	106.9	-20.7	263.2
2	Erosion	-288.3	-678.8	0.0	-96.3	-820.9	-1884.3
	Deposition	303.3	259.2	916.1	0.0	272.4	1751.0
	Net	15.0	-419.6	916.1	-96.3	-548.4	-133.3
3	Erosion	0.0	-188.8	-0.6	-18.8	-141.7	-349.8
	Deposition	44.4	0.0	135.6	94.8	10.0	284.9
	Net	44.4	-188.8	135.1	76.0	-131.7	-65.0
4	Erosion	-82.2	-54.0	-56.1	-19.4	-223.1	-434.9
	Deposition	4.0	49.6	98.7	52.9	56.1	261.3
	Net	-78.2	-4.4	42.6	33.4	-167.1	-173.6
5	Erosion	-349.0	-60.3	-13.5	-185.3	-580.2	-1188.3
	Deposition	69.1	326.9	258.2	328.4	40.0	1022.5
	Net	-279.9	266.6	244.7	143.1	-540.2	-165.8
6	Erosion	-11.2	-50.5	0.0	-207.0	-26.5	-295.3
	Deposition	20.1	19.0	187.2	11.0	256.8	494.2
	Net	8.9	-31.5	187.2	-196.0	230.3	198.9
7	Erosion	-203.6	-256.2	-382.8	-195.8	-21.1	-1059.5
	Deposition	47.5	407.1	81.6	0.0	103.6	639.8
	Net	-156.1	150.9	-301.2	-195.8	82.5	-419.7
8	Erosion	-86.4	-16.6	-5.3	-3.5	-171.0	-282.8
	Deposition	40.5	50.0	143.9	37.1	0.0	271.6
	Net	-45.9	33.5	138.6	33.6	-171.0	-11.2
9	Erosion	-72.5	0.0	-20.5	-12.6	0.0	-105.7
	Deposition	0.0	57.1	55.1	54.5	104.4	271.1
	Net	-72.5	57.1	34.6	41.9	104.4	165.4

Rainfall year starts in September and ends in May

4.4.2.3 Sediment Yield at the Outlet of Rills

Runoff traps measured sediment yield at the outlet of rills. The results show (Table 4.22) that sediment yield varied between 0.0014 and 0.44 Mg ha^{-1} for different rainfall events. The sediment yield from rill 7 on 4th April, 2006 was not included due to breaching of the ridges. The annual sediment yield varied between 0.03 and 0.427 Mg ha^{-1}. The average annual sediment yield for all cases was estimated at 0.18 Mg ha^{-1}. Average annual sediment yield for all control cases was estimated at 0.13 and for intervention area it was 0.22 Mg ha^{-1}. The sediment yield from intervention area was little less than double the sediment yield from intervention area. The disturbances in the intervention area could be responsible for this higher yield.

Table 4.22. Sediment Yield at the Outlet of Rills

Rill No	Treatment	Catchment Area (m^2)	Sediment yield (Mg ha^{-1})					
			4/4/2006	25/10/06	3/1/2007	5/12/2007	5/18/2007	Annual
1	Rest	289	0.189	0.1430	0.0015	0.0037	0.012165	0.160
2	Rest	935	0.203	0.1029	0.0037	0.0030	0.0075	0.117
3	Rest	350	0.247	0.1194	0.0063	0.0081	0.037768	0.172
4	Vi-6	266	0.147	0.00	0.00	0.0027	0.028548	0.031
5	Rest	1372	0.049	0.0474	0.0021	0.0014	0.002296	0.053
6	Vc-6	426	0.092	0.2517	0.0023	0.0041	0.013336	0.271
7	Vc-12	263	3.890	0.0010	0.0038	0.1540	0.021709	0.180
8	Vc-12	293	0.368	0.3139	0.0082	0.0624	0.043003	0.427
9	Vi-12	431	0.090	0.0896	0.0059	0.0495	0.044072	0.189
Average annual value for combine cases (Mg ha^{-1})								0.178
Average annual from all controls (Mg ha^{-1})								0.126
Average annual from all treatments (Mg ha^{-1})								0.220

4.4.3 Sediment Yield at Catchment Scale

Catchment-scale sediment delivery was measured in three streams at upstream of purposely constructed weirs. The catchment area at the weir sites varied from 5.1 to 36.30 ha. The results (Table 4.23) showed that the sediment yield varied between 0.02 and 1.1 Mg ha^{-1} for different rainfall amounts. The annual sediment yield varied between 1.25 and 1.49 Mg ha^{-1}. Relatively high sediment at catchment scale as compared with micro-catchment and rill scales is linked to the steep upper catchment that potentially generated high runoff and sediment yield. It also depicted that regardless of disturbed land the contribution of the intervention area to the sediment yield was proportionately low. Flat slope in the middle reach in the intervention area was mainly responsible for low the low contribution at catchment scale. It indicated that MCWH did not significantly affect the sediment yield at the catchment scale. It was also noticed that most of annual runoff and sediment loss resulted from a fewer larger events that occurred during period when soils were nearly saturated. The results depicted that one such runoff event on 18th July 2007 contributed to about 64–72% of the annual sediment yield for different catchment sizes.

Table 4.23. Sediment Yield of Small Catchment

Location	Catchment Area (ha)	Sediment Yield (Mg ha^{-1})					
		4/4/2006	10/3/2006	10/25/2006	3/1/2007	5/18/2007	Annual
Weir-1	36.30	0.12	0.06	0.24	0.08	0.87	1.25
Weir-2	21.00	0.10	0.13	0.24	0.06	1.07	1.49
Weir-3	5.10	0.05	0.02	0.25	0.24	0.91	1.42

4.4.4 Sediment Enrichment

Determining the sediment enrichment at the outlets of rills and weirs measured the affect of MCWH on soil quality. Representative sediment samples at the outlets of the rills and at the weirs were analyzed for main chemical properties for two runoff events (Tables 4.24 and 4.25). The organic matter in control (0.99%) was comparable with the organic matter measured at the rill outlets for both events (0.82 and 1.0%). The organic matter (OM) in sediment at catchment scale was 0.86% for runoff event on 25th October, 2007 and 2.9% on 4th April, 2006. The higher value of the OM in case of runoff event on 4th April, 2007 can be linked to high manure concentration by the grazing livestock in the upper catchment during the season. Comparing with the control the extractable phosphorous (Olsen p) was around two times higher in sediment at the rills outlet and 2.5 to 3 times higher in sediment at the catchment outlets. The extractable potassium in sediment both at rill and catchment scale was lower than the control. The total nitrogen at rill scale was 1 to 2 times and at catchment scale it was about three times higher than the control. Results do show significant difference of Olsen p and total nitrogen and sediment enrichment in these cases varied from 1 to 3 times. However, the insignificant difference of organic matter can be linked to the soil degradation.

Table 4.24. Comparison of Soil Parameters in Control and Sediment Deposition Areas after Runoff Event 4th April, 2006

Treatments	Sample ID	Sample location	OM	Olsen-P	Extr. K	Mineral Nitrogen (ppm)		
						NH_4-N	NO_3-N	Min-N
			%	ppm	ppm	ppm	ppm	ppm
Control area (June 2005)								
Baseline	Block A	Control	1.18	7.2	340.9	2.3	12.8	15.1
	Block B	Control	0.96	8.3	381.4	11.4	9.5	20.8
	Block C	Control	0.84	8.8	327.6	3.2	8.2	11.4
		Average	*0.99*	*8.1*	*350.0*	*5.6*	*10.1*	*15.8*
At sediment trap at the outlet of each measured rill (After runoff event 4th April 2006)								
Rill trap 1	RT-1	Rill outlet	0.78	15.4	99.8	8.0	21.3	29.3
Rill trap 2	RT-2	Rill outlet	1.61	24.3	203.8	17.2	26.1	43.2
Rill trap 3	RT-3	Rill outlet	0.83	17.8	185.8	10.6	23.4	34.0
Rill trap 4	RT-4	Rill outlet	1.34	21.8	213.0	21.3	26.3	47.7
Rill trap 5	RT-5	Rill outlet	1.50	20.7	136.2	8.2	19.5	27.7
Rill trap 6	RT-6	Rill outlet	1.91	23.1	160.2	14.5	24.2	38.7
Rill trap 7	RT-7	Rill outlet	0.60	10.0	185.8	5.3	31.6	36.9
Rill trap 8	RT-8	Rill outlet	1.08	14.9	194.7	13.7	28.8	42.5
Rill trap 9	RT-9	Rill outlet	0.78	22.6	194.7	12.1	18.0	30.1
		Average	*0.82*	*15.8*	*191.7*	*10.4*	*26.1*	*36.5*
In main gullies at upstream of weirs (After runoff event 4th April 2006)								
Weir-1	W-1–1	0.5	3.51	29.2	251.9	30.0	26.1	56.1
	W-1–2	6.0	3.65	29.7	251.9	22.0	45.5	67.5
	W-1–3	12.0	2.31	28.1	232.1	16.9	61.3	78.2
Weir-2	W-2–1	0.5	2.24	26.9	232.1	31.8	20.2	52.0
	W-2–2	10.0	2.41	25.3	241.9	26.5	22.4	48.9
	W-2–3	20.0	3.20	35.8	222.5	20.6	38.0	58.6
Weir-3	W-3–1	0.5	2.49	23.9	177.1	25.8	26.9	52.7
	W-3–2	5.0	4.90	30.6	213.0	25.3	37.2	62.6
	W-3–3	10.0	1.50	15.0	128.5	12.4	25.5	37.9
		Average	*2.91*	*27.2*	*216.8*	*23.6*	*33.7*	*57.2*

Table 4.25. Comparison of Soil Parameters in Control and Sediment Deposition Areas after Runoff Event 25th October, 2006

Treatments	Sample ID	Sample location	OM	Olsen-P	Extr. K	Mineral Nitrogen (ppm)		
						NH_4-N	NO_3-N	Min-N
			%	ppm	ppm	ppm	ppm	ppm
Control area (June 2005)								
Baseline	Block A	Control	1.18	7.2	340.9	2.3	12.8	15.1
	Block B	Control	0.96	8.3	381.4	11.4	9.5	20.8
	Block C	Control	0.84	8.8	327.6	3.2	8.2	11.4
		Average	*0.99*	*8.1*	*349.9*	*5.6*	*10.1*	*15.8*
At sediment trap at the outlet of each measured rill (After runoff event 25 Oct 2006)								
Rill trap 1	RT-1	Rill outlet	0.85	13.3	171.3	16.0	5.4	21.4
Rill trap 2	RT-2	Rill outlet	1.81	17.3	287.4	13.6	8.3	21.8
Rill trap 3	RT-3	Rill outlet	0.53	4.9	123.4	4.6	6.4	11.0
Rill trap 4	RT-4	Rill outlet	1.07	16.2	235.7	8.7	12.5	21.3
Rill trap 5	RT-5	Rill outlet	1.07	18.8	188.7	4.5	10.8	15.3
Rill trap 6	RT-6	Rill outlet	1.00	22.3	225.9	4.5	11.1	15.7
Rill trap 7	RT-7	Rill outlet	0.92	11.9	696.8	9.4	3.8	13.1
Rill trap 8	RT-8	Rill outlet	0.89	8.7	405.0	5.3	3.4	8.6
Rill trap 9	RT-9	Rill outlet	0.89	14.9	235.7	16.6	13.69	30.3
		Average	*1.00*	*14.3*	*285.5*	*9.3*	*8.37*	*17.6*
In main gullies at upstream of weirs (After runoff event 25 Oct, 2006)								
Weir-1	W-1–1	0.5	0.74	20.0	213.0	7.2	10.7	18.0
	W-1–2	6.0	0.56	23.0	194.7	5.0	43.5	48.5
	W-1–3	12.0	0.35	25.6	160.2	4.5	27.9	32.3
Weir-2	W-2–1	0.5	1.51	23.6	251.9	15.9	106.2	122.0
	W-2–2	10.0	1.02	19.8	194.7	22.4	39.3	61.6
	W-2–3	20.0	0.74	17.6	144.0	14.1	29.8	43.9
Weir-3	W-3–1	0.5	1.41	26.1	160.2	22.9	25.5	48.4
	W-3–2	5.0	0.70	14.9	386.1	10.5	54.9	65.4
	W-3–3	10.0	0.70	12.5	93.1	4.4	19.2	23.6
		Average	*0.86*	*20.3*	*199.7*	*11.9*	*39.7*	*51.6*

4.4.5 Decay of MCWH Structures

Periodic collection of data on decay of MCWH ridges over the study period and its analysis showed (Fig. 4.51) that ridges decay was highest for Pakistani treatment, followed by manually constructed semi-circular bunds, and lowest in Vallerani treatments. Overall, the decay was low, which was linked to low rainfall. A linear decay trend (Table 4.26) takes a form of the following equation

$$H = at + c \tag{4.5}$$

Where '*t*' is time in month (represented by *x*), '*H*' is lowering of ridge in cm (represented by *y*), '*a*' is coefficient and '*c*' is constant. The values of '*a*' varied between 0.04 and 0.06 and '*c*' is set to zero to meet initial conditions (at time t_o the decay is zero). These equations were developed within time domain of 24 month. The results show an effective/half life as 20, 25 and 30 years for Pakistani, manual and Vallerani implement, respectively. Nevertheless, high return period rainfalls (10–25 years) may accelerate and affect the overall decay rate.

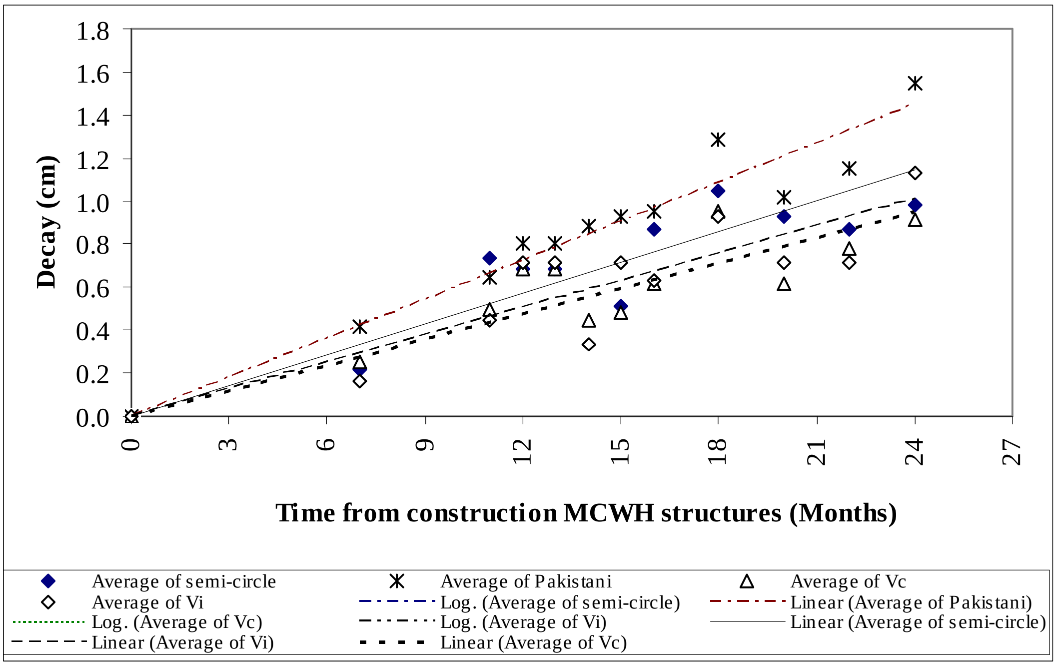

Figure 4.51. Decay of MCWH Structures in Relation to Time

Table 4.26. Ridge-decay Trends

Ridge Techniques	Decay Trend Equation	R^2
Pakistani implement	y = 0.0603x; where, *x* is decay time in months and *y* is lowering in ridge height in cm.	0.93
Manual bund (semi-circles)	y = 0.0479x; where *x* and *y* already defined	0.76
Vallerani continuous	y = 0.0395x; where *x* and *y* already defined	0.75
Vallerani intermittent	y = 0.042x; where *x* and *y* already defined	0.76

4.4.6 Estimation of Sediment Yield by RUSLE2 Model

4.4.6.1 Model Conceptualization

Water erosion assessment by the RUSLE2 for this study was conceptualized as,

- Overland flow length was kept as 45.7 m; a default value for this model. For study area, it largely varied between 40 and 50 m.
- Slope was fairly uniform in intervention area and average slope steepness was about 3%. Therefore, uniform slope template was used.
- The sediment delivery (SD) for control was estimated for entire overland flow length segment (45.7 m). However, SD for intermediate segment length was computed to know the trend.
- Soil loss and SD with MCWH were estimated for overland flow segment length of 6, 12 and 18 m for Vc-6 technique, 6, 12 and 24 for Vi-6, 12, 24 and 36 for Vc-12 and 24, 36 and 48 m for Vi-12 technique. It was based on the layout structure of these techniques. For example, a segment length of 18 m for Vc-6 will allow two sediment basins at 6 and 12 m to assess the effect of 2 intermediate continuous ridges in between. However, in case of intermittent ridges double the segment length was used to accommodate two sediment basins to simulate sediment routing through these ridges.
- Management practices included the ridges across the slope and highly disturbed land due to machine operation.

4.4.6.2 Development of Input Data Files

Four main data input files were developed including climate, soil, topography and land use. Rainfall and runoff drive major water erosion process. Monthly rainfall erosivity was computed by using continuous rainfall data at Qaryatin, MRC and the study area from 1996–1997 to 2006–2007 (Table 4.27). Mean-monthly rainfall, erosivity (EI30) and temperature data was used in climatic data input file. A 10-yr 24-h rainfall was estimated as 35 mm and was also used as an input. The model computed EI for 10-yr 24-h rainfall 280 MJ mm ha^{-1} h^{-1} and average annual erosivity (R) as 154 MJ mm ha^{-1} h^{-1}. Soil texture was sandy clay loam. Topography input data used the uniform slope of 3% average steepness. The land use practices used smooth and bare soil with no disturbances and up and down slope for control. For MCWH, the management included machine operation, ridges at given interval across the slope and intermediate sediment basins.

Table 4.27. Monthly Rainfall Erosivity for the Study Area.

Year	EI30												
	Jan	Feb	Mar	Apr	May	Jun	Jul	Aug	Sep	Oct	Nov	Dec	Annual
1996–97	17.6	0.9	19.8	4.2	12.6	0.3	0.0	0.0	0.0	0.0	188.8	81.5	325.7
1997–98	1.5	27.3	27.4	11.3	0.1	0.0	0.0	0.0	0.0	0.0	77.8	4.2	149.6
1998–99	1.5	27.3	27.4	11.3	0.1	0.0	0.0	0.0	8.7	0.0	0.0	2.5	78.8
1999–00	37.6	2.2	12.6	2.4	0.0	0.0	0.0	0.0	0.0	3.4	0.0	1.8	60.0
2000–01	1.2	25.2	1.6	33.8	5.9	0.0	0.6	0.0	0.0	9.8	1.2	9.4	88.7
2001–02	29.1	15.7	2.5	11.4	11.4	0.0	0.0	0.0	0.0	0.0	2.0	1.2	73.3
2002–03	2.0	24.5	0.0	0.0	0.0	0.0	0.0	0.0	0.0	2.8	53.6	7.2	90.1
2003–04	38.6	0.0	0.0	0.0	0.0	0.0	0.0	0.0	0.0	0.2	73.5	1.0	113.3
2004–05	61.6	66.8	0.3	24.4	38.0	0.0	0.0	0.0	0.0	2.9	152.0	29.6	375.6
2005–06	20.6	9.7	2.6	19.7	0.2	0.0	0.0	0.0	0.0	2.2	8.9	0.7	64.6
2006–07	0.6	7.0	1.3	1.5	106.7	0.0	0.0	0.0	0.0	39.0	0.5	0.7	157.3
Mean	19.3	20.7	10.6	13.3	19.4	0.1	0.1	0.0	1.2	5.5	50.8	12.7	143.4
EI30 dist.	0.13	0.14	0.07	0.09	0.14	0.0	0.0	0.0	0.01	0.04	0.35	0.09	1.06
Rainfall	13.5	14.5	20.9	11.9	14.7	0.2	0.0	0.0	0.3	8.0	14.4	12.8	110.6

4.4.6.3 Soil Loss and Sediment Yield Estimates

For control conditions, the sediment yield varied between 0.6 and 0.9 Mg ha^{-1} yr^{-1} for overland flow segments between 5 and 45.7 m. The maximum sediment yield (0.93 Mg ha^{-1} yr^{-1}) was estimated for the segment length 45.7 m and minimum (0.62 Mg ha^{-1} yr^{-1}) for the segment length 5 m. The entire soil loss within the segments was delivered to the end of segments because of slope uniformity and smooth and bare soils. Annual sediment yield in relation to slope length (Fig. 4.52) showed an increasing trend in sediment yield with increase in slope length. This was due to the fact that kinetic energy of flow increased with the slope length and induced erosion. Fitting the linear equation to the data gave the following relationship

$$q_s = aL_s + b \quad (R^2 = 0.94) \qquad (4.6)$$

Where 'L_s' is overland flow segment length in m, 'q_s' is annual sediment rate in Mg ha^{-1} yr^{-1} and '*a*' and '*b*' are coefficient and constant, respectively. The values of '*a*' and '*b*' in the above equation is *0.0072* and *0.629*, respectively. This equation was developed in segment length domain between 5 and 45.7 m. However, it is to be noted that for the given set of climatic, erosivity, topography and soil data a minimum soil loss around 0.60 Mg ha^{-1} yr^{-1} should be expected even for a smallest overland flow segment (slope length → 0).

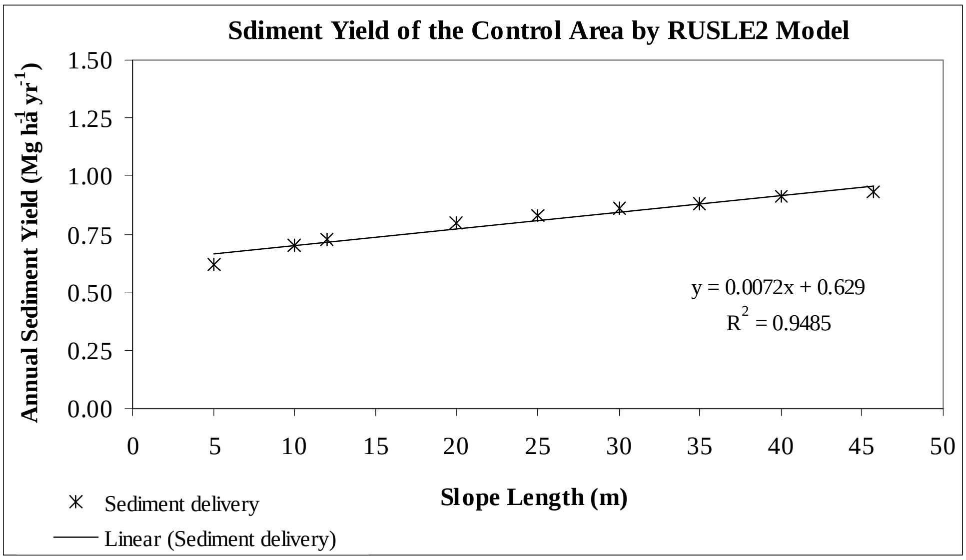

Figure 4.52. Annual Sediment Yield in Relation to Slope Length under Control Conditions

For intervention area the soil loss from eroded area and sediment delivery at the end of the overland flow length were modeled as

- For Vallerani continuous ridges, the soil loss was equal to the soil loss from eroded portion for entire segment length. The sediment delivery at the end of overland flow length was computed by assuming no routing effect, if ridge in between did not intercept (Vc-6 for 6 m and Vc-12 for 12 m slope lengths), sediment routing through one sediment basin if one intermediate ridge intercepted (Vc-6 for 12 m and Vc-12 for 24 m slope lengths) and sediment routing through two sediment basins if two intermediate ridges intercepted the flow (Vc-6 for 18 m and Vc-12 for 36 m slope lengths)

- For Vallerani intermittent ridges, the soil loss from eroded portion followed the similar pattern. In this study, the entire slope length was assumed to be eroded portion due to uniform slope and shorter length profile. However, the sediment delivery for intermittent ridges was modeled considering that out of 4 m width of a micro-catchment, 1.2 m (43% of the total width) delivered runoff/sediment at the end of the segment uninterruptedly. Nevertheless, remaining 2.8 m (57% of the total width) routed the runoff through sediment basins. Therefore sediment delivery by the 43% of the width of a micro-catchment equals the soil loss by the segment and for rest of the 57% width; the actual sediment delivery was 57% of the theoretically computed sediment delivery with intermediate sediment basins. The total sediment delivery for Vi, therefore, was estimated as 43% of the soil loss plus 57% of the sediment delivery with one intermediate sediment basin. For example, for Vi-6, 43% of eroded soil for 12 m slope length plus 57% of the computed sediment delivery for 12 m slope length. In case of Vi-12, the total sediment delivery will be equal to 43% of eroded soil for 24 m slope length plus 57% of sediment delivery for 24 m slope length.

The computations showed (Table 4.28) that for the Vallerani continuous ridges (Vc), the sediment delivery varied from 0.25 Mg ha^{-1} yr^{-1} for Vc-6 with 12 m segment length to 1.8 Mg ha^{-1} yr^{-1} for Vc-6 for 6 m segment length. In the case of Vc-6 with 12 m spacing, the intermediate ridge had intercepted the runoff and reduced the sediment delivery to the end of the segment. However, in the case of Vc-6 with 6 m spacing, the entire soil loss was delivered to the end of overland flow length as no ridge existed in between. For Vc-12; considering 24 and 36 m overland flow length, the sediment delivery was dropped from 2.3 (total soil loss from 12 m segment length) to around 0.33 Mg ha^{-1} yr^{-1}, due to routing effect of intermediate ridges.

Vi-6 and Vi-12 techniques, due to intermittent effect, responded differently. The difference in structural layout resulted in difference in soil loss and sediment yield. The soil loss for Vi-6 (12 m slope length with one sediment basin and 24 m slope length with two sediment basins) was 1.13 and 0.31 Mg ha^{-1} yr^{-1}. For Vi-12 the sediment yield was 1.48 and 0.40 Mg ha^{-1} yr^{-1} for 24 and 48 m overland flow length. Flow interception by the intermediate ridges reduced sediment delivery.

The results showed that the intermediate continuous ridges (Vc) reduced the sediment delivery to about 10% of the soil loss from the segments with 12 and 18 m length. However, in the case of Vallerani intermittent (Vi), one intermediate ridge, was able to reduce sediment delivery by about 50% of the total soil loss from the segments. Two intermediate ridges, in this case, have reduced the sediment delivery to about 10% of the soil loss from the segment. Comparing the effect of ridges with the control, it showed that the soil loss with MCWH was about 3–4 times higher than control, but sediment delivery with MCWH was about 50% of the sediment delivery without MCWH. Interception of runoff by the intermediate ridges was responsible for reduced sediment delivery for MCWH.

Table 4.28. Soil Loss and Sediment Yield with MCWH

MCWH Techniques	Slope Length (m)	Number of Ridges (Sediment basins) in between	Soil Loss and Sediment Yield (Mg ha^{-1} yr^{-1})	
			Soil loss eroded portion	Sediment Delivery (sediment leaving end of slope)
Vc-6	6	0	1.8	1.8
Vc-6	12	1	2.3	0.25
Vc-6	18	2	2.7	0.27
Vc-12	12	0	2.3	2.3
Vc-12	24	1	3.0	0.33
Vc-12	36	2	3.4	0.34
Vi-6	12	1	2.3	1.13
Vi-6	24	2	3.0	0.31
Vi-12	24	1	3.0	1.48
Vi-12	48	2	3.8	0.40

4.4.7 Summary of Sediment Yield

The sediment yield varied from 0.77 to 1.21 Mg ha^{-1} yr^{-1} at micro-catchment scale and 0.12 to 0.22 Mg ha^{-1} yr^{-1} at the rill scale for the study period (Table 4.29). At both the scales, the intervention area produced more sediment than the control area. The lower sediment yield at the rill scale was due to erosion, transport and deposition process driven by concentrated flows within the rills and sediment routing effect of these channels. However, breaching of the ridges in the three rills during one runoff event produced more than 10 times higher sediment and significantly increased the annual sediment yield at this scale. This adds complexity to the erosion assessment at the rill scale with MCWH structures. It is therefore important to note that storms of higher return periods (5–10 years or bigger) due to high flow concentration may cause breaching of the ridges and generate unprecedented erosion with MCWH structures. We also faced erosion measurement difficulties at this scale. Firstly, difficulty in achieving the accuracy in measurement of sheet erosion by pins due to very small scale (some times fraction of millimeters) and its multiplied effect. Secondly, the catch traps or settling tanks were not able to absorb runoff from bigger storms that may have produced a large fraction of the total sediment yield. Consequently, overflowing could take some sediment with runoff resulting in underestimation. During the study period some of the catch traps were replaced with settling tanks in order to avoid loss of sediment with runoff.

The sediment yield at the catchment scale ranged between 1.3 and 1.5 Mg ha^{-1} yr^{-1} at the catchment scale (Table 4.29). It showed that (i) the unit sediment yield at catchment scale was higher than at micro-catchment and rill scales, which is unusual and (ii) there was an insignificant difference of sediment yield between catchment 3 (without MCWH) and catchments 1 and 2 (partly with MCWH). Higher sediment yields at catchments scale than micro-catchment and rill scales were due to contribution of highly degraded upper catchment with steep slopes and incised small gullies as a result of heavy storm in May 2007. Insignificant difference of sediment yield from catchments 1 and 2 with MCWH and catchment 3 without MCWH can be explained from the distinctive sediment production potential of the upper and lower catchments. The upper catchment due to steep topography and shallow soils is not suitable for MCWH. The proportionate contribution of lower catchment with MCWH to the overall sediment yields at catchment scale was low, which resulted into a trivial difference in the sediment yields. It has also indicated that the MCWH in this environment does not affect sediment yield at catchment scale, significantly.

A comparison of the soil loss and sediment delivery by RUSLE2 Model (Table 4.27) showed a reasonable match between measured and simulated data. However, due to its flexibility, the model was able to produce results for many scenarios, which were difficult to achieve through measurement due to time and resource limitations for this study.

Table 4.29. Summary of Sediment Yield at Different Scales

Measurement Scale	Unit Sediment Yield (Mg ha^{-1} yr^{-1})
Micro-catchment Scale	
Runoff micro-catchments	1.21
Gerlach Trough	0.77
Rill Scale	
Annual sediment yield in control	0.12
Annual sediment yield with MCWH	0.22
Annual sediment yield with breaching	2.62
Catchment Scale	
Catchment 1, with partial MCWH	1.30
Catchment 2, with partial MCWH	1.50
Catchment 3, without MCWH	1.40
Estimation by RUSLE2 Model	
Soil loss and sediment delivery (5–45.7 m segment length) without MCWH (control)	0.6–0.9
Soil loss from segments (6–48 m length) for different Vc and Vi treatments	1.8–3.8
Sediment delivery from segments (6–48 m lengths) for i) For Vc treatments ii) For Vi treatments	 0.25–0.34 0.31–1.48

4.4.8 Tolerable Soil Loss

A tolerable soil loss (T) is the maximum annual amount of soil, which can be removed before the long term natural soil productivity is adversely affected. The T value for Darling Downs, Queensland in Australia was adopted as 10 Mg ha^{-1} yr^{-1} for land on 2–10% for crops on slopes (Rose, 1994). Soil-loss tolerance for all crop land soils in USA was assigned ranging from 2 Mg per ha per year for fragile soils to 11 Mg ha^{-1} yr^{-1} for soils not readily damaged by erosion (Toy *et al.* 2002). The main factors were soil formation rate from parent material, rate of top soil formation, reduction of crop yield, change in soil properties, soil depth, loss of organic matter, sediment deposition problem, likelihood of rills and gully formation, sediment delivery and feasible, economic and socially acceptable conservation practices (Mannering, 1981; McCormack and Young, 1981). The top soil formation rate was estimated as 11 Mg ha^{-1} yr^{-1}, which sets the upper limit of soil loss tolerance (McCormack and Young, 1981). An average soil formation rate from its parent material was estimated at 1.0 Mg ha^{-1} yr^{-1} with a variation of 0.1–3 Mg per ha per year depending on climate and other factors (Morgan 1991). The soil loss tolerance in relation to rill and inter-rill erosion was set to be 15 Mg ha^{-1} yr^{-1}, at which rills begins to form (Toy *et al.* 2002). Foster (2003), for RUSLE model, adopted a soil-loss tolerance value of 4 to 5 Mg ha^{-1}. The maximum soil loss in the study area varied between 0.12 and 1.4 Mg ha^{-1} Yr^{-1} for control and from 0.22 to 3.8 Mg ha^{-1} yr^{-1} with MCWH for different treatments and scales. In total, the study area produced about 300 Mg yr^{-1} of sediment from 2.5 km^2 area. This soil loss should not be a major problem in the study environment. The lower soil losses in the study area could be attributed to the lower rainfall and its erosivity.

4.5 Runoff and Soil Loss Prediction Equations

This study developed some prediction equations (Table 4.30) for water and sediment loss assessment in the study area. These equations are valid only in the given domains for certain set of conditions. Extrapolation to certain degree may be made with caution. For other environments and conditions, the equations may be used as guiding research tool.

Table 4.30. Prediction Equations for Estimation of Runoff and Sediment Loss

Description	Prediction Equation	Explanation of Variables	R^2	Limitations
Runoff yield in relation to event rainfall at micro-catchment scale	$q = 4.6P - 17.71$ $P \geq 3.9$	*P* is event rainfall in mm and *q* is event runoff in $m^3\ ha^{-1}$	0.65	Micro-catchment area between 13 and 50 m^2 and event rainfall between 5 and 22 mm
Runoff Yield in relation to event rainfall at site scale	$q = a\,Ln(P) + c$ $P \geq 1.82$ *a* is coefficient (11.32) and *c* is intercept (-6.75).	*q* is unit runoff yield ($m^3\ ha^{-1}$), *P* is event rainfall in mm. *p* must be +ve integer	0.96	For Vi-6 technique only. The soil-water averaged for 15 locations to estimate runoff
Runoff/ rainfall ratio in relation to event rainfall (catchment scale)	$\frac{R_o}{P} = 0.22P - 0.115$ $P \geq 0.53$	*P* is event rainfall in mm and R_o is event runoff in mm. *p* must be +ve integer	0.85	Small catchment (area ~ 21 ha)
Sediment Yield in relation to event rainfall at Micro-catchment Scale	$q_s = 0.02P - 0.091$ $P \geq 4.6$	*P* is event rainfall in mm, q_s is sediment rate per unit area in Mg ha^{-1}	0.59	Micro-catchment area between 13 and 50 m^2 and event rainfall between 5 and 22 mm
Sediment yield vs. runoff yield at Micro-catchment scale. Runoff plot (RP) and Gerlach Trough (GT) methods	$q_s = a\,Ln(q) + c$ $q \geq 3.63$ *(RP)* $q \geq 1.75$ *(GT)* *a* is *0.066* (RP) and *0.071* (GT) and *c* is *(-0.085)* for RP and *(-0.124)* for GT.	q_s is sediment yield in Mg ha^{-1} and *q* is runoff yield in $m^3\ ha^{-1}$. *q* must be +ve integer	0.23 (RP) & 0.49(GT)	Micro-catchment area between 13 and 90 m^2 and event rainfall between 5 and 22 mm
Annual sediment yield in relation to slope length	$q_s = 0.0072L_s + 0.63$ $5 < L_s < 45.7$	L_s is slope length in m, q_s is annual sediment rate in Mg $ha^{-1}\ yr^{-1}$.	0.94	Overland flow length with uniform slope
Ridge decay function. Vi, Intermittent Sc, Semicircle P, Pakistani Vc, Continuous	$H = aT + c$ '*a*' was 0.06 (P), 0.046 (Sc), 0.042 (Vi) and 0.04 (Vc) and '*c*' was set to zero.	*t* is time in month, *H* is decay in cm, *a* is coefficient and *c* is constant.	0.75 (Vi) 0.76 (Sc) 0.90 (P) 0.75 (Vc)	Equation based on 24 month data and event rainfall between 5 and 22 mm.

4.6 Shrub Survival and Growth

Periodic collection of shrub data and its analysis resulted in the highest shrub survival rate of *Atriplex halimus* (87%) followed by *Salsola vermiculata* (87%) and *Atriplex licuclada* (68%) by the end of season 2004–05 (Table 4.31). This year received an above average rainfall (127.5 mm), but plantation in late January 2005 missed half of the rainfall season from September 2004 to January 2005 and the shrubs benefited only from 50 mm rainfall that has occurred during February and May 2005. The average survival rate by the end of second rainfall season (2005–06) was 71% for *Atriplex halimus* followed by *Salsola vermiculata* (56%) and *Atriplex licuclada* (31%). Due to very low survival rate in control in the past—Some *et al.* (2004) showed 2% survival rate in similar trial in same environment, the shrubs were not planted in control.

Table 4.31. Shrub Survival for Different MCWH Techniques and Treatments

Year	Rainfall	Species	Survival Rate (%) for MCWH Techniques						Average
	(mm)		Vi-12	Vi-6	Vc-12	Vc-6	P-12	P-6	
2004–05	127.5	AH	92	80	98	81	91	77	87
May, 2005		SV	86	70	89	73	82	82	87
		AL	73	61	79	54	85	58	68
2005–06	44.1	AH	75	77	71	79	64	62	71
May, 2006		SV	75	68	47	69	59	17	56
		AL	30	32	22	43	30	26	31

AH= Atriplex Halimus, SV = Salsola Vermiculata and AL = Atriplex Licuclada
Vi-12 = Vallerani intermittent with 12 m spacing, Vi-6, Vallerani intermittent with 6 m spacing, Vc-12 = Vallerani continuous with 12 m spacing, Vc-6 = Vallerani continuous with 6 m spacing and P-12 and P-6 stand for Pakistani implement with 12 and 6 m spacing respectively

Examination of the shrub survival across the MCWH techniques showed insignificant difference (Fig. 4.53). In general, the Vallerani treatments performed slightly better. The shrub survival for MCWH techniques did not differ significantly. Very low water requirement for survival and capability of MCWH to harvest runoff from small events could be the reasons for low variations. Nevertheless, the performance of different techniques and treatments could be visible for medium to high rainfall events.

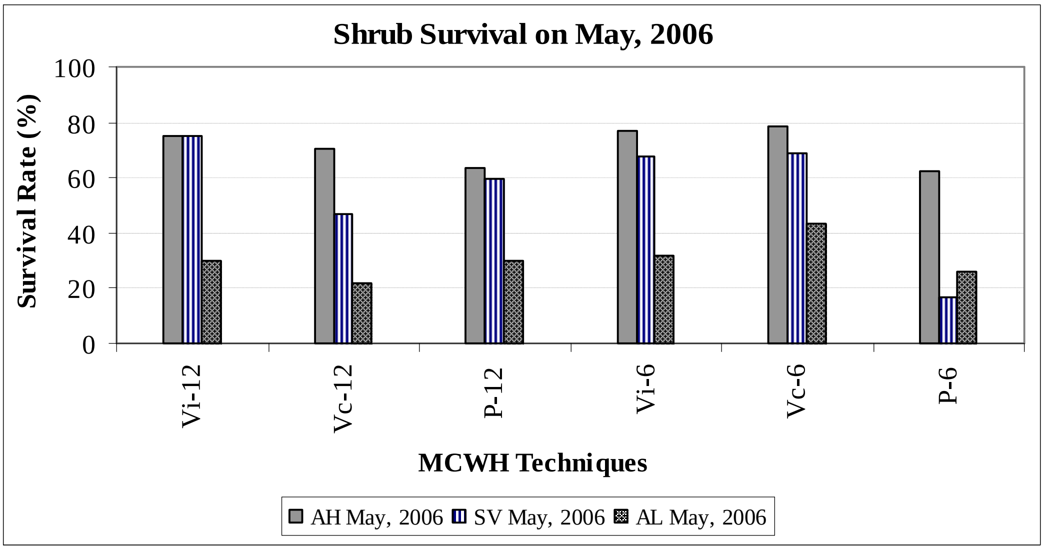

Figure 4.53. Shrub Survival in Relation to MCWH Techniques and Treatments

Shrub growth in relation to shrub species show that *Atriplex halimus* performed better followed by *Atriplex licuclada* and *Salsola vermiculata* (Fig. 4.54). The growth of *Atriplex halimus* varied between 50,000 and 350,000 cm^3, *Atriplex licuclada* between 10,000 and 150,000 cm3 and *Salsola vermiculata* less than 25,000 for various techniques and treatments. Examining the effect of MCWH techniques and treatments on the shrubs growth (Fig. 4.55) showed that the performance of Vi-12 was best followed by Vc-12 and P-12. For 6-m spacing Vc-6 performed better than Vi-6 and P-6. The better performance of 12-m spacing ridges was due to bigger micro-catchment area. It seems that better water concentration at plant location in case of Vallerani intermittent ridges (Vi-12) was responsible for relatively higher growth. Shrub growth in relation to time (Fig. 4.54) showed an increasing trend followed by power equation of the form

$$V = aT^b \qquad (4.6)$$

Where *'V'* is volume of shrub in cm^3, *'T'* is time, *'a'* is coefficient and *'b'* is exponent of the power equation. The parameters of the regression equations for each species are given in Table 4.32. Overall on the basis of better survival and growth rates *Atriplex halimus* can be regarded as better performing species in the drylands disregards of MCWH techniques and catchment area.

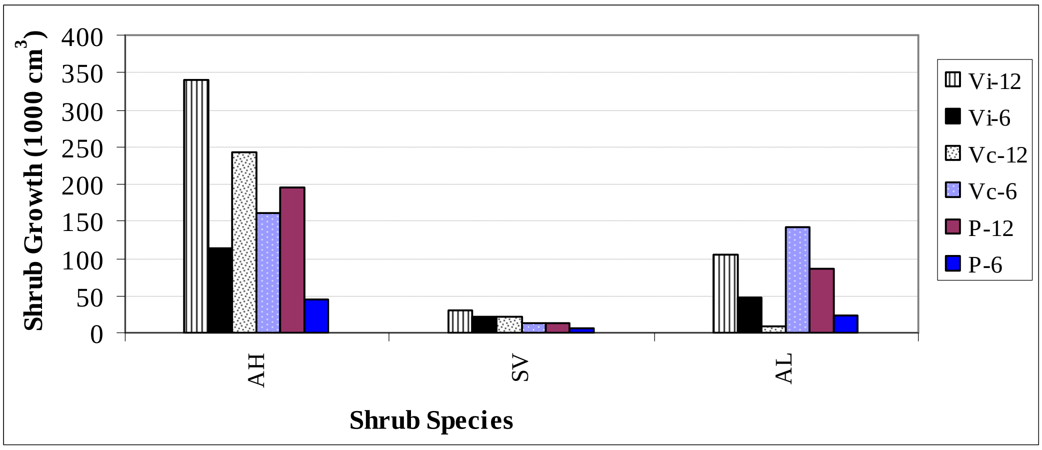

Figure 4.54. Shrub Growth in Relation to Species

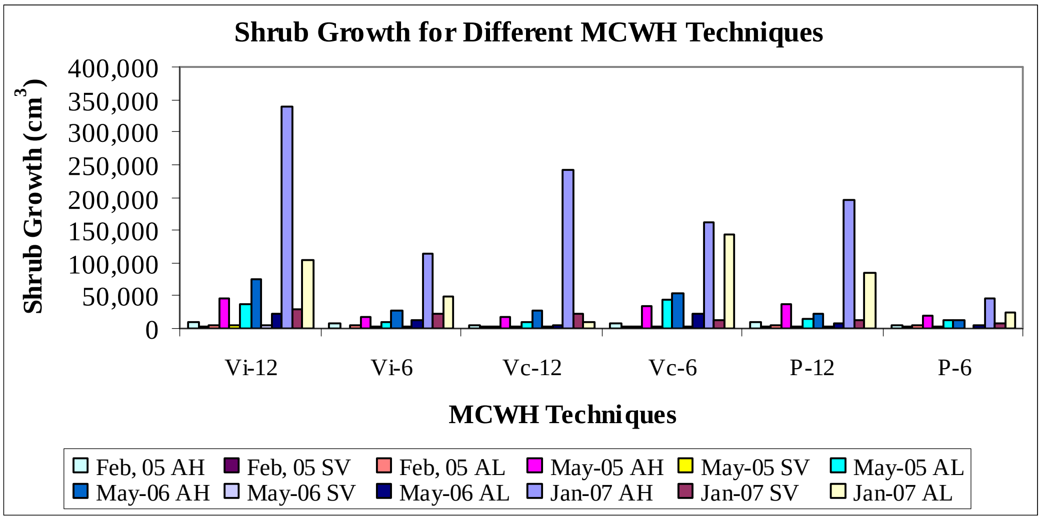

Figure 4.55. Shrub Growth in Relation to Different MCWH Techniques and Treatments

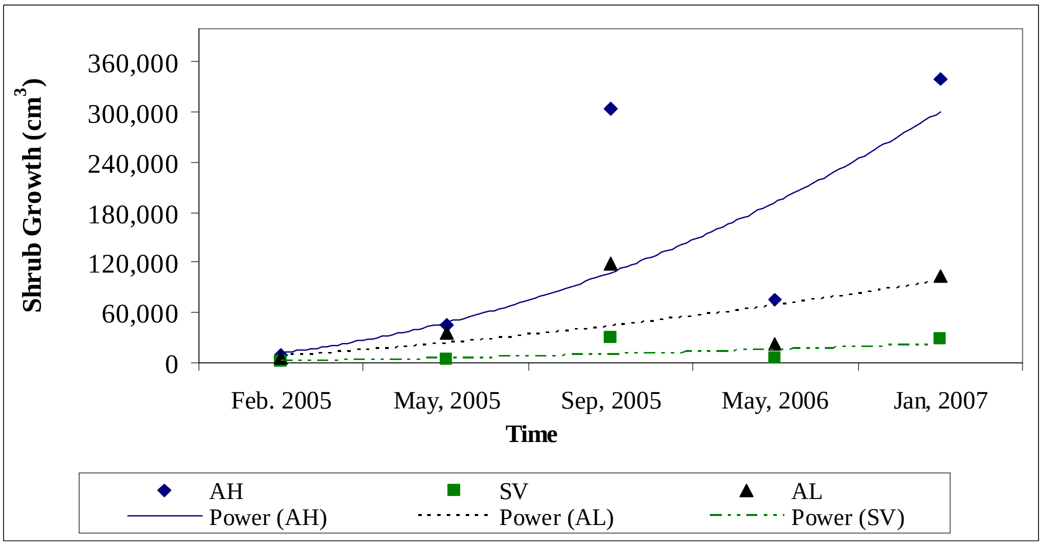

Figure 4.56. Shrub Growth in Relation to Time

Table 4.32. Regression Equation for Growth of three Shrub Species

Species	Regression Equation	R^2
Atriplex halimus (AH)	$y = 11961x^{2.0037}$	0.77
Atriplex licuclada (AL)	$y = 1770.9x^{1.5667}$	0.62
Salsola vermiculata (SV)	$y = 7862.2x^{1.5626}$	0.60

5. CONCLUSIONS AND RECOMMENDATIONS

5.1 Conclusions

This study provided a unique opportunity to evaluate the effect of MCWH on water, soil and vegetation cover in a drier environment. The following conclusions have been drawn on the basis of results obtained from the study for the prevailing agro-ecological environment.

Low rainfall is responsible for the deficit soil-water during dominant period in a year. High temporal variability of rainfall with dry conditions prevailing for 30% of the time and long dry spells between rainfall events further reduces the possibility of rehabilitation of the vegetative cover without water harvesting.

Most of the runoff occurs as a result of high intensity short duration rainfall, if it follows good antecedent soil-moisture conditions. This is the major cause of soil loss.

The soil texture in the study area is sandy clay loam, which is deficit in nutrients and is most vulnerable to crust formation. It discourages infiltration and encourages runoff. In this context, MCWH can help in harvesting the runoff and storing it as soil-water near the plant location.

At the micro-catchment scale, the annual runoff yield (varied between 200 and 400 m^3 ha^{-1}) is too low to support olive cultivation – a largely adopted production system in the region, or rainfed agriculture. However, if harvested, this runoff can revitalize vegetative cover and support range-based production system.

At the site scale, the annual runoff yield per unit area was about half to one-third of the runoff yield at the micro-catchment scale. The partial water diversions into rills and small gullies were responsible for low runoff yield at this scale.

At the catchment scale, the annual runoff per unit area (varied between 370 and 489 m^3 ha^{-1}) was relatively higher. The major contribution by the upper catchment area and flow diversions by the rills from the intervention area were responsible for the higher runoff yield.

At the micro-catchment scale, the average annual sediment yield was about 1.6 times higher with MCWH. Land disturbances and loose material from the ridges may have contributed to the increased sediment loss with MCWH. The unit sediment yield increased with the rainfall and runoff yield. The relationship was linear between rainfall and sediment yield and logarithmic between runoff and sediment yields. The estimates made using RUSLE2 Model are also comparable with the measured sediment loss.

At the rill scale, the sediment yield with MCWH was about 1.7 times higher than the control. The overall sediment yield at the rill scale was lower than at micro-catchment scale. Sediment routing through rill system reduced the sediment yield per unit area of the rills.

RUSLE2 modelled the effect of MCWH on sediment loss and delivery well. It estimated the sediment delivery by about 0.27 to 0.40 Mg ha^{-1} yr^{-1} across the ridges, which was about $1/5^{th}$ to $1/10^{th}$ of the sediment loss. MCWH increased the sediment loss by about 1.6 times within an overland flow length, but it reduced the sediment delivery to less than $1/5^{th}$ of the sediment loss.

At the catchment scale, the annual sediment yield varied between 1.25 and 1.49 Mg ha^{-1}. The relatively high sediment yield at catchment scale than other scales was due to major contribution of the upper catchment and gully erosion during two high rainfall events.

Ridges developed by Pakistani implement decayed at faster rate than manual bunds and Vallerani implement (Photo in Annex D). A linear decay trend estimated the effective/half life of the ridges as 20, 25 and 30 years for Pakistani, manual and Vallerani implement, respectively. Nevertheless, the rains of high return periods (10–25 years) may accelerate the decay at a faster rate.

In total, the study area produced about 300 Mg yr^{-1} of sediment from 2.5 km^2 area including rills and gullies, which is 1.2 Mg ha^{-1} yr^{-1}. This sediment is much less than the soil loss tolerable limits of 10 Mg ha^{-1} yr^{-1} adopted in Queensland, Australia and 4 to 5 Mg ha^{-1} yr^{-1} adopted by RUSLE model for agricultural land. It is also less than the top soil formation rate of 11 Mg ha^{-1} yr^{-1} (McCormack and Young, 1981) and comparable with an average soil formation rate of 1.0 Mg ha^{-1} yr^{-1} with a variation of 0.1–3 Mg ha^{-1} yr^{-1} from its parent material (Morgan 1991). Considering the range as main land use and insignificant downstream consequences, this sediment loss should not be a major problem for the study area.

The runoff potential of the micro-catchments varied between 5 and 80% of the incidental rainfall. By virtue of its capacity to capture a small local runoff, which may not be available at larger scales, the MCWH has a potential to secure most of this runoff.

The overland flow length decreases runoff and increases sediment loss per unit length. A good design of the MCWH system should consider the optimization of the overland flow length, which maximize runoff and minimize soil loss.

There was an insignificant effect of MCWH on the runoff yield at catchment scale. High runoff production potential of the upper catchment area overwhelmed the effect of MCWH on runoff reduction at the catchment scale. It infers that the MCWH does not substantially affect the runoff yield and downstream water availability.

The soil-water was low in the micro-catchment area and reasonably good in the planted area. The runoff inducement by the MCWH structures was responsible for the higher soil-water at the plant location. The soil-water varied temporally from very low in summer (around 11%, close to the wilting point), moderate in winter and good in spring (around 22%, close to the field capacity). The measurements after 24 hours of rainfall showed high water contents in soil layer between 15 and 30 cm depth, followed by soil layer from 0 to 15 cm, 30 to 45 cm and 45 to 60 cm. There was hardly any change in soil-water below 60 cm depth.

Shrub survival rate was low for *Atriplex licuclada* (31%) and high for *Atriplex halimus* (71%). The survival rate of the shrubs was relatively better in Vallerani techniques than in the Pakistani method. Regarding, shrub growth, *Atriplex halimus* performed better followed by *Atriplex licuclada* and *Salsola vermiculata*. The results do not help to conclude on performance of MCWH technique. Finally, on the basis of better survival and growth rates, the shrub *Atriplex halimus* can be regarded as the better performing species irrespective of MCWH techniques and catchment area.

An assessment of water and soil losses through measurement worked well with the support of simulations by RUSLE2 model. RUSLE2 model has the ability to reasonably simulate the changes in land use caused by MCWH. It also incorporated the effects of certain parameters such as 24 hours-10 years rainfall and the sediment delivery across the ridges, which was not possible by measurements within study period and domain.

5.2 Recommendations

The runoff and soil erosion study is complex because of interaction of many variables such as the rainfall timing, duration, amount and intensity, soil properties, vegetation densities and the land management practices. Only careful field observations can produce reliable data.

The conclusions from this study are based on three years of data. A long term data can only incorporate the effects of high inter-annual rainfall variability and dry spells.

MCWH change the landscape significantly by retaining and diverting flows and causing damages to the structures at locations of flow concentration near rills. Further investigations are needed to improve the design and implementation of the MCWH.

Linking the research result on micro-catchment scale to the macro-/ catchment is a challenge. An appropriate methodology that holds well for up-scaling of results from small to large scale and downscaling of results from large to small scale is needed.

Further investigations are needed to improve the methodology to measure runoff and sediment loss rates at all the spatial scales, in general and at rill and site scales in particular.

The soil erosion and its conservation involve geophysical, agro-climatic and socio-economic factors. Soil tolerable limit offers a firm basis for conservation planning. Assessment of soil tolerable limit for the study environment can lead to an appropriate policy guideline for conservation planning of natural resources facing overexploitation.

REFERENCES

Adepetu. J.A. and Adebusuyi, B.A. 1985. Available data-base for soil-testing programme in Nigeria and further requirements for its development. Paper presented at workshop on soil fertility survey of Nigeria. In: Adepetu, J.A. Nabhan, H. and Osinubi, A. (eds). 1996. Simple soil, water and plant testing techniques for soil resource management. Proceedings of training course held in Ibadan, Nigeria, 16–27 September, 1996. IITA and FAO Rome, 2000.

Adepetu. J.A. 1990. Soil-test data interpretation in soil-testing programme. In: Adepetu, J.A. Nabhan, H. and Osinubi, A. (eds). 1996. Simple soil, water and plant testing techniques for soil resource management. Proceedings of training course held in Ibadan, Nigeria, 16–27 September, 1996. IITA and FAO Rome, 2000.

Agassi, M., Shainberg, I. and Morin, J., 1981. Effect of electrolyte concentration and soil sodicity on infiltration rate and crust formation. Soil Science Society American Journal 45: 848–851. Cited in: Agassi, M. (ed.) (1996). *Soil Erosion, Conservation and Rehabilitation.* Marcel Dekker, Inc., USA.

Agassi, M., Morin, J. and Shainberg, I., 1985. Effect of raindrop impact energy and water salinity on infiltration rates of sodic soils. Soil Science Society American Journal 49: 186–190. Cited in: Agassi, M. (ed.) (1996). *Soil Erosion, Conservation and Rehabilitation.* Marcel Dekker, Inc., USA.

Albergel, J. 1988. Genese et predetermination des crues au Burkina Faso. Collection Etudes et theses, ORSTOM, Paris. In: Taur, W. and Humborg, G. 1992. Runoff Irrigation in Sahel Zone. Technical Centre for Agriculture and Rural Cooperation (CTA), Wageningen, The Netherlands and Verlag Josef Margraf Scientific Books P.O. Box 105, Weikersheim Germany.

Aldon, E.f. and H.W. Springfield, 1975. Using polyethylene to harvest water for growing shrubs. In: Proceedings of Water Harvesting symposium, Phoenix, AZ, ARS W-22, USDA, pp. 251–257.

Al-Durrah, M. and Bradford, J. M., 1981. New methods of studying soil detachment due to water-drop impact. Soil Science Society America, Journal, 45: 949–953.

Alexander, G.N., 1972. Effect of catchment area on flood magnitude. Journal of Hydrology, No. 4, pp 493–498.

Ali, A., Oweis, T., Rashid, M., El-Naggar, S. and AbdulAal, A., 2007. Water Harvesting Options in Dryland Catchments at Different Spatial Scales. Journal of Land Use and Water Resources Research, 7(2007) 1–13.

Anschutz, J., Kome, A., Nederlof, M., de-Neef, R., and Van-de-VEN, T., 1997. Water harvesting and soil-moisture retention. Agrodok series no 13, Agromisa Foundation and Technical Centre for Agriculture and Rural Cooperation (CTA) Wageningen, The Netherlands.

Anaya, M.G. and Tovar, J.S., 1975. Different soil treatments for harvesting water for radish production in the Mexico Valley. In: Proceeding of Water Harvesting Symposium, Phoenix AZ ARS W-22, USDA, pp. 315–320.

Arnold, J.G., Williams, J.R. Srinvasan R., and King, K.W., 1995. Soil and Water Assessment Tool. Theoretical document. USDA Agricultural Research Services, Grassland, Soil and Water Research Laboratory, Texas, and Texas A & M university, USA.

Arteaga, F.E., and Rantz, S.E. 1973. Application of the source-area concept of storm runoff to a small Arizona watershed. Journal of Research US Geological Survey, Vol 1, No. 4, pp 225–240.

Bedient, P. B. and Hubber, W. C., 1992. Hydrology and floodplain analysis. Addison-Wesley, New York.

Behailu, M. 2001. Key note speech. Workshop on the experience of water harvesting in the drylands of Ethiopia: Principles and practices

Bell, F.C. 1979. Precipitation. In: Goodball, D. W. and Perry, R.A. eds). Arid Land Ecosystems. Cambridge University Press, Cambridge, 373–393.

Ben-Hur, M.I., I. Shamberg, D. Bakker and R. Keren. 1985. Effect of soil texture and CaCO3 contents on water infiltration in crusted soils as related to water salinity. Irrigation Science 6: 181–194.

Benkobi, L., Trlica, M.J. and Smith, J.L., 1993. Evaluation of refined surface cover sub-factor for use in RUSLE. Journal of Range Management 47(1993):74–78. Cited in Christopher Jones, 2001. RUSLE application on Arizona rangelands. Rangeland management: Arizona Ranchers management Guide, Arizona Cooperative Extension, USA.

Benson, M.A. 1962. Factors influencing the occurrence of floods in a humid region of diverse terrain. US Geological Survey Water Supply Paper 1580-B

Bergkamp, G., 1998. A hierarchical view of interactions of runoff and infiltration with vegetation and micro-topography in semi-arid shrub lands. Catena 33:201–220.

Betson, R.P. 1964. What is watershed runoff? Journal of Geographical Research, 69(8):1541–1551.

Betson, R.P. and Maurius, J.B. 1969. Source areas of storm runoff. Water Resource Research, vol. 5, no 3, pp 574–582.

Beven, K. 2002. Runoff generation in semi-arid areas. In: Bull, L.J. and Kirkby, M.J. 2002. Dryland Rivers: Hydrology and geomorphology of semi-arid channels. John Wiley and Sons, ltd.

Blanchard, B.J., McFarland, M.J., Schmugge, T.J. and Rhoades, E., 1981. Estimation of soil-moisture with API algorithms and microwave emission. Water Resource Bulletin, American Water Resources Association, Vol. 17 No. 5, pp 767–774.

Boers, Th.M., and Ben-Ashar, J., 1982. A review of rainwater harvesting. Agriculture Water Management, 5:145–158.

Boers, Th.M., Zondervan, J., and Ben-Asher, J., 1986b. Microcatchment Water Harvesting (MCWH) for arid zone development. In: Agriculture Water Management 12, 21–39.

Boers, T.M. 1994. Rainwater Harvesting in Arid and Semi-arid Zones. PhD. Dissertation Wageningen Agriculture University, The Netherlands.

Bosznay, M., 1989. Generalization of SCS Curve Number method. Journal of Irrigation and Drainage Engineering. ASCE, 115(1), 139–144.

Bouyoucos, G. L., 1962. Hydrometer method improved for making particle-size analysis of soils. American Agronomy Journal, 53: 464–465.

Boughton, W. C., 1966. A mathematical model for relating runoff to rainfall with daily data. In: Ravi, V. and Williams J. R., 1998. Estimation of infiltration rate in the vadose zone: Compilation of simple mathematical models, volume 1, EPA/600/R-97/128a. United State Environmental Protection Agency.

Bowersock, G.W., 1994. Roman Arabia. Harvard, Press, USA.

Branson, F.A. 1976. Water use on rangelands. In: Watershed Management on Range and Forest Lands, 193–209. Proceedings fifth US/Australian Rangelands Panel, Boise, Idaho.

Bremner, J. M. and C. S. Mulvaney, 1982. Nitrogen total. Pp 595–624. In: Methods of soil analysis, A. L. Page (ed). Agronomy number 9, Part 2: Chemical and Micro-biological properties, 2nd edition. American Society of Agronomy, Madison, WI, USA.

Brice, J.B., 1966. Erosion and deposition in the loess-mantled Great Plain, Medicine Creek drainage basin, Nebraska. *USGS Professional paper, 352H*, 235–339.

Bristow, K.L., Smetten, K.R.J., and Ross, P.J., 1994. Water entry into sealing, crusting and hard setting soils: A review and illustrating simulation study. In: So, H.B., G.D. Smith, S.R. Raine, B.M. Schafer and R.J. Loch (eds). *Sealing, crusting and hard setting soils: Productivity and conservation*. Australian Society of Soil Science Inc. Brisban Australia, pp183–203.

Brown, L.C., and Foster, G.R., 1987. Storm erosivity using idealized intensity distribution. Transaction of American Society of Agriculture Engineers 30(2):379-386.

Bruins, H.J., Evenari M., and Nessler, U., 1986. Rainwater harvesting agriculture for food production in arid zones: the challenge of the African famine. Applied Geography, 6:13–33.

Brunori, F., Penzo, M. C., and Torri, D., 1989. Soil shear strength: its measurement and soil detachability. Catena 16: 59–71.

Bryan, R.B., Yair, A. and Hodges, W.K. 1978. Factors controlling the initiation of runoff and piping in Dinosaur Provincial Park badlands, Alberta Canada.

Zeitschrift fur Geomorphologie N.F., Suppl. Bd 29, pp151–168, Berlin, Germany.

Bull, L.J., Kirkby, M.J., Shannon, J. and Hooke, J.M., 2000. The variation in estimated discharge in relation to the location of storm cells in South East Spain. Catena, 38(3), 191–209.

Bull, L.J. and Kirkby, M.J. 2002. Dryland Rivers Characteristics and Concepts. In: Bull, L.J. and Kirkby, M.J. (Eds). 2002. Dryland Rivers: Hydrology and Geomorphology of Semi-arid Channels. John Willey and Sons Ltd.

Buringh, P., 1981. An assessment of losses and degradation of productive agriculture land in the world. Working Group on Soil Policy, Food and Agriculture Organization, United Nation, Rome, Italy.

Cazier, D. J., and Hawkins, R. H., 1984. Regional application of the Curve Number method. In: water today and tomorrow, proceedings of ASCE Irrigation and Drainage Division Special Conference, ASCE, New York.

Chapman, R.W., 1978. The evidence for prehistoric water control in South East Spain. Journal of Arid Environments, 1:261–274.

Charles, B., Ashok, S., Rama, M.R. and Butterworth J., 2002. Mitigation the potential unintended impacts of water harvesting. Paper presented at IWRA, International Regional Symposium " Water for Human Survival", 26–29th November, 2002, New Delhi, India.

Chepil, W.S., 1953. Factors that influence cold structure and erodibility of soil by wind: I soil texture, Soil Science, 75: 473–483. Cited in: Visser, S. and W. Cornelis (eds). Wind and Rain Interaction in Erosion, Chapter 5, pp 71–78. Tropical Resource Management Papers no. 50 (2004) Wegeninegn University and Research Center, the Netherlands.

Chevallier, P.,Claude, J.,Pouyaud, B. and Bernard, A. 1985. Hydrolgie de la mared'Oursi (Burkina Faso). ORSTOM, Collection Travaux et Documents, No. 190 Paris; quoted in: Taur, W. and Humborg, G. 1992. Runoff Irrigation in Sahel Zone. Technical Centre for Agriculture and Rural Cooperation (CTA), Wageningen, The Netherlands and Verlag Josef Margraf Scientific Books P.O. Box 105, Weikersheim Germany.

Chow, V. T., 1959. Open Channel Hydraulics. McGraw-Hill International.

Chow V.T., Maidment D.R., Mays L.W. 1988. Applied Hydrology. McGraw Hill International.

Clark, E. H., 1985. The off-site costs of soil erosion. Journal of Soil and Water Conservation 40: 19–22.

Critchley, W., Reij, C., 1988. Water Harvesting for Plant Production. World Bank Technical Paper no. 91. Washington, DC.

Critchley, W. and K., Siegert,, 1991. Water Harvesting: A Manual for the Design and Construction of Water Harvesting Schemes for Plant Production. 133 pp. AGL Miscellaneous Paper no. 17, FAO, Rome, Italy.

Critchley, W., Reij, C. and Seznec, A., 1992. Water Harvesting for Plant Production. Volume 2. Case Studies and Conclusions from Sub-Saharan Africa. World Bank Technical Paper, 157.

Cudworth, A.G., 1989. Flood hydrograph manual. US Department of Interior, Bureau of fReclamation, Washington, DC.

De Poley, J. 1974. Mechanical properties of hillslopes and their relation to gullying in central and semi-arid Tunisia. Reported in: Poesen, J., L. Vandekerckhove, J. Nachtergaele, D. Oostwoud Wijdenes, G. Verstraeten and B. Van Wesemael, 2002. Gully erosion in dryland environment. In: Bull, L.J. and M.J. Kirkby, 2002. Dryland ***Rivers: Hydrology and Geomorphology of Semi-arid Channels***. John Wiley and Sons, Ltd.

Dudal, R., 1981. An evaluation of conservation needs. In: Soil Erosion by Wind and Water: Problems and Prospects, R., Lal (ed), 1994. Soil and Water Conservation Society, Ankeny, USA.

Duely, F.L. 1939. Surface factors affecting the rate of intake of water by soils. American Soil Science Society, Proceedings 4:60–64. Cited in: Agassi, M. (ed.) (1996). ***Soil Erosion, Conservation and Rehabilitation***. Marcel Dekker, Inc., USA.

Dunin, F.X. 1976. Infiltration: Its simulation for field conditions. In: Roda, J.C. (ed), Facets of Hydrology, chapter 8, pp 199–227. John Wiley and Sons. New York.

Dunne, T. and Balck R.D. 1970a. An experimental investigation of runoff production in permeable soils. Water Resource Research, Vol. 6, No. 2, pp 478–490.

Eagleson, P., 1978. Climate, soil and vegetation. A simplified model of soil moisture movement in the liquid phase. Water Resource Research, 14:722–730.

Eger, H., 1988. Runoff Agriculture. Riechert, Wiesbaden, Germany.

Ellison, W.D., 1947. Soil erosion studies. III: Some effects of erosion on infiltration and surface runoff. Agriculture Engineering 28: 245–248. Cited in: Agassi, M. (ed.) (1996). *Soil Erosion, Conservation and Rehabilitation*. Marcel Dekker, Inc., USA.

El-Naggar, S., Perrier, E.R. and Shykhoun, M., 1988. Evaluation of farm resource management in the northwest coast of Egypt. In Proceedings of Workshop for the Northwest Coastal Region. Alexandria/Mersa Matrouh, Egypt, April 1988. ARC-SWRI/ICARDA-FRMP.

Emmett, W. W. 1970. The hydraulics of overland flow on hillslopes. Geological Survey Professional Paper 662-a, U.S. Department of Interior.

Epstein, E. and Grant. W.J. 1973. Soil crust formation affected by raindrop impact. Reported in: Agassi, M. (ed.) (1996). *Soil Erosion, Conservation and Rehabilitation*. Marcel Dekker, Inc., USA.

Evans, R. 1980. Mechanics of water erosion and their spatial and temporal controls: an empirical viewpoint. In: M. J. Kirkby and R.P.C. Morgan (eds), Soil erosion. Chichester, Wiley: 109–128

Evenari, M., Shanan L., and Tadmor N.H., 1968. Runoff farming in the desert. I. Experimental layout. In: Agronomy journal 60: 29–32

Evenari, M., Shanan, L., and Tadmor, N. H., 1971. The Negev, the Challenge of a Desert. Harvard University Press, Cambridge, Mass, USA.

Falkenmark, M., Lundqvist, J. and Widstrand, C., 1990. Coping with water scarcity-implications of biomass strategy for communities and policies. Water Resources Development. 6(1): 29–43, March 1990. http://www.epw.org.in/showArticles.php?root=2003&leaf=11&filename=6557&filetype=html

FAO. 1978. Reports of the agro-ecological zones projects, World Soil Resources Report 48 vol. 14, FAO Rome.

FAO. 1980. Land Evaluation for Development. FAO, Rome, Italy.

FAO, 1981. Arid zone hydrology for agricultural development. FAO irrigation and drainage paper no 37. Food and Agriculture Organization of the United Nation, Rome, Italy.

FAO. 1988a. World Agriculture: Towards 2000, an FAO study. Ed. Alexandratos N. London.

FAO. 1990a. The Conservation and Rehabilitation of African Lands: An International Scheme ARC/90/4, Rome, 38p.

FAO, 1992. Crop water requirement. Irrigation and Drainage Paper no. 24. FAO Rome.

FAO, 1993. Field measurement of soil erosion and runoff. Food and Agriculture Organization of the United nations Rome, Italy.

FAO, 1994. Water Harvesting for Improved Agricultural Production. Proceedings of the FAO Expert Consultation, Cairo, Egypt, 21–25 November, 1993. Water Reports, 3. FAO, Rome, Italy.

Flanagan, D.C. and M. Nearing, 1995. USDA-Water erosion prediction project. Hillslope profile and watershed model documentation, NSERL Report No. 10, WEPP Technical Document, USDA-ARS National Soil Erosion Research Laboratory, West Lafayette, Indiana 47907, USA.

Flerchinger, G. N, Waltts, F. J., and Bloomsbug, G L., 1988. Explicit solution to Green-Ampt equation for non-uniform soils.

Fogel, M.M. 1969. Effect of storm rainfall variability on runoff from small semi-arid watersheds. Transactions of ASAE, 12(6):808–812.

Fogel, M.M. and Duckstein, L. 1973. Prediction of convective storm runoff in semi-arid regions. IAHS publication no. 97, pp 465–480.

Foster, G.R. 1971. The overland flow process under natural conditions. In: Biological effects in the hydrological cycle. Proceedings of Third International Seminar for Hydrology. Purdue University West Lafayette.

Foster, G.R., 1982. Modeling the erosion process. In: Hann, C.T., Johnson, H.P. and Brakensiek, D.L. (eds.), *Hydrological Modeling of Small Watersheds* ASAE Monograph no. 5, St. joseph, Michigan 49085.

Foster, G.R., Young, R.A., Romkens, M.J.M., and Onstad, C.A., 1985. Processes of soil erosion by water. Cited in: Cited in: Agassi, M. (ed.) (1996). *Soil Erosion, Conservation and Rehabilitation.* Marcel Dekker, Inc., USA.

Foster, G.R., 1986. Understanding ephemeral gully erosion. *In Soil Conservation, National Academy of Science Press*, Washington DC, 2, 90–125.

Foster G.R., 1991. Advances in wind and water erosion prediction. Journal of Soil and Water Conservation, 46:27–29.

Frasier, G.W., Cooly, K.R., and Griggs, J.R. 1979. Performance evaluation of water harvesting catchments. Journal of Range Management 32(6), November 1979.

Freeze, R.A. 1982. The influence of hillslope hydrological processes on the stochastic properties of stream flow. Statistical analysis of rainfall and runoff. Proceedings of International Symposium on Rainfall-runoff Modeling held May 18–21, 1981 at Mississippi State University, USA.

Gatot I.S., Duchesne J., Forest F., Perez P., Cudennec, C., Prasetyo T., and Karama S. 1999. Rainfall-runoff harvesting for controlling Erosion and Sustaining Upland Agriculture Development. In: Sustaining the Global Farm. Stott, D.E., Mohtar R.H. and Steinhardt, G.C. (eds.), 2001. Selected papers from 10th International Soil Conservation Organization Meeting May 24–29 Purdue University and USDA-ARS National Soil Erosion Research Laboratory.

Ghadiri, H. and Payne, D., 1981. Raindrop impact stress. Journal of Soil Science 32: 41–49.

Glymph, L.M., 1951. Relation of sedimentation to accelerated erosion in the Missouri River Basin, Technical paper 102, USDA, Soil Conservation Services USA.

Gollany, H.T., T.E. Schumacher, P.D. Evenson, M.J. Lindstrom and G.D. Lemme. 1991. Aggregate stability of an eroded and desurfaced typic Argiustoll. Soil Science Society of America Journal 55:811–826.

Govers, G., 1985. Selectivity and transport capacity of thin flows in relation to rill erosion. Catena, 12, 35–49.

Govers, G., 1992. Relationship between discharge, velocity and flow area for rills eroding loose, non-layered material. Earth Surface Processes and Land-forms 17: 515–528.

Graf, W.L. 1988. Fluvial process in Dryland Rivers. Springer-Verlag, Berlin.

Gray, D.M. 1961. Interrelationships of watershed characteristics. Journal of the Geophysical Union, vol. 66, No 4, pp 1215–1223.

Green, W.H. and Ampt, G.A., 1911. Studies on Soil Physics, I. Flow of air and water through soils. *Journal of American Agronomic Society*, 4:1–24.

Gregory, K.J. and Walling, D.E. 1968. The variation of drainage density within a catchment. IAHS Publication No. 13, pp 61–68.

Grissinger, E.H., 1996a. Rill and gullies erosion. In: Aggassi, M. (ed.) Soil Erosion, Conservation and Rehabilitation Marcel Dekker, Inc., New York, USA, pp 153–161.

Grissinger, E.H., 1996b. Reclamation of gullies and channel erosion. In: Aggassi, M. (ed.) Soil Erosion, Conservation and Rehabilitation Marcel Dekker, Inc., New York, USA, pp 301–310.

Hadley, R.F. and Lusby G. C. 1967. Runoff and hillslope erosion resulting from high-intensity thunderstorm near Mack, Western Colorado. Water Resource Research 3(1):139–143.

Hairsine, P.b. and Rose, C.W., 1991. Rainfall detachment and deposition: sediment transport in the absence of flow driven processes. Soil Science Society American Journal 55: 320–324.

Hann, C.T., Barfield, B.J. and Hayes, J.C. 1994. Design Hydrology and Sedimentology for Small Catchments. Academic Press Inc., San Diego, California, USA.

Hauge, C., 1977. Soil erosion definitions. California Geology, 30, 202–203. Cited in: Bull, L.J. and M.J. Kirkby, 2002. Dryland *Rivers: Hydrology and Geomorphology of Semi-arid Channels*. John Wiley and Sons, Ltd.

Hewlett, J.D. and Hibbert R.A. 1967. Factors affecting the response of small watersheds to precipitation in humid areas. Forest Hydrology: Proceedings of National Science Foundation Advanced Science Seminar (International Symposium on Forest Hydrology), ed. William, E. Sopper, pp275–280, Oxford.

Horton, R.E., 1932. Drainage-basins characteristics. Transactions of American Geophysical Union, pp 350–361.

Horton, R.E., 1933. The role of infiltration in hydrological cycle. Transaction American Geographical Union, vol. 14, pp 446–460.

Horton, R.E. 1940. Approach toward a physical interpretation of infiltration capacity. Proceedings of Soil Science Society of America, 5(339–417).

Holton, H.N., 1961. A concept for infiltration estimates in watershed engineering. USDA-ARS 41–51.

Huang, C., Bradford, J. M. and Cushman, J. H., 1982. A numerical study of raindrop impact phenomena: the rigid case. Soil Science Society of America Journal, 46: 14–19.

Huggins L.F. and Burney, J.R., 1982. Surface runoff, storage and routing. In: Hann, C.T., Johnson, H.P., Brakensiek, D.L. (1982), Hydrological modeling of small watersheds. American Society of Agriculture Engineers. Monograph no. 5, Michigan, USA.

Huibers, F.P. 1985. Rainfed agriculture in a semi-arid tropical climate: aspects of land and water management for red soils in India. Doctoral thesis, Agriculture University Wageningen, The Netherlands.

Imeson, A.C. and Kawaad, F.J.P.M., 1980. Gully types and gully prediction. Cited in: Bull, L.J. and M.J. Kirkby, 2002. Dryland *Rivers: Hydrology and Geomorphology of Semi-arid Channels*. John Wiley and Sons, Ltd.

ISNAR. 1992. Summary of agriculture research policy. International quantitative perspectives International Services for National Agriculture research (ISNAR), Netherlands, The Hague, 24p.

Jastrow, J.D. and R.M. Miller. 1991. Methods for assessing the effects of biota on soil structure. Agricultural Ecosystem and Environment 34:9279–303.

Jones, C., 2001. RUSLE application on Arizona rangelands. Rangeland management: Arizona Ranchers Management Guide, Arizona Cooperative Extension, USA. Website: http://www.sedlab.olemiss.edu/rusle/

Kemper, W.D. and E.J. Koch, 1966. Aggregate stability of soils from Western US and Canada. US Department of Agriculture Technical Bulletin 1355.

Kemper, W.D., Rosenau, R.C., and Dexter, A.R., 1987. Cohesion development in disrupted soils as affected by clay and organic matter content and temperatures. Soil Science Society American Journal 51: 860–867.

Kiepe, P. 1995. No runoff, no soil loss: Soil and water conservation in hedgerow barrier system. In: van Loon, E. E. 2001. Overland flow: interfacing models with measurements. PhD thesis, Wageningen Agriculture University, The Netherlands.

Kincaid, D.R., Gardner, J.L. and Schreiber, H.A. 1963. Soil and vegetation parameters affecting infiltration under semi-arid conditions. IAHS publication no. 65, pp 440–453.

Kirpich, Z.P., 1940, Time of concentration of small agricultural watersheds, *Civil Engineering*, 10(6):362.

Kolarkar, A.S., Murthy, K. & Singh, N., 1983. Khadin - a method of harvesting water for agriculture in the Thar desert. Journal of Arid Environments, 6:59–66.

Kovda,, V. A., 1983. Loss of productive land due to salinization. Ambio 12: 91–93. In: Soil Erosion Research Methods, Soil erosion by wind and water: problems and prospects, R., Lal, 1994. Soil and Water Conservation Society, Ankeny IA and St. Lucie Press Delray Beach FL, USA.

Landon, J.R. (ed). 1984. A handbook of soil survey and agriculture land evaluation in the tropics and sub-tropics. Booker Tropical Soil Manual, UK.

Langbein, W. B. and S. A., Schumm, 1958. Yield of sediment in relation to mean annual precipitation. Transaction of the American Geophysical Union 39: 1076–1084.

Lenzen, C.J., R.L.Gordon and A.M. Mcquitty. 1985. “Excavation at Tell Irbid and Beit Ras, Jordan Annual of Department of Antiquities Vol. XXIX.

Lal, R., 1994. Soil erosion by wind and water: problems and prospects. In: Lal, R. (ed.), Soil Erosion Research Methods (second edition). Soil and Water Conservation Society, Ankeny IA and St. Lucie PressDelray Beach FL, USA.

Leopold, L.B., Emmett W.W. and Myrick, R.M, 1966. Channel and hillslope processes in semi-arid area in New Mexico. ***Professional paper 352-G***, USGS, Washington, DC.

Lin, Xi. 1999. Flash floods in arid and semi-arid zones. International Hydrological Program, Technical Documents in Hydrology No. 23. UNESCO, Paris, pp, 2–8.

Linsley, R.K., Kohler, M.A. and Paulhus, J.L.H. 1949. Applied Hydrology. McGraw-Hill, New York.

Linsley, R.K., Kohler, M.A. and Paulhus, J.L.H. 1958. Hydrology for Engineers. McGraw Hills, New York.

Mannering, J.V. 1981. The use of soil loss tolerance as a strategy for soil conservation. In: R.P.C. Morgan (ed.), Soil Conservation: Problems and Prospects, pp. 337-349. Willey, New York.

Martinez-Mena, M., Albaladejo, J. and Castillo, V.M. 1998. Factors influencing surface runoff generation in Mediterranean semi-arid environment: Chicamo watershed, SE Spain. Journal of Hydrological Processes 12: 741–754.

Mays, L. W., 2004. Water Resources Engineering. John Willey and Sons Inc.

McCormack, D.E., and Young, K.K. 1981. Technical and societal implications of soil loss tolerance. In: R.P.C. Morgan (ed.), Soil Conservation: Problems and Prospects, pp. 337-349. Willey, New York.

Meyer, L.D, Foster, G.R., and Romkens, M.J.M., 1975b. Source of soil eroded by water from upland slopes. In: Present and prospective technology for predicting sediment yields and sources. ARS-S-40, USDA-Agriculture Research Services, pp, 177–189.

Middleton, N.J. and Thomas, D.S.G. 1997. World Atlas of Desertification, 2nd Edition. UNEP/Edward Arnold London.

Morgan, R.P.C., L. Martin and C.A. Noble, 1986. Soil erosion in the United Kingdom: A case study from mid-Bedfordshire. Silsoe College Occasional Paper no. 14. cited in: Morgan R.P.C., 1995. Soil Erosion and Conservation Second Edition, Longman Scientific and Technical, Longman Group Ltd.

Morgan R.P.C., 1991. Strategies for erosion control. In: D.A. Davidson (ed.), Soil Erosion and Conservation, pp 162-185. Wiley, New York.

Morgan R.P.C., 1995. Soil Erosion and Conservation Second Edition, Longman Scientific and Technical, Longman Group Ltd.

Morin, J. and Binyamini, Y., 1977. Rainfall infiltration into bare soils Water Resource Research 13:813–817. Cited in: Agassi, M. (ed.) (1996). *Soil Erosion, Conservation and Rehabilitation.* Marcel Dekker, Inc., USA.

Moss, A.J., Green P., and Hutka, J., 1982. Small channels: their experimental formation, nature, and significance. *Earth Surface: Process Landforms 7*:401–415.

Moss, A.J. and Green, T.W., 1986. Errosive effect of large water drops (gravity drops) that fall from plants. Australian Journal of Soil Research 26: 9–20.

Moss, A.J., 1988. Effects of flow velocity variation on rain-driven transportation and the role of rain impact in the movement of solids. Australian Journal of Soil Research 26: 443–450.

MRMP, 1992. Project Preparation Report. Matrouh Resource Management Project, Matrouh, Egypt.

MRMP, 2000. Farm Survey Report. Matrouh Resource Management Project, Matrouh, Egypt.

Murphy, J.B., Wallace, D.E. and Lane, L.J. 1977. Geomorphic parameters predict hydrograph characteristics in the Southwest. Water Resource Bulletin, American Water Resource Association, vol. 13, no.1, pp 25–38.

Mutcheler, C.K. and Young, R.A., 1975. Soil detachment by raindrops. In Proceedings of Sediment Yield Workshop, Oxford M.S. USDA, ARS-S-40, pp 113–117.

Myers, L.E. 1975. Water harvesting 2000 B.C. to 1974 A.D. In: Proceedings Water Harvesting Symposium, phoenix AZ, ARS W-22, USDA, pp. 1–7

Nearing M.A., Bradford J.M., and Parker, S.C., 1991. Soil detachment by shallow flow at low slopes. Soil Science Society, American Journal 49: 547–552.

Nearing, M.A., 1991. A probabilistic model of soil detachment by shallow turbulent flow. *Transaction of ASAE, 34:* 81–85.

Oosterbaan, R.J., 1983. Moderen interferences in traditional water resources in Baluchistan. International Land Reclamation Institute (ILRI) Annual Report, 1982: p 23–34 Wageningen, Netherlands.

Osborn, H.B. and Lane, L.J. 1969. Precipitation-runoff relationships for very small semi-arid rangeland watersheds. Water Resource Research, WRR 5(2):419–429

Osborn, H.B. and Renard, K.G. 1973. Thunderstorm runoff on the Walnut Gulch Experimental Watershed, Arizona, USA. IAHS, publication no 128. pp 126–140.

Oweis, T., Hachum, A. and Kijne, J., 1999. Water Harvesting and Supplemental Irrigation for Improved Water Use Efficiency in Dry Areas. SWIM paper no. 7. System-wide Initiative on Water Management, ICARDA and IWMI. International Water Management Institute PO Box 2075, Sri Lanka.

Pacey, A. and Cullis, A., 1999. Rainwater harvesting: the collection of rainfall and runoff in rural areas. Intermediate Technology Publications, London, HK.

Palmer R.S., 1965. Water drop impact forces. Transaction of ASAE 8: 69–72.

Parr, J.F. and Stewart B.A. 1990. Improving rainfed farming for semi-arid tropics: implications for soil and water conservation. Soil conservation society of America, Ankeny, Iowa, USA.

Parlange, J.Y. and Haverkamp, R. 1989. Infiltration and ponding time. In: Unsaturated Flow in Hydrologic Modeling. Theory an dPractice. Ed. Morel-Seytoux, 95–126. Kluwer Academic Publishers, Boston.

Patra, K. C., 2002. Hydrology and Water Resources Engineering. Narosa Publishing House, New Delhi.

Perace, A.J., 1976. Magnitude and frequency of erosion by Hortonian overland flow. Journal of Geology 84: 65–80. Cited in: Morgan R.P.C., 1995. Soil Erosion and Conservation Second Edition, Longman Scientific and Technical, Longman Group Ltd.

Philip, J.R. 1957. The theory of infiltration: 4. Sorptivity and Algebraic infiltration equations. Soil Science 84: 257–264.

Philip, J.R. 1969. Theory of infiltration. Advances in Hydroscience 5:215–296. Academic Press, New York.

Piest, R.F., Bradford J.M. and Spomer, R.G., 1975. Mechanisms of erosion and sediment movement from gullies. *Publication ARS-S-40,* Agricultural Research Services, UDA.

Poesen, J. 1985. An improved splash transport model *Zeitschift Geomorphologie* 29:193–211. In: Morgan, R.P.C. 1995. Soil Erosion and Conservation. Longan Scientific Publication.

Poesen, J., 1993. Gully typology and gully control measures in the European loess belt. Cited in: Bull, L.J. and M.J. Kirkby, 2002. Dryland *Rivers: Hydrology and Geomorphology of Semi-arid Channels*. John Wiley and Sons, Ltd.

Poesen, J., L. Vandekerckhove, J. Nachtergaele, D. Oostwoud Wijdenes, G. Verstraeten and B. Van Wesemael, 2002. Gully erosion in dryland environment. In: Bull, L.J. and M.J. Kirkby, 2002. Dryland *Rivers: Hydrology and Geomorphology of Semi-arid Channels*. John Wiley and Sons, Ltd.

Ponce, V.M. 1989. Engineering Hydrology: Principles and Practices. Prentice-Hall, Eaglewood Cliffs, NJ, 1989.

Ponce, V. M. and Hawkins R. H., 1996. Runoff curve number: Has it reached maturity? Journal of Hydrological Engineering, vol. 1 No. 1, Jan 1996, pp 11–18.

Prinz, D., 1994. Water harvesting - past and future. In Sustainability of Irrigated Agriculture. L.S. Pereira (ed), Proceedings of NATO Advanced Research Workshop, Vimiero, 21–26 March 1994. Balkeman, Rotterdam.

Prinz, D. and Singh, A. K., 2000. Water Resources in Arid Regions and their Sustainable Management. Annals of Arid Lands. Special Issue on Research. Institute of Water Resource Management, Hydraulic and Rural Engineering, University of Karlsruhe, Germany.

http://www.google.com/scholar?q=Water+Resources+in+Arid+Regions+and+their+sustainable+management+Dieter+Prinz+and+Anupam+Singh&btnG=Google+Scholar+Search&num=25

Puech, C. and Chabi-Gonni, D. 1984b. Reported in: Taur, W. and Humborg, G. 1992. Runoff Irrigation in Sahel Zone. Technical Centre for Agriculture and Rural Cooperation (CTA), Wageningen, The Netherlands and Verlag Josef Margraf Scientific Books P.O. Box 105, Weikersheim Germany. Page 57.

Radoane, M., Ichim, I. and Radoane, N., 1995. Gully distribution and development in Moldavia, Romania. Catena, 24, 127–146.

Rallison, R.E. and Miller. N., 1981. Past, present and future SCS runoff procedure. In: Singh, V. P. (ed.). Rainfall runoff relationship. Water Resource Publication, Littleton, CO.

Ramasastari, K.S. and Seth, S. M., 1985. Rainfall and runoff relationship. Report RN-20, National Institute of Hydrology, Roorkee, Utar Pardesh, India.

Rauws, G. and Govers, G., 1988. Hydraulic and soil mechanical aspects of rill generation on agricultural soils. Journal of Soil Science 39: 111–124.

Ravi, V. and Williams J. R., 1998. Estimation of infiltration rate in the vadose zone: Compilation of simple mathematical models, volume 1, EPA/600/R-97/128a. United State Environmental Protection Agency.

Reij, C., Mulder, P., and Begemann, L., 1988. Water Harvesting for Plant Production. 120 pp. Technical paper No. 91, World Bank, Washington, DC, USA.

Renard, K.G. and Keppel, R.V. 1968. Hydrographs of ephemeral streams in Southwest. Journal of Hydraulics Division. Proceedings ASCE, Vol 92, HY 2, pp 33–52.

Renard K.G. and Simanton, J.R., 1990. Application of RUSLE to rangelands. Watershed planning and analysis in action, pp 164–173. Symposium proceedings of IR conference watershed management, ASCE, Durango, CO, 1990.

Renard, K.G., Foster, G.R., Weesies, G.A., Mccool, D.K., and D.c. Yader, 1996. United State Department of Agriculture (USDA), Agriculture Handbook No. 703, Predicting soil erosion by water: A guide to conservation planning with Revised Universal Soil Loss Equation (RUSLE) USDA Agricultural Research Services.

Renard, K.G., Foster, G.R. Weesies, G.A., Mccool, D.K., and Yader, D.c. 1997. Predicting soil erosion by water: A guide to conservation planning with Revised Universal Soil Loss Equation (RUSLE). United State Department of Agriculture (USDA), Agriculture Handbook No. 703, USDA Agricultural Research Services.

Renard K.G., 1999. Personal telephonic conversation and e-mail correspondence with Jones C., Tucson, AZ, September 1999. Cited in Christopher Jones, 2001. RUSLE application on Arizona rangelands. Rangeland management: Arizona Ranchers management Guide, Arizona Cooperative Extension, USA.

Richard, L. A. 1931. Capillary conduction of liquids through porous mediums. Physics, volume 1.

Richard, L. A., 1954. Diagnosis and improvement of saline and alkali soils. USDA Agriculture Handbook 60. Washington, D.C.

Roche, M. 1963. Hydologie de surface. Gautheir-Villars editeur, Paris. Cited in: Taur, W. and Humborg, G. 1992. Runoff Irrigation in Sahel Zone. Technical Centre for Agriculture and Rural Cooperation (CTA), Wageningen, The Netherlands and Verlag Josef Margraf Scientific Books P.O. Box 105, Weikersheim Germany. Page 57.

Rodier, J., and Ribstein, P. 1988. Estimation of floods in small Sahelian basins under 10 km^2. In french: Estimation des caracteristiques de la crue decennale pour les petits basins versants du Sahel couvrant de 1 a 10 km2. ORSTOM, Montepellier. 108 p + Annexes.

http://www.bondy.ird.fr/pleins_textes/pleins_textes_6/b_fdi_35–36/39698.pdf#search=%22Rodier%20%2B%20runoff%20%2B1988%20%22

Rose, C.W., 1985. Developments in soil erosion and deposition models. *Advances in Soil Science, 2 (1–63)*.

Rose, C.W., 1994. Research progress on soil erosion processes and a basis for soil conservation practices. In: R. Lal (ed.), Soil Erosion Research Methods, pp 159-177. Soil and Water Conservation Society Ankeny, IA, USA

Ryan, J, Masri, S., Garabet, S., Diekmann, J., and Habib, H. 1997. Soils of ICARDA's Agricultural Experimental Station and Sites:Climate, Classification, Physical and Chemical Properties and Land Uses. International Center for Agricultural Research in the Dry Area, Aleppo, Syria.

Sala, M., Rubio, J.L. and Garcia-Ruiz, J.M. (Eds.), 1991. Soil erosion studies in Spain. Cited in: Dryland Rivers: Hydrology and Geomorphology of Semi-Arid Channels, Bull, L.J. and Kirkby, M.J. (Eds.), Chapter 1: Dryland River Characteristics and Concepts. John Willey and Sons, 2002.

Salvucci, G. D. and Entekhabi, D., 1994. Explicit expressions for Green-Ampt (delta function diffusivity) infiltration rate and cumulative storage. Water Resource Research, 30:2661–26663.

Savat, J., 1979. Laboratory experiments on erosion and deposition of loess by laminar sheet flow and turbulent rill flow. In: Morgan R.P.C., 1995. Soil Erosion and Conservation Second Edition, Longman Scientific and Technical, Longman Group Ltd.

Scogging, S.M. and Thornes, J.B. 1979.Infiltration characteristics in the semi-arid environment. IAHS publication no 128, pp 159–168.

Seginer. I., 1966. Gully development and sediment yield. Journal of hydrology, 4, 236–253.

Shanan, L.A. and Schick, A.P. 1980. A hydrological model for the Negev Desert Highlands: effects of infiltration, runoff and ancient agriculture. Hydrological Science Journal 25:269–282]. In: Simmers, Ian (ed). 2003. Understanding Water in a dry environment.

Sharma, K.D., 1986. Runoff behavior of water harvesting micro-catchments. Agriculture Water Management, 11: 137–144.

Sharma, P.P., 1996. Interrill erosion. In: Agassi, M. (ed.) (1996). *Soil Erosion, Conservation and Rehabilitation*. Marcel Dekker, Inc., USA.

Sharma, P.P. and Gupta, S.C., 1989. Sand detachment by single raindrops of varying kinetic energy and momentum. *Soil Science Society, American Journal 45*:1031–1034.

Sharon, D. 1972. The spottiness of rainfall in a desert area. Journal of Hydrology, Vol. 17, 1972.

Shiferaw, B. and Holden, S., 1998. Resource degradation and adoption of land conservation technologies in the Ethiopian Highlands: A case study in Andit Tid, North Shewa. Agriculture Economics, 18 (3), 233–248.

Simanton, J.R., Weltz, M.A., West, L.T., and Wingate, G.D., 1987. Rangeland experiment for water erosion prediction project. American Society of Agricultural Engineers, paper no. 87–2545, MI, USA.

Simmers, I. (2003). Hydrological process and water resource management. In: Simmers I. (ed). Understanding water in dry environment; Hydrological process in arid and semi-arid zones. IAH publication no 23.

Simons, D.B., Li R.M. and Associates, 1982. Engineering Analysis of Fluvial System. Fort Collins Colorado 80522, USA. Published by BookCrafters, Inc., Chelsea, Michigan, U.S.A.

Skaggs, R.W. and Khaleel, R. 1982. Infiltration, hydrologic modeling of small watersheds. American Scoiety of Agricultural Engineers, MI, USA.

Skaggs, R.W. 1982. Infiltration. In: Hann, C.T., Johnson, H.P. and Brakensiek, D.L. (ed), 1982. Hydrological modeling of small watersheds. ASAE Monograph, Amrican Society of Agricultural Engineers, Michigan, USA.

Slattery, M.C. and R. B., Bryan, 1992. Hydraulic conditions for rill incision under simulated rainfall: a laboratory experiment. Earth Surface Processes and Landforms 17: 127–146.

Sobulo, R.A. and Adepetu, J.A. 1987. Soil testing and fertilizer formulation for crop production in Nigeria. In: Adepetu, J.A. Nabhan, H. and Osinubi, A. (eds).

1996. Simple soil, water and plant testing techniques for soil resource management. Proceedings of training course held in Ibadan, Nigeria, 16–27 September, 1996. IITA and FAO Rome, 2000.

Somerhalter, T., 1987. Boden-und wasserkonservierende Mabnahmen im Queddai, Tschad, DED, Berlin. Cited in: Water Harvesting: History, Techniques and Trends, Prinz, D. 1996. Zeitschrift fűr Bewässerungswirtschaft, 31, Jahrgang, Heft 1/1996, Seite 64–105.

Somme, G., Oweis, T., Abdulal, A., Bruggeman, A. and Ali, A. 2004. Micro-catchment water harvesting for improved vegetation cover in the Syrian Badia. On-farm Water Husbandry Series No. 3. International Center for Agricultural Research in The Dry area, Aleppo, Syria.

Snyder, F. F., 1938. Synthetic unit-graphs, ransaction of American Geophysics Union, Vol 19, pp 447–454. Reported in: Chow V.T., Maidment D.R., Mays L.W. 1988. Applied Hydrology. McGraw Hill International.

Soil Science Society of America, 1996. Glossary of Soil Science Terms. Soil Science Society of America, Madison, USA.

Springer, E. P., McGurk, B. J., Hawkins, R. H. and Coltharp, G. B., 1980. Curve Number from watershed data. Proceedings of ASCE, Irrigation and Drainage, Symposium on Watershed Management, Volume II, 938–950, ASCE, NewYork.

Stern P.H. 1979. Small-scale irrigation. Intermediate Technology Publication London.

Stocking, M. A. and Murnaghan, N. 2000. Handbook of the Field Assessment of Land Degradation. Overseas Development Group University of East Anglia Norwich, UK. Helen Rose, Marketing Executive Earthscan Publication Ltd 120 Pentonville Road, London N1 9JN. Web. http://www.unu.edu/env/plec/l-degrade/index-toc.html

Subramanya, K. 1994. Engineering Hydrology. Tata McGraw-Hill Publishing Company Limited, New Delhi. P 235

Swartzendruber, D., 1974. Infiltration of constant-flux rainfall into soil as analyzed by the approach of Green-Ampt. Soil Science 117:272–281.

Syrian Ministry of Environment and UNDP, 1997. Biological Diversity: National Report, Biodiversity strategy and action plan project (SYR/97/G31), Tolyani, P.O. Box 3773, Damascus, Syria.

Takei A., Kobaski, S. and Fukushima, Y. 1981. Erosion and sediment transport measurement in a weathered grnite mountain area. In: Erosion and Sediment Transport Measurement, Proceedings of the Florence Symposium, IAHS Publication no. 133, pp. 493–502.

Taur, W. and Humborg, G. 1992. Runoff Irrigation in Sahel Zone. Technical Centre for Agriculture and Rural Cooperation (CTA), Wageningen, The Netherlands and Verlag Josef Margraf Scientific Books P.O. Box 105, Weikersheim Germany.

Taylor, A.B. and Schwarz, H.E. 1952. Unit-hydrograph lag and peak flow related to basin characteristics. Transaction American Geophysical Union, vol. 33. no 2, pp 235–246.

Tenbergen, B. 1991. Reported in: Oberle, A. 2004. GIS-Based Identification of Suitable Areas for Various Kinds of Water Harvesting in Syria. PhD Dissertation, Karlsruhe University, Germany.

Terstriep, M.L. and Stall, J.B. 1974. The Illinois Urban Drainage Area Simulator. ILLUDAS. ISWS-74-Bul 58. State of Illinois Department of Registration and Education, Urbana, IL.

Thames, J.L., 1989. Watershed management in arid zones. In: FAO 1989, Role of forestry in combating desertification. FAO Conservation Guide 21, Food and Agriculture Organization of the United Nations, Rome, Italy.

Tikue, G.G. 2002. Water harvesting practices in Raya Valley Integrated Agriculture Development Program Observation areas. In: Hailu, M. (ed.) (2002). Workshop on the experience of water harvesting in the drylands of Ethiopia: principles and practices (December 2001), Ethiopia. Dryland coordination group report no 19, Norway.

Tilahun, K., 2006. Analysis of rainfall climate and evapotranspiration in arid and semi-arid regions of Ethiopia using data over the last half a century. *Journal of Arid Environments, Volume 64, Issue 3, February 2006, Pages 474–487.*

Thompson, J.R., 1964. Quantitative effect of watershed variable on the rate of gully head advancement. *Transactions, American Society of Agricultural Engineers, Vol. 7, No. 1*.

Thornes, J.B. 1994. Catchment and channel hydrology. In: Abrahams A.D. and Parsons A.J. (eds). Geomorphology of Desert Environment. Chapman and Hall, London, 257–287.

Troch, P. A., Smith, J. A., Wood, E. F. and de Troch, F. P. 1994. Hydrologic controls of large floods in a small basin: central Appalachian case study. Journal of Hydrology, 156.

Torri, D., Sfalanga M. and Chisci, G., 1987. Threshold conditions for incipient riling. Catema Supplement 8: 97–105.

Toy, T.J., Foster, G.R. and Renard, K.G., 2002. Soil Erosion: Process, Prediction,

Measure and Control. John Wiley and Sons, Inc. New York.

Truman, C.C., Bradford J.M., and Ferris, J.E., 1990. Influence of antecedent water content and rainfall energy on soil aggregate breakdown. *Soil Science Society, American Journal 54*: 1385.

UNEP, 1983. Rain and Stormwater Harvesting in Rural Areas. A Report by the United Nations Environnemental Programme, 238 pp. Tycooly International Publishing, Dublin, Ireland.

UNEP. 1991. External Evolution of the Plan of Action to Combat Desertification, Report of the Executive Director, prepared for the 16th session of the Governing Council UNEP, Nairobi.

UNEP, 1992. World Atlas of Desertification. Edward Arnold, London.

UNEP, 2000. Rainwater harvesting and utilization. United Nation Environmental Program. An Environmentally Sound Approach for Sustainable Urban Water Management: An Introductory Guide for Decision-Makers.

http://www.unep.or.jp/ietc/publications/urban/urbanenv-2/9.asp

UNESCO, 1977. Climatic zonation of the arid and semi-arid regions. In: Reij, C., Mulder, P. and Begemann, L. (1988). Water harvesting for plant production. The World Bank Technical Paper no. 91, Washington, D.C.

USACE, 1944. Hydrology, San Gabriel Riverand the Rio Hondo above Whitter Narrows flood control basin. US Army Core of Engineers, Los Angeles.

USACE, 1987. Derivation of rainfall-runoff model to compute n year floods for Orange County watersheds, US Army Core of Engineers, Los Angeles.

USACE. 1994. Flood runoff analysis, Engineering manual, EM 1110–2–1417, table 6.1, US Army Core of Engineers, Washington, DC.

USACE-HEC. 1998. HEC-1, flood hydrograph package user's manual. Hydrological Engineering Center, Davis, CA.

USACE-HEC., 2000. Hydrological modeling system, HEC-HMS. Technical reference manual. US Army Core of Engineers, Hydrological Engineering Center, Washington DC.

USDA-NRCS, 1996. Soil Survey Laboratory Methods Manual. Soil Survey Investigation Report No. 42, US Department of Agriculture, Natural Resources Conservation Service.

USDA-SCS, 1966. Procedures for determining rates of land damages, land depreciation and volume of sediment produced by gully erosion. *Technical release no. 32, Geology, July, 1966*, United State Department of Agriculture, Soil Conservation Services.

USDA-SCS, 1972. National Engineering Handbook. Hydrology, Section 4. U.S. Department of Agriculture, Soil Conservation Services.

USDA-SCS, 1985. Hydrology. National Engineering Handbook, Section 4," United State Department of Agriculture, Soil Conservation Services. Government printing office Washington DC

USDA-SCS, 1986. Urban Hydrology for Small Watershed. *Technical Release 55*. U.S. Department of Agriculture, Soil Conservation Services.

Valentin, C., Hoogmoed, W. and Andriesse, W., 1991. The maintenance and enhancement of low fertility soil. In: Evaluation for sustainable land management in the developing world. IBSRAM Proceedings: Technical Papers Vol. 2.

Walkley, A., 1947. A critical examination of a rapid method for determining organic carbon in soils: Effect of variations in digestion conditions and of organic soil constituents. Journal of Soil Science, 63: 251–263.

Vandekerchove, L., Poesen, J., Oostwoud D.W., and Gyssels, G., 2001. Short-term bank gully retriate rates in Mediterranean environments. Catena, 44, 133–161. Cited in: Gully erosion in dryland environment. In: Bull, L.J. and M.J. Kirkby, 2002. Dryland *Rivers: Hydrology and Geomorphology of Semi-arid Channels*. John Wiley and Sons, Ltd.

Van-Rooy, M.P. 1965. A rainfall anomaly index independent of time and space. *Notos* 14: 43, Weather Bureau of South Africa 14(1965). Cited in: Tilahun, K. 2006. Analysis of rainfall climate and evapotranspiration in arid and semi-arid regions of Ethiopia using data over the last half a century. Journal of Arid Environments, Feb. 2006.

Visser, S.M. and Leenders, J.K., 2004. The role of crust formation in the interaction between wind and water erosion in the Sahel. In: Visser, S. and W. Cornelis (eds). Wind and Rain Interaction in Erosion, Chapter 5, pp 71–78. Tropical Resource Management Papers no. 50 (2004) Wegeninegn University and Research Center, the Netherlands.

Vogel, H., 1990. Deterioration of a mountainous agro-ecosystem in the Third World due to Emigration of rural labor. In: Soil Erosion and Conservation, R.P.C. Morgan, 1995. Second Edition, Longman Scientific and Technical, Longman Group Ltd.

Wahlin, L. 1997. The family cistern: 300 years of household water collection in Jordan. *Ethnic Encounter and Culture Change,* ed. Sabour and Vikor, 233 1/N 49. Nordic Middle East conference at Joensuu in the Finnish Karelia, 19–22 June 1995.

Wallace, D.E. and Lane, L.J. 1976. Geomorphic thresholds and their influence on surface runoff from small semi-arid watersheds. American Water Resource Association, Arizona Section. Proceedings of the Meeting of the Arizona Section, pp 169–176, Tucson, Arizona.

Wei, T.C. and Larson, C.C. 1971. Effects of areal and time distribution of rainfall on small watershed runoff hydrographs. Bull. 30. Water Res. University of Minnesota, March, 1971.

Weltz, M.A., Renard, K.G. and Simanton, J.R., 1987. Revised Universal Soil Loss Equation for western rangelands. Strategies for classification and management of native vegetation and food production in arid zones pp 104–111. USDA Forest services Rocky Mountains. Forest and range experiment station report RM-150, 1987, USA.

Williams, J.R. and Berndt, H.D. 1977. Sediment yield prediction based on watershed hydrology. Transaction ASAE, 20(6):1100–1104.

Williams, J. R., Ouyang, Y., Chen, J and Ravi, V., 1998. Estimation of infiltration rate in Vadose zone: Application of selected mathematical models, volume II, EPA/600/R-97/128b. United State Environmental Protection Agency.

Wischmeier, W.H. and D.D. Smith, 1951. Rainfall energy and its relation to soil loss. Transaction of American Geophysics. Un. 39: 285–308.

Wischmeier, W.H. and Smith, D.D. 1965. Predicting rainfall-erosion losses from cropland east of the Rocky Mountains, Agriculture Handbook No. 282, USDA-ARS. Cited in, Simons, D.B., R.M. Li and Associates, 1982. Engineering Analysis of Fluvial System. Fort Collins Colorado 80522, USA. Published by BookCrafters, Inc., Chelsea, Michigan, U.S.A.

Wischmeiere, W.H. and L.V. Mannerring. 1969. Relation of soil properties to its erodibility. Soil Science Society America. Proceedings 33:131–137. Cited in: Agassi, M. (ed.) (1996). *Soil Erosion, Conservation and Rehabilitation*. Marcel Dekker, Inc., USA.

Wischmeier, W.H., Johnson, C.B. and Cross, B.V., 1971. A soil erodibility nomograph for farmland and construction sites. Journal of Soil and Water Conservation 26: 189–93.

Wischmeier, W.H. and Smith, D.D. 1978. Predicting rainfall erosion losses: A guide to conservation planning. USDA Science and Education Administration, Agriculture Research Agriculture Handbook No. 537. U.S. Government printing office Washington D.C.

World Resource Institute, 2003. Earth trends: Country profile. http://earthtrends.wri.org

Wright-McLaughlin Engineers. 1969. Urban Storm Drainage Criteria Manual. Denver Regional Council of Governments, Denver Colorado.

Yair, A. and Klein, M. 1973. The influence of surface properties on flow and erosion processes on debries covered slopes in an arid area. Catena, Vol.1, pp 1–18, Gottingen.

Yair, A. and Lavee, H. 1974. Areal contribution to runoff on scree slopes in an extreme arid—a simulated rainstorm experiment, Zeitschrift fur Geomorphologie, N.F. Suppl. Bd. 21 pp 106–121, Berlin

Yair A. Sharon D. and Lavee, H. 1978. An instrumented watershed for the study of partial area contribution of runoff in the arid zone. Zeitschrift fur Geomorphologie, N.F. Suppl. Bd. 21 pp 106–121, Berlin.

Young, A., 1969. Present rate of land erosion. Nature 224: 851–852. In: Soil Erosion and Conservation, R.P.C., Morgan, 1995. Second Edition, Longman Scientific and Technical, Longman Group Ltd.

Zaunderer, J. and C.F.,Hutchinson, 1988. A review of water harvesting techniques in the arid southwestern US and North Mexico. Un-published paper produced for World Bank Sub-Saharan Water Harvesting Study. In: Water Harvesting: A Manual for the Design and Construction of Water Harvesting Schemes for Plant Production. Critchley, W. and K., Siegert, 1991. AGL Miscellaneous Paper no. 17, FAO, Rome, Italy.

CURRICULUM VITAE

I was born in Mohammadi Pur village of District Kasur, Pakistan in 1957 and attended the Government High School Chunian and Dyal Singh College Lahore, where I completed my secondary school education from the Board of Intermediate and Secondary Education, Lahore. I graduated in Civil Engineering from the University of Engineering and Technology, Lahore, Pakistan in 1982. I pursued my post-graduate study and earned a degree in Master of Science in Water Resource Engineering from the Asian Institute of Technology Bangkok, Thailand in 1993. I also earned a Post-Graduate Diploma in International Affairs from the Punjab University, Lahore in 1997. I recieved trainings in Alluvial Channel Hydraulic Design by USBR, Geographical Information System (GIS) from AIT and Information Technology and Computer Applications (ITCA) from Hyderabad, Pakistan.

I worked for National Engineering Services of Pakistan (NESPAK) from 1982 to 1999 at different positions from Junior Hydraulic Engineer to Principal Engineer. Most of my experience with the NESPAK was in hydraulic design, river basin planning and large hydraulic structures including feasibility studies, design and project implementation. Working in tropical arid and semi-arid areas, diversified my experience. My major assignments with the NESPAK included; planning and design of large irrigation and drainage systems, flood management and development of flood forecasting and early warning systems for the Indus basin, hydro-power development, water and soil conservation and mathematical modeling and scale model studies.

I joined ICARDA as Water and Soil Engineer in 2000 on Matrouh Natural Resource Management Project Egypt and worked in natural resource management, water harvesting and integrated watershed management and, soil conservation with emphasis on combating desertification on six major projects. I extensively travelled in West Asian and North African countries and acquired a great deal of knowledge through working with the communities and the national scientists. I attended and organized several workshops/seminars and greatly contributed to capacity building of the national scientists.

ANNEX A: THEORETICAL BASIS OF RUNOFF ESTIMATE

Annex A-1: Some Commonly Used Infiltration Models

A-1.1 Horton equation

Horton (1940) found that the following empirical equation fits experimentally to the infiltration.

$$i(t) = i_c + (i_o - i_c)e^{-kt} \tag{A.1}$$

Where, ***i(t)*** is infiltration rate at time *t*, i_o and i_c are initial and final infiltration rates, respectively and *k* is the measure of the rate of decrease in infiltration rate.

This equation requires knowledge of i_o, i_c and *k* for its application. Infiltration in this equation is a function of time without considering variations in rainfall intensity, which is an important contributing parameter (Hann, *et al.* 1994). If i_c is known from data, the other parameters of equation (A.1) can be estimated by modifying the equation.

$$i(t) - i_c = (i_o - i_c)e^{-kt} \tag{A.2}$$

Taking logarithm of both sides of the equation (3)

$$\ln[i(t) - i_c] = \ln(i_o - i_c) - kt \tag{A.3}$$

Linear regression of $ln[i(t)-i_c]$ versus *t* can result into $-k$ as slope and i_o as $exp(a)+i_c$, where ***a*** is the intercept of the regression.

A-1.2 Kostiakov's Equation

Kostiakov (1932) proposed the following empirical equation to estimate infiltration.

$$i(t) = a\, t^{-b} \tag{A.4}$$

Where, *I* is infiltration rate at time *t* and α *(α>0)* and β *(0< β<1)* are empirical constants. Integrating equation (A.4) over a time domain (T) results in cumulative infiltration.

$$I(t) = \frac{a}{1-b} t^{(1-b)} \qquad \text{(A.5)}$$

The constants α and β can be determined by curve-fitting equation (A.5) to experimental data for cumulative infiltration, *I(t)*. Infiltration rate, *i*, becomes zero as $t \rightarrow \infty$ rather than approach a non-zero value, Kostiakov proposed that the equation (A.4) and (A.5) should be used for $t < t_{max}$, where, $t_{\max} = [a/K_s]^{(1/b)}$ and K_s is saturated hydraulic conductivity of the soil. Kostiakov equation describes infiltration quite well at smaller time, but becomes less accurate at larger times (Philip, 1957; Parlange and Haverkamp, 1989). It has one parameter and requires less data for its application.

A-1.3 Mezencev's Equation

Mezencev (Philip, 1957) in order to overcome the limitations of large time step in Kostiakov Equation suggested estimation of infiltration by using equation (A.6) and (A.7) instead (A.4) and (A.5).

$$i(t) = i_f + a\, t^{-b} \qquad \text{(A.6)}$$

and

$$I(t) = i_f\, t + \frac{a}{1-b} t^{(1-b)} \qquad \text{(A.7)}$$

Where, i_f, represents final infiltration rate for steady state conditions. All other parameters have already been defined.

A-1.4 Holton's Equation

Holton (1961) proposed a two-parameter empirical equation to estimate infiltration rate. The equation explicitly depends on available pore space for soil-moisture storage at a particular time.

$$i(t) = i_f + ab(w - I)^n \qquad \text{(A.8)}$$

Where, *i(t)* is infiltration rate (cm hr^{-1}) at time step *t*, if is final infiltration rate, ω is the initial moisture deficit or the pore space per unit area of cross-section initially available for water storage (cm), *I* is the cumulative infiltration (cm) at time *t* so that (ω-*I*) is the unfilled capacity of the soils to store water, ***a*** is constant related to surface condition varying between 0.25 and 0.8, ***b*** is a scaling factor and ***n*** is exponent and was equal to 1.4 for many soils. Due to more physical basis and description of infiltration and recovery of infiltration capacity during period of low or no rainfall, the Holton equation is considered superior than Horton model (Hann *et al.*, 1994). This equation has been found suitable for inclusion in catchment models, because of soil water dependence and satisfactory progress in prediction of runoff (Dunin, 1976).

A-1.5 Boughton's Equation

Boughton (1966) proposed the following rainfall-runoff relationship.

$$R = P - F_r \tanh\left(\frac{P}{F_r}\right) \qquad \text{(A.9)}$$

Where, F_r is an empirical parameter and infiltration is estimated by

$$I = P - R \qquad \text{(A.10)}$$

Where, *I* is infiltration, *P* is rainfall and *R* is runoff, all in same units. Dunin (1976) reported some success by using these equations if interpretation of initial soil-moisture deficit is desired.

Ravi and Williams (1998), provides an exhaustive list of infiltration models. A brief description of some of the simplistic infiltration models is given in Table A-1.

Table A-1. Some Simplistic Infiltration Models (adapted from Ravi and Williams, 1998)

Model name	Model Description
Philip (1957)	$Y = T^{1/2} + lT$ Where, T and Y are dimensionless time and cumulative infiltration respectively and have same meaning for all equations in this table. λ is constant that varies between 0 and 1.
Philip (1969)	$Y = \frac{1}{4}[2T^{1/2}\exp(-T/p) + (2T+p)\,erf\{(T/p)^{1/2}\} + 2T]$
Knight (1973)	$Y = \frac{p}{4}\ln[1 + erf(4T/p)^{1/2}] + T$
Parlange (1975)	$2Y - [1 - \exp(-2T^{1/2})] = 2T$
Brutsaert (1977)	$Y = T + \left[\frac{T^{1/2}}{\left(1 + aT^{\frac{1}{2}}\right)}\right]$; where α is either 2/3 or 1.
Collis-George (1977)	$Y = T + \frac{1}{N}\left[\tanh(N^2T)\right]^{1/2}$; where N is a dimensionless constant that varies between 1 and 4.
Swartzendruber and Clague (1989)	$Y = T + \frac{1}{a}\left[1 - \exp(-aT^{1/2})\right]$; where α is constant related to soil hydraulic parameters and is equal to 2.

A-1.6 Richards Equation

Darcy's law and continuity equation can describe the one-dimensional form of unsteady unsaturated flow in porous media (Richard, 1931). The theoretical-based equation can be written as

$$\frac{\partial q}{\partial t} = \frac{\partial}{\partial z}\left(D(q)\frac{\partial q}{\partial z}\right) - \frac{dK}{dq}\frac{\partial q}{\partial z} \quad \text{[θ-based equation]} \qquad \text{(A.11)}$$

Similarly h-based form of the Richard equation can be written as

$$C\frac{\partial h}{\partial t}=\frac{\partial}{\partial z}\left(K(h)\frac{\partial h}{\partial z}\right)-\frac{dK}{dh}\frac{\partial h}{\partial z} \text{ [h-based equation]} \qquad (A.12)$$

Where, θ is soil-water contents (volume of water by total volume), K is hydraulic conductivity, z is coordinate direction, +ve upward, h is soil water potential, and D is soil-water diffusivity, $K(d\Psi/d\theta)$, which has dimension [L^2/T]. The parameters D and K vary markedly with water contents or pressure head, which add difficulty in solving the Richard equation (Skaggs, 1982). Specifying, the applicable boundary conditions is another difficulty. For homogenous soil, $\partial K/\partial z = 0$, the equation (A.11) is transformed in

$$\frac{\partial q}{\partial t}=\frac{\partial}{\partial z}\left(D\frac{\partial q}{\partial z}\right) \qquad (A.13)$$

Philip (1969) presented several limitations of using the Richard equation including:

- Colloidal swelling and shrinking of soils may cause significant changes in soil permeability.
- Air-movement may become important in condition when it differ significantly from atmospheric pressure
- Evaporation during re-distribution of infiltrated water increase the importance of thermal effects.
- Soil hysteresis may become significant after infiltration ceases and redistribution begins.
- Flow is one dimensional; this is reasonable for rainfall and irrigation over large area.

A-1.7 Green-Ampt Model

Green and Ampt (1911) derived first physically based equation of infiltration of water into soil. The results of this equation also match with empirical observation. The equation can be derived from Darcy's law in the following form.

$$i(t) = K\left[\frac{y\Delta q}{I(t)}\right] + 1 \qquad \text{(A.14)}$$

Where *i (t)* is time dependent infiltration rate, *Ψ* is the pressure head *Δθ* is change in water contents across the wetting front and ***I(t)*** is cumulative infiltration at time *t*. The cumulative infiltration can be computed from

$$I(t) = K(t) + y\Delta q \ln\left(1 + \frac{I(t)}{y\Delta q}\right) \qquad \text{(A.15)}$$

The above equation can be solved by iterative method. For iteration purpose, as a first estimate, ***I(t)*** is assumed equal to ***K(t)***. The equations (A.14) and (A.15) are applicable for non-ponding depths or where ponding depth is negligible. For ponding condition *Ψ* should be replaced with *Ψ+d,* where d is ponding depth. The value of Δθ can be computed from

$$\Delta\theta = \theta_e - \theta_i = \theta_e - S_e\theta_e = (1 - S_e)\,\theta_e \qquad \text{(A.16)}$$

$\theta_e = \eta - \theta_r$ (Chow *et al.* 1988) (A.17)

Where, $\theta_{i,}$ initial water contents, θ_r residual water contents, S_e is effective saturation, and η, is the total porosity. The values of Green-Ampt functions are given in literature in tabular forms (Hann, *et al.* 1994; Mays, 2004).

Williams *et al.* (1998) presented many form of Green-Ampt model including Green-Ampt non-homogenous model for layered system (Flerchinger *et al.*, 1988), Green-Ampt explicit model for ponding (Salvucci and Entekhabi, 1994), constant flux Green-Ampt model for non-ponding conditions (Swartzendruber, 1974) and infiltration/exfiltration model for wetting and drying conditions (Eagleson, 1978).

A-1.8 Initial and Constant Loss Rate Models

The initial and constant loss rate models work on the concept that maximum potential rate of precipitation loss, i_c, is constant throughout an event. If, p_t is the maximum areal precipitation (MAP) depth during a time interval $t \rightarrow t+\Delta t$, the excess rainfall, pe_t, during the interval is given by

$$pe_t = \begin{cases} p_t - i_c \,;\; if\; p_t > i_c \\ 0 \qquad\quad otherwise \end{cases} \tag{A.18}$$

Where, p_t is rainfall at time t, pe_t is rainfall excess at time t. An initial loss, I_a can be added to the model to incorporate interception and detention storage. No runoff occurs, till the accumulated precipitation on the pervious area exceeds the initial loss volume. Thus, the rainfall excess can be presented as

$$pe_t = \begin{cases} 0 \quad if \sum p_i < I_a \\ p_t - i_c \quad if \sum p_i > I_a \; and \; p_t > i_c \\ 0 \quad if \sum p_i > I_a \; and \; p_t < i_c \end{cases} \tag{A.19}$$

USACE (1994: EM 1110–2–1417), recommended initial loss for forest from 10–20% and maximum 12.75 mm (0.5 inch) and 2.5–5 mm (0.1–0.2 inch) for impervious area. USDA-SCS (1986) and Skaggs and Khaleel (1982) suggested infiltration (loss) rates for various soils (Table A-2).

Table A-2. Infiltration Loss Rate for Different Soil Textures (from USDA-SCS, 1986 and Skaggs and Khaleel, 1982)

Soil group	Description	Loss rate (mm h^{-1})*
A	Deep sand, deep loess, aggregated silts	7.6–10.1 (0.3–0.4)
B	Shallow loess, sandy loam	3.8–7.6 (0.15–0.3)
C	Clay loams, shallow sandy loam, soils low in organic content and soil usually high in clay	1.3–3.8 (0.05–0.15)
D	Soils that swell significantly when wet, heavy plastic clays and certain saline soils	0.0–1.3 (0.0–0.05)

*The values in the parenthesis show loss range in inch per hour

A-1.9 SCS Curve Number Approach

The Soil Conservation Services of USDA (USDA-SCS, 1972, 1985) combines (a) total precipitation (b) an initial rainfall abstraction, (c) a time variable infiltration rate during storm and (d) antecedent soil-moisture to translate event rainfall into runoff (Huggins and Burney, 1982). It is a semi-empirical model that was developed on 20 years of study and data from many medium to large catchments all over the United States. The storms included were fairly long duration. The model provides consistent basis for estimating the runoff under varying land use and soil type (Rallison and Miller, 1981). The development of SCS Curve Number method followed a hypothesis that "ratio of actual retention to potential retention (F/S) is equal to the ratio of actual runoff to potential runoff, also called effective rainfall or direct runoff (Q/P_e)".

$$\frac{F}{S} = \frac{Q}{P_e} \tag{A.20}$$

Where, F is actual water retention in a catchment and equal to (P_e - Q), S is potential maximum retention, Q is actual runoff or direct runoff and P_e is potential runoff and is equal to (P - I_a) i.e. total rainfall less the initial abstraction and P is total rainfall. From continuity principle,

$$P = Q + F + I_a \tag{A.21}$$

Substituting the value of P_e as (P - I_a) and value of F from equation (A.21) into equation (A.20) and simplifying results into:

$$Q = \frac{(P - I_a)^2}{(P - I_a + S)} \tag{A.22}$$

Equation (2.23) provides the basis for estimation of direct runoff from any given storm. Nevertheless, it does not incorporate time explicitly into the formulation. The application of method to a rainfall hyetograph requires that time be incorporated in a simple way in equation (A.22) (USACE, 1994).

$$Q(t) = \frac{(P(t) - I_a)^2}{(P(t) - I_a + S)} \tag{A.23}$$

Where $Q(t)$ is cumulative runoff at time t and $P(t)$ is cumulative rainfall minus I_a at time t. The incremental runoff depth over a period $\Delta t = t_2 - t_1$ can be calculated from

$$\Delta Q = Q(t_2) - Q(t_1) \tag{A.24}$$

Where, ΔQ is incremental runoff depth in relation to runoff depths at time t_1 and t_2. In equation (A.23), I_a and S are two unknown to be determined. In order to further simplification the SCS suggested $I_a = kS$, where k is initial abstraction ratio.

Based on the study from various small (less than 4 hectares) experimental watersheds with considerable scatter in data, USDA-SCS (1985) adapted a value of 0.2 for k (50% of data points lay within *0.095 £ k £ 0.38*). It resulted in $I_a = 0.2S$. A value of the k (*0.0 £ k £ 0.3*) has been documented in a number of studies encompassing various geographic locations in the USA and elsewhere (Springer *et al.* 1980; Cazier and Hawkins 1984; Ramasastri and Seth 1985; Bosznay 1989). With value of k = 0.2, the equation (A.23) results in

$$Q = \frac{(P - 0.2S)^2}{(P + 0.8S)} \quad \text{for P > 0.2S,} \tag{A.25}$$

Where, Q is runoff, P is rainfall and S represents abstraction losses.

The equation (A.25) is valid for a value of $P>0.2S$. The potential retentions S may vary between zero and infinity. SCS mapped the S into dimensionless parameter *CN*, keeping its value between 0 and 100 for practical convenience and suggested

$$S = \left[\frac{1000}{CN} - 10\right] \quad \text{in Imperial units (S in inches)} \tag{A.26}$$

and

$$S = 25.4\left[\frac{1000}{CN} - 10\right] \quad \text{in Metric units (S in mm)} \tag{A.27}$$

It shows that potential retention is zero for *CN=100* (upper bound) means all rainfall transformed into runoff. Conversely, for a *CN=0*, the potential retention would be infinity. It should be noted that spatial and temporal variability of storm and antecedent moisture conditions could affect the value of *S*. The first two can be incorporated with the selection of composite curve number, while the last one is explained as that the *S* and *CN* in equations (A.26) and (A.27) represents average soil-moisture conditions and can be referred as S_2 and CN_2, respectively. The Curve Number for antecedent condition 1 (dry or low moisture) and 3 (wet or high moisture) can be estimated by (Chow *et al.*, 1988),

$$CN_1 = \frac{4.2\,CN_2}{10 - 0.058\,CN_2} \tag{A.28}$$

$$CN_3 = \frac{23\,CN_2}{10 + 0.13\,CN_2} \tag{A.29}$$

The value of CN_2 can be determined from the SCS tabulated data for different soil groups and land use conditions, which are available from a number of sources (e.g. Chow *et al.*, 1988; Hann *et al.*, 1994; Mays, 2004).

Ponce and Hawkins (1996) reported, its simplicity, predictability, stability, its reliance on one parameter and its representativeness to major runoff producing catchment properties as the main advantages of SCS Curve Number method. They also reported marked sensitivity to the choice of curve number, absence of clear guidance on antecedent moisture condition variations, different level of accuracy for different biomes, absence of an explicit provision for spatial scale effect and fixing of initial abstraction ratio as 0.2 as the weaknesses of the model.

Annex A-2: Two Commonly Used Unit Hydrograph Methods for Estimation of Direct Runoff

A-2.1 Snyder's unit hydrograph

Snyder (1938) estimated the unit hydrograph (UH) from catchment parameters. He considered lag time, peak flow and total time base as critical characteristics of a UH. According to him rainfall duration of a standard UH is related to lag time and time to peak.

$$t_p = 5.5 t_r \tag{A.30}$$

Where, t_p is catchment lag time and t_r is rainfall duration. For a standard UH, he showed that

$$t_p = C_1 C_t \left(L L_c \right)^{0.3} \tag{A.31}$$

Peak discharge per unit of catchment area in m^3 sec^{-1} km^{-2} (ft^3 sec^{-1} mi^{-2}) of the standard UH can be estimated from

$$q_p = \frac{C_2 C_p}{t_p} \tag{A.32}$$

Where, t_p is in hours, L is length of main stream in kilometers (or miles in English units) from the outlet to the upstream divide, L_c is the distance in kilometers (or miles in English units) from the outlet to a point on the stream nearest the centroid of the catchment area, C_1 = 0.75 (or 1.0 for English system), C_2 = 2.75 (640 for English system) and C_t and C_{p} are coefficients derived from gauged basin in similar environments. The values of C_t and C_p can be computed from gauged basin by measuring L and L_c from map of the catchment area and estimating the values of effective duration t_R in hours, catchment lag time t_{pR} in hours, and peak discharge per unit drainage area q_{pR} in m^3 sec^{-1} km^{-2} cm^{-1} (ft^3 sec^{-1} mi^{-2} in^{-1} in English system) from observed hydrograph. For $t_{pR} = 5.5\ t_R$, then $t_R = t_r$, $t_{pR} = t_p$ and $q_{pR} = q_p$. By knowing these values, C_t and C_p can be computed by using equations (A.31) and (A.32). In case, $t_{pR} \neq 5.5\ t_R$ or it shows a significant difference, the standard basin lag can be computed by solving equations (A.30) and (A.33) below, simultaneously for t_r and t_p. The values of C_t and C_p are then computed from equations (A.31) and (A.32).

$$t_p = t_{pR} + \frac{t_r - t_R}{4} \tag{A.33}$$

Bedient and Hubber (1992) reported that C_t typically range from 1.8 to 2.2, although it has been found to vary from 0.4 in mountainous area to 8.0 along the Gulf of Mexico. They also reported that C_p range from 0.4 to 0.8 where larger value of C_p is associated with smaller value of C_t.

The relation between peak discharge, q_p and the peak discharge per unit of drainage area, q_{pR} of the required unit hydrograph is

$$q_{pR} = \frac{q_p t_p}{t_{pR}} \tag{A.34}$$

The base time can be estimated assuming triangular shape of the unit hydrograph by

$$t_b = \frac{C_3}{q_{pR}} \tag{A.35}$$

Where t_b is time base of unit hydrograph in hours and C_3 is 5.56 in MKS system (1290 for English system). The width of the unit hydrograph can be computed by

$$W = C_w q_{pR}^{-1.08} \tag{A.36}$$

Where, W is width of unit hydrograph in hours, C_w is 1.22 in MKS system (440 for English system) for 75% of the width and 2.14 (770, English system) for 50% of the width. Usually one-third of the width is distributed before the peak of unit hydrograph and two-third after the peak (Chow *et al.*, 1988).

USACE (1944) has proposed an alternate form of equation (A.31) in order to estimate unit hydrograph parameter t_p.

$$t_p = CC_t\left(\frac{LL_c}{\sqrt{S}}\right)^N \tag{A.37}$$

Where S is overall slope of longest water course from point of concentration to the boundary of the catchment area and N is an exponent, commonly taken as 0.33 (USACE-HEC 2002). Some others (Cudworth, 1989; USACE, 1987) related t_p with t_c, where t_c is time of concentration and can be estimated from catchment parameters. Most of the time t_p is estimated as 50–75% of t_c.

A-2.2 SCS dimensionless unit hydrograph

It is dimensionless and single-peaked synthetic unit hydrograph that shows discharge as ratio of discharge q to peak discharge q_p, (q/qp), and the time by the ratio of time t to time of rise of unit hydrograph, T_p, (t/T_p). T value of q_p can be estimated by the following equation,

$$q_p = C\frac{A}{T_p} \tag{A.38}$$

Where, C is 2.08 in MKS system (483.3 in the English system), and A is drainage area in km^2 (or mi^2 in English units). The T_p can be calculated from

$$T_p = \frac{\Delta t}{2} + t_{lag} \tag{A.39}$$

Where t_{lag} is basin lag defined as the time difference between the center of mass of rainfall excess and the peak of the unit hydrograph and $t_{lag} \approx 0.6t_c$ and t_c is time of concentration, Δt is duration of effective rainfall.

$$t_c = t_{sheet} + t_{shallow} + t_{channel} \tag{A.40}$$

Equation (A.40) shows the total time for sheet, shallow concentrated and channel flows. The time for channel flow can be estimated from Manning equation.

$$V = \frac{KR^{2/3}S^{1/2}}{n} \tag{A.41}$$

Where, V is velocity, K is constant and is taken as 1.0 for MKS system (1.486 for English units), R is hydraulic radius, S is longitudinal slope and n is Manning roughness coefficient and can be estimated from text book (Chow, 1959). Time in channel can then be estimated from

$$t_{channel} = \frac{L}{V} \tag{A.42}$$

Where L is channel length. Sheet flow (10–100 m) can be calculated from

$$t_{sheet} = \frac{0.007(NL)^{0.8}}{P_2^{0.5}S^{0.4}} \tag{A.43}$$

Where, N is overland flow roughness coefficient (Table A-3), L is flow length, P_2 is 2-year, 24-hour rainfall depth in inches and S is slope. The equation (A.43) is based on the approximate solution of kinematic wave model. Velocity for shallow concentrated flow (largely prevails at about 100 m of sheet flow) can be estimated from.

$$V = \begin{Bmatrix} 16.1345\sqrt{S} & \textit{for unpaved surface} \\ 20.3282 & \textit{for paved surface} \end{Bmatrix} \tag{A.44}$$

The travel time can be estimated by using equation (A.42).

Table A-3. Roughness Coefficient for Overland Sheet Flow (After USACE-HEC, 1998)

Description	Value of N
Smooth surface (Concrete, asphalt, gravel or bare soil)	0.011
Fallow (no residue)	0.05
Cultivated soil	
Residue cover ≤ 20%	0.06
Residue cover > 20%	0.17
Grass	
Short grass prairie	0.15
Dense grasses, including species such as weeping love grass, buffalo grass, blue grass, and native grass mixtures.	0.24
Bermuda grass	0.41
Range	0.13
Woods (Consider cover to height of 3 cm only, which obstructs sheet flow)	
Light underbrush	0.40
Dense underbrush	0.80

Annex A-3: Theoretical Basis of Erosion Estimation at Interrill and Rill Scales

Sediment continuity equation is described by rates of change of sediment along distance and sediment concentration with time.

$$\frac{\partial G}{\partial x} + r_s \frac{\partial}{\partial t}(CY) = D_f + D_i \qquad \text{(A.45)}$$

Where, G is sediment load (kg/s/m), x is downslope distance (m), p_s is sediment particles mass density, C is sediment concentration in the flow (volume of sediment/ volume of water), Y is flow depth, D_f is rill erosion or deposition rate (kg/s/m^2) and D_i is inter-rill sediment delivery to rill. D_i is considered to be independent of X. D_f is positive for detachment and it is negative for deposition.

Steady-state sediment continuity equation is simplified form of sediment continuity equation, where time dependent temporary storage term is dropped. Considering quasi-steady-state conditions the sediment continuity equation can be written as

$$\frac{dG}{dx} = D_f + D_i \qquad \text{(A.46)}$$

Equation (A.46) is the first order ordinary differential equation of sediment flow and can be solved analytically. Inter-rill sediment delivery D_i can be estimated from

$$D_i = K_i I^2 S_f \qquad \text{(A.47)}$$

Where, K_i is an inter-rill erodibility parameter and is empirical-based, I is average rainfall intensity integrated over the duration of rainfall excess and S_f is slope factor. Based on data from 18 rangeland sites, Simanton *et al.* (1987) developed a relationship between interrill erodibility K_i and soil properties. The baseline K_i is predicted from

$$K_i = 1000[1810 - 1910 sand - 6327 OM - 846 q_{fc}] \qquad \text{(A.48)}$$

Where, K_i is baseline interrill erodibility parameter for a rangeland soil (kg sm^{-4}), *sand* is the fraction of sand (0 to 1), *OM* is fraction of organic matter (0 to 1), and q_{fc} is the volumetric water content of the soil at 0.033 MPa (m^3 m^{-3}). If predicted K_i is < 10,000 kg sm^{-4}, then K_i is set equal to 10,000. If K_i is > 2,000,000 kg sm^{-4}, then set K_i equal to 2,000,000. The above equation was developed with the following variable ranges (Table A-4).

Table A-4. Values of Variables Used in Determination of Erodibility Parameters (Source: Flanagan and Nearing, 1995; WEPP Technical Document)

Variable	Range	Units
Sand	0.08 to 0.88	Fraction
OM	0.005 to 0.112	Fraction
q_{fc}	0.04 to 0.40	m^3 m^{-3}

Flanagan and Nearing, (1995) on the basis of USDA rangeland rainfall simulation experiments also proposed the optimized values of interrill erodibility K_i, rill erodibility K_r and critical shear stress τ_c (*pa*) (Table A-5).

Table A-5. Interrill Erodibility K_i, Rill Erodibility K_r and Crititcal Shear Stress τ_c in Relation to Soil Texture (Source: Flanagan and Nearing, 1995).

Soil texture	Values for different soil texture observed at four experimental sites		
	K_i (kg sm^{-4})	K_r (kg sm^{-4})	τ_c(pa)
Sandy loam	270, 285, 445, 485, 422, 223	5.3, 1.2, 1.7, 2.1, 1.1, 4.6	0.502, 0.313, 0.576, 0.528, 0.712, 0.136
Sandy clay loam	263	3.5	1.306
Silty clay	1195	16.2	4.36
Loam	315, 357, 972, 469, 903, 238	3.2, 1.5, 1.0, 8.3, 0.9, 0.4	0.025, 1.16, 0.05, 1.88, 0.001, 0.031
Clay	1030, 947	2.0, 1.5	0.426, 3.27
Gravelly sand loam	186	3.3	0.288
Sand	20	30.2	5.71

Note: K_i times 1,000 equals measured K_i. K_r divided by 10,000 equals measured K_r

Based on the 18 WEPP field study sites, the suggested minimum and maximum values for K_i, K_r and τ_c are given in Table A-6.

Table A-6. Minimum and Maximum Values for Ki, Kr and τ_c (Source: Flanagan and Nearing, 1995)

Description	K_i ($kg\ s\ m^{-4}$)	K_r ($s\ m^{-1}$)	τ_c (Pascals)
Minimum value	10,000	0.00001	0.3
Maximum value	2,000,000	0.004	7

Baseline interrill soil erodibility for rangeland is adjusted by following the procedure given below.

$$K_{iadj} = K_{ib}\left(RK_{i\,\text{cov}}\right)\left(RK_{ift}\right) \qquad \text{(A.49)}$$

Where, K_{iadj} is the adjusted interrill erodibility, K_{ib} is the baseline interrill erodibility for rangeland soils, RK_{icov} is the adjustment factor for rangeland cover and RK_{ift} is the adjustment fro freezing and thawing. The RK_{icov} for ground cover is estimated from

$$RK_{i\,\text{cov}} = e^{-7.0(inr\,\text{cov} + can\,\text{cov})} \qquad \text{(A.50)}$$

Where, *inrcov* is interrill cover (0–1) and *concov* is the canopy cover (0–1). S_f in equation (A.47) can be computed by using following relationship

$$S_f = \left(1.05 - 0.85\exp^{(-0.85\sin q)}\right) \qquad \text{(A.51)}$$

Rill erosion or deposition D_f in Equation (A.46) can be estimated from

$$D_f = D_c\left[1 - \frac{G}{T_c}\right] \qquad \text{(A.52)}$$

Where, D_c ($kg\ s^{-1}\ m^{-2}$) is detachment capacity by clean water flow, G ($kg\ s^{-1}\ m^{-1}$) is sediment load, and T_c ($kg\ s^{-1}\ m^{-1}$) is sediment transport capacity in rill. *Dc* is estimated from

$$D_c = K_r\left(t - t_c\right) \qquad \text{(A.53)}$$

Where K_r ($s\ m^{-1}$) is the soils rill erodibility parameter, t (pa) is shear stress of flow acting on the soil particles, and t_c (pa) is soils critical hydraulic shear strength or rill detachment threshold parameter. Rill detachment is considered zero if flow shear stress is less than the critical shear stress for the soil. The relationship between detachment rate and flow shear stress was developed on the basis of hydraulic flume studies. The hydraulic shear stress can be defined as

$$t = gRS \tag{A.54}$$

Where, g is unit weight, R is hydraulic radius and S is channel slope. τ_c in equation (A.54) can be estimated from

$$t_c = 3.23 - 5.6 sand - 24.4 orgmat + \frac{0.9 r_d}{1000} \tag{A.55}$$

Where τ_c is the critical shear stress of flow necessary to detach soil (pa), *sand* is *fraction* of sand (0–1), *orgmat* is *fraction* of organic matter (0–1) and p_d is dry soil bulk density ($kg\ m^{-3}$). A range of the variables used to develop above relationship is given below (Table A-7).

Table A-7. Values of Variables used in Determination of Erodibility Parameters (Source: Flanagan and Nearing, 1995)

Variables	Range	Units
sand	0.08 to 0.88	fraction
orgmat	0.005 to 0.112	fraction
ρ_d	1200 to 1800	Kg m^{-3}

Based on research on 18 rangeland sites, the baseline value of k_r for rangeland can be computed by

$$k_r = 0.0017 + 0.0024 clay - 0.0088 orgmat - \frac{0.00088 r_d}{1000} - 0.00048 root10 \tag{A.56}$$

Where, k_r is the baseline rill erodibility for rangeland (s m^{-1}), *clay* is soil clay contents (0–1) *orgmat* is organic matter content of the surface soil (0–1), p_d is dry soil bulk density (kg m^{-3}) and ***root10*** is total root mass in the top 10 cm of the soil surface (kg m^{-2}). The values of these parameters can be selected from Table A-8.

Table A-8. Range of the Variables Used to Develop the Equation.

Variables	Range of values	Units
Clay	0.033–0.422	Fraction
orgmat	0.005–0.112	Fraction
ROOT10	0.02–4.10	Kg m^{-2}
ρ_d	1200–1800	Kg m^{-3}

Sediment transport capacity of a rill T_c is estimated from

$$T_c = k_t t^{3/2} \qquad \text{(A.57)}$$

Where t is flow shear stress in ***pa***, and k_t is the transport coefficient (m$^{0.5}$ s^{2} kg$^{-0.5}$). The net deposition rate is computed when sediment load G in greater than the sediment transport capacity T_c, therefore for deposition the rill erosion equation will be

$$D_f = \left[{V_f}/{q} \right] \left[T_c - G \right] \qquad \text{(A.58)}$$

Where, V_f is effective fall velocity of sediment particles (m s^{-1}) and q is unit discharge (m^{3}s^{-1}m^{-1}). This equation considers that detachment of soils in rills occur if the hydraulic shear stress of the flow exceeds a critical value and sediment in the flow is less than the transport capacity of the flow. On the other hand, the deposition in the rills occurs when the sediment load in the flow is greater than the transport capacity of flow.

Annex A-4: Some Empirical Models of Gully Erosion Assessment

One such equation that estimates the gully surface area was developed on the basis of data collected in western Iowa, USA.

$$Y = 0.01 X_1^{0.982} X_2^{-0.044} X_3^{0.7954} X_4^{-0.2473} e^{-0.036 X_5} \qquad (A.59)$$

Where, Y is growth in gully surface area in acres for a given time period, X_1 is an index of surface runoff in inches, X_2 is the terraced area of the watershed in acres, X_3 is the gully length at the beginning of time period in feet, X_4 is length from the end of gully to the catchment divide in feet and X_5 is the deviation of the precipitation in inches from normal during time period.

A regression model for gully head advance (Thompson, 1964) based on the field study of gully activity in several locations was developed in the United States.

$$R = 0.15 A^{0.49} S^{0.14} P^{0.74} E^{1.00} \qquad (A.60)$$

Where, R is average annual gully head advance, in ft; A is drainage area in acres; S is slope of approach channel, as a percentage; P is annual summation of rainfall, in inches, from rainfall equal to or greater than 0.5 in/24 h; and E is clay content of eroding soil profile, as a percentage by weight.

USDA-SCS (1966) proposed following equation for gully head advance.

$$R = 1.5 A^{0.46} P^{0.20} \qquad (A.61)$$

Where, R and A are already defined above. P is the summation of 24-h rainfall totals of 0.5 in. or more occurring during the time period, converted to an average annual basis, in inches.

Seginer (1966), suggested that gully erosion problems of a locality can be evaluated from an equation of the form

$$R = C\ A^b \qquad (A.62)$$

Where R is average annual medium-term (15 year) lineal gully head advance (m yr^{-1}) determined by historic or geologic study, or calculated; A is area of drainage basin (km^2); and C and b are constants. The value of C varies between 2.1 and 6 depending on the catchment characteristics and value of b as 0.5.

Based on gully head advancement study in Romania, Radoane *et al.* (1995), suggested following regression models.

$$R = aA^b L^c E^d P^e \text{ (For gullies cut in marls and clays)} \quad (A.63)$$

and

$$R = a + bA + cE + dL + eP \text{ (for gullies cut in sandy rock)} \quad (A.64)$$

Where, R is medium-term (14-years) retreat rate (m yr^{-1}) for gully head, A is area of drainage basin at the upstream of gully head (ha), L is gully length (m) and P is slope of drainage basin (m/100m) and ***a, b, c, d, e*** are empirical coefficients or exponents.

Vandekerchove *et al.* (2001) based on a study of 46 active gullies in Southern Spain found that drainage basin area was the most important factor explaining the short-term (2-year) gully head cut. They gave the following relationship

$$V_e = 0.04 A_p^{0.38} \quad (R^2 = 0.39) \quad (A.65)$$

Where, V_e is eroded volume (m yr^{-1}), A_p is drainage basin area (m^2).

The relationship between total eroded volume (V in m^3, represent long-time gully headcut) and the original drainage area (A_o in m^2), resulted in

$$V = 1.71 A_o^{0.60} \quad (R^2 = 0.65) \quad (A.66)$$

Comparing both the above equations shows a greater variability (exponent and R^2 value).

Main factors that can affect gully erosion may include land use, catchment size, gully size, soil type and the momentum of the fluid. None of the above equations consider all these factors. The equations presented are linear multiplicative or power models except for equation (A.64). Zero value of any variable in these equations will result zero gully erosion, which may not be correct. For example; zero terraced area in a catchment in equation (A.59), yields zero gully erosion, which may not be true. Equations (A.60) and (A.61) consider rainfall event more than 0.5 inch (12.5 mm). Rainfall events in dry areas such as study site less than 12.5 mm are rare and smaller rainfall events can produce runoff to cause gully erosion. This factor in these equations limits their applicability for the dryland catchment.

ANNEX B: EXPERIMENTAL DESIGN AND LAYOUT

Annex B-1. Experimental Design

S. No	Block/ strip	Treatment	Spacing (m)	Strip width (m)	Length along contour (m)	No. of rows	[1]No. of rows less 1	[2]Total length (m)	[3]L/S6 (m)	[4]CM/ S6	[5]No of Shrubs	Order
1	A 1	Vi - 12	12	108	425	9	8	3400	567	95	190	6-3-2-1-5-4
2	A 2	Vc - 6	6	72	675	12	11	7425	1238	207	207	3-2-4-1-5-6
3	A 3	P- 12	12	60	750	5	4	3000	500	84	168	6-1-2-5-4-3
4	A 4	P- 6	6	60	825	10	9	7425	1238	207	207	1-3-5-4-2-6
5	A 5	Vi - 6	6	36	1250	6	5	6250	1042	174	174	4-6-2-3-5-1
6	A 6	Rest		36	1250							
7	A 7	Vc - 12	12	36	1250	3	2	2500	417	70	140	5-6-1-2-4-3
8	B 1	Vc - 6	6	36	1250	6	5	6250	1042	174	174	4-1-5-2-6-3
9	B 2	Rest		36	1325							
10	B 3	P- 6	6	36	1225	6	5	6125	1021	171	171	3-1-5-6-4-2
11	B 4	P- 12	12	36	1275	3	2	2550	425	71	142	5-2-1-4-6-3
12	B 5	Vi - 6	6	36	1225	6	5	6125	1021	171	171	6-2-5-3-1-4
13	B 6	Vc - 12	12	36	1100	3	2	2200	367	61	123	1-4-2-6-5-3
14	B 7	Vi - 12	12	36	1075	3	2	2150	358	60	120	6-1-2-4-3-5
15	C 1	Vi - 6	6	42	1000	7	6	6000	1000	168	168	1-4-3-2-6-5
16	C 2	Rest		51	875							
17	C 3	P- 12	12	60	800	5	4	3200	533	89	179	5-3-1-2-4-6
18	C 4	Vc - 6	6	60	725	10	9	6525	1088	182	182	4-1-3-5-6-2
19	C 5	Vi - 12	12	72	625	6	5	3125	521	87	174	4-3-1-2-6-5
20	C 6	P - 6	6	102	450	17	16	7200	1200	201	201	3-5-6-4-1-2
21	C 7	Vc - 12	12	120	375	10	9	3375	563	94	188	6-3-2-5-1-4

Notes:

[1] First row neglected to avoid interference

[2] Length along contours multiply by effective rows

[3] Length available per combination of method of plantation and shrub species (L/6)

[4] Catchment area per combination

[5] Two shrubs per catchment for 12 m spacing and one for 6 meter spacing

Contributing width to one micro-catchment is 4 meters (2.8 meter length of intermittent micro-catchment and 1.2 meters space between the micro-catchment).

Order	Shrub and method
1	Shrub-Atriplex
2	Shrub-Salsola
3	Shrub-Leuclolada
4	Seed-Atriplex
5	Seed-Salsola
6	Seed-Leuclolada

Annex B-2. Typical Field Layout of MCWH Structures

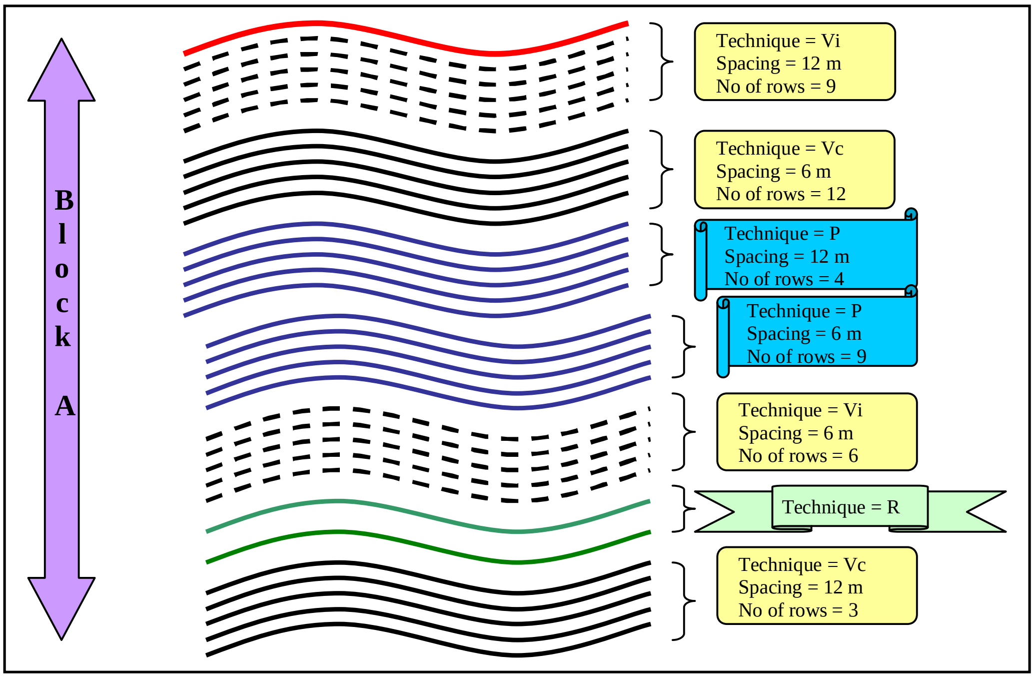

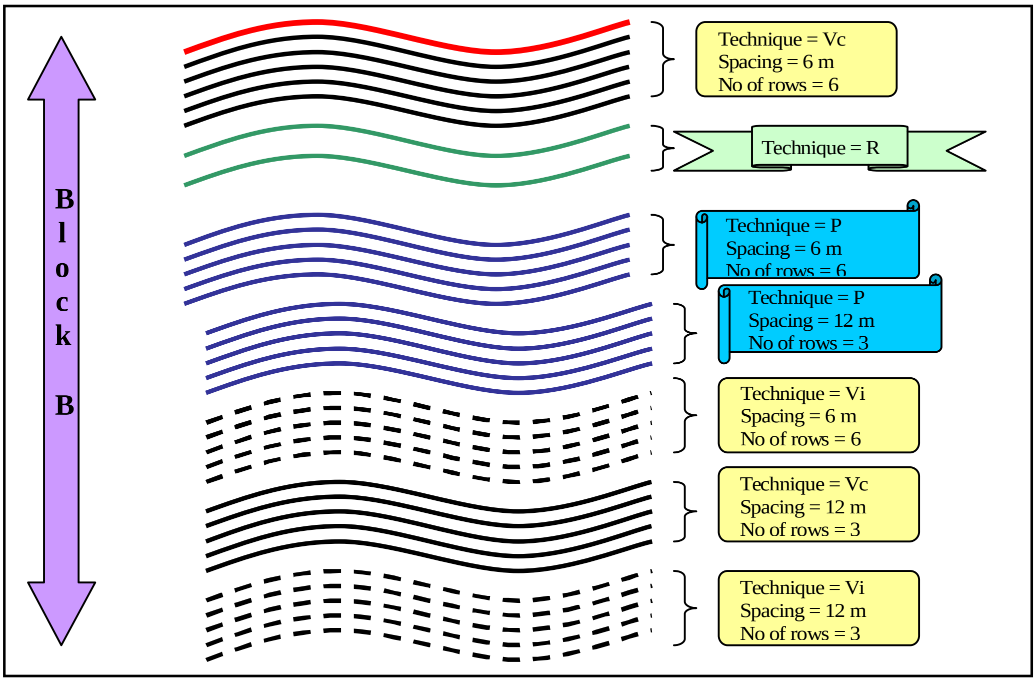

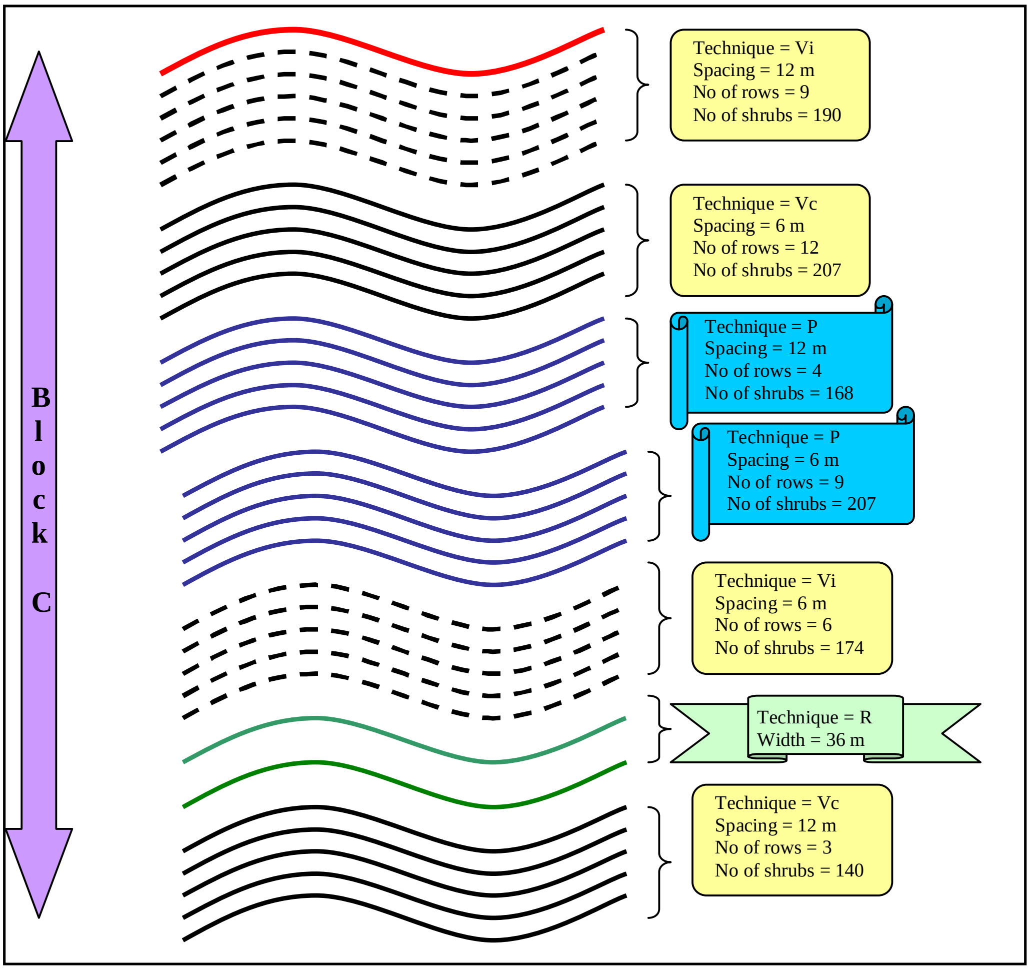

Block C
Technique = Vi
Spacing = 12 m
No of rows = 9
No of shrubs = 190
Technique = Vc
Spacing = 6 m
No of rows = 12
No of shrubs = 207
Technique = P
Spacing = 12 m
No of rows = 4
No of shrubs = 168
Technique = P
Spacing = 6 m
No of rows = 9
No of shrubs = 207
Technique = Vi
Spacing = 6 m
No of rows = 6
No of shrubs = 174
Technique = R
Width = 36 m
Technique = Vc
Spacing = 12 m
No of rows = 3
No of shrubs = 140

ANNEX C: RUNOFF AND SEDIMENT YIELD

Annex C-1: Unit Sediment Yield of the Micro-Catchments for Different Rainfall Events

Table C-1.1. Annual Sediment Yield at Micro-catchment Scale by Runoff Plot Method

Catchment area (m^2)	Micro-catchment-Scale Sediment Yield (Mg ha^{-1}) for Different Rainfall Events							
	5/5/2005	4/4/2006	10/3/2006	10/25/2006	3/1/2007	5/12/2007	5/18/2007	Annual
Rainfall (mm)	*13.1*	*6.1*	*5.1*	*21.1*	*15.4*	*17.1*	*21.8*	
13.80	0.065	0.194	0.163	0.143	0.017	0.174	0.494	0.991
14.40	0.035	0.123	0.228	0.017	0.002	0.029	0.343	0.618
16.00	–	0.098	0.043	0.488	0.024	0.073	0.980	1.608
16.80	0.042	0.211	0.000	1.651	0.084	0.293	0.648	2.676
17.40	0.126	0.263	0.273	0.028	0.012	0.946	0.258	1.517
18.00	0.022	0.091	0.000	0.045	0.060	2.021	0.779	2.906
24.00	–	0.042	0.042	1.406	0.009	0.033	0.412	1.901
24.30	–	0.125	0.000	0.021	0.017	0.211	0.288	0.537
25.20	–	0.072	0.019	0.933	0.006	0.637	0.698	2.293
27.60	0.043	0.057	0.201	0.124	0.007	0.060	0.163	0.555
30.00	0.010	0.021	0.013	0.001	0.009	0.056	0.454	0.533
33.60	0.014	0.161	0.034	0.709	0.025	1.431	0.341	2.540
36.00	–	0.063	0.012	1.007	0.027	0.636	0.342	2.023
39.00	–	0.187	0.085	0.024	0.042	0.033	0.081	0.265
42.25	–	0.041	0.000	0.268	0.010	0.017	0.157	0.451
47.52	–	0.082	0.000	0.030	0.068	0.092	0.600	0.789
48.00	–	0.085	0.000	0.415	0.020	0.011	0.188	0.634
49.44	–	0.073	0.000	0.044	0.026	0.024	0.123	0.217
50.40	–	0.096	0.049	0.444	0.003	0.098	0.499	1.093
Average Annual Sediment Yield (Mg ha^{-1} yr^{-1})								1.271

Annual Sediment Yield was computed for rainfall year starting from September and ending in May

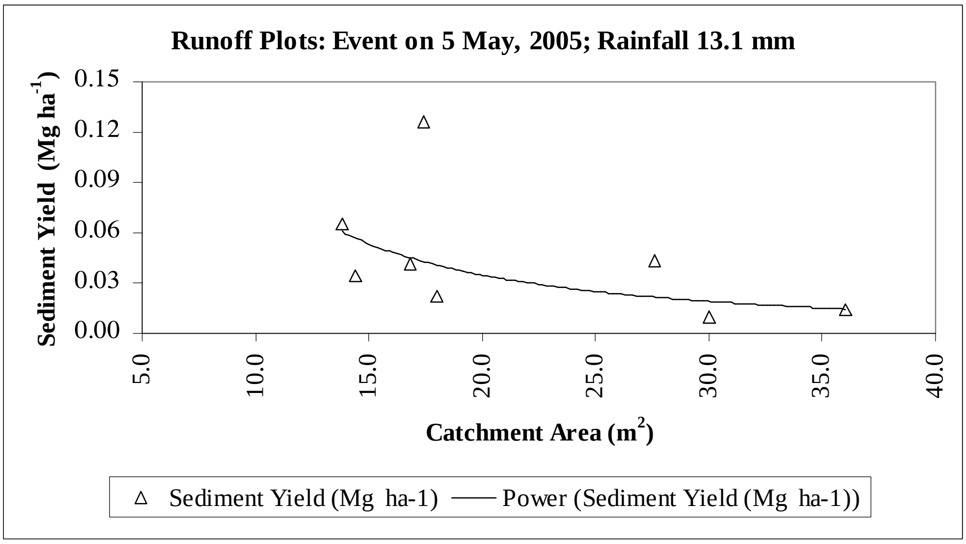

Figure C-1.1. Relationship between Micro-Catchment Area and Sediment Yield for Rainfall Event on May 5, 2005.

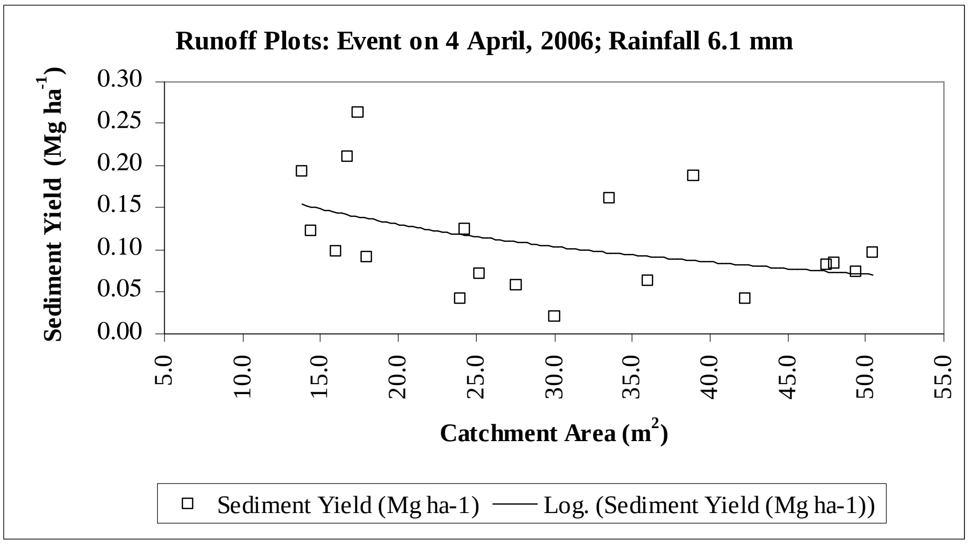

Figure C-1.2. Relationship between Micro-Catchment Area and Sediment Yield for Rainfall Event on April 4, 2006.

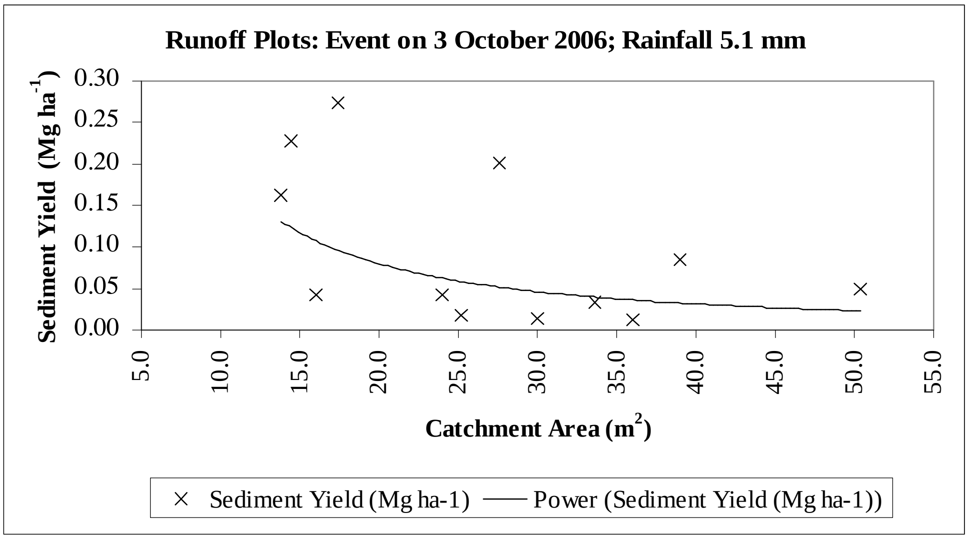

Figure C-1.3. Relationship between Micro-Catchment Area and Sediment Yield for Rainfall Event on October 3, 2006.

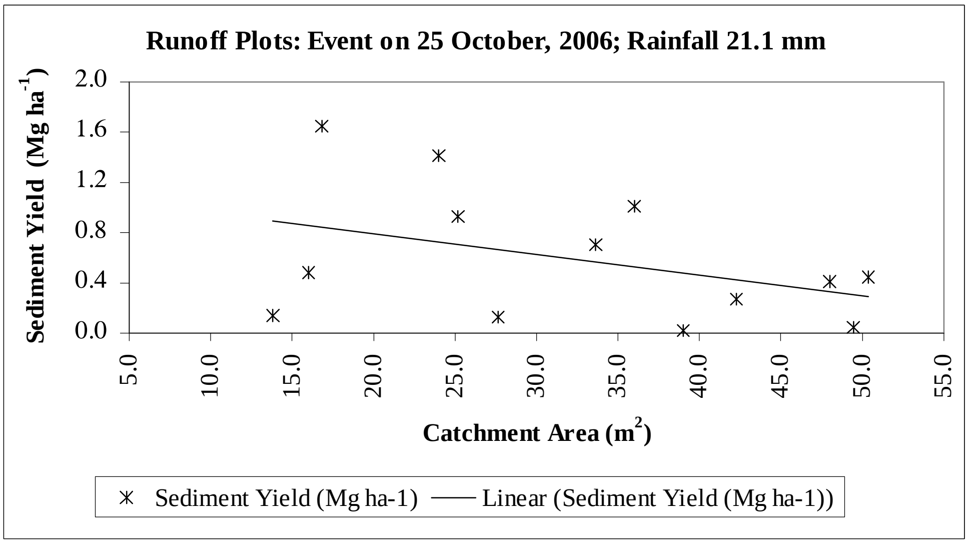

Figure C-1.4. Relationship between Micro-Catchment Area and Sediment Yield for Rainfall Event on October 25, 2006.

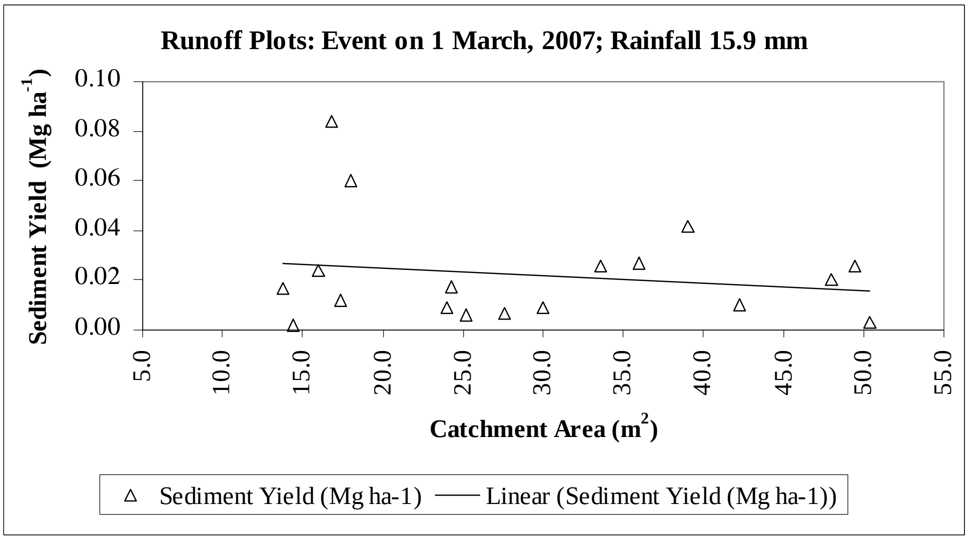

Figure C-1.5. Relationship between Micro-Catchment Area and Sediment Yield for Rainfall Event on March 1, 2007.

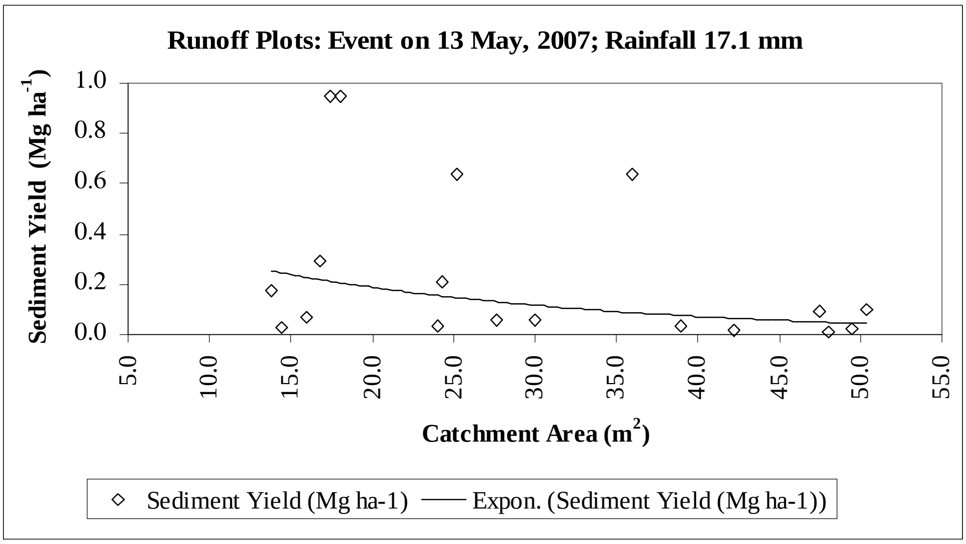

Figure C-1.6. Relationship between Micro-Catchment Area and Sediment Yield for Rainfall Event on May 12, 2007.

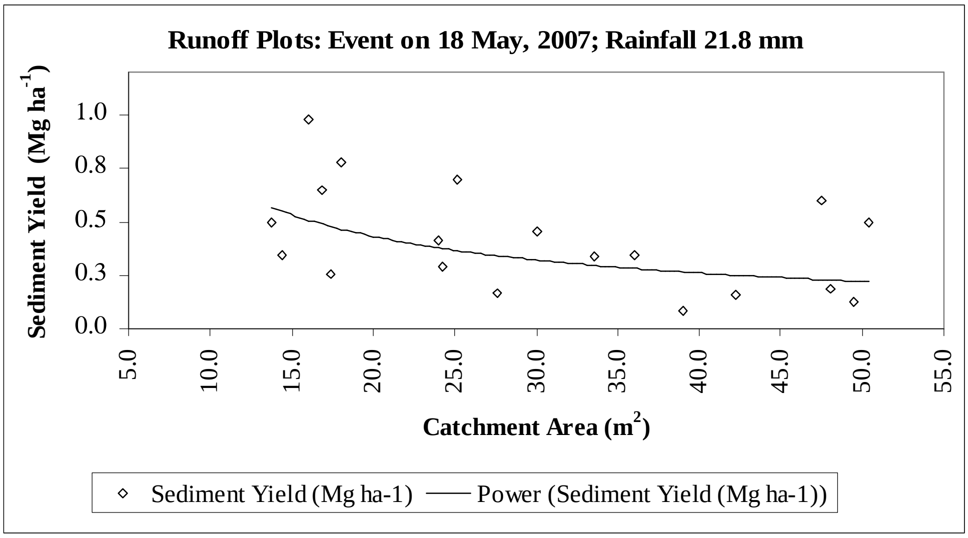

Figure C-1.7. Relationship between Micro-Catchment Area and Sediment Yield for Rainfall Event on May 18, 2007.

Table C-1.2. Sediment Rate in Relation to MCWH Techniques and Treatments (Runoff Plot Method).

MCWH Techniques/ Treatments	Micro-catchment-Scale Sediment Rate (Mg ha^{-1})							
	5/5/05	4/4/06	10/3/06	10/25/06	3/1/07	5/12/07	5/18/07	Annual (Mg ha^{-1} yr^{-1})
Sc-6	0.08	0.16	0.22	0.06	0.01	0.38	0.37	1.04
Vi-6	0.03	0.11	0.04	0.49	0.04	0.13	0.58	1.28
Vc-6		0.10	0.04	0.68	0.02	0.44	0.52	1.70
Sc-12	0.03	0.10	0.21	0.01	0.02	0.07	0.26	0.57
Vi-12	0.01	0.09	0.04	0.17	0.02	0.68	0.22	1.13
Vc-12		0.09	0.02	0.98	0.04	0.61	0.46	2.11

Table C-1.3. Sediment Rate for Different Micro-Catchment Areas and Rainfall Events (Gerlach Trough Method.

Trough No	Slope (%)	MC Area (m^2)	Sediment Yield (Mg ha^{-1})					
			4-May-05	4-Apr-06	25-Oct-06	1-Mar-07	18-May-07	Annual
GT-1	4	11	0.06	0.735	0.092	0.159	0.341	0.59
GT-2	6	12	0.02	0.024	0.100	0.058	0.066	0.22
GT-3	2	20	0.017	na	0.056	0.036	0.051	0.14
GT-4	6	22	0.013	0.209	0.126	0.390	0.105	0.62
GT-5	6	20	0.021	0.075	0.130	0.263	1.073	1.47
GT-6	2	27	0.027	na	0.066	0.228	0.212	0.51
GT-7	4	55	0.011	na	0.030	0.042	0.159	0.23
GT-8	2	90	0.002	0.084	0.066	0.095	0.223	0.38
GT-9	6	17	0.022	na	0.040	0.527	0.329	0.90
GT-10	4	17	0.042	na	0.076	0.058	0.092	0.23
GT-11	4	89	na	0.065	0.028	0.023	0.039	0.09
Average								0.49

The annual sediment yield was computed for rainfall year that starts from September and ends in May. However, it missed two runoff events during 2006-2007 that could not be recorded.

Annex C-2: Erosion and Sediment Deposition at Rill Scale

Annex C-2.1: Erosion and Sediment Deposition Pattern in Inter-Rill Area for Different Rainfall Events

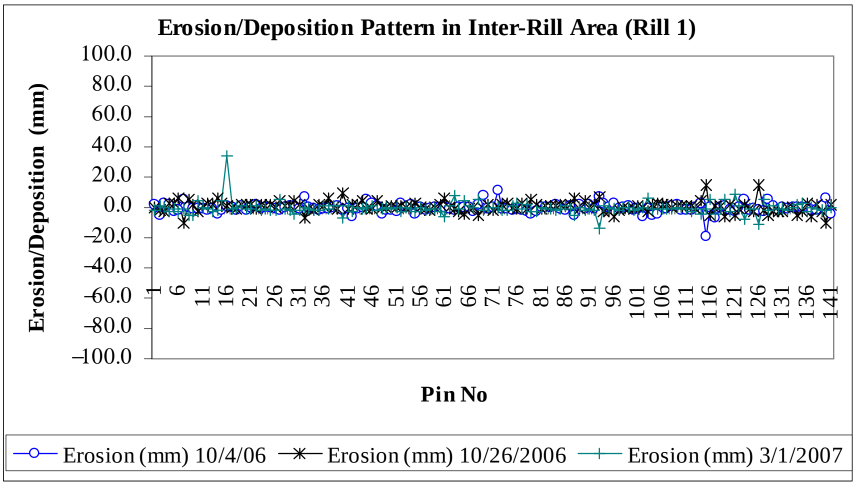

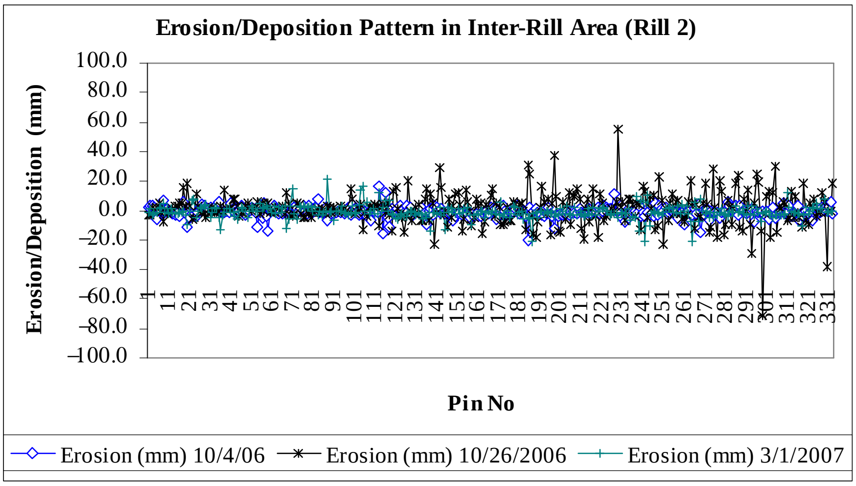

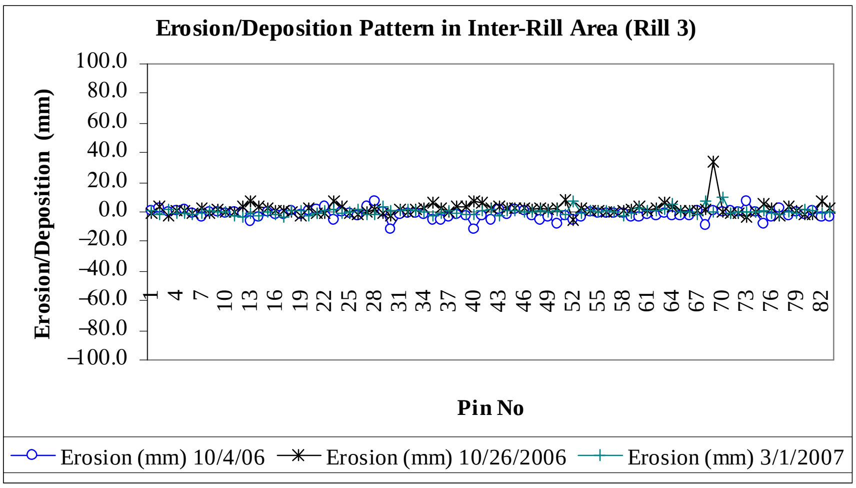

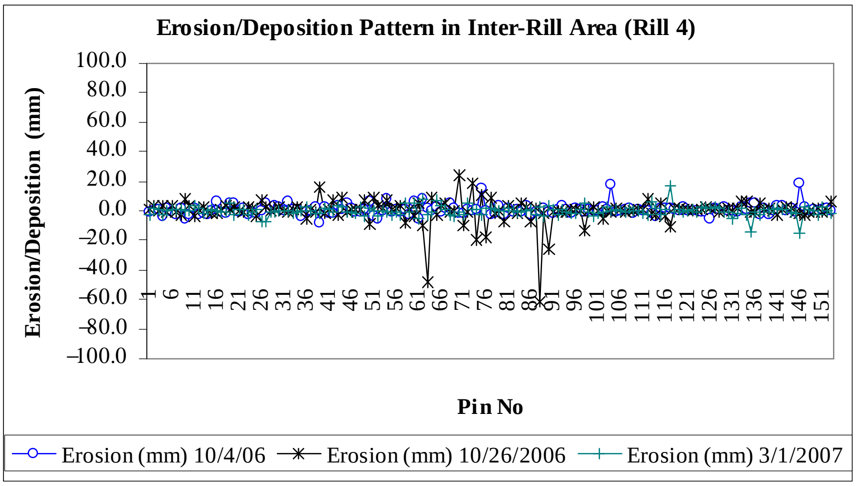
Erosion/Deposition Pattern in Inter-Rill Area (Rill 4)
Erosion/Deposition (mm)
Pin No
Erosion (mm) 10/4/06
Erosion (mm) 10/26/2006
Erosion (mm) 3/1/2007

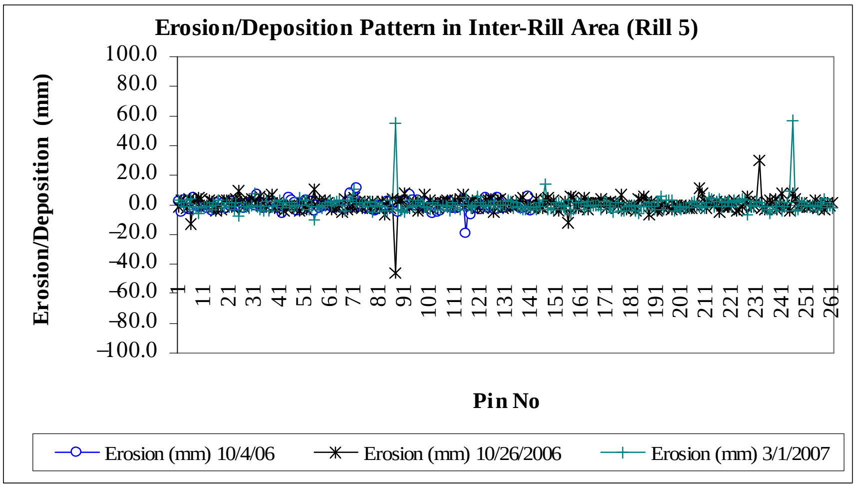
Erosion/Deposition Pattern in Inter-Rill Area (Rill 5)
Erosion/Deposition (mm)
Pin No
Erosion (mm) 10/4/06
Erosion (mm) 10/26/2006
Erosion (mm) 3/1/2007

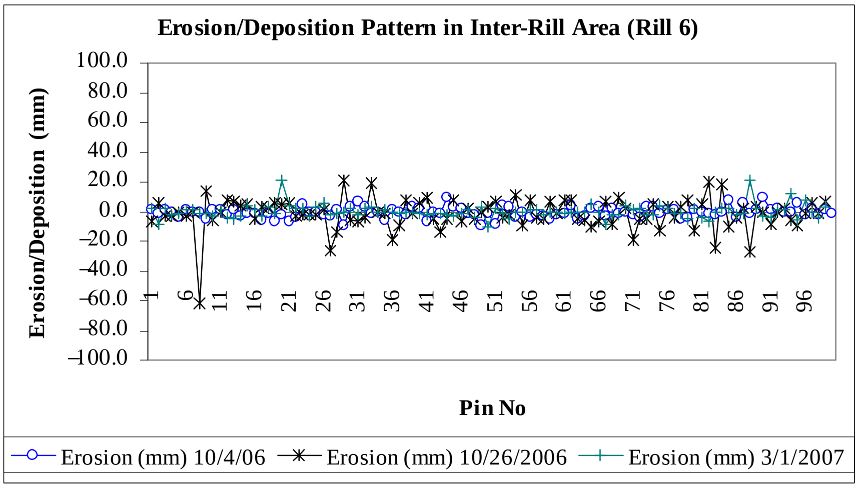
Erosion/Deposition Pattern in Inter-Rill Area (Rill 6)
Erosion/Deposition (mm)
Pin No
Erosion (mm) 10/4/06
Erosion (mm) 10/26/2006
Erosion (mm) 3/1/2007

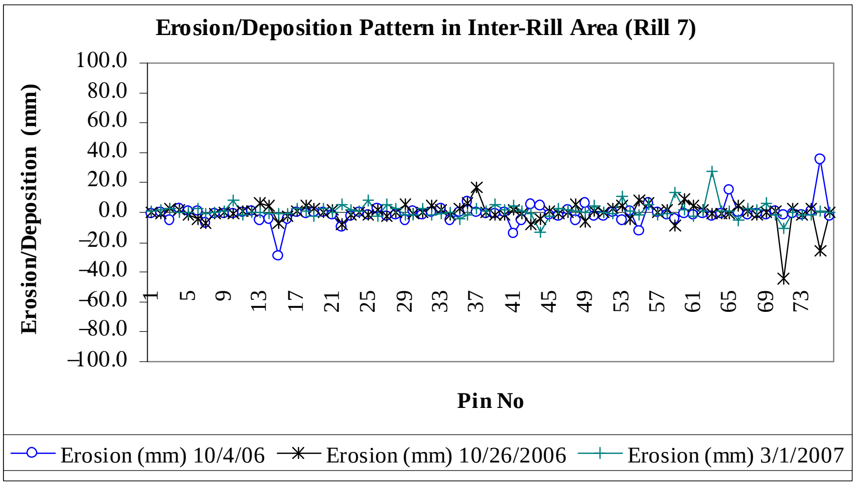
Erosion/Deposition Pattern in Inter-Rill Area (Rill 7)
Erosion/Deposition (mm)
Pin No
Erosion (mm) 10/4/06
Erosion (mm) 10/26/2006
Erosion (mm) 3/1/2007

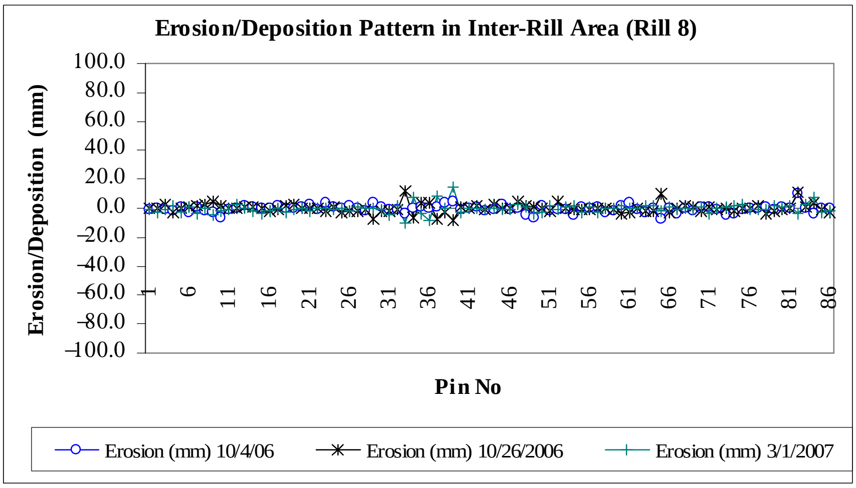
Erosion/Deposition Pattern in Inter-Rill Area (Rill 8)
Erosion/Deposition (mm)
Pin No
Erosion (mm) 10/4/06
Erosion (mm) 10/26/2006
Erosion (mm) 3/1/2007

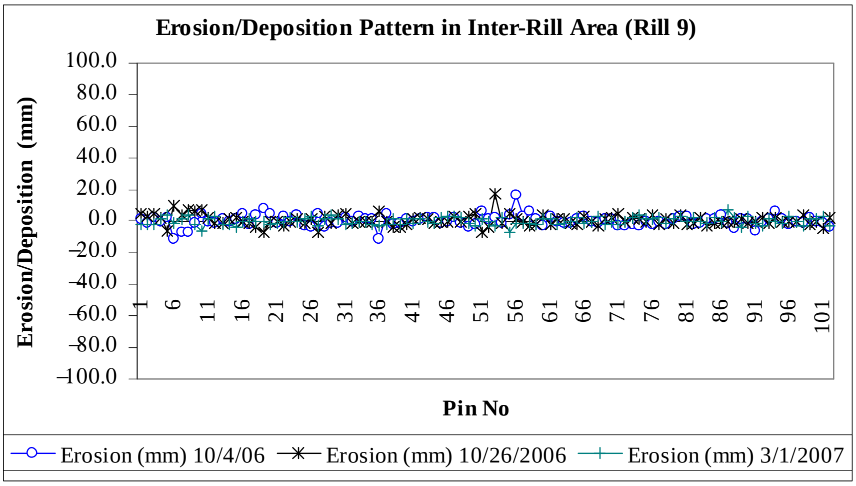
Erosion/Deposition Pattern in Inter-Rill Area (Rill 9)
Erosion/Deposition (mm)
Pin No
Erosion (mm) 10/4/06
Erosion (mm) 10/26/2006
Erosion (mm) 3/1/2007

Annex C-2.2: Erosion and Sediment Deposition Pattern in Rills Area for Different Rainfall Events

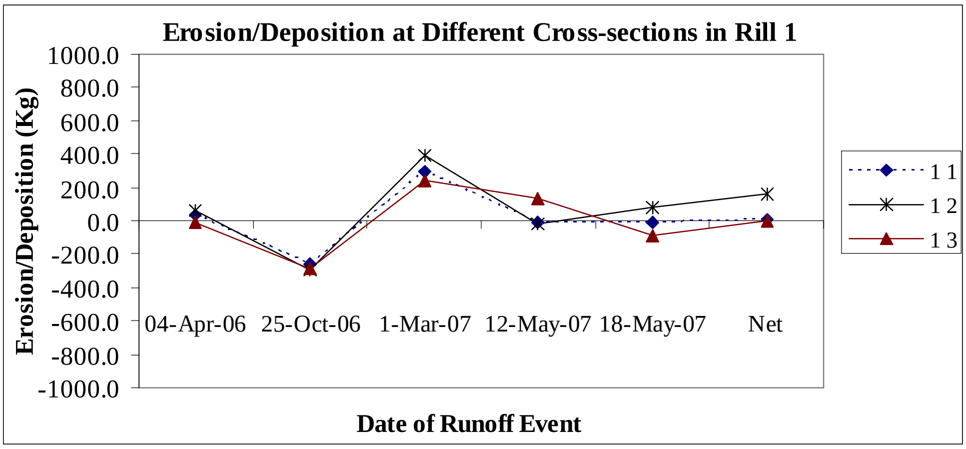

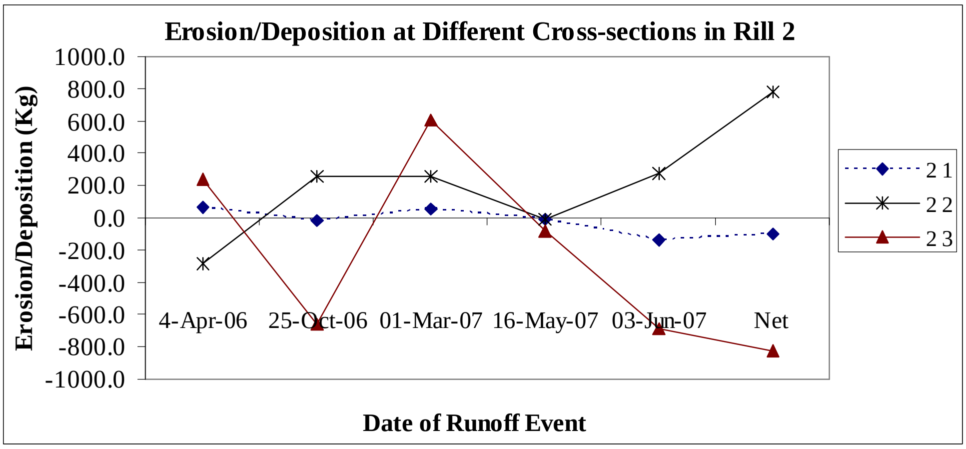

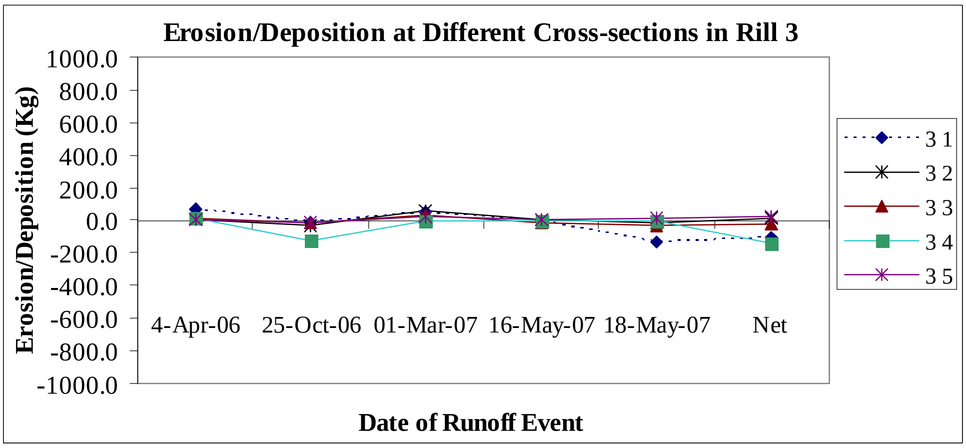

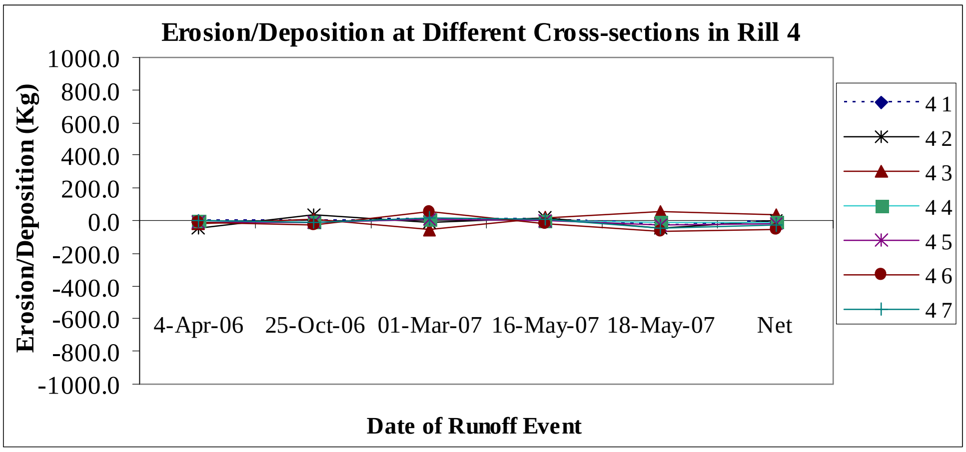
Erosion/Deposition at Different Cross-sections in Rill 4
Erosion/Deposition (Kg)
1000.0
800.0
600.0
400.0
200.0
0.0
-200.0
-400.0
-600.0
-800.0
-1000.0
4-Apr-06
25-Oct-06
01-Mar-07
16-May-07
18-May-07
Net
4 1
4 2
4 3
4 4
4 5
4 6
4 7
Date of Runoff Event

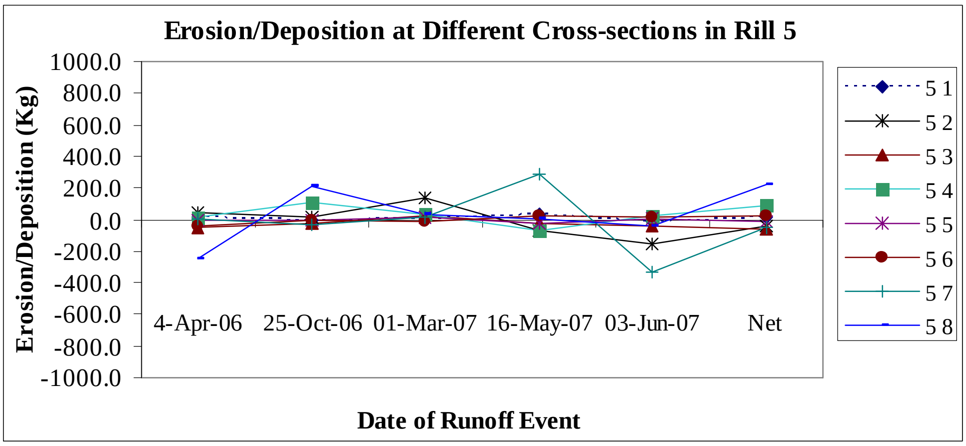
Erosion/Deposition at Different Cross-sections in Rill 5
Erosion/Deposition (Kg)
1000.0
800.0
600.0
400.0
200.0
0.0
-200.0
-400.0
-600.0
-800.0
-1000.0
4-Apr-06
25-Oct-06
01-Mar-07
16-May-07
03-Jun-07
Net
5 1
5 2
5 3
5 4
5 5
5 6
5 7
5 8
Date of Runoff Event

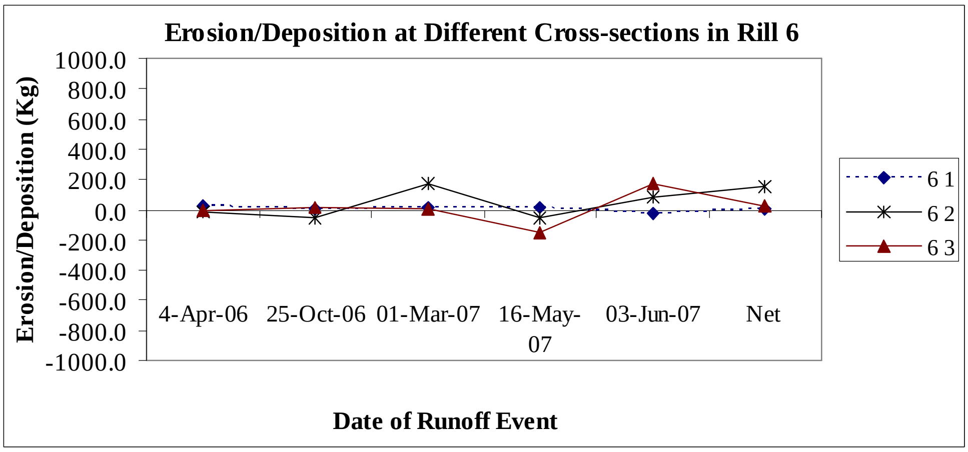
Erosion/Deposition at Different Cross-sections in Rill 6
Erosion/Deposition (Kg)
1000.0
800.0
600.0
400.0
200.0
0.0
-200.0
-400.0
-600.0
-800.0
-1000.0
4-Apr-06
25-Oct-06
01-Mar-07
16-May-07
03-Jun-07
Net
6 1
6 2
6 3
Date of Runoff Event

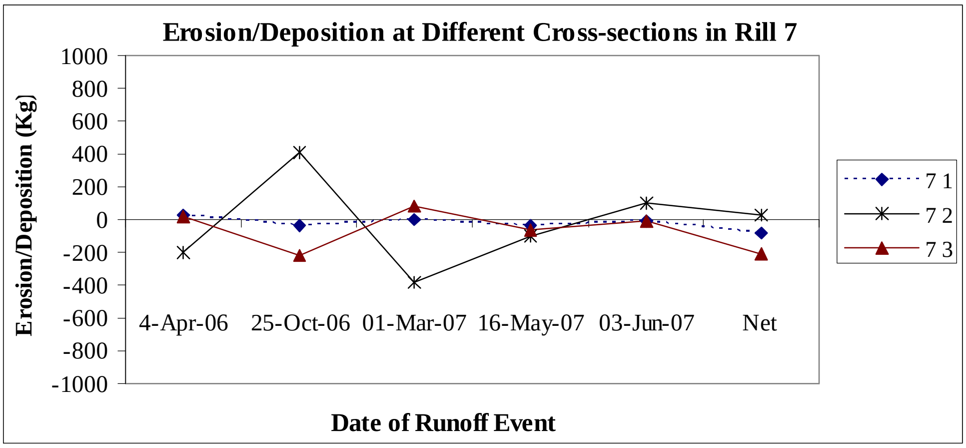
Erosion/Deposition at Different Cross-sections in Rill 7
Erosion/Deposition (Kg)
1000
800
600
400
200
0
-200
-400
-600
-800
-1000
4-Apr-06
25-Oct-06
01-Mar-07
16-May-07
03-Jun-07
Net
Date of Runoff Event
7 1
7 2
7 3

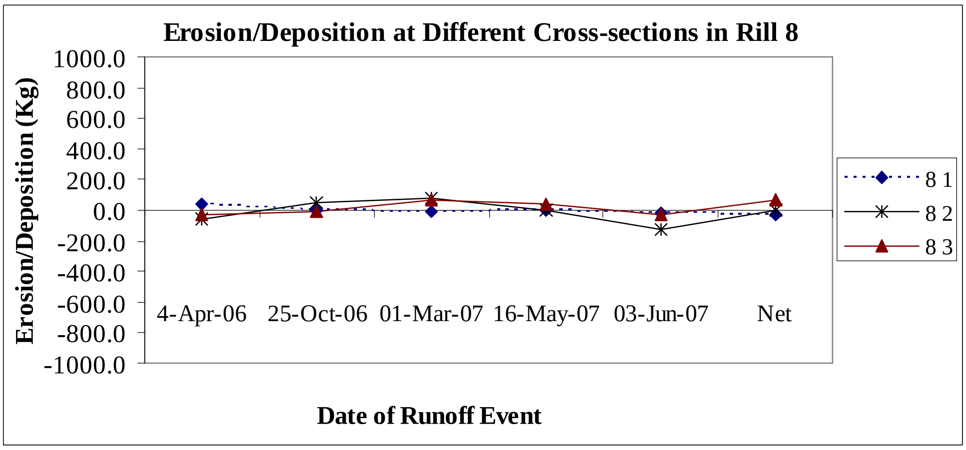
Erosion/Deposition at Different Cross-sections in Rill 8
Erosion/Deposition (Kg)
1000.0
800.0
600.0
400.0
200.0
0.0
-200.0
-400.0
-600.0
-800.0
-1000.0
4-Apr-06
25-Oct-06
01-Mar-07
16-May-07
03-Jun-07
Net
Date of Runoff Event
8 1
8 2
8 3

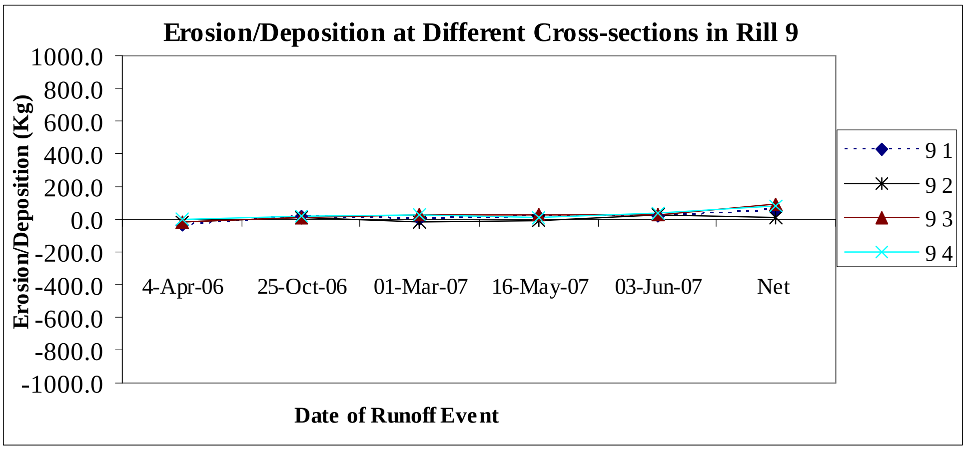
Erosion/Deposition at Different Cross-sections in Rill 9
Erosion/Deposition (Kg)
1000.0
800.0
600.0
400.0
200.0
0.0
-200.0
-400.0
-600.0
-800.0
-1000.0
4-Apr-06
25-Oct-06
01-Mar-07
16-May-07
03-Jun-07
Net
Date of Runoff Event
9 1
9 2
9 3
9 4

ANNEX D: SOME SELECTED PHOTOGRAPHS FROM THE STUDY AREA

Photo 1. An Automatic Weather Station at the Study Site

Photo 2. Automatic Rain Gauge at the Site for Rainfall Measurement

Photo 3. Use of Total Station Maintained the Accuracy in Layout of the Structures

Photo 4. The Work on the Construction of Weir is in Progress

Photo 5. Construction of Weirs in Gullies and Automatic Data Loggers Facilitated Real-time Measurement of Stage Hydrographs

Photo 6. Data Logging for Each Runoff Event

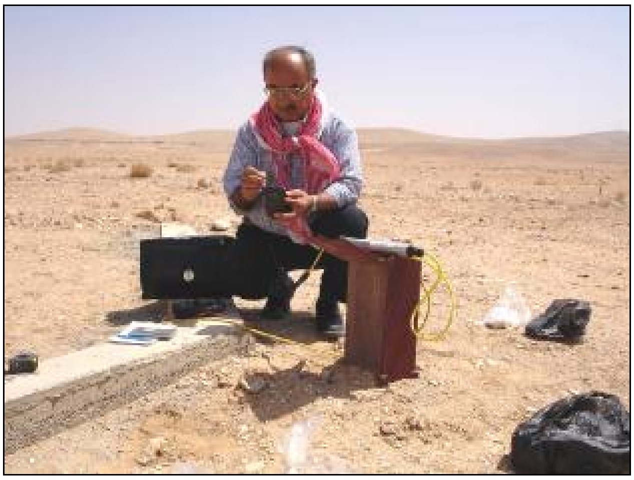

Photo 7. Accuracy of Data Logger Requires a Regular Battery Voltage Check

Photo 8. Sediment in Front of the Weirs was Measured for each Runoff Event

Photo 9. Installation of Bridge Frames for Rill Measurement were checked for Horizontal and Vertical Controls

Photo 10. Prof. Yazar Visits the Site and Discusses the Implementation and Data Collection Methodology

Photo 11. Installation of Runoff and Sediment Tanks in Progress

Photo 12. A Tank with Runoff and Sediment after a Runoff Event

Photo 13. Engineer Explains the Layout of the Gerlach Trough

Photo 14. Twenty Four Ridge Frames Measured the Ridge Decay Rate

Photo 15. Precision in Measurement Requires Check for Horizontal and Vertical Controls for Ridge Bridge Frame

Photo 16. Runoff at the Shrub Location Satisfies that the MCWH Functions Properly

Photo 17. The Micro-catchments Harvested the Local Runoff Even from a Small Rainfall Event

Photo 18. Blooming the Desert—MCWH Made Shrub Cultivation Possible in an Environment of Annual Rainfall Around 120 mm

Photo 19. Vallerani Implement that can Develop Continuous and Intermittent Ridges

Photo 20. Board of Trustees of CIMMYT and ICARDA Scientists at the Research Site

Photo 21. A Group Photo of the Field Team at the Research Site